Thermodynamic analysis of biomass gasification and torrefaction

Mark Jan Prins

Thermodynamic analysis of biomass gasification and torrefaction

PROEFSCHRIFT

ter verkrijging van de graad van doctor aan de Technische Universiteit Eindhoven, op gezag van de Rector Magnificus, prof.dr. R.A. van Santen, voor een commissie aangewezen door het College voor Promoties in het openbaar te verdedigen op woensdag 16 februari 2005 om 16.00 uur

door

Mark Jan Prins

geboren te Haaksbergen

Dit proefschrift is goedgekeurd door de promotoren:

prof.dr.ir. F.J.J.G. Janssen
en
prof.ir. C. Daey Ouwens

Copromotor:
dr.ir. K.J. Ptasinski

Dit onderzoek is uitgevoerd in het kader van het Stimuleringsprogramma Energieonderzoek, dat is opgezet door NWO (Nederlandse organisatie voor Wetenschappelijk Onderzoek) en Novem (Nederlandse Onderneming voor Energie en Milieu). NWO en Novem geven geen garanties voor de juistheid en/of volledigheid van de onderzoeksgegevens en -resultaten. Tevens is een deel van het onderzoek ondersteund door SDE (Stichting Duurzame Energie) met Shell Global Solutions als industriële partner.

CIP-DATA LIBRARY TECHNISCHE UNIVERSITEIT EINDHOVEN

Prins, Mark J.

Thermodynamic analysis of biomass gasification and torrefaction /
by Mark J. Prins. – Eindhoven : Technische Universiteit Eindhoven, 2005.
Proefschrift. – ISBN 90-386-2886-2
NUR 913
Trefwoorden: synthese gas bereiding / biomassa; vergassing / roosteren; torrefactie /
hout / thermodynamica / vrije energie; exergie / duurzame ontwikkeling
Subject headings: fuel gas manufacturing / biomass gasification / roasting; torrefaction /
wood / thermodynamics / free energy; exergy / sustainable development

Cover design by Tanja Gielen
Cover photograph by Wouter van den Hoogen
Printed in the Netherlands by Ridderprint bv

Aan mijn broer Michiel,
die begaan was met mensen

Table of Contents

Chapter 1

Introduction

This chapter highlights the problem of world energy supply, which calls for increased use of renewable resources such as biomass. An introduction into biomass gasification is presented and the objective and structure of this thesis are outlined.

1.1 The trilemma of energy, economy and environment

The world population has increased at an explosive rate from 1.65 billion to just over 6 billion in the 20th century, and continues to increase. In the same century, mankind has consumed over 875 billion barrels of oil and it is very likely that even more oil will be consumed in the present century. Annual energy use in developing countries has risen from 55 to 212 kg oil equivalent over the last thirty years, while developed countries use as much as 650 kg oil equivalent per person (BP Statistical Review of World Energy, 2003).

In his book 'Trilemma: Three major problems threatening world survival', Yoda (1995) foresees a three-fold challenge in the 21st century: how can we achieve economic growth, supply food and energy resources, while conserving the environment? To overcome the Trilemma, we cannot continue much longer to consume finite reserves of fossil fuels, the use of which contributes to global warming. Preferably, the world should move towards more sustainable energy sources such as wind energy, solar energy and biomass. However, the above-mentioned challenges may not be met solely by introduction of sustainable energy forms. We also need to use energy more efficiently. Developing and introducing more efficient energy conversion technologies is therefore important, for fossil fuels as well as renewable fuels.

This thesis addresses the question how biomass may be used more efficiently and economically than it is being used today. Wider use of biomass, a clean, renewable and CO_2 neutral feedstock may extend the lifetime of our fossil fuels resources and alleviate global warming problems. Another advantage of using of biomass as a source of energy is to make developed countries less interdependent on oil-exporting countries, and thereby reduce political tension. Furthermore, the economies of agricultural regions growing energy crops benefit as new jobs are created.

1.2 Primary energy sources: past, present and future

Biomass, in particular wood, has historically been an important energy source for fires, ovens and stoves. During the Industrial Revolution, coal displaced biomass because of its high energy content and because it is available in large quantities at low cost. At the beginning of the 20th century, oil (which was discovered in the U.S. in 1859) supplied only 4% of the world's energy. Decades later it became the most important energy source. Figure 1.1 shows the primary energy consumption in developed countries and developing countries. Especially developed countries are highly dependent on oil, which supplies about 96% of their transportation energy. With world energy demand projected to rise by about 40% from now to 2020, it is possible that natural gas, which supplies almost 25% of the world's energy demand today, overtakes oil as the most important energy source. This trend is also supported by environmental concerns such as global warming which have resulted in calls for increased use of natural gas. Looking beyond the era of natural gas, coal may become increasingly used, but this requires CO_2 sequestration.

Eventually, fossil fuel reserves will dwindle. Can the oldest fuel, biomass, make a comeback? Annually, photosynthesis stores 5-8 times more energy in biomass than man currently consumes from all sources. Biomass, currently the fourth largest energy source in the world, could therefore in principle become the main energy source. Several scenarios for the future (e.g. Shell, 2001) predict a strong increase in the use of biofuels between 2025 and 2050.

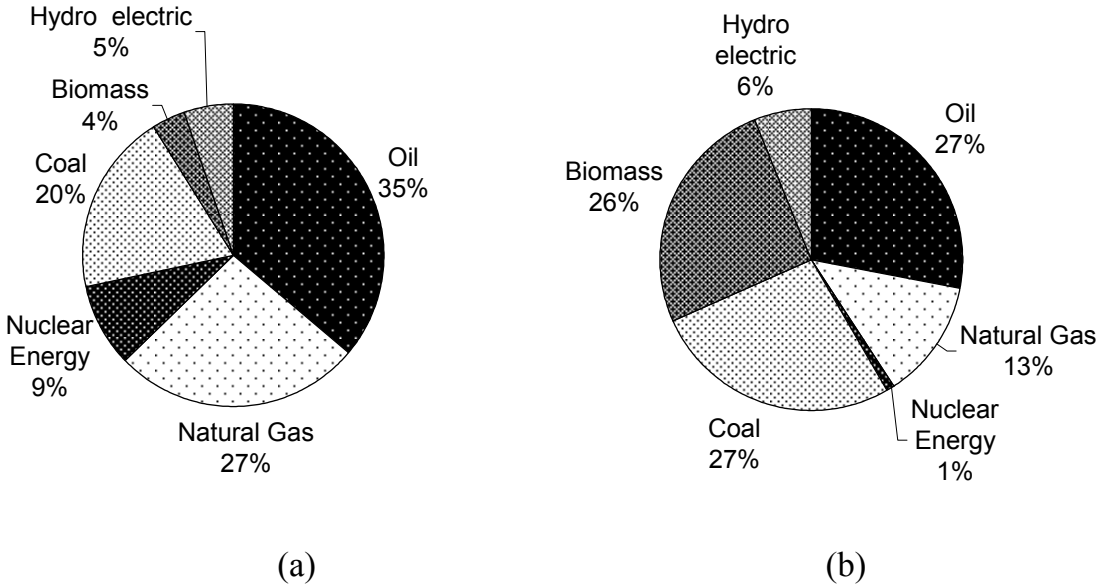

(a) (b)

Figure 1.1: Primary energy consumption in a) developed countries, b) developing countries (BP Statistical Review of World Energy, June 2003; biomass consumption from Hall and House, 1995)

1.3 Biomass gasification

Gasification involves the production of a gaseous fuel by partial oxidation of a solid fuel. The gasification of coal and biomass began in about 1800 and by about 1850 gas light for streets was commonplace. Before the construction of natural gas pipelines, there were many "gasworks" serving larger town and cities in Europe and the US. During the petroleum shortages of World War II, almost a million gasifiers were used to run cars, trucks, and buses using primarily wood as a fuel. These gasifiers were mothballed after the return to peace and the availability of inexpensive petroleum fuels. However, the oil crisis in the 1970's and 1980's has inspired continued research and development of coal gasifiers. Since the 1990's, concerns about global warming shifted the focus to biomass as a gasifier fuel.

Due to its higher efficiency, it is desirable that gasification becomes increasingly applied in future rather than direct combustion. Gaseous fuels can be easily distributed for domestic and industrial use, used in electricity producing devices such as engines, gas turbines and fuel cells, or for chemical synthesis of liquid fuels and chemicals.

Several types of gasifiers have been developed; an overview is shown in Fig. 1.2. These gasifiers have different hydrodynamics (especially the way in which the solid fuel and the gasification agent are contacted), gasification agents (air, oxygen and/or steam) and operating conditions such as temperature and pressure. The most important types are fixed-bed gasifiers, operated in counter-current, co-current or cross-current mode, fluidized bed gasifiers and entrained flow gasifiers.

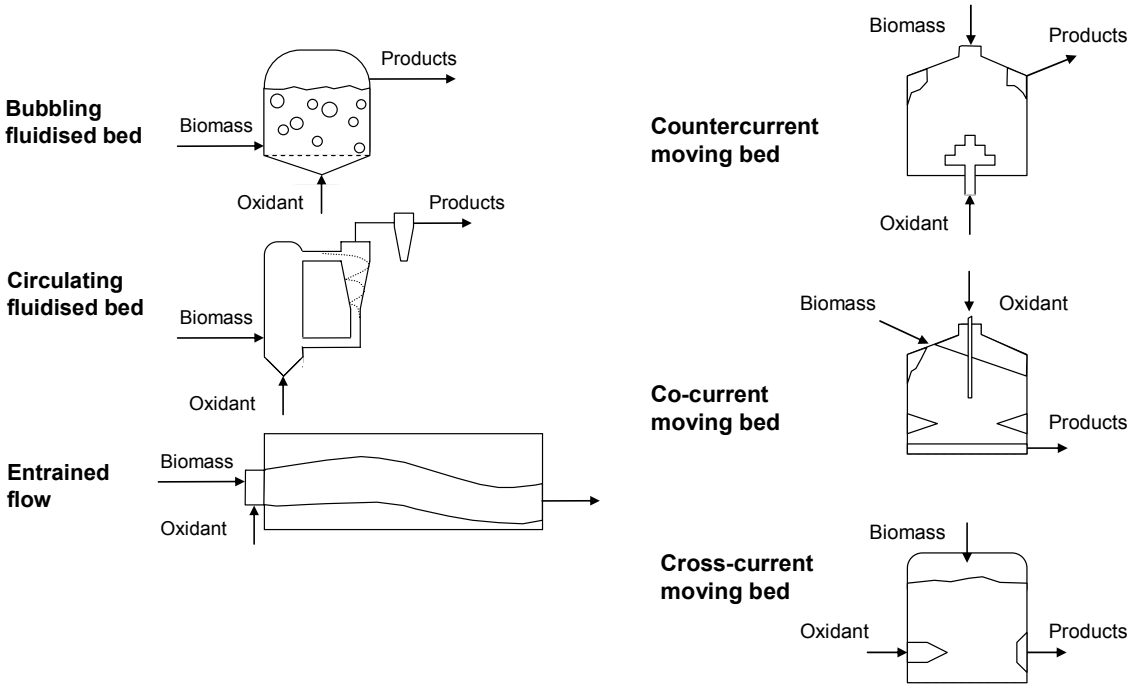

Figure 1.2: Overview of gasifier types (Stassen et al., 2002); courtesy Biomass Technology Group, Netherlands

Despite the long experience with biomass gasifiers, reliable and large-scale operation continues to be suffering from several problems. As it is difficult to scale-up fixed-bed gasifiers to a large capacity, most large scale biomass gasifiers are based on bubbling fluidized bed or circulating fluidized bed technology. Sand is used as a heat carrier and the operating temperature is limited to 900-950°C to prevent ash sintering problems. At these relatively low gasification temperatures, tarry components are formed. Upon cooling of product gas, condensation of these tars can lead to choking of equipment and piping. Although many technologies have been developed to tackle the tar problem, such as physical separation, thermal and catalytic cracking, these methods add to the complexity and the cost.

Gas clean-up problems would be largely avoided if biomass were gasified in entrained flow or flame gasifiers at elevated temperatures up to 1700°C. However, this requires the use of pure oxygen and the removal and handling of molten ashes. Although this technology has been demonstrated in the coal gasifier in Buggenum (the Netherlands), the properties of biomass pose specific problems. Firstly, the low calorific value and the hygroscopic nature of biomass (which leads to a high moisture content, even after drying) have a negative effect on the efficiency of gasification. Secondly, the fibrous structure of wood makes it difficult to grind the material to the desired size. For co-feeding of biomass with coal in thermal processing plants, a separate feed route is needed because the biomass cannot be grinded small enough.

1.4 Research objective

The objective of this study is to find out how the energy (or more precisely: exergy, i.e. the work content) of a biofuel can be preserved as much as possible in the product gas of a gasifier. This is relevant because efficient conversion processes are required for renewable resources in order to compete with fossil fuels.

The topic is studied from a fundamental point of view with the help of thermodynamics. This comprises the first law, which states that energy can never be lost, and the second law, which states that the quality of energy will always degrade in irreversible processes. Biomass is thus regarded as a certain amount of work potential (that was previously fixed by photosynthesis), which decreases with every conversion step. The clue is to develop optimised processes, in which the work potential is largely retained, so that a high proportion of useful work is delivered.

1.5 Outline of the thesis

The thesis continues in Chapter 2 with results from multi-disciplinary research about the use of biomass as a sustainable energy source. The current research project has formed part of a larger research programme entitled ‘Biomass as a sustainable energy source: environmental load, cost-effectiveness and public

acceptance', in which researchers from engineering sciences and social sciences have cooperated. The programme was conducted within the scope of the Incentives Programme for Energy Research, founded by NWO (Netherlands Organisation for Scientific Research) and Novem (Netherlands Agency for Energy and Environment).

Multi-disciplinary discussions about the question which biofuels are most attractive for a gasifier have raised a more general question, i.e. what is the effect of the composition of the fuel on the efficiency that can be attained in a gasifier? Subsequently, the rest of the thesis is dedicated to this topic.

The main research results are presented in two parts: Chapters 3-6 and Chapters 7-9. All these chapters have been (or will be) published in peer-reviewed journals.

The first part of the thesis comprises energy and exergy analyses of gasification and combustion processes. It addresses several research questions that are relevant in the light of the objective, notably:

- How should the efficiency of a gasifier be evaluated? *(Chapter 3)*
- Why is gasification more efficient than combustion? *(Chapter 4)*
- Can the efficiency be optimized by tuning the process conditions? *(Chapter 4)*
- How do biofuels compare with fossil fuels such as coal? *(Chapter 5)*
- Can biomass gasification be effectively integrated into complex process schemes, such as production of Fischer-Tropsch fuels from biomass? *(Chapter 6)*

An important conclusion reached in the first part of the thesis is that it may be attractive to improve the fuel properties of biomass (particularly wood and straw) prior to gasification. The second part of the thesis focuses consequently on a pre-treatment technology for gasifiers, namely on torrefaction, a technology whereby wood is roasted at temperatures in the range of 250-300°C. Torrefaction increases the relatively low energy density of biomass, lowers its moisture content, and reduces the electricity required for size reduction of fibrous biomass. Research questions that are addressed are:

- How fast are the kinetics of the torrefaction process, depending on process conditions? *(Chapter 7)*
- What products are formed, and in which quantities? *(Chapter 8)*
- How can torrefaction be combined with gasification, and why would this be advantageous? *(Chapter 9)*

Finally, Chapter 10 presents conclusions, recommendations and an outlook for biomass-based energy.

References

BP Statistical Review of World Energy (2003). See also: http://www.bp.com/

Hall DO, House JI (1995). Biomass: a modern and environmentally acceptable fuel. Solar Energy Materials and Solar Cells 38:521-542.

Shell (2001). Energy needs, choices and possibilities. Scenarios to 2050. See also: http://www.shell.com/

Stassen HEM, Prins W, Swaaij WPM van (2002). Thermal conversion of biomass into secondary products: the case of gasification and pyrolysis. In: Palz W, Spitzer J, Maniatis K, Kwant K, Helm P, Grassi A, editors. Twelfth European Biomass Conference, Amsterdam, Netherlands. p.38-44.

Yoda S, editor (1995). Trilemma: three major problems threating world survival. Tokyo: Central Research Institute of Electric Power Industry.

Chapter 2

Biomass as a sustainable energy source

Various types of biomass are compared with regard to availability, technical suitability as a gasifier fuel and societal acceptance. Wood and straw are desirable because they are abundant and clean (low moisture and ash content), but the public seems to prefer energy from waste streams such as manure and green waste. Improved communication strategies are recommended to inform the public that energy from wood is renewable and CO_2-neutral.

2.1 Introduction

In a joint research programme, researchers from the Departments of Chemical Engineering and Technology Management at Eindhoven University of Technology have cooperated with the aim of contributing to a successful implementation strategy for the introduction of energy from biomass. Such an introduction may be hampered by technical barriers (e.g. reliable gasifier operation, presence of tars) as well as non-technical barriers (e.g. availability and cost of biofuels, public acceptance). Hence, a multi-disciplinary approach is advisable.

Biomass is a very general term which comprises all organic matter that originates from photosynthesis. It is not a well-defined and often inhomogeneous feedstock, whose composition may vary depending on origin, physical location, age, season and other factors. Biomass types include many types of wood, plants, vegetable oils, green waste, and materials such as manure and sewage sludge. These biofuels differ in many aspects, such as their availability, cost, suitability as a gasifier fuel, and also in their acceptance by the public. In this chapter, these aspects are treated for various biofuels from the viewpoints of engineering and social sciences (the latter is referred to as: Hübner and Meijnders, 2004).

2.2 Availability of biomass

In its Third Energy Green Paper (Dutch Ministry of Economic Affairs, 1995), the Dutch government has set the ambitious target that 10% of energy supply in the Netherlands should come from renewable resources by the year 2020. This translates into a total of 288 PJ per annum, of which over a third is projected to come from biomass (75 PJ) and waste (45 PJ). Since 1999, several energy resources previously perceived as renewable are no longer considered as such, notably the

plastic fraction contained in waste and electricity production from industrial heat pumps. Therefore, the target for biomass should be increased to at least 100 PJ. This number is the amount of fossil fuel energy avoided; it is equivalent with a required amount of biomass of at least 130 PJ_{th} (thermal input), as electricity generation from biomass is less efficient than from fossil fuels at the present state of technology.

Table 2.1: Availability of biomass in the Netherlands (from Arts et al., 1999)

NTA code	Main group	Total availability (PJth)	Short term availability (PJth)
100	Wood	62	24
200	Grass and straw	18	12
300	Manure	96	6
400	Sludge	19	6
500	Waste from food industry	101	9
600	Green waste	10	0
700	Other	7	6
	Total	313	63

Several studies have been carried out to find out how much biomass is potentially available in the short and long term in the Netherlands. Arts et al. (1999) studied the total amount of biomass available, as well as the fraction that is not utilised and therefore available on a short term. Results are shown in Table 2.1. The total biomass potential is estimated at 313 PJ_{th}, with organic waste streams from the food industry and manure as the largest biomass streams. However, the majority of these streams is sold as feed for cattle, as fertilizer in agriculture, or as a raw material for industry. The short term availability of biomass for energy purposes is only 63 PJ_{th}; wood, grasses and straw are the types of biomass with the highest short term availability. Another study by Weterings et al. (1999) estimates a higher number of 76 PJ_{th}. Nevertheless, it is clear that several actions must be taken to meet the targets formulated for biomass based energy: growing energy crops in the Netherlands, import of biomass from EU countries or the rest of the world, and/or implementation of government policies to promote energy from biomass streams currently used for other purposes.

2.3 Technical suitability of biomass for gasification

Biomass gasifiers are considered omnivorous and flexible towards the feedstock that is to be processed. A wide range of biomass sources, such as traditional

agricultural crops, dedicated energy crops, residues from agriculture and foresting as well as organic wastes can be gasified. This is generally regarded as a real advantage, because it means that the most available and usually economically most attractive feedstock can be selected. However, the question is whether all the biomass types can be converted with comparable efficiencies. These biomass types differ in chemical composition, heating value, ash and moisture content. The Phyllis database, maintained by the Energy research Centre of the Netherlands (2004), provides information about these properties. Comparison of the various types of biomass listed in Phyllis shows that the higher heating value of biomass does not vary much (standard deviations of 4-7%) and lies generally in the range of 19-21 MJ/kg. Contrarily, variations in moisture content and ash content are especially large (standard deviations of 50-120%). Figure 2.1 shows the average moisture and ash content for various biomass types; this gives insight into the differences between these types, but it must be kept in mind that the values for individual biomass streams may vary largely.

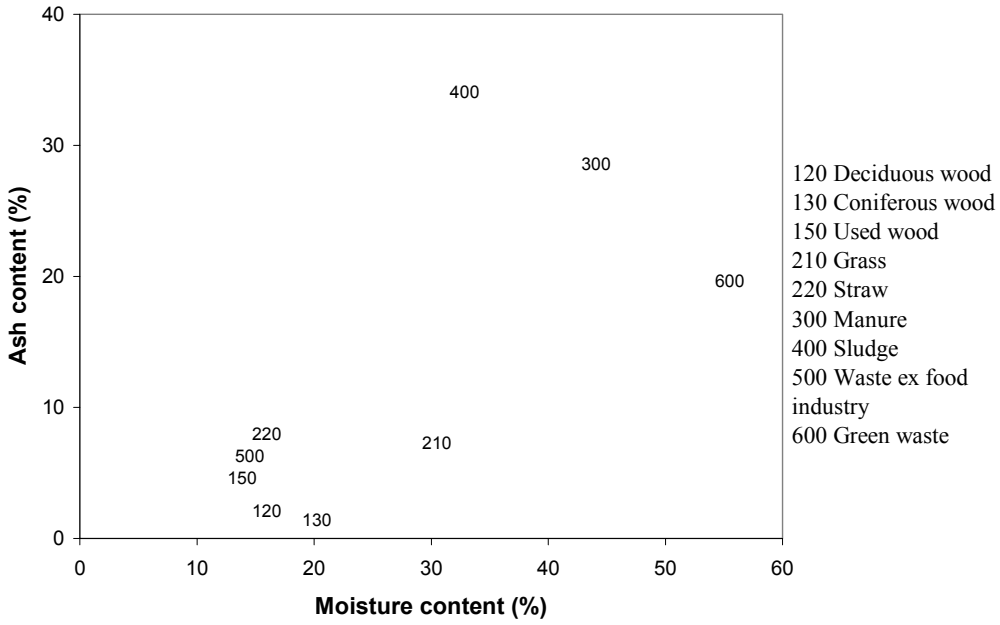

Figure 2.1: Average moisture and ash content of different biomass streams (data from Phyllis database, Energy research Centre of the Netherlands, 2004)

From Fig. 2.1, two sorts of biomass streams may be distinguished: ‘dry’ streams including wood, straw, and waste from the food industry (e.g. nut shells and husks from rice, corn, etc.) and ‘wet’ streams comprising manure, sludge and green waste, with grass somewhere in between. The dry streams are regarded as more suitable for thermal processing technologies, i.e. combustion, gasification and pyrolysis. Evaporation of moisture in a thermal processing apparatus reduces the energy efficiency, although this problem is less severe if waste heat is available for pre-drying. Furthermore, the processing and disposal of large amounts of ash poses

problems. Therefore, other technologies are more suitable for the wet streams, such as anaerobic digestion and hydrothermal upgrading (HTU®; Goudriaan et al., 2001). Since transport of wet biomass is costly, these technologies must be applied on a smaller scale.

2.4 Public acceptance of energy from biomass

Hübner and Meijnders (2004) have studied the attitudes of green electricity consumers towards different feeding materials. Their method started with a so-called sorting task, where 38 laypeople were asked to group 28 biomass materials into categories. It was concluded that the categories made by laypeople overlapped largely with those in the Phyllis database, which was set up by experts. These categories were: energy crops, farmed wood, used wood, green waste, animal powder (including cadavers), and manure. From statistical analysis using multidimensional scaling, two dimensions were found to relevant: floristic order (wood – crops) and life cycle (new – waste).

A survey was subsequently done among 330 green electricity consumers throughout the Netherlands, in which their attitudes towards the six biomass input categories were measured. The respondents were asked whether they had a preference for one of these materials as a source of electricity. They could mention their two most preferred materials as well as two most rejected materials. Some just mentioned one material, others two. In total 89% answered to have a preference, 75% said they would reject certain materials. For the part of the population that indicated to have a preference or rejection, the results are shown in Fig. 2.2. It can be observed that the respondents have a preference for using waste materials, such as green waste, manure and used wood, as energy sources. The concept of growing crops or wood for energy purposes was not favoured by the respondents.

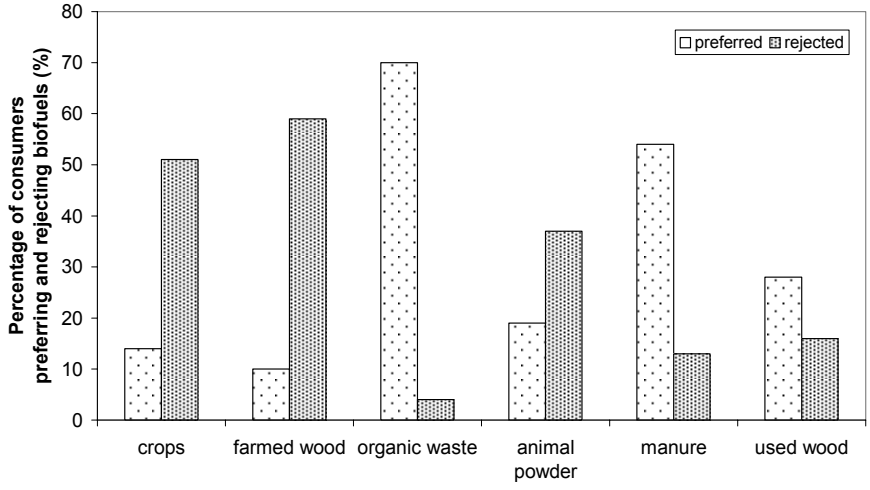

Figure 2.2: Biomass feeding materials preferred and rejected by electricity consumers (Hübner and Meijnders, 2004)

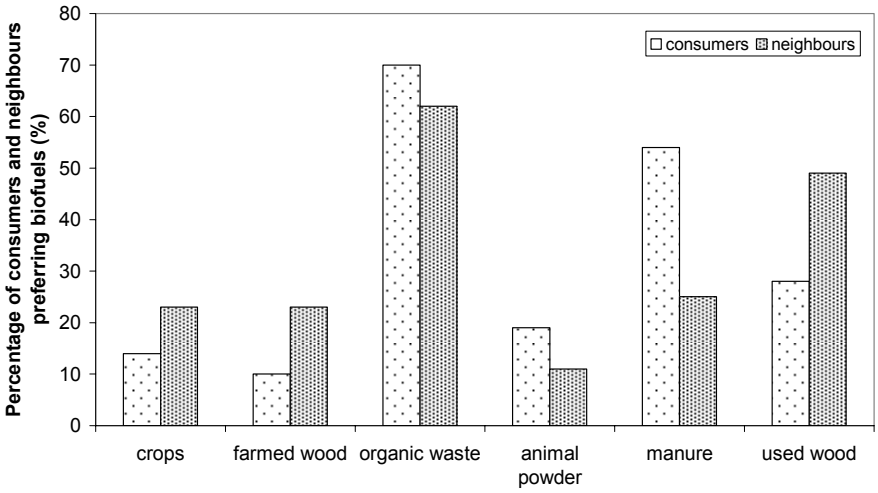

Figure 2.3: Biomass feeding materials preferred by electricity consumers and neighbours of biomass-based power stations (Hübner and Meijnders, 2004)

The respondents were also asked about their general attitude towards renewable energy in comparison with fossil fuel energy. On a scale from -3 (highly undesirable) to +3 (highly desirable), they rated renewable energy as desirable (biomass) to highly desirable (wind and solar energy). Natural gas was rated as slightly desirable, coal as slightly undesirable and nuclear energy as undesirable.

A second survey was carried out among 374 neighbours, i.e. residents living nearby biomass-based power stations. These power stations were located in 6 different locations and comprised combustion, stand-alone gasification, co-gasification with coal and anaerobic digestion installations. Amongst other questions, the neighbours were asked whether they had a preference for certain types of biomass for the production of electricity. The results are shown in Fig. 2.3. The preferences of neighbours deviate from those of electricity consumers: although both groups prefer the use of waste streams, the neighbours have a stronger preference for clean waste streams (e.g. used wood) above dirty waste streams (e.g. manure).

2.5 Conclusions and discussion

Most gasifiers, in laboratories, demonstration scale or in commercial operation, use wood or straw as biomass input material. This is logical considering the abundant availability of these materials, and the low ash and moisture content which makes them suitable for thermal processing. However, it must be realized that electricity consumers are not yet convinced that energy from wood is truly renewable. More research is needed to find out why they do not perceive biomass to be as ‘green’ as wind and solar energy. Perhaps this is related to the possibility of emissions from biomass based energy and uncertainty whether biomass is grown in an environmentally friendly way.

A strategy that could be followed is cascaded use of wood, whereby it is applied as a construction material until the end of its life cycle, when waste wood is used as an energy source. However, the amount of waste wood may be insufficient, so that growing wood for energy purposes may be unavoidable. This calls for good communication strategies, e.g. by informing the public that wood stems from a forest which is managed with good stewardship (an example is certification by the Forest Stewardship Council) and that wood is processed in a clean and efficient way.

References

Arts PAM, Beek A van, Benner JHB (1999). BIO-MASSTERCLASS: A survey of streams and an initiative for price indexation, Novem-EWAB report 9916. Rotterdam, Netherlands: Bureau for Communication and Advice on Energy and Environment (in Dutch).

Dutch Ministry of Economic Affairs (1995). Third Energy Green Paper (Derde Energienota). Den Haag, Netherlands.

Energy research Centre of the Netherlands (2004). Phyllis database. See also: http://www.ecn.nl/phyllis

Goudriaan F, Beld B van de, Boerefijn FR, Bos GM, Naber JE, Wal S van der, Zeevalkink JA (2001). Thermal efficiency of the HTU® process for biomass liquefaction. In: Bridgwater AV, editor. Progress in Thermochemical Biomass Conversion. Oxford: Blackwell Science Ltd. p. 1312-1325.

Hübner G, Meijnders AL (2004). Public acceptance of energy from biomass. In: 18th IAPS conference, Vienna, Austria.

Weterings RAPM, Bergsma GC, Koppejan J, Meeusen-van Onna MJG (1999). Availability of waste and biomass for electricity generation in the Netherlands, Novem-GAVE report 9911. Apeldoorn, Netherlands: TNO-MEP.

Chapter 3

Thermodynamics of gas-char reactions: first and second law analysis[‡]

In energy transformation processes such as combustion, gasification and reforming of fossil and renewable fuels, the conservation of energy (first law of thermodynamics) as well as the quality of energy (second law of thermodynamics) is important. This study focuses on the conversion of biomass with air and/or steam into gaseous components and char, represented by solid carbon (graphite). Energy and exergy (available energy) losses are analysed by calculating the composition of a dry, ash-free typical biomass feed represented by $CH_{1.4}O_{0.59}N_{0.0017}$ in equilibrium with varying amounts of air and/or steam. The analysis is carried out for adiabatic systems at atmospheric pressure, with input of biomass and air at ambient conditions and steam at atmospheric pressure and temperature of 500K.

For air gasification, energy and exergy in the product gas have a sharp maximum at the point where all carbon is consumed, the carbon boundary point. This is the optimum point for operating an air-blown biomass gasifier. For gasification with steam, operation at the carbon boundary point is also optimal, but thermodynamic process losses hardly increase when adding more steam when required. The efficiency of steam and air-blown gasification was compared using the definition of rational efficiency. Although gasification by steam is more efficient (87.2% vs. 80.5%), this difference is expected to level off if exergy losses for the production of steam are taken into account. The choice between steam and air as a gasifying medium therefore seems to depend more on the required gas compositions. For steam gasification, the product gas contains mainly methane and carbon dioxide, while hydrogen, carbon monoxide, and (at least 38%) nitrogen are the main product gases for air gasification.

3.1 Introduction

In processes, such as combustion, gasification, hydrogenation and steam reforming, fossil and renewable fuels are converted into a different fuel and/or heat and/or electricity. For example, gasification of a fuel involves converting the chemical energy contained in the fuel into chemical energy contained in the gaseous products and sensible energy of the produced gas. According to the first law of thermodynamics, energy can never be lost. Therefore it is justified to state that

[‡] Published in Chem.Eng.Science 58 (13-16):1003-1011, 2003.

energy conversion processes do not have energy losses, except for losses from the process system into the environment. However, the second law of thermodynamics should also be considered. Energy conversion processes are accompanied by an irreversible increase in entropy, which leads to a decrease in exergy (available energy). Thus, even though the energy is conserved, the quality of energy decreases because energy is converted into a different form of energy, from which less work can be obtained.

For a fuel containing carbon, hydrogen and oxygen, at fixed pressure, the temperature of the CHO system is determined by the equivalence ratio (ER, the amount of air added relative to the amount of air required for stoechiometric combustion). Depending on ER, a thermochemical fuel conversion process may be classified as pyrolysis (ER=0), gasification (ER=0.25-0.50) or combustion (ER $\geq$ 1). For a dry- and ash-free biomass fuel of typical composition, Desrosiers (1979) has calculated the gas phase compositions, temperatures and energy distribution curves at varying equivalence ratios. However, no reference was made to the second law of thermodynamics and no results were presented for the exergy. Therefore it is the objective of this chapter to show to which extent exergy is lost in thermochemical biomass conversion processes.

Desrosiers also considered the conversion of biomass by addition of steam. Depending on the amount of steam added and the steam conditions, this process is known as steam pyrolysis (a solid residue is formed) or steam gasification (no solid residue is formed). Therefore, another objective of this paper is to determine how air gasification of biomass can be compared to steam gasification of biomass. The criterion for this comparison is again based on exergy; i.e. to which extent is the work potential of the biomass fuel conserved in the products. In this chapter, the following issues will be described: the conversion of biomass by air and steam, the comparison of efficiencies for both processes and finally comparison of the gas phase compositions.

3.2 Approach

The energy conversion processes studied can be shown in a triangular C-H-O-diagram as shown in Figure 3.1. The composition at any point in the diagram can be computed at a given temperature and pressure by calculation of the gas phase compositions in equilibrium with solid carbon (graphite). Methods to calculate the complex equilibria are described in appendix A: they are based on either minimizing the Gibbs free energy of the system or solving the applicable reaction equilibria in conjunction with the material balance.

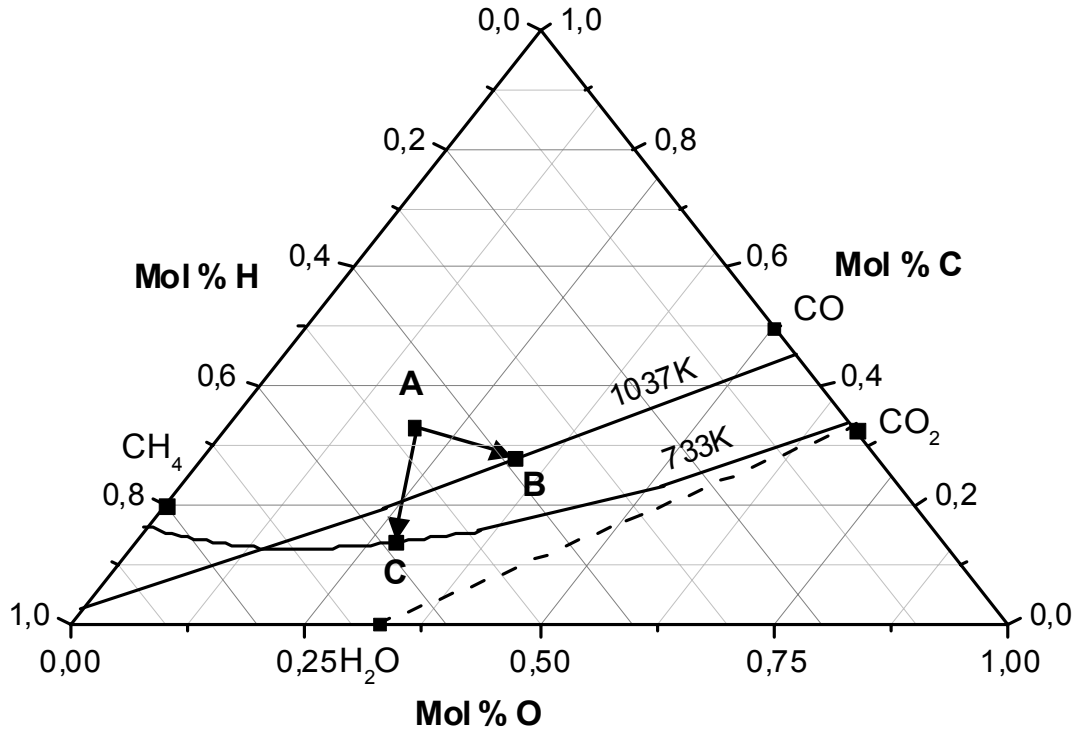

Figure 3.1: Molar triangular diagram indicating A: biomass feed, B: biomass in equilibrium with air at carbon boundary, C: biomass in equilibrium with steam of 500K at carbon boundary

In the triangular diagram, several lines are shown, the so-called carbon deposition boundaries. Above the solid carbon boundary, solid carbon exists in heterogeneous equilibrium with gaseous components, while below the carbon boundary no solid carbon is present. Most hydrocarbon fuels are located above the carbon boundary, which means that if these fuels are brought to chemical equilibrium, solid carbon is formed. This implies that in order to avoid solid carbon formation and achieve complete gasification, oxygen and/or hydrogen must be added. Oxygen and hydrogen sources are H_2, H_2O, O_2, air or CO_2.

The following reactions are relevant for carbon conversion into gaseous components:

$$C + 2\,H_2 = CH_4 \qquad (3.1)$$

$$C + H_2O = CO + H_2 \qquad (3.2)$$

$$C + CO_2 = 2\,CO \qquad (3.3)$$

In steam and air gasification, all these reactions occur so that the endothermic water-gas and Boudouard reactions are coupled to the exothermic methane formation reaction. Coupling of endothermic and exothermic reactions is very attractive in order to achieve a high thermodynamic efficiency. For hydrogasification, the temperature should be kept low so that the first reaction is

predominant. On the contrary, for endothermic carbon dioxide gasification, a high temperature is required and the third reaction is predominant. Endo- en exothermic reactions are not coupled for hydrogasification and carbon dioxide gasification. Therefore, this paper focuses entirely on conversion of biomass by addition of air, steam and mixtures thereof.

The biomass fuel considered in this work is represented by a general formula of $CH_{1.4}O_{0.59}N_{0.0017}$ (as in Desrosiers, 1979) and indicated by point A in the triangular diagram. When oxygen is added, the composition moves into the direction of point B; at this point, all carbon is present in the gaseous phase as carbon monoxide, carbon dioxide or methane. If more oxygen is added, the line between CO_2 and H_2O is crossed, meaning that the fuel has been completely combusted (and free oxygen becomes present). An equivalence ratio of 1, corresponding to complete oxidation, requires 1.475 g of oxygen, or 6.331 g of air per g of biomass. Eq. 3.4 describes this (neglecting the small amount of nitrogen contained in biomass.):

$$CH_{1.4}O_{0.59} + 1.055\,O_2 + 3.996\,N_2 \longrightarrow CO_2 + 0.7H_2O + 3.996\,N_2 \qquad (3.4)$$

If steam is added to the biomass fuel, the composition moves to point C so that the carbon boundary is also crossed. This happens at a lower temperature, because the reactions between biomass and steam are endothermic and those between biomass and air are exothermic.

In this chapter, the distribution of energy and exergy along the lines A-B and A-C, and lines from A to points lying between B and C are analysed. This analysis is restricted to adiabatic systems at atmospheric pressure. This means that biomass (at a temperature of 25°C) and air (at a temperature of 25°C) and/or steam (at a temperature of 500K) are brought to equilibrium, with the products, gases and char, leaving the system at system temperature T.

3.3 Energy and exergy calculations

The energy distribution of the biomass conversion process can be obtained from the energy balance:

$$\sum_{IN} H_j = \sum_{OUT} H_k \qquad (3.5)$$

where $\sum_{IN} H_j$ and $\sum_{OUT} H_k$ are enthalpy flow of all entering and leaving material streams, respectively.

The exergy balance of the biomass conversion process can be represented in the following form using exergy values of all streams entering and leaving the process:

$$\sum_{IN} \mathrm{E}_j = \sum_{OUT} \mathrm{E}_k + I \qquad (3.6)$$

where $\sum_{in} E_j$ and $\sum_{OUT} E_k$ are exergy flow of all entering and leaving material streams, respectively. The difference between exergy and energy balance is that exergy is not conserved but subjected to dissipation. It means that the exergy leaving any process step will always be less than the exergy in. The difference between all entering exergy streams and that of leaving streams is called irreversibility ***I***. Irreversibility represents the internal exergy loss in process as the loss of quality of materials and energy due to dissipation. The losses of exergy (available work) are due to entropy production generated during fluid flow, heat and mass transfer and chemical reactions.

The exergy of a stream of matter E depends on its composition (chemical exergy E_o) and its temperature and pressure (physical exergy E_{ph}):

$$E = E_0 + E_{ph} \tag{3.7}$$

The standard chemical exergy of a pure chemical compound ε_o is equal to the maximum amount of work obtainable when a compound is brought from the environmental state, characterized by the environmental temperature T_o and environmental pressure P_o, to the dead state, characterized by the same environmental conditions of temperature and pressure, but also by the concentration of reference substances in standard environment. For instance, the standard reference substance for carbon is CO_2 at the concentration of about 300 ppm, as it represents the lowest thermodynamic value of all carbon containing compounds. The values of standard chemical exergy of pure compounds can be calculated from the thermodynamic date and are tabulated. The chemical exergy of the mixture $\varepsilon_{o,M}$ is determined by the composition and concentration of components in the mixture:

$$\varepsilon_{0M} = \sum_i x_i \varepsilon_{oi} + RT_0 \sum_i x_i \ln x_i \tag{3.8}$$

It should be noticed that the chemical exergy of the mixture is always lower than the sum of exergy of individual components, as the second term in the above equation represent so-called exergy of mixing and is always negative.

The physical exergy of a pure compound of a mixture can be easily calculated using enthalpy and entropy data for the given system:

$$\varepsilon_{ph} = (h - h_o) - T_0(s - s_0) \tag{3.9}$$

where h and s are enthalpy and entropy of a system at given temperature and pressure, and h_o and s_o are the values of these functions at the environmental temperature and pressure.

For the gaseous components considered in the equilibrium calculations, enthalpy and entropy data were obtained from the Aspen Plus database. For the biomass fuel,

thermodynamic properties are not available. Therefore, the statistical correlation of Szargut and Styrylska (1964) was used:

$$\varepsilon_{0,\,biomass} = \beta \cdot LHV_{biomass} \qquad (3.10)$$

where $LHV_{biomass}$ is the lower heating value, i.e. net enthalpy of combustion of the biomass.

$$\beta = \frac{1{,}0412 + 0{,}2160 \cdot \frac{z_{H_2}}{z_C} - 0{,}2499 \cdot \frac{z_{O_2}}{z_C} \cdot \left[1 + 0{,}7884 \cdot \frac{z_{H_2}}{z_C}\right] + 0{,}0450 \cdot \frac{z_{N_2}}{z_C}}{1 - 0{,}3035 \cdot \frac{z_{O_2}}{z_C}} \qquad for: \ \frac{z_{O_2}}{z_C} \le 2.67 \qquad (3.11)$$

where z_{O2}, z_C, z_{H2} and z_{N2} are the weight fractions of oxygen, carbon, hydrogen and nitrogen, respectively in the biomass. The biomass considered has a higher heating value of 22.21 kJ/g and lower heating value of 20.9 kJ/g. The chemical exergy was calculated using the above-mentioned method at 23.34 kJ/g.

3.4 Results

3.4.1 Conversion of biomass by air

For the conversion of biomass by air, Figure 3.2a shows the energy contained in the products in kJ/g wood versus the equivalence ratio. These results are equivalent to those of Desrosiers. The gross heat of combustion contained in the gas initially rises when air is added due to conversion of solid carbon. At the solid carbon boundary, addition of more air leads to a decrease in the combustion energy and an increase in sensible energy of the gas. The total energy is constant and equals the energy in the feed. Figure 3.2b, showing the exergy contained in the gaseous products versus the equivalence ratio, also exhibits a maximum for the gas at the point where all carbon is consumed. This maximum is lower because some gaseous products formed such as carbon monoxide and hydrogen has a lower chemical exergy than heating value of combustion. Beyond this maximum the total exergy decreases, because the decrease in chemical exergy is not fully compensated by the increase in physical exergy.

3.4.2 Conversion of biomass by steam

Figure 3.3a shows the energy contained in the products for conversion of biomass with steam of 500 K and atmospheric pressure (the study of Desrosiers was based on steam of 1000 K, but this has only a small influence on the system temperature and compositions). Notice that the total energy is not constant because the energy of steam is added to the wood. An almost linear increase in heating value of the gas and almost linear decrease in heating value of the char can be observed upon addition of steam. Beyond the carbon boundary point, no more carbon is gasified, but the heating value of the gas does not decrease when more steam is added (unlike

gasification with air). The exergy contained in the process inputs and outputs is shown in Fig. 3.3b. The exergy in the feed increases because steam is added. It is interesting that the difference between exergy in the feed and in the total products (internal exergy loss or irreversibility) occurs already when no steam is added, and hardly increases upon addition of steam.

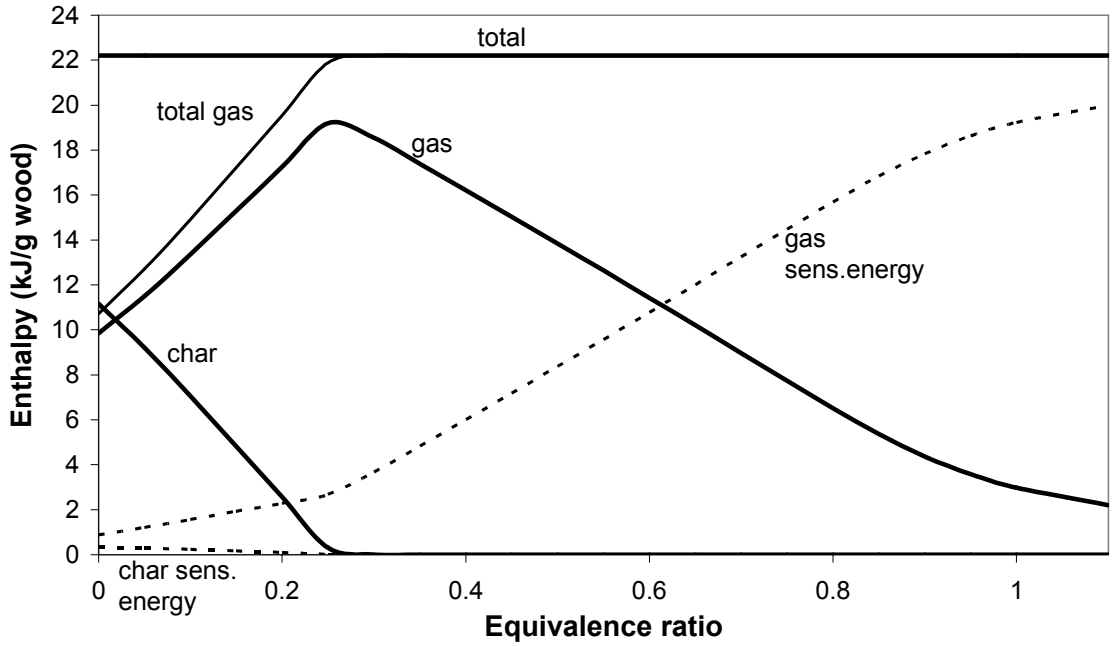

(a)

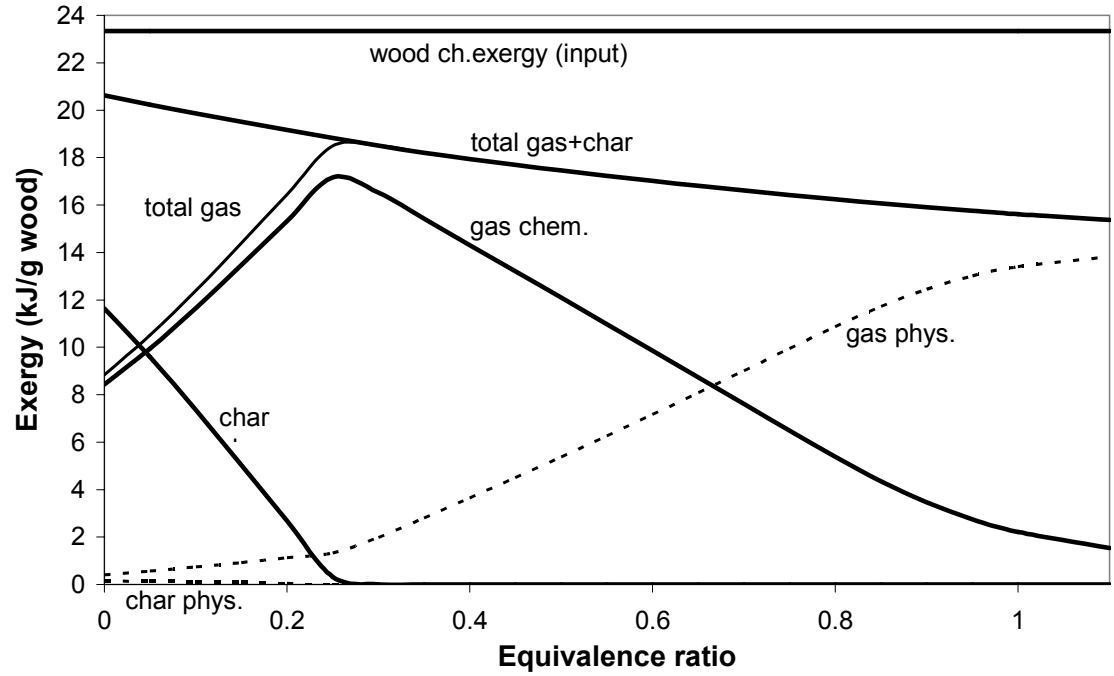

(b)

Figure 3.2: Distribution of energy and exergy to the product gas and char for biomass conversion by air: (a) energy (b) exergy

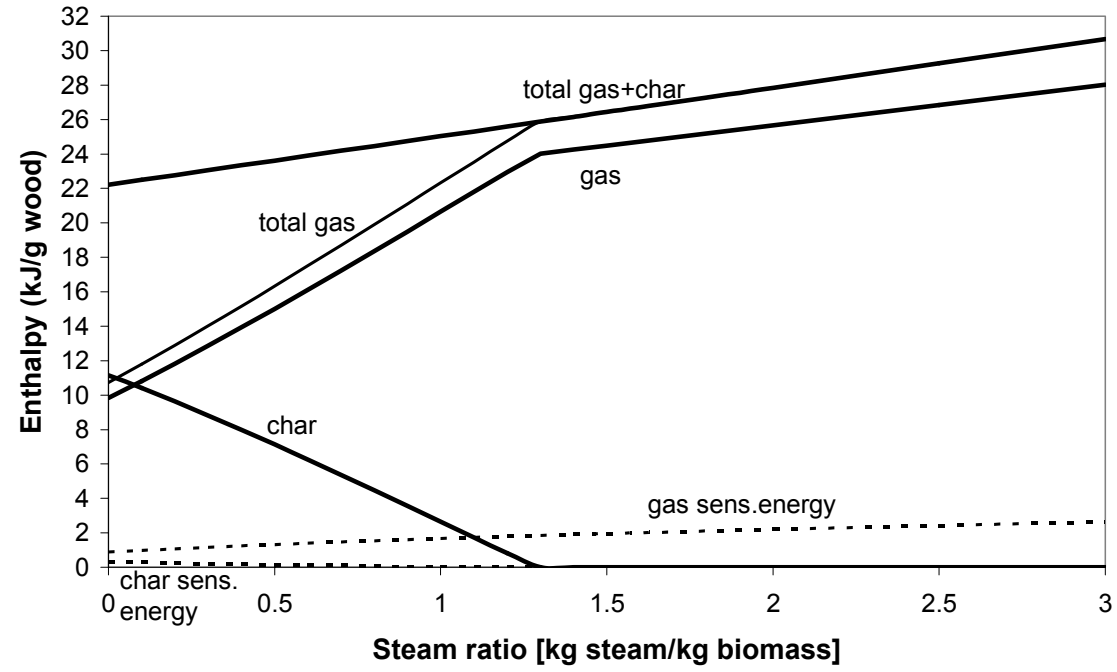

(a)

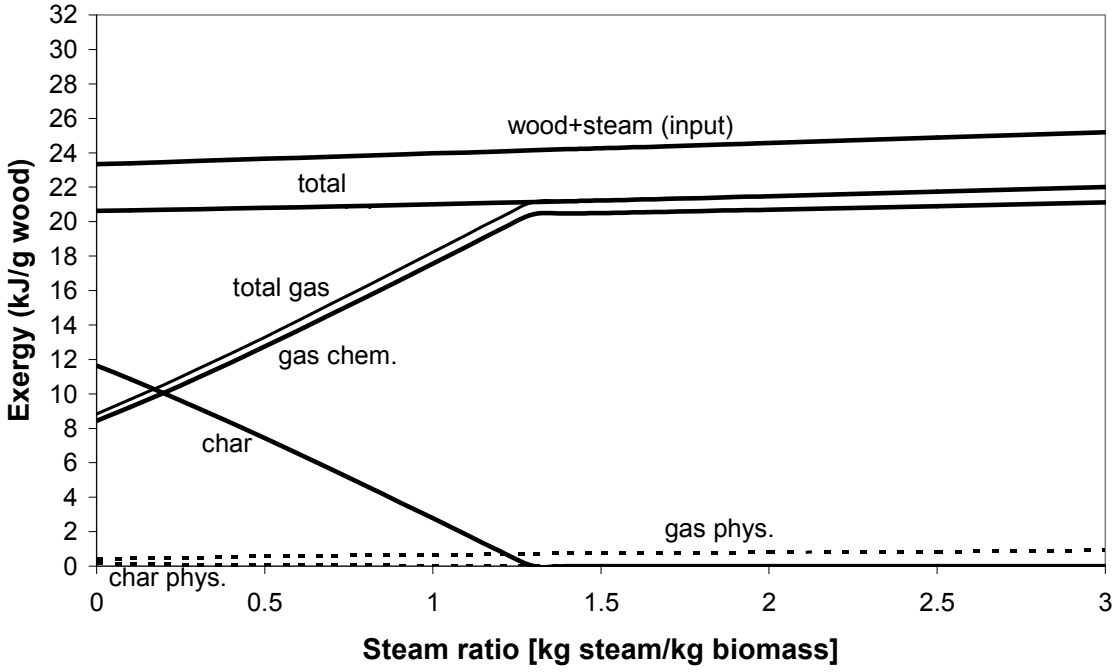

(b)

Figure 3.3: Distribution of energy and exergy to the product gas and char for biomass conversion with steam: (a) energy (b) exergy

3.4.3 Comparison of efficiencies for biomass gasification using air or steam

The efficiency of conversion of biomass to gaseous products can be defined in numerous ways. Efficiencies could be energy-based, e.g. the heating value of the gaseous products divided by the heating value of the biomass feed. This has a number of drawbacks. First, it is unclear whether the higher or lower value, i.e. gross or net heat of combustion, should be used. Secondly, only the so-called cold-gas efficiency can be calculated by neglecting the energy in the unconverted char as well as the sensible heat of the produced gas (if this were not done, a 'hot-gas efficiency' of 100% would be obtained because the system is adiabatic). Most important, the increase in entropy due to conversion of a solid fuel into gaseous compounds is disregarded. Basing the efficiencies on exergy avoids these drawbacks. However, there are various possibilities to define the exergetic efficiency of a process, which requires careful consideration.

Most chemical engineers define efficiency as the ratio of desired output over input. If only gas is regarded as a desired product, the efficiency could be defined as the sum of exergy of desired products divided by the total process inputs:

$$\Psi_1 = \frac{E_{gas}}{E_{biomass} + E_{steam} + E_{air}} \qquad (3.12)$$

The exergy of air is zero because it is a reference component at reference conditions (1 atm, 25°C).

The unconverted carbon could also be seen as a useful product because this could be recovered as a product and/or re-introduced in a gasifier. In that case, the efficiency is calculated by dividing the exergy contained in the product gas and char by the exergy contained in the process inputs:

$$\Psi_2 = \frac{E_{gas} + E_{char}}{E_{biomass} + E_{steam} + E_{air}} \qquad (3.13)$$

Grassmann (1950) has defined efficiency as the ratio of exergy gains to losses. This definition is also known as the rational or intrinsic efficiency. In this process, energy is transferred from a solid fuel to a gaseous product. The char is not regarded as a product, but as unconverted solid fuel. The rational efficiency thus becomes:

$$\Psi_3 = \frac{E_{gas} - E_{steam} - E_{air}}{E_{biomass} - E_{char}} \qquad (3.14)$$

Figures 3.4a and 3.4b show these three different efficiency definitions for conversion of biomass by air or steam, respectively. The location of the carbon boundary point is seen at ER=0.255, respectively steam:biomass ratio of 1.30 kg:kg. As can be expected, the efficiencies are (almost) equal if no char is produced. In the situation where char is present, the efficiency based on exergy of output gas is

found to under predict, compared to the rational efficiency. On the contrary, the efficiency based on exergy of output gas and char is found to over predict compared to the rational efficiency.

It is important to realize that the carbon boundary is indeed the optimum point of operation for an air-blown biomass gasifier, as was postulated by Double and Bridgwater (1985). Gasification at the carbon boundary point is more efficient than slow pyrolysis without addition of air, 80.5% vs. 76.8%. This can be explained by the fact that the exothermic oxidation of carbon by air is coupled to endothermic water-gas reaction and Boudouard reaction. As long as solid carbon is present in the system, addition of air increases the exergy contained in the produced gas.

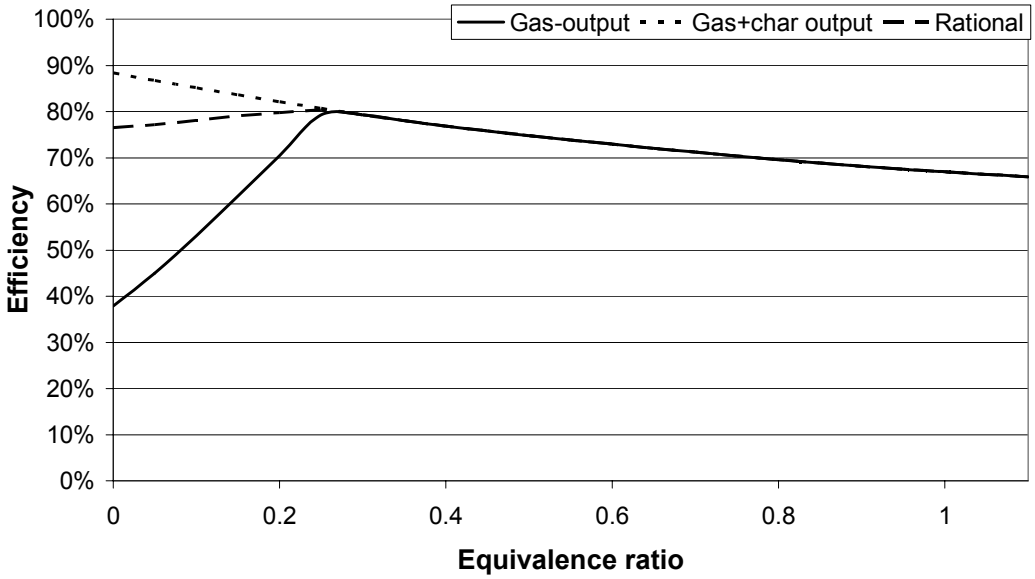

(a)

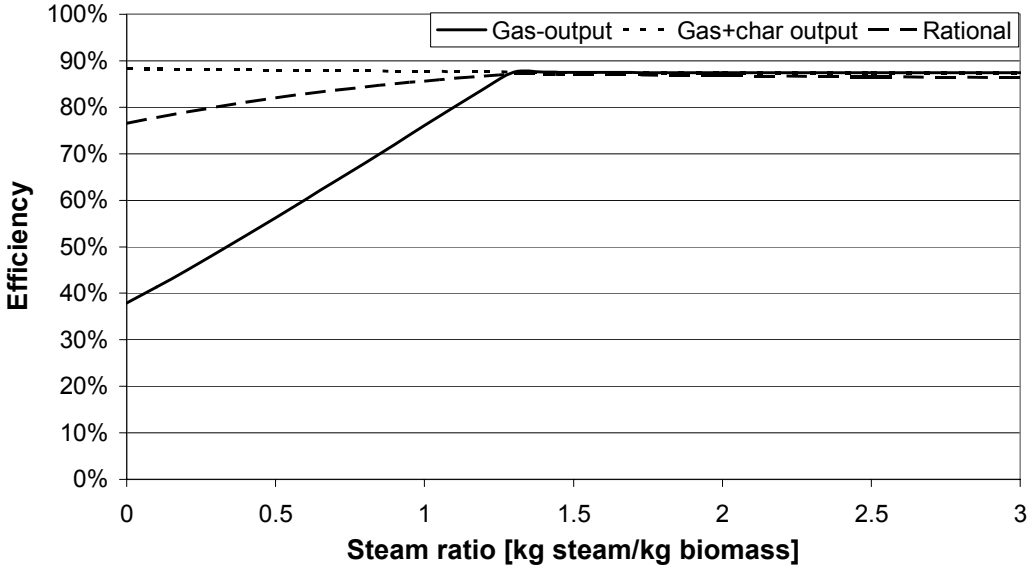

(b)

Figure 3.4: Efficiencies for conversion of biomass using (a) air, (b) steam

It can be observed that the efficiency of air gasification is sensitive to equivalence ratio (due to over oxidation), whereas the efficiency of steam gasification is not very sensitive to the steam:biomass ratio. The optimum efficiency of steam gasification is higher than the optimum efficiency of air gasification. However, exergy losses during production of the steam for steam gasification were not considered. If steam has to be generated on purpose, e.g. in a boiler, with efficiency below 30%, the overall efficiency for steam gasification is the same or even lower than for air gasification. Although this can be improved (e.g. by optimising the steam conditions or by using steam from a combined heat and power plant), the difference in efficiency between steam and air gasification is expected to be small.

3.4.4 Comparison of gas phase compositions for biomass gasification using air/steam mixtures

Figure 3.5 shows the amount of steam required to reach the carbon boundary at various equivalence ratios and the corresponding carbon boundary temperatures. For gasification of dry biomass using mixtures of air and steam, the efficiency lies between that of air gasification (80.5%) and of steam gasification (87.2%).

The choice of gasifying medium does not only depend on the thermodynamic efficiency of the gasifier, but also on the application of the produced gas down-stream of the gasifier. For points on the carbon boundary line, i.e. at optimum gasification conditions, gas phase compositions for gasification of dry biomass using steam and/or air are shown in Fig. 3.6. Compared to air blown gasification, steam gasification produces more methane because apart from oxygen, hydrogen is also introduced into the system. The carbon boundary is reached at a much lower temperature, so that formation of methane and carbon dioxide become thermodynamically favoured.

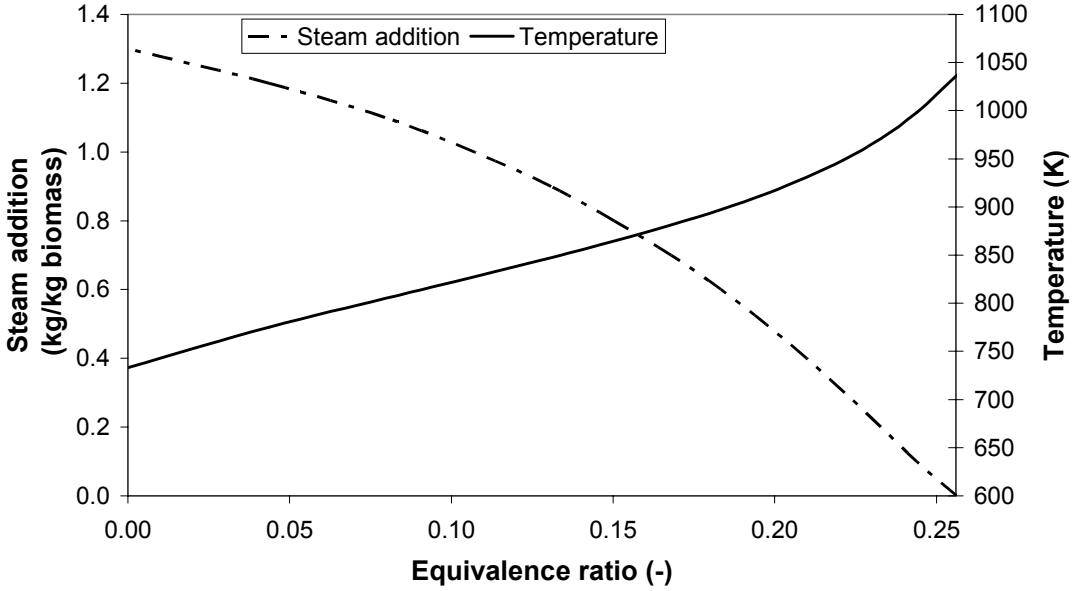

Figure 3.5: Required steam addition and corresponding carbon boundary temperature for conversion of biomass at different equivalence ratios

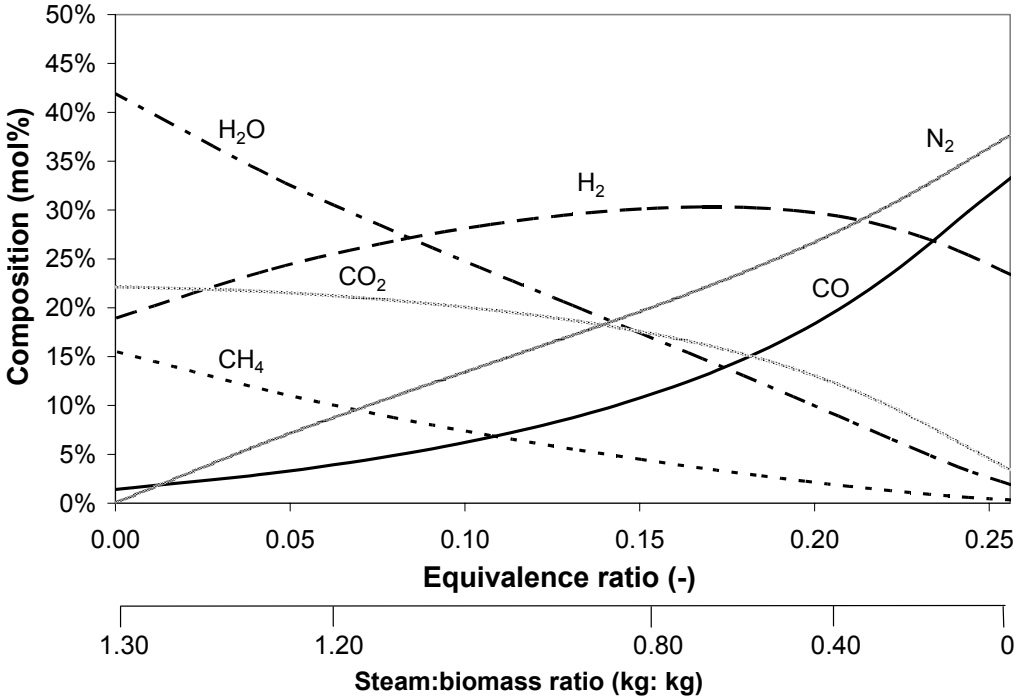

Figure 3.6: Gas phase compositions for conversion of biomass using air/steam mixtures

3.5 Conclusions and discussion

By defining the rational efficiency, based on exergy content of biomass feed and gaseous and solid products, it was possible to prove that gasification of biomass is intrinsically more efficient than slow pyrolysis (reaching chemical equilibrium) or combustion.

Using the above-mentioned efficiency, gasification of biomass using air was compared to gasification using steam. The difference in thermodynamic efficiency between air and steam gasification of dry, ash-free biomass is relatively small, especially if exergy losses that take place for the production of steam are taken into account. In practice, the efficiencies will be lowered by the presence of moisture in the biomass.

For the choice between steam and air gasification, the required gas composition is also important. If methane is the desired product, steam gasification is the preferred method. Apart from methane, the gas is composed of steam and carbon dioxide. If methane production is to be avoided, with hydrogen and carbon monoxide the desired products, e.g. for Fischer-Tropsch synthesis and hydrogen production, air gasification is more suitable. In this case, the product gases will contain at least 38% of nitrogen. This dilution can only be avoided by using pure oxygen for gasification or by CO_2 gasification driven by external heat. In both cases, additional exergy losses will take place outside of the gasifier.

Appendix A: Calculation of chemical equilibrium in a CHO system

Methods for calculating the composition in a CHO system at chemical equilibrium are well established in the literature (Cairns and Tevebaugh, 1964; Baron et al., 1976). This can be done by stoichiometric or non-stoichiometric methods, which both give the same results. These methods are incorporated in today's standard process simulation software, e.g. in Aspen Plus the REQUIL respectively RGIBBS unit operations can be used to calculate the reaction equilibria.

The non-stoichiometric method is based on minimizing the total Gibbs free energy in the system without specification of the possible reactions taking place. This requires identification of the possible products, for which thermochemical data must be available. Using a general-purpose equilibrium calculation program developed by NASA, Desrosiers (1979) showed that under gasification conditions (with temperatures between 600 and 1500K), the only species present at concentrations greater than 10^{-4} mol% are H_2, CO, CO_2, CH_4, H_2O and solid carbon (graphite).

The stoichiometric approach starts by selecting from all the possible species containing the elements C, H and O only those species that are present in the greatest amounts, i.e. those species having the lowest value of the free energy of formation. For a system composed of six components and three elements, there are 3 independent reactions, which are given in Table 3.1. In the region where no solid carbon exists, this reduces to 2 independent reactions. Solving these reaction equilibria together with the mass and energy balances gives the desired equilibrium composition.

Table 3.1: Important reactions in gasification

Reaction	ΔH (850°C) (kJ/mol)	ΔG (850°C) (kJ/mol)
(1) $C + 2\ H_2 = CH_4$	-91.0	33.1
(2) $C + H_2O = CO + H_2$	135.8	-25.4
(3) $C + CO_2 = 2\ CO$	169.8	-26.2
(2-3) $CO + H_2O = CO_2 + H_2$	-34.0	0.9
(1-2) $CO + 3\ H_2 = CH_4 + H_2O$	-226.6	58.3
$C + O_2 = CO_2$	-395.0	-396.0

Assumptions:

- Uniform temperature and pressure are assumed
- No information about reaction pathways/ formation of intermediates
- Tar is not modelled – solid carbon is used as a model component, which is a measure for the extent of tar formation
- No information about the rate of reactions, i.e. whether equilibrium is attained in practice.

If the residence time in the system is sufficiently long, e.g. for an air-blown moving bed gasifier, the equilibrium model is well verified; see Groeneveld (1984). However, for a steam-blown gasifier, equilibrium may not be reached due to the lower operating temperatures. In that case, steam-reforming catalysts may help in avoiding kinetic restrictions.

References

Baron RE, Porter SH, Hammond OH (1976). Chemical equilibria in carbon-hydrogen-oxygen systems. Cambridge: MIT Press.

Cairns EJ, Tevebaugh AD (1964). CHO gas phase compositions in equilibrium with carbon, and carbon deposition boundaries at one atmosphere. Journal of Chem. and Eng. Data 9(3):453-462.

Desrosiers R (1979). Thermodynamics of gas-char reactions. In: Reed TB, editor. A survey of biomass gasification. Colorado: Solar Energy Research Institute.

Double JM, Bridgwater AV (1985). Sensitivity of theoretical gasifier performance to system parameters. In: Palz W, Coombs J, Hall DO, editors. Energy from biomass, 3rd EC conference, Venice. p. 915-919

Grassman P (1950). On the common definition of efficiency. Chemie-Ingenieur-Technik 22(4):77-80 (in German).

Groeneveld MJ (1984). The co-current moving bed gasifier. Ph.D thesis, Twente University of Technology, Netherlands. Chapter IV.

Szargut J, Styrylska T (1964). Approximate evaluation of the exergy of fuels. Brennst. Wärme Kraft 16(12):589-596 (in German).

Chapter 4

Energy and exergy analyses of the oxidation and gasification of carbon[‡]

Exergy losses in gasification and combustion of solid carbon are compared by conceptually dividing the processes into several subprocesses: instantaneous chemical reaction, heat transfer from reaction products to reactants (internal thermal energy exchange) and product mixing. Gasification is more efficient than combustion because exergy losses due to internal thermal energy exchange are reduced from 14-16% to 5-7% of expended exergy, while the chemical reactions are relatively efficient for both processes. The losses due to internal thermal energy exchange may be reduced by replacing air with oxygen, although this introduces additional process losses for separation of oxygen from air, or alternatively, preheating of air by heat exchange with product gas. For oxygen-blown gasification of fuels with high calorific value, such as solid carbon, it is advisable to moderate the temperature by introduction of steam. At optimum gasification temperatures in the ranges of 1100-1200 K (for atmospheric pressure) and 1200-1300 K (for 10 bar pressure), up to 75% of the chemical exergy contained in solid carbon can be preserved in the chemical exergy of carbon monoxide and hydrogen.

4.1 Introduction

In combustion processes, energy is conserved if heat losses to the environment are minimized. However, the quality of energy decreases; the irreversible combustion of fuels in power producing plants consumes at least 30% of the fuel's exergy (Moran and Shapiro, 1998). The losses, known as irreversibilities, can be easily quantified by evaluating the exergy values and changes of component input and output streams and energy interactions. However, this does not deliver the detailed information about the specific process phenomenon that causes the exergy changes (Lior, 2001). To gain insight into irreversibilities occurring in energy conversion processes, and contribute to the development of more innovative energy conversion systems, detailed exergy analyses are essential. However, only few such analyses have been performed so far. Dunbar and Lior (1994) have studied the destruction of exergy in combustion processes in detail for adiabatic, constant pressure systems, while Caton (2000) has studied adiabatic, constant volume systems. De Groot (2004) has done an advanced exergy analysis of high temperature fuel cell systems.

[‡] Published in Energy 30 (7):982-1002, 2005.

Dunbar and Lior conceptually separated the oxidation into three sub-processes: (1) combined diffusion/fuel oxidation, (2) internal thermal energy exchange (heat transfer) and (3) the product constituent mixing process. The research showed that the majority of the exergy destruction occurs during thermal energy exchange between hot reaction product molecules and reactant molecules. The fuel oxidation itself was found to be relatively efficient. Based upon these fundamental insights, a recommendation was made to perform oxidation in fuel cells. This largely avoids liberation of thermal energy, so that the oxidation process is significantly more efficient. For the fuels considered in the study, hydrogen and methane, oxidation in a low-temperature fuel cell (such as Proton Exchange Membrane fuel cell) respectively high-temperature fuel cell (such as Molten Carbonate or Solid Oxide fuel cell) is very attractive. In practice, many solid fuels such as coal, refinery bottoms, wood, lignite, etc. are used for power generation. These fuels cannot be directly oxidized in fuel cells, at least not using present day technology. However, it is possible to gasify the solid fuels using a sub-stoichiometric amount of oxidant (25-50% of the amount needed for combustion), so that the produced gas could be subsequently used in a fuel cell.

The objectives of this chapter are therefore to quantify exergy losses of gasification processes, compare the results with combustion processes, and finally to investigate the source of exergy losses in both processes. This should give a fundamental explanation why the exergy losses of gasifying fuels (where fuels are only partially oxidized) are smaller than those of combusting fuels. A further objective of this chapter is to find out whether the exergy losses in a gasifier may be minimized by optimization of process parameters such as temperature, pressure and choice of gasifying medium. Various gasifying media can be used for the gasification of fuels: apart from oxygen and air, steam, hydrogen or carbon dioxide may be used. Injecting steam into an oxygen- or air-blown gasifier moderates the gasification temperature, changes the product gas composition and also influences the thermodynamic efficiency.

For a detailed thermodynamic analysis of combustion and gasification of industrial solid fuels, the thermodynamic properties of these fuels must be known. Therefore, solid carbon (graphite) was selected as a model compound in this study. This is the only thermodynamically stable solid carbon-containing material at temperatures above 600K (until its sublimation temperature of 3700K). For all other industrial fuels, combustion is accompanied by thermal decomposition, also known as pyrolysis. Depending on process variables such as heating rate, particle size and volatile content of the fuel, hundreds of pyrolysis products may be formed. Thermodynamic data such as the heat capacity and its dependency on temperature are not known for all pyrolysis products. Furthermore, there is scattered information about the heat of pyrolysis (Rath et al., 2003). Nevertheless, the results obtained in

this study for solid carbon may be generalized also to other solid carbonaceous fuels.

This chapter comprises two parts. In the first part, the oxidation of solid carbon with air is analyzed at atmospheric pressure. By varying the air/fuel ratio, thermodynamic losses of gasification and combustion can be compared. In the second part of the chapter, attention is focused completely on gasification. The possibility of improving gasification efficiency by replacing air with oxygen is investigated. Furthermore, the carbon-oxygen gasification system is extended to a C-H-O system by introducing steam into the reaction system. The effect of steam on the magnitude of thermodynamic losses is studied at atmospheric pressure and at an elevated pressure of 10 bar.

4.2 Methodology

4.2.1 Reaction equilibria

The oxidation of solid carbon is described by the following equations:

$$C(s) + O_2\ (g) \longrightarrow CO_2\ (g) \qquad (4.1)$$

$$C(s) + 1/2\ O_2\ (g) \longleftrightarrow CO\ (g) \qquad (4.2)$$

The Boudouard equilibrium reaction also applies:

$$C(s) + CO_2\ (g) \longleftrightarrow 2\ CO\ (g) \qquad (4.3)$$

The system is composed of four components and two phases; the phase rule indicates that four constraints on the system are necessary for a complete definition of the system. These constraints were chosen to be pressure, O_2/C ratio (equivalence ratio) and two independent chemical reaction equations 4.1 and 4.3, which include all four species. The temperature of the system is an output variable. Note that reaction equation 4.2 is not independent because it can be obtained by addition of reaction equations 4.1 and 4.3.

If steam is added in gasification or combustion of solid carbon, the C-O system is extended to a C-H-O system. Methods for calculating the composition in a C-H-O system at chemical equilibrium are well established in the literature (e.g. Cairns and Tevebaugh, 1964). This can be done by stoichiometric or non-stoichiometric methods, which both give the same results. The non-stoichiometric method is based on minimizing the total Gibbs free energy in the system without specification of the possible reactions taking place. The stoichiometric approach starts by selecting from all the possible species containing the elements C, H and O only those species that are present in the greatest amounts, i.e. those species having the lowest value of the free energy of formation. For a C-H-O system, besides C(s), CO_2, CO and O_2 also H_2O, H_2 and CH_4 are considered. According to the phase rule, seven components

and two phases result in seven degrees of freedom. These have been pressure, O_2/C ratio (equivalence ratio), H_2O/C ratio (steam to carbon ratio) and four reaction equations, being Eqs. 4.1 and 4.3 plus two additional equations:

$$C(s) + H_2O\,(g) \longleftrightarrow CO\,(g) + H_2\,(g) \qquad (4.4)$$

$$C(s) + 2\,H_2\,(g) \longleftrightarrow CH_4\,(g) \qquad (4.5)$$

Solving these reaction equilibria together with the mass and energy balances gives the desired equilibrium composition and the system temperature. Figure 4.1 shows the equilibrium constants for Eqs. 4.2-4.5. For an accurate calculation of these equilibrium constants, it is important that thermodynamic data are available at very high temperatures (over 4000 K can be achieved in carbon oxidation). Especially the heat capacities of all components must be accurately known as a function of temperature. Commonly used third-order polynomial equations give large deviations at temperatures above 1000 K. To overcome this problem, we have used the equation developed by Barin (1989) for both solid carbon and gaseous products:

$$C_{p,i} = -c_{n,i} - 2d_{n,i}T - 6e_{n,i}T^2 - 12f_{n,i}T^3 - \frac{2g_{n,i}}{T^2} - \frac{6h_{n,i}}{T^3} \qquad (4.6)$$

In this equation, Cp is the heat capacity in J mol^{-1} K^{-1}, and c-g constants of various units. For each component i, multiple sets of parameters from 1 to n are used to cover multiple temperature ranges. These temperatures ranges extend to 4726.85 K.

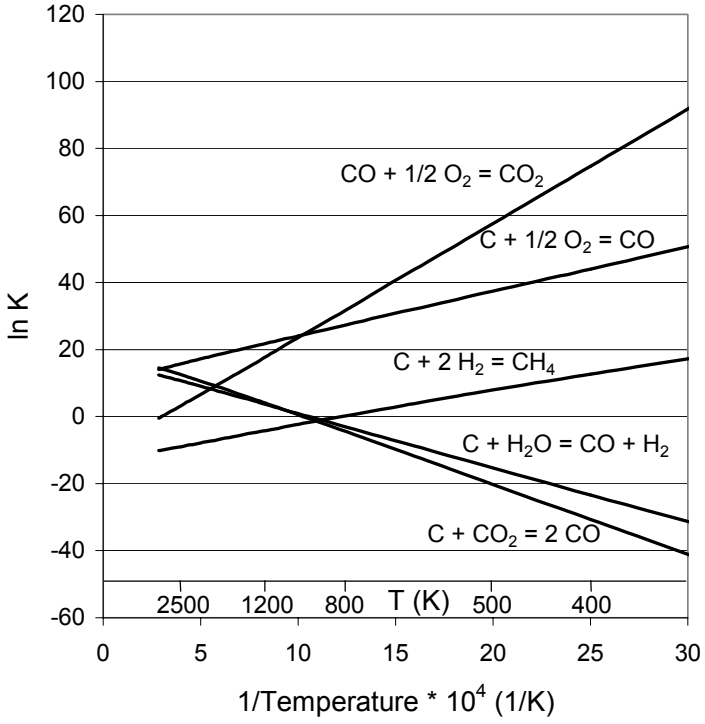

Figure 4.1: Logarithm of equilibrium constants versus inverse temperature for solid carbon oxidation and reforming reactions

4.2.2 Global analysis

The global analysis considers a reactor at atmospheric pressure in which solid carbon and oxygen (or air, consisting of 21% oxygen and 79% nitrogen) are introduced at an environmental temperature of 25°C. These react with each other and the product gases and residual fuel leave the reactor at an elevated temperature. The reactor is regarded as zero-dimensional, i.e. there are no spatial variations in temperature or composition. Neither is there any change effected with time because all forward and reverse reactions are assumed to reach chemical equilibrium. In real equipment, temperature and composition gradients are present along the main flow path. Also, it is possible that kinetic limitations occur so that chemical equilibrium is not reached. Nevertheless, the equilibrium model presents valuable information as it shows the thermodynamic constraints of the system.

For the exergy balance over the reactor, four streams must be considered: incoming solid fuel, incoming gas, unconverted solid fuel, and produced gas. The exergy balance for the gasifier thus becomes:

$$\varepsilon_{\text{fuel}} + \varepsilon_{\text{gas\_in}} = \varepsilon_{\text{fuel\_unconv.}} + \varepsilon_{\text{gas\_prod}} + I \qquad (4.7)$$

In which $\varepsilon_{\text{fuel}}$, $\varepsilon_{\text{gas\_in}}$, $\varepsilon_{\text{fuel\_unconv.}}$, $\varepsilon_{\text{gas\_prod}}$ are the exergy (sum of chemical and physical exergy) of the fuel, incoming gas, unconverted solid fuel, and produced gas, respectively, and I the process irreversibilities, all in J.

The overall exergetic efficiency of the process η_{overall} can be defined in various ways, as discussed in Appendix B. This study uses the most stringent definition:

$$\eta_{\text{overall}} = \frac{(\varepsilon_{\text{gas\_prod.}} - \varepsilon_{\text{gas\_in}})}{(\varepsilon_{\text{fuel}} - \varepsilon_{\text{fuel\_unconv.}})} \qquad (4.8)$$

An alternative definition of exergetic efficiency can be obtained by neglecting the temperature-dependent part of the physical exergy of the product gas. This will be called the chemical efficiency η_{chem}:

$$\eta_{\text{chem}} = \frac{(\varepsilon^{ch}_{\text{gas\_prod}} + \varepsilon^{ph,\Delta P}_{\text{gas\_prod}} - \varepsilon_{\text{gas\_in}})}{(\varepsilon_{\text{fuel}} - \varepsilon_{\text{fuel\_unconv.}})} \qquad (4.9)$$

Where: ε^{ch} is the chemical exergy and $\varepsilon^{ph,\Delta P}$ the pressure-dependent part of physical exergy, both in J.

Both definitions are considered in this study. Strictly speaking, the former definition of Eq. 4.8 is more correct. However, it is important to realize that additional losses in the process system take place outside of the gasifier or combustor (Moran and Shapiro, 1998). In practice, it is difficult to convert the physical exergy due to the elevated temperature of product gas completely into work. Often, this gas is first quenched to a temperature below 900°C, passed through a synthesis gas cooler to

generate steam, which subsequently drives a steam turbine. Process losses occur in all these steps. The definition of Eq. 4.9 is useful in order to point out under which conditions the chemical exergy of the fuel is maximally conserved.

4.2.3 Detailed analysis

To understand the observed overall efficiency, it is necessary to analyse the overall process irreversibilities in more detail. Similar to Dunbar and Lior (1994), the approach is to assume hypothetical sequences of subprocesses and calculate the entropy production for each subprocess. In this way, the total irreversibilities can be broken down into individual contributions. The following physicochemical processes are considered to contribute to the global entropy production: (i) reactant diffusion (ii) fuel oxidation (iii) heat transfer between product molecules and reactant molecules and (iv) product mixing. Considering that oxygen is normally rapidly consumed in a gasifier, it is assumed that fuel oxidation is instantaneous. Two cases will be considered: an isothermal case, where heat transfer is very rapid so that the oxidation takes place isothermally, and an adiabatic case, where heat transfer is very slow so that the oxidation takes place adiabatically. In practice, heat transfer will be between these two extremes.

Figures 4.2a and 4.2b illustrate the subprocesses occurring when solid carbon and gasifying medium are introduced into a hot reactor. These are conceptually assumed to take place as follows: gasifying medium (oxygen or air, and optionally steam) and solid fuel are heated to the reactor temperature T_r. Entropy production due to mixing between reactant gases is considered. Mixing between solid fuel and gasifying medium is not taken into account because this does not happen on a molecular scale. As soon as the solid fuel and gasifying medium contact each other, chemical reactions take place. For the isothermal case of Fig. 4.2a, the reaction heat is removed swiftly to the surrounding reactant molecules. For the adiabatic case of Fig. 4.2b, the product molecules become much warmer (up to 2000°C) than the surrounding reactant molecules. When heat transfer takes place from product molecules to reactant molecules, it is possible that subsequent reactions occur because chemical equilibria change with temperature. Finally, the product molecules mix with the remaining global system constituents.

Exergy balances can be made for all the subprocesses. As an illustration, an exergy balance is presented for the sub-process of heating the fuel to the global reactor temperature:

$$I_{\text{heating\_fuel}} = T_o \Delta s_{\text{heating\_fuel}} = (\varepsilon_{in} - \varepsilon_{out}) + \varepsilon^Q \qquad (4.10)$$

$$(\varepsilon_{in} - \varepsilon_{out}) = (h_{in} - h_{out}) - T_o (s_{in} - s_{out}) \qquad (4.11)$$

$$\varepsilon^Q = (h_{out} - h_{in}) \cdot (1 - \frac{T_o}{T}) \qquad (4.12)$$

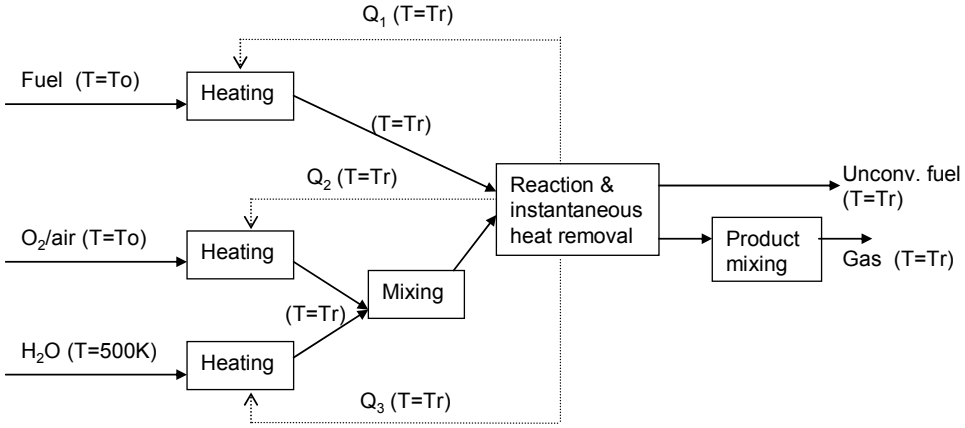

(a)

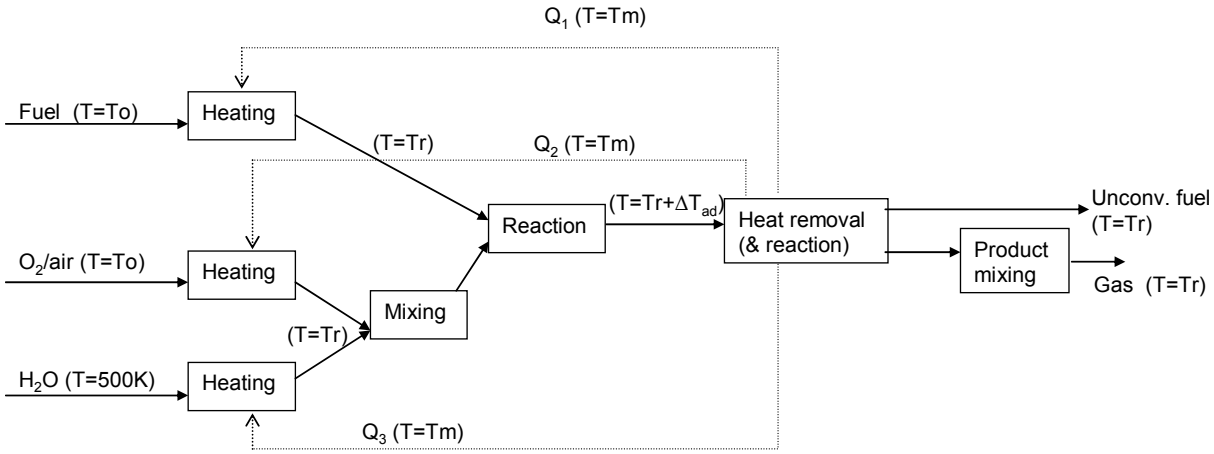

(b)

Figure 4.2: Hypothetical subprocesses for (partial) oxidation of solid carbon, (a) isothermal case (b) adiabatic case

In these equations, h is the enthalpy in J, s the entropy in J/K, T_o the environmental temperature (298.15 K or 25°C) and ε^Q the thermal exergy in J. For all equations, the subscripts indicate the corresponding subprocess.

Dividing Eq. 4.10 by T_o gives the entropy production Δs in J/K of this sub-process:

$$\Delta s_{\text{heating\_fuel}} = (s_{out} - s_{in}) - \frac{(h_{out} - h_{in})}{T} \qquad (4.13)$$

The difference between Fig. 4.2a and Fig. 4.2b lies in the temperature T (in Eqs. 4.12 and 4.13) at which the heat of reaction is liberated. For the isothermal case, this temperature equals the reactor temperature T_r. For the adiabatic case, the heat removal block in Figure 4.2b operates in reversible mode if the entropy production equals zero:

$$\Delta s_{\text{heat\_removal}} = (s_{out} - s_{in}) - \frac{(h_{out} - h_{in})}{T_m} = 0 \qquad (4.14)$$

which gives the mean thermodynamic temperature T_m at which the reaction heat is liberated:

$$T_m = \frac{h_{out} - h_{in}}{s_{out} - s_{in}} = \frac{h_{Tr+\Delta Tad} - h_{Tr}}{s_{Tr+\Delta Tad} - s_{Tr}} \tag{4.15}$$

Where ΔT_{ad} is the adiabatic temperature rise in K for the adiabatic case of Fig. 4.2b.

The overall irreversibilities equal the sum of the irreversibilities of the subprocesses:

$$I_{\text{overall}} = I_{\text{heating\_fuel}} + I_{\text{heating\_O}_2\text{/air}} + I_{\text{heating\_steam}} + I_{\text{reactant\_mixing}} + I_{\text{chemical\_reaction}} + I_{\text{product\_mixing}} \tag{4.16}$$

It is advantageous to divide the individual contributions of the total irreversibility by the expended exergy, which gives the relative exergy loss δ, also termed efficiency defect (Kotas, 1980):

$$\delta_i = \frac{I_i}{\Delta\varepsilon_{\text{expended}}} = \frac{I_i}{(\varepsilon_{\text{fuel}} - \varepsilon_{\text{fuel\_unconv.}})} \tag{4.17}$$

The sum of these efficiency defects is the fraction of the expenditures lost through irreversibility:

$$1 - \eta_{\text{overall}} = \sum_i \delta_i = \frac{\sum_i I_i}{\Delta\varepsilon_{\text{expended}}} \tag{4.18}$$

4.3 Oxidation of solid carbon with air

4.3.1 Results of global analysis

Figure 4.3 shows the temperature, fraction of unreacted carbon and thermodynamic efficiency for oxidation of solid carbon with air as a function of equivalence ratio (ER). The ER is defined as the amount of oxygen added for gasification relative to the amount of oxygen required for complete combustion. An ER of 1 corresponds to stoichiometric combustion of the fuel; in this case, this corresponds to 1 mol O_2/mol C. At the carbon boundary, where the carbon is totally gasified, ER equals 0.5. The overall efficiency reaches a maximum at the carbon boundary, where a temperature of 1222°C is attained. Addition of more air beyond this ER leads to a relatively strong temperature increase because carbon is not present so that the endothermic reaction of Eq. 4.3 cannot take place.

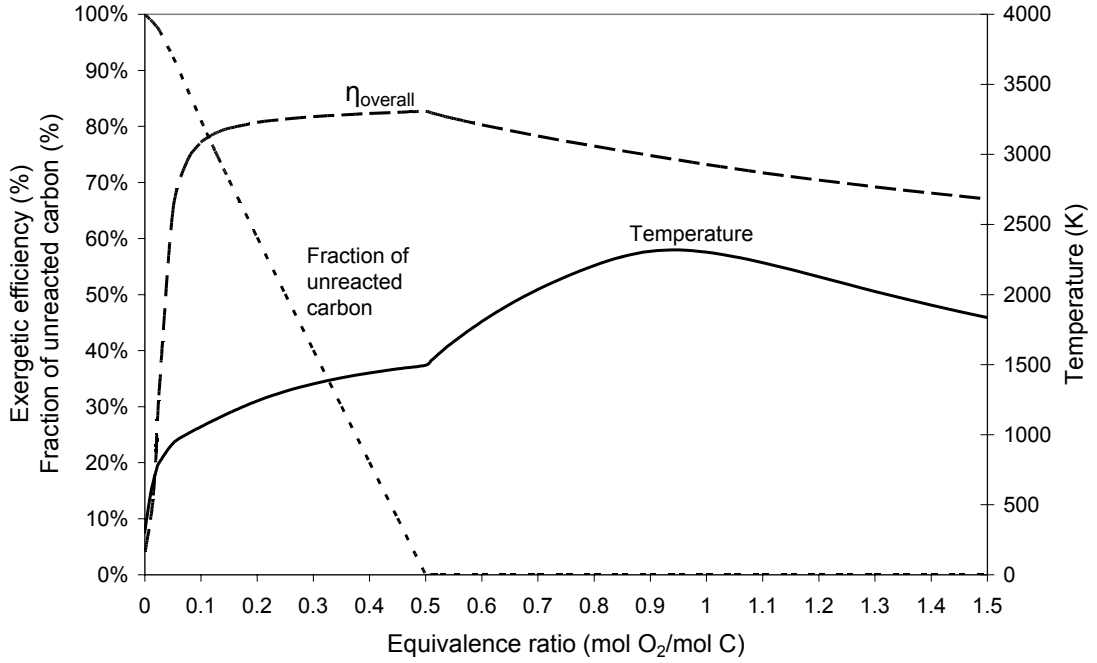

Figure 4.3: Efficiency, fraction of unreacted carbon and system temperature for air-blown oxidation of solid carbon versus equivalence ratio

Figure 4.4 gives the gas phase compositions of the oxidation process. In the left hand side of this figure, at low equivalence ratios, mainly carbon dioxide is formed, but as the temperature rises the equilibrium shifts to carbon monoxide. At an ER of 0.5, all carbon is partially oxidized to carbon monoxide. Addition of more oxygen leads to further combustion to carbon dioxide, and especially for combustion with excess air (ER above 1) free oxygen is present in the product gas.

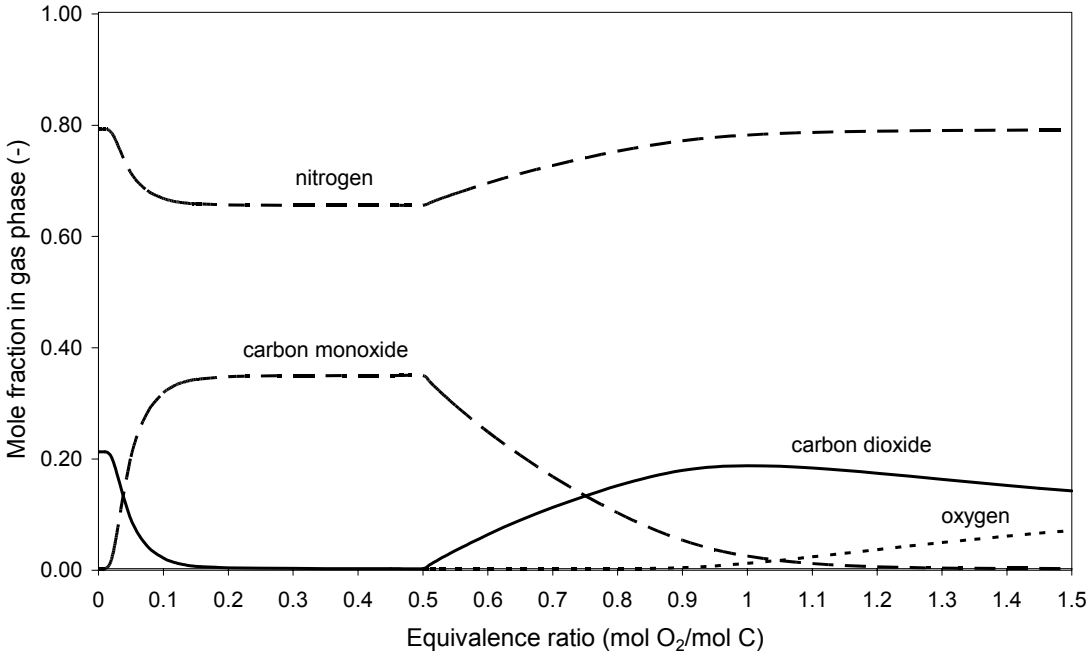

Figure 4.4: Gas phase composition for air-blown oxidation of solid carbon versus equivalence ratio

4.3.2 Results of detailed analysis

Figures 4.5a and 4.5b show the relative exergy losses for the sub-processes of carbon oxidation using air, for the adiabatic case and isothermal case respectively. The relative exergy loss was defined in Eq. 4.17 as the irreversibility for each sub-process divided by the consumed chemical exergy of the fuel. Since the overall efficiency is the same for both cases, the sum of these relative exergy losses is equal. The difference lies in the fact that for the adiabatic case, a higher reaction temperature is reached. A high temperature is favourable for the exothermic carbon oxidation reaction, because from a thermodynamic point of view it is best to carry out an exothermic reaction at the highest possible temperature.

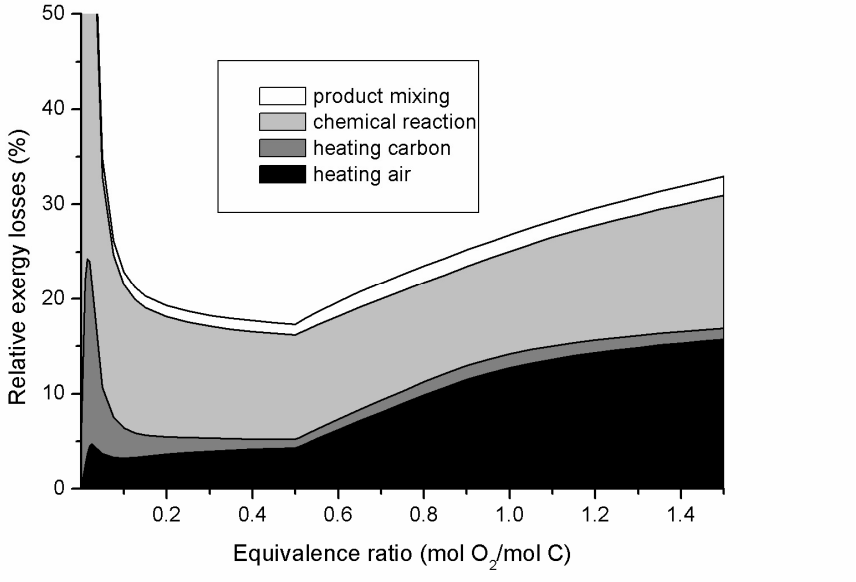

(a)

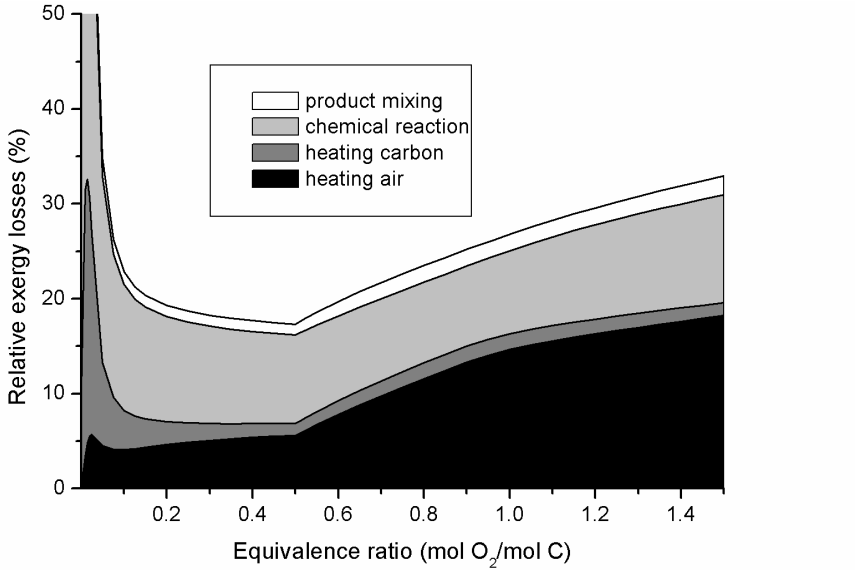

(b)

Figure 4.5: Relative exergy losses for subprocesses in air-blown oxidation of solid carbon versus equivalence ratio, (a) isothermal case (b) adiabatic case

Therefore, the relative exergy losses due to chemical reaction are smaller for the adiabatic case than for the isothermal case. This is compensated in other sub-processes, specifically heating of reactants to the reactor temperature. Since $T_m > T_r$, it is found in Equation 4.13 that for the adiabatic case, the entropy production for heating of fuel (and gasifying medium) is larger than for the isothermal case. In other words, heat is downgraded more in temperature. The differences between the isothermal and adiabatic case have been found to be relatively small.

The relative exergy loss of the various subprocesses are discussed below:

- The relative exergy losses in the subprocesses of heating fuel and gasifying medium (internal thermal energy exchange) initially increase from ER=0 to ER=0.015. This happens when carbon starts to become oxidized and the resulting reaction heat is downgraded to a temperature not much higher than the environmental temperature. Upon further addition of oxidant, more reaction heat is liberated but it is downgraded less and conserved as physical exergy. This explains the initial maxima which correspond to a temperature around 400°C (notice that this is rather theoretical situation because at such low temperatures, the rate of carbon oxidation is infinitely slow). Beyond ER=0.5, the losses for the subprocess of heating of carbon increase slightly, while the losses for the subprocess of heating of air increase strongly due to the temperature rise of the system and the increased amount of air required for combustion.
- The relative exergy loss resulting from chemical reaction decreases with equivalence ratio in the range of ER=0 to ER=0.5, as a result of the temperature rise. The oxidation reaction proceeds efficiently (loosing 10-12% of expended fuel exergy) for both gasification, in which the combustion reaction of Eq. 4.1 drives the endothermic reforming reaction of Eq. 4.3, and combustion, in which the combustion reaction creates a very high system temperature. At ER>1, the reaction proceeds less efficiently as the temperature drops due to the excess of air added.
- The relative exergy loss related to product mixing is fairly small.
- The sum of relative exergy losses has a minimum at ER=0.5, the point where the overall efficiency is the highest.

For combustion, i.e. equivalence ratios from 1 to 1.5, it is found that the losses due to internal energy exchange are larger than those due to chemical reaction. This is in good agreement with results obtained by Dunbar and Lior (1994). It can be concluded that combustion is less efficient than gasification due to internal heat transfer, i.e. increased downgrading of reaction heat for heating the fuel and the gasifying medium, while the chemical reactions are relatively efficient for both processes.

4.4 Gasification of solid carbon

4.4.1 Gasification by air or oxygen

4.4.1.1 Results of global analysis

In order to decrease the exergy losses for heating up the gasifying medium to the reactor temperature, oxygen can be used instead of air. This has the benefit that a much smaller gas volume needs to be heated, and hence the exergy losses in the gasifier are smaller. Figures 4.6a and 4.6b compare the temperatures and thermodynamic efficiencies for air-blown and oxygen-blown gasification, respectively.

The choice of gasifying medium has a very large effect on the temperature, which increases at the carbon boundary from 1495 K to 3457 K when air is replaced by oxygen. As expected, the overall efficiency at the carbon boundary increases (from 82.7 to 87.6%). However, the industrial production of oxygen for the gasifier, usually based on cryogenic distillation processes, also requires work, which should be included in the analysis. The electricity consumption of large-scale cryogenic oxygen plants is approximately 380 kWh/ton oxygen (Simbeck et al., 1983), which translates into a low exergetic process efficiency of 9.1%. Furthermore, this electricity must be produced, e.g. from gasification product gas using gas turbines or fuel cells; an exergetic efficiency of 50% is commonly assumed for this process. Correcting the overall efficiency with process irreversibilities for production of oxygen and electricity (and steam, if applicable) results in a net overall efficiency $\eta_{overall,\ net}$ and net chemical efficiency $\eta_{chem,\ net}$. These efficiencies are also shown in Figure 4.6b and are found to be lower for oxygen-blown gasification than for air-blown gasification.

However, the use of oxygen does have other advantages such as operation at lower equivalence ratio, smaller equipment size of gasifier and downstream equipment, and possibly savings in compression cost of produced gas, but also disadvantages such as the investment cost for an oxygen plant and safety aspects related to storage and production of oxygen. Therefore, the choice of gasifying medium is not only determined by energetic considerations, but also by process economics, which depend on the scale of the gasification process.

Considering the chemical efficiency, as defined in Eq. 4.9, it is very interesting to observe that this does not have a maximum at the carbon boundary, but already at an equivalence ratio around 0.15 for gasification with air or 0.10 for gasification with oxygen. At these equivalence ratios, temperatures around 1200 K are reached, so that the equilibrium of endothermic gasification reaction of Eq. 4.3 lies sufficiently to the right. The exothermic oxidation of carbon is coupled with endothermic reforming of carbon and a high efficiency is obtained. Addition of more oxygen leads to a higher temperature, but since this has little effect on the

reaction equilibria, it does not increase the chemical exergy of product gas. Due to the temperature rise of product gas, its physical exergy and the overall efficiency do increase.

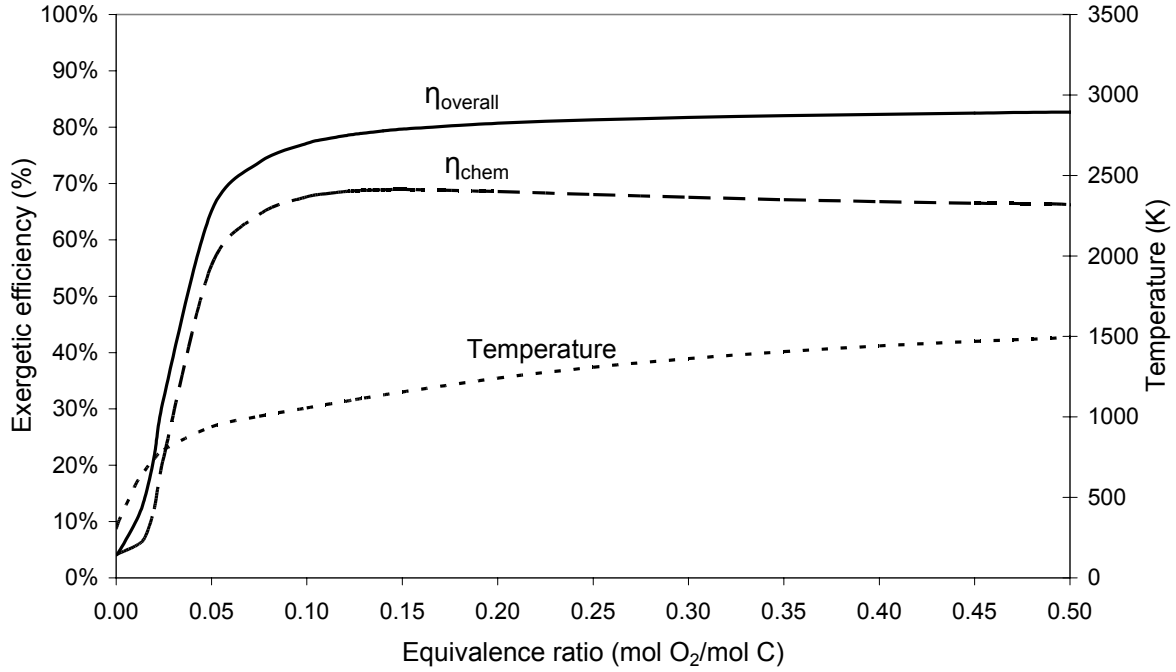

(a)

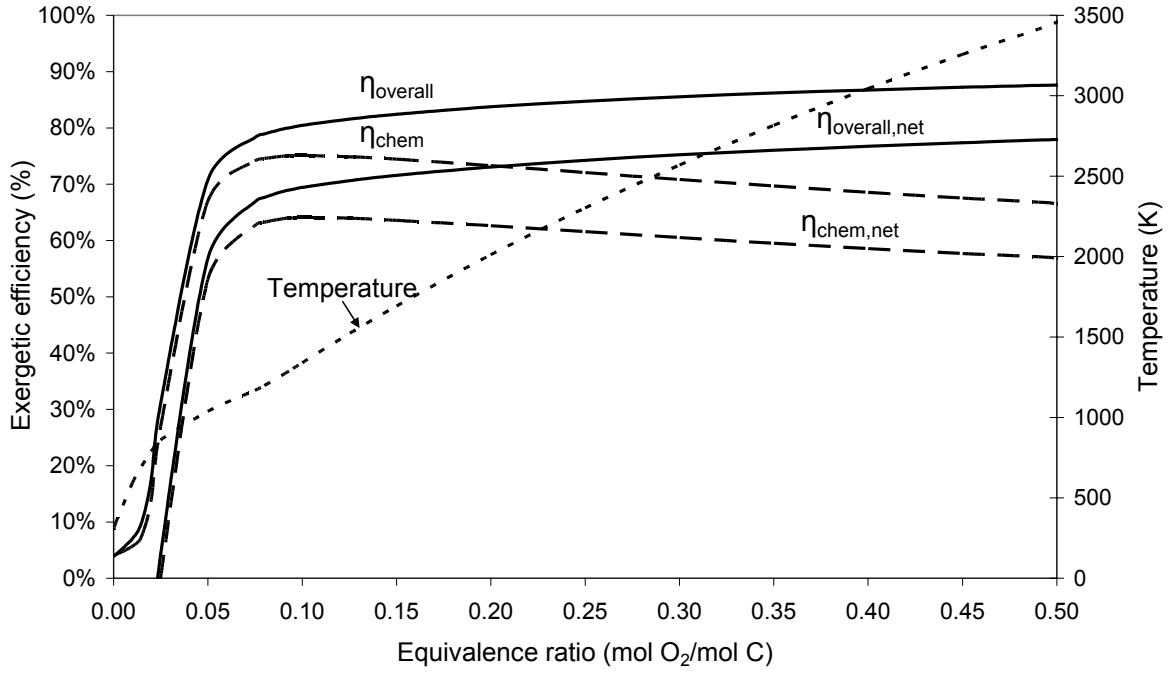

(b)

Figure 4.6: Overall efficiency, chemical efficiency and system temperature for gasification of solid carbon versus equivalence ratio, (a) air-blown (b) oxygen-blown

Table 4.1: Comparison of relative exergy losses and exergetic efficiencies (both in %) for air- and oxygen-blown gasification of solid carbon (at equivalence ratio of 0.5)

	Air-blown gasification		Oxygen-blown gasification	
	Isothermal case	**Adiabatic case**	**Isothermal case**	**Adiabatic case**
Heating carbon	0.9	1.2	2.0	2.5
Heating oxygen or air	4.3	5.6	1.9	2.3
Chemical reaction	11.0	9.4	8.5	7.6
Product mixing	1.1	1.1	negl.	negl.
Sum of relative losses	17.3		12.4	
Oxygen separation from air			4.9	
Electricity for oxygen separation			5.3	
Total losses			22.6	
Exergetic efficiency	82.7		77.4	
chemical contribution	66.3		56.4	
physical contribution	16.4		21.0	

4.4.1.2 Results of detailed analysis

The relative exergy losses and thermodynamic efficiencies for gasification of carbon with air and oxygen are shown in Table 4.1, both for the isothermal and adiabatic case. These two cases show similar trends. The chemical reaction becomes more efficient for oxygen-blown gasification because of the higher temperature. The relative exergy loss for the subprocess of heating gasifying medium to the reactor temperature reduces by more than a factor of 2 if air is replaced with oxygen. Still, a larger reduction could have been expected considering that the gas volume added is 4.76 times smaller. To explain the disappointing improvement, it must be realized that the reaction heat, which is liberated at a very high temperature in oxygen-blown gasification, is downgraded more. This also explains why the relative exergy losses for heating carbon increase.

The irreversibilities in a cryogenic oxygen plant, which are equivalent to 40 kJ/mol oxygen, are larger than irreversibilities avoided in the gasifier by using pure oxygen instead of air. The latter can be calculated at 28 kJ/mol oxygen by setting up an exergy balance for heating the nitrogen (3.76 mol per mol of oxygen) from environmental temperature to a gasification temperature of 1495 K. In practice, these may be reduced by preheating of air, e.g. by heat exchange with product gas.

Summarizing, the very high temperature corresponding to complete gasification of carbon using oxygen has two drawbacks. Firstly, although the overall efficiency is high, almost ¼ of exergy is present in the form of physical exergy, which is difficult to use. Secondly, exergy losses for heating up the reactants and especially for oxygen and electricity production are relatively large. To alter the ratio of physical and chemical exergy in the product gas, and further decrease exergy losses, steam

can be added to the gasifier. In this way, less oxygen could be used and the temperature in the system is moderated. Note that a similar effect could be obtained by CO_2 addition, but steam addition is more practical. The effect of such steam addition on overall efficiency and conservation of chemical exergy in product gas is therefore studied in the next section.

4.4.2 Gasification by steam/oxygen mixtures

4.4.2.1 Results of global analysis

The purpose of this section may be illustrated in a triangular C-H-O-diagram as shown in Figure 4.7. In the triangular diagram, the solid and the dashed lines show the so-called carbon deposition boundaries at 1 atm and 10 bar, respectively, for various temperatures. Above the solid carbon boundary, solid carbon exists in heterogeneous equilibrium with gaseous components, while below the carbon boundary no solid carbon is present. In order to gasify solid carbon, it is necessary to add oxygen and/or hydrogen-containing gases. Gasification of carbon as studied in the previous section can be represented by the bold solid line, which runs from the C vertex along the C-O axis until the carbon boundary line is reached in point I. This carbon boundary line corresponds to a temperature of 1500 K, but it was previously calculated that the actual system temperature is much higher (3457 K).

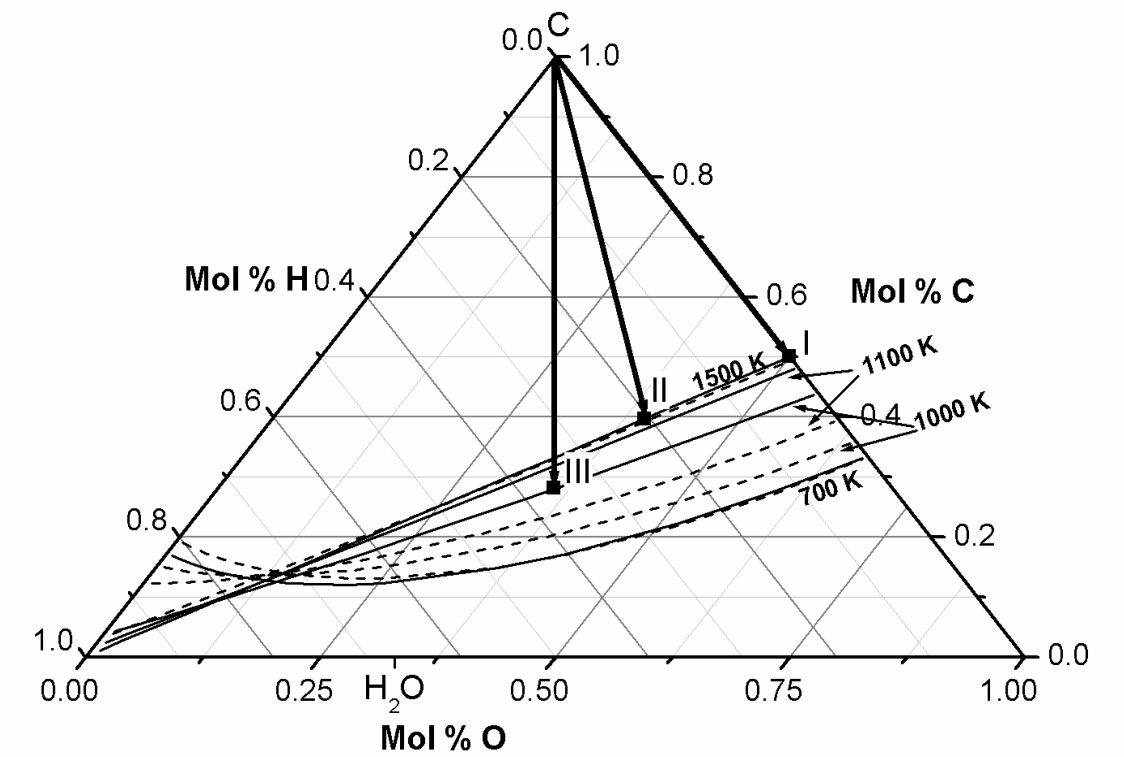

Figure 4.7: Molar triangular C-H-O-diagram indicating solid carbon boundaries at atmospheric pressure (solid lines) and 10 bar pressure (dashed lines) and possible gasification pathways

Therefore, we may replace part of the oxygen by steam, which implies that oxygen is supplied in a different form. This reduces the system temperature, but as long as the temperature does not drop below 1500 K, there is no influence on the reaction equilibria, so that the final O/C ratio of 1 does not change. The line from the C vertex to point II in Figure 4.7 represents this. Finally, if the temperature drops below 1500 K, the carbon boundary is reached at a lower temperature, e.g. point III, so that the final O/C ratio increases and relatively more oxygen or steam is required.

Figure 4.8 shows the amount of steam (at an inlet temperature of 500 K) required to reach the carbon boundary and the corresponding temperature, for atmospheric pressure and a pressure of 10 bar. In the right hand side of the figure, from the linear slope of the steam:carbon line, it is clear that 1 mole of oxygen can be replaced by 2 moles of steam. As soon as the equivalence ratio drops below 0.37, the temperature is below 1500 K, and the slope of the steam:carbon line starts to increase. This is because a carbon boundary line corresponding to a lower temperature in the C-H-O diagram is applicable, so that relatively more oxygen must be added to achieve complete gasification. Comparing the required steam addition at 10 bar and 1 atm, it is seen that at higher equivalence ratios slightly less steam is required at 10 bar, whereas at low equivalence ratios slightly more steam is required at 10 bar. This can be explained because at higher pressure, the carbon boundary lines move downwards in the right side of the C-H-O diagram (reaction Eqs. 4.3 and 4.4 are not favoured by pressure), while they move upwards in the left side of the C-H-O diagram (reaction Eq. 4.5 is favoured by pressure).

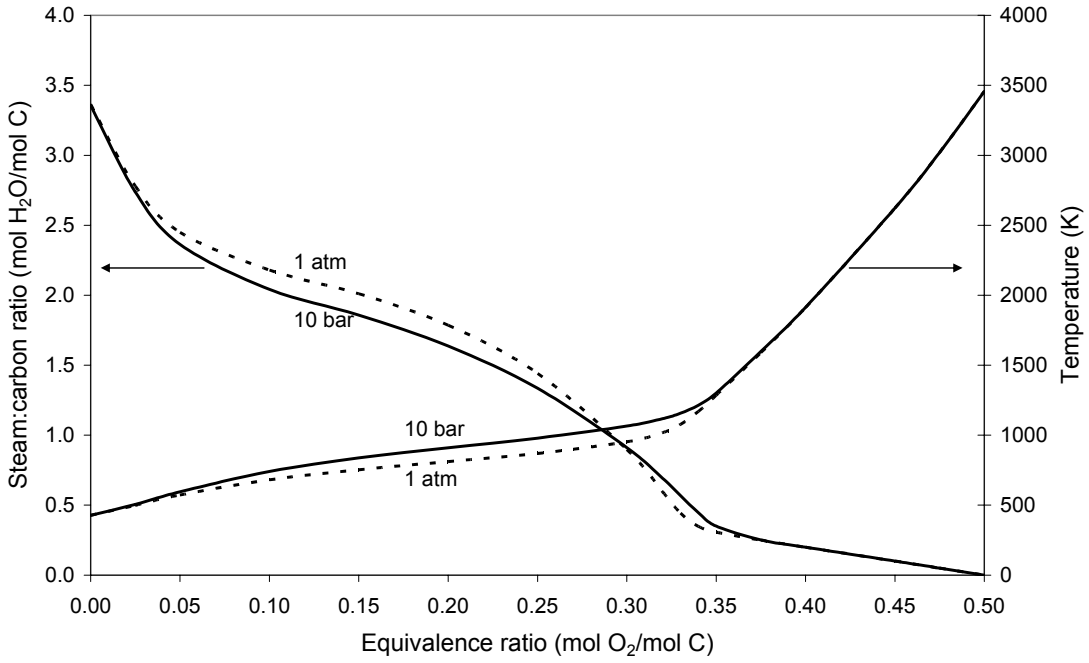

Figure 4.8: Required steam addition and corresponding temperature for complete gasification of solid carbon at different equivalence ratios

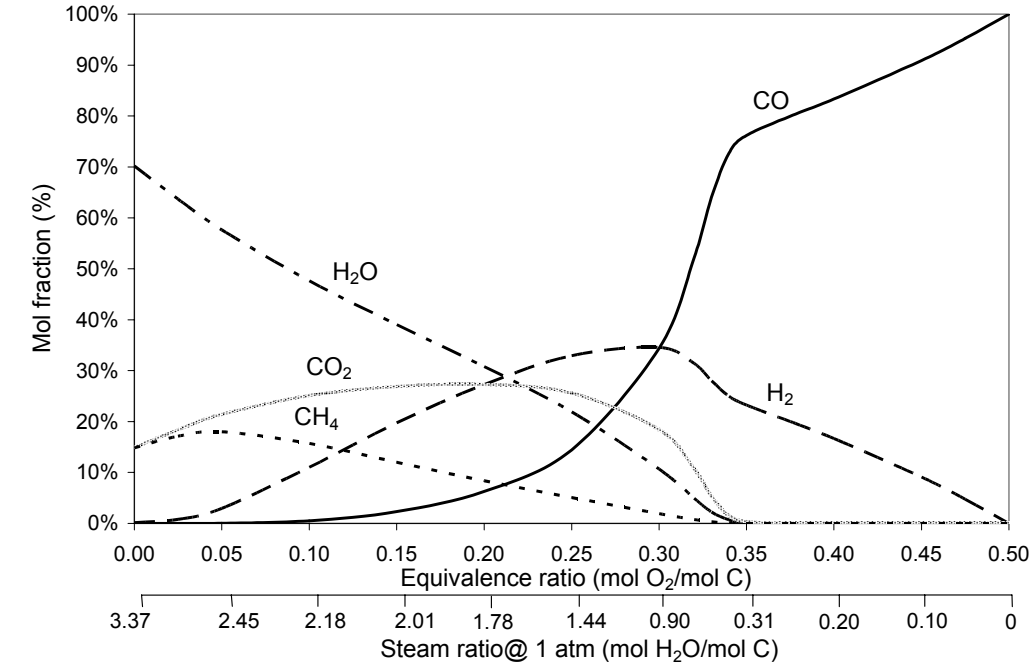

(a)

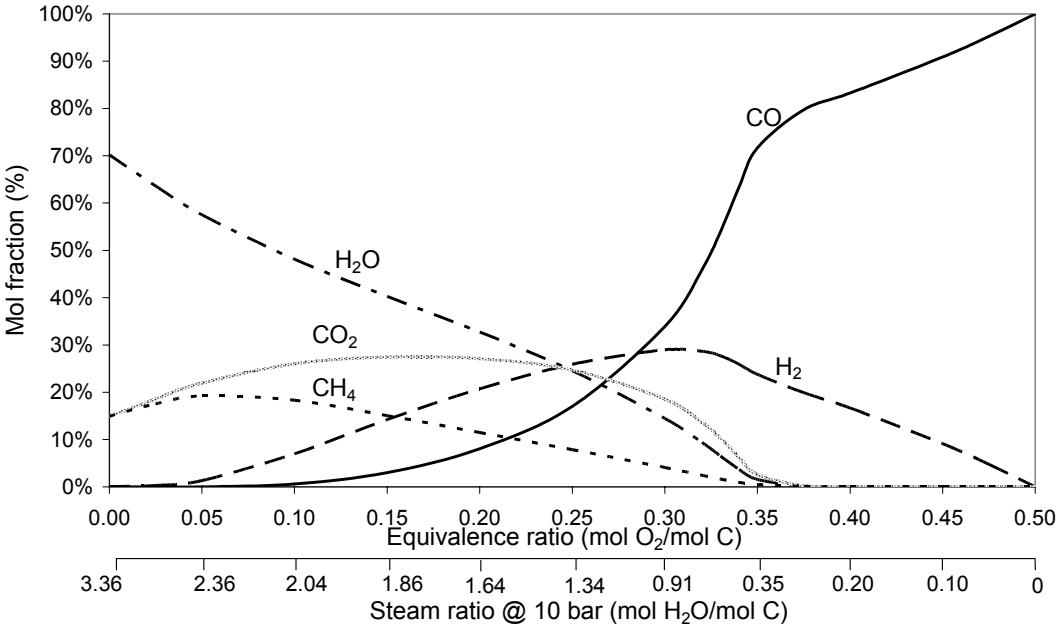

(b)

Figure 4.9: Gas phase composition for gasification of solid carbon using oxygen/ steam mixtures, (a) at atmospheric pressure (b) at 10 bar pressure

Figure 4.9 shows the gas phase compositions as a function of equivalence ratio and added steam (in a ratio that achieves complete gasification of carbon). Going down from an equivalence ratio of 0.5 down to 0.35, there is a linear increase in hydrogen concentration and linear decrease in carbon monoxide concentration. This could be expected because increasing the steam to oxygen ratio implies that reaction Eq. 4.4 increasingly replaces reactions Eqs. 4.1 and 4.3; in other words, more carbon is

reformed by steam rather than partially oxidized. Below an equivalence ratio of 0.35, the temperature has become low enough for formation of CO_2 and CH_4; also not all the steam that is added reacts away. At higher pressures, this point moves to an equivalence ratio of 0.37 since pressure promotes formation of CO_2 and CH_4.

The thermodynamic efficiency of complete gasification of carbon at various oxygen/steam ratios is shown in Figs. 4.10a-b, for both atmospheric pressure and a pressure of 10 bar. Figure 4.10a shows the efficiency for the gasifier only, while Fig. 4.10b shows net efficiencies, which incorporate irreversibilities occurring in production of oxygen and required electricity, and also for the production of steam. This study considers steam at 500 K and atmospheric pressure. Due to the low Carnot-factor of the steam, the efficiency of steam production would be less than 20% if it were produced in a boiler. If steam is produced by heat exchange with product gas, higher efficiencies are achievable; 50% is used as a conservative estimate. Interestingly, the efficiencies observed for pressurized gasification are slightly lower than for atmospheric gasification. However, this analysis is restricted only to the chemical reaction and does not involve possible compression work. If it is desirable to have the product gas available at elevated pressure, the work required to compress the producer gas respectively to inject the fuel into a pressured gasifier has to be taken into account.

Figure 4.10a demonstrates that, starting from ER=0.5, replacement of oxygen by steam improves the overall efficiency only slightly, but the chemical efficiency is improved substantially. An apparent local optimum is observed for atmospheric gasification at an ER of 0.33-0.34, corresponding to a temperature in the range of 1100-1200 K, and for pressurized gasification at an ER of 0.34-0.35, corresponding to a temperature of approximately 1200-1300 K. Such a local optimum was not found for gasification of fuels with low calorific value, such as biomass, because its carbon boundary temperature is below 1100 K (see Chapter 3). Intuitively, one might expect that an optimum gasification temperature exists. To understand this, it must be realized that in a gasifier, exothermic oxidation and endothermic reforming reactions are coupled. If the temperature in the gasifier is too low, the equilibria for the endothermic reforming reactions are unfavourable; on the other hand, if the temperature is too high, these equilibria are very favourable but too much oxidation takes place. This could be generalized to other reactors in which endothermic and exothermic reactions are coupled, such as autothermal methane reformers. The reason that the efficiency is further improved to the left of the local optimum is that formation of methane begins to occur. To prove this, hypothetical lines were calculated, where methane formation was not taken into account, and shown in Figure 4.10. Unless methane is the desired product, operation to the left of the local optimum is not recommended. In practice, the relatively low temperature promotes formation of not only methane, but also higher hydrocarbons (and possibly undesired tars).

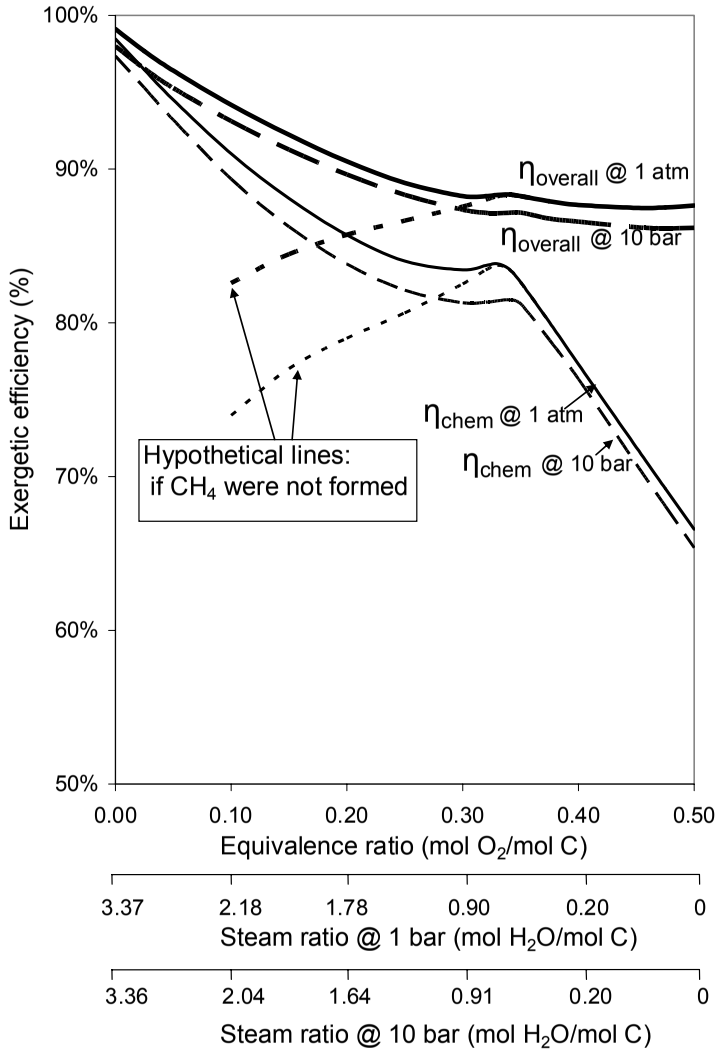

(a)

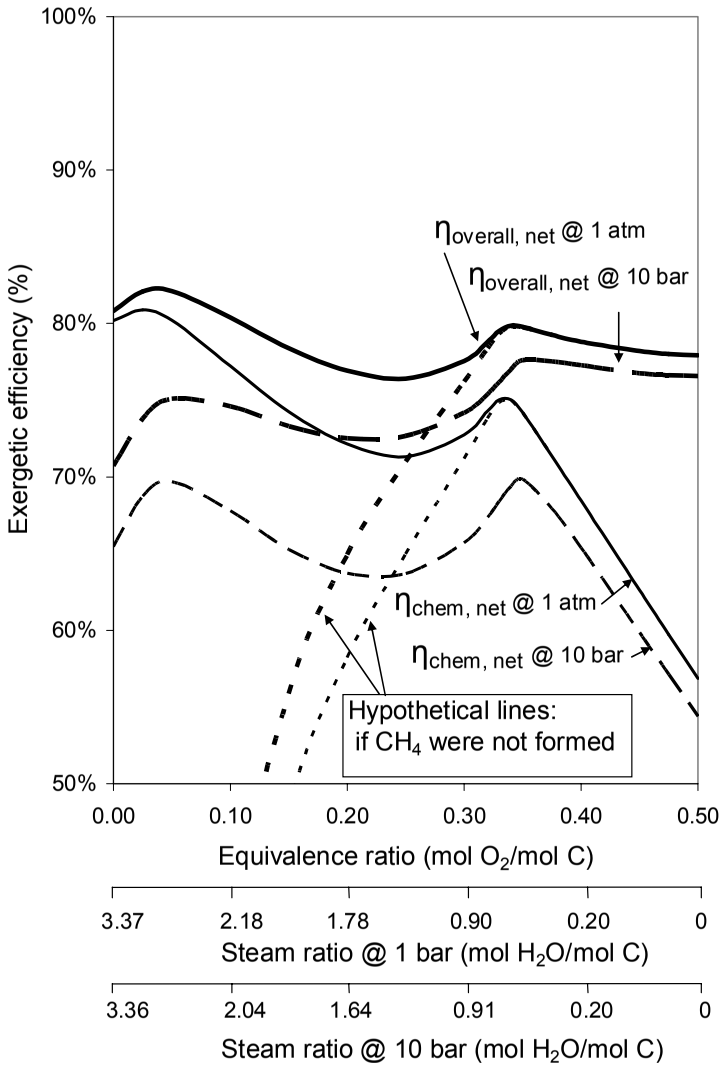

(b)

Figure 4.10: Chemical and overall efficiency for complete gasification of solid carbon using oxygen/steam mixtures at atmospheric pressure and 10 bar pressure, (a) gasifier efficiency (b) net efficiency

The net efficiencies in Figure 10b are considerably lower, but a similar increase in chemical efficiency (from 56.9% to 75.0%) is observed when the gasification temperature is moderated by introduction of steam. The local optimum becomes more pronounced, because steam requirements and associated exergy losses for steam production become much larger when the gasification temperature drops below 1100 K. Moderation of the gasification temperature is theoretically also feasible for air-blown gasification, but the benefits are smaller. In this case, the chemical efficiency increases from 66.3% to 75.4%, which is comparable to oxygen-blown gasification, although the overall efficiency remains higher. In practice, fuels with lower calorific value than pure carbon are used, so that steam injection into air-blown gasifiers is not recommended.

4.4.2.2 Results of detailed analysis

The relative exergy losses of gasification of carbon in the presence of steam can be seen in Figure 4.11, for the isothermal case. The main consequence of steam introduction is that losses for production of oxygen (and required electricity) and in the sub-processes of heating oxygen and heating fuel to the gasifier temperature are largely reduced. This is the benefit of operating at lower gasification temperatures. Below an equivalence ratio of 0.35, there is a strong increase in the exergy losses of steam production due to the increased amount of steam required for complete gasification. Furthermore, two things are apparent: up to 2% of exergy is lost due to product mixing since unreacted steam mixes with the reaction product, and the chemical reactions become more efficient due to formation of methane.

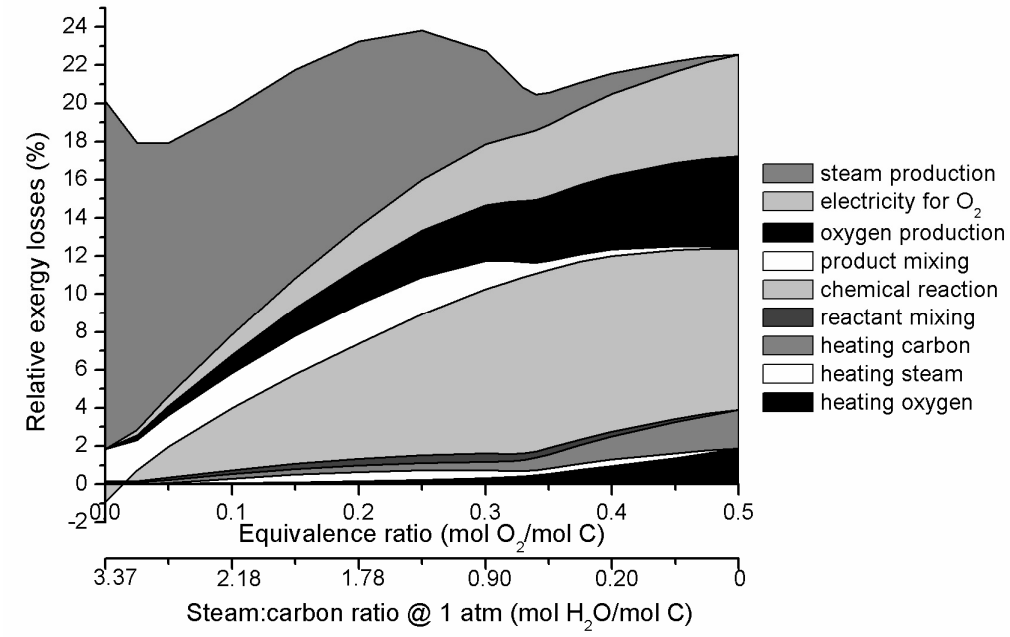

Figure 4.11: Relative exergy losses for subprocesses in complete gasification of solid carbon at atmospheric pressure using oxygen/steam mixtures (isothermal case)

In fact, if carbon is reacted only with steam, the following reaction takes place:

$$2\,C(s) + 2\,H_2O\,(g) \longrightarrow CH_4\,(g) + CO_2\,(g) \qquad \Delta G_{298} = +11.96\ kJ/mol\ CH_4 \qquad (4.19)$$

This reaction is thermodynamically up-hill and could take place only theoretically because an excess of steam cools down from its inlet temperature of 500 K, thus driving the reaction. In practice, the rate of reaction is infinitely slow. It must also be kept in mind that also other hydrocarbon products are thermodynamically stable at such low temperatures.

4.5 Conclusions and discussion

To compare exergy losses in gasification and combustion of solid carbon, the processes were conceptually divided into several subprocesses: instantaneous chemical reaction, heat transfer from reaction products to reactants (internal thermal energy exchange) and product mixing. For stoichiometric combustion of carbon with air, exergy losses due to internal thermal energy exchange (14-16% of expended exergy) are larger than those due to the chemical reaction (9-11% of expended exergy). In gasification, i.e. partial oxidation of the fuel, the reaction remains very efficient while the exergy losses related to internal thermal energy exchange (5-7% of expended exergy) are reduced due to the lower temperature. While the exergy losses due to chemical reaction are inherent, those due to internal thermal energy exchange are in principle avoidable. Methods to reduce these losses are replacement of air with oxygen, although this introduces additional process losses for separation of oxygen from air, or alternatively, preheating of air by heat exchange with product gas.

These results were obtained by focusing on the combustion respectively gasification units. However, it is important to realize that additional losses in the overall process system take place outside of the gasifier or combustor. For combustion, the exergy of product gas is present mainly in physical form, which is usually converted into electricity using relatively inefficient steam-Rankine cycles. For gasification, the product has a high chemical exergy, which can be converted into electricity using more efficient gas turbines, fuel cells or combined cycle technologies. In order to maximize the chemical exergy present in the product gas, for oxygen-blown gasification of fuels with high calorific value, such as solid carbon, it is advisable to moderate the temperature by introduction of steam. Optimum gasification temperatures in the ranges of 1100-1200 K (for atmospheric pressure) and 1200-1300K (for 10 bar pressure) have been observed. Operation at lower temperatures is not recommended as it leads to formation of methane and possibly higher hydrocarbons. Rather, the gasifier should be operated just above the optimum temperature, e.g. between 1200-1400K for atmospheric pressure and 1300-1500K for elevated pressures. In this way, up to 75% of the exergy contained in solid fuels

can be converted into chemical exergy of carbon monoxide and hydrogen. This conclusion may be generalized to other chemical reactors in which exothermic oxidation reactions and endothermic reforming reactions are coupled, such as autothermal methane reformers.

Appendix B: Definition of exergetic efficiency for gasification processes

To evaluate the performance of industrial processes, Grassmann (1950) has defined efficiency as the ratio of delivered exergy ("Nutzen") to expenditures ("Aufwand"):

$$\eta = \frac{\varepsilon_{\text{delivered}}}{\varepsilon_{\text{expended}}} = 1 - \frac{I}{\varepsilon_{\text{expended}}} \tag{4.20}$$

The efficiency equals zero, when the expended exergy is completely dissipated, while the efficiency becomes unity for a completely reversible process, for which I is always zero.

It is not always straightforward to identify which terms in the exergy balance should be classified as deliveries or expenditures. This may lead to different, sometimes subjective, definitions of efficiency. Baehr (1968) has systematically investigated the number of possible definitions. For a system with K ingoing exergy flows and N outgoing exergy flows, the number of possible efficiency definitions W equals:

$$W = K \cdot N \tag{4.21}$$

In gasification and combustion processes, two ingoing flows (solid fuel and gasifying medium) and two outgoing flows (product gas and possibly unconverted solid fuel) must be considered. The efficiency can thus be defined in four different ways:

$$\eta_I = \frac{\varepsilon_{unconv.fuel} + \varepsilon_{prod.gas}}{\varepsilon_{fuel} + \varepsilon_{gas.medium}} \tag{4.22}$$

$$\eta_{II} = \frac{\varepsilon_{prod.gas}}{(\varepsilon_{fuel} - \varepsilon_{unconv.fuel}) + \varepsilon_{gas.medium}} \tag{4.23}$$

$$\eta_{II} = \frac{\varepsilon_{unconv.fuel} + (\varepsilon_{prod.gas} - \varepsilon_{gas.medium})}{\varepsilon_{fuel}} \tag{4.24}$$

$$\eta_{IV} = \frac{(\varepsilon_{prod.gas} - \varepsilon_{gas.medium})}{(\varepsilon_{fuel} - \varepsilon_{unconv.fuel})} \tag{4.25}$$

If the exergy of the gasifying medium can be neglected, e.g. when air is used at atmospheric conditions (both chemical and physical exergy are zero), efficiencies η_I and η_{III} become equal and likewise efficiencies η_{II} and η_{IV}. Note that the unconverted fuel may leave the process at an elevated temperature, therefore it has

not only chemical but also physical exergy. This physical exergy term is regarded as exergy that has not yet been expended.

Efficiencies based on exergy differences result in lower values than those based on summation of in- and out-going exergy flows. For a biomass gasifier, it was found in Chapter 3 that η_I over predicts the gasification efficiency. The most stringent criterion η_{IV} relates better to the function of the gasifier, as it indicates the increase in exergy of gas divided by the decrease in exergy of solid fuel.

For η_I, the trivial result is obtained that the efficiency becomes unity when no fuel is consumed and no gas is produced, i.e. when the equivalence ratio approaches zero. For η_{IV}, the efficiency for ER→0 can be calculated, realizing that the temperature approaches the environmental temperature T_o. This means that the heat from carbon oxidation is dissipated at a low temperature level, so that only the chemical exergy is preserved. (Note that this is a rather theoretical case because oxidation of carbon at room temperature is kinetically limited). The limit of the efficiency η_{IV} for ER→0 therefore becomes, using respectively oxygen and air:

$$\eta_{oxygen} = \frac{(\varepsilon_{CO_2} - \varepsilon_{O_2})}{(\varepsilon_C)} = \frac{(19.87 - 3.97)}{(410.26)} = 3.88\% \qquad (4.26)$$

$$\eta_{air} = \frac{(0.21 \cdot \varepsilon_{CO_2} + 0.79 \cdot \varepsilon_{N_2} + RT_o(0.21 \ln 0.21 + 0.79 \ln 0.79) - \varepsilon_{air})}{(0.21 \cdot \varepsilon_C)} = \\ = \frac{(0.21*19.87 + 0.79*0.72 - 1.27 - 0)}{(0.21*410.26)} = 4.02\% \qquad (4.27)$$

References

Baehr HD (1968). On the definition of exergetic efficiency. A systematic study. Brennstoff-Wärme-Kraft 20(5):197-200 (in German).

Barin I (1989). Thermochemical data of pure substances: Part I and II. Weinheim, Germany: VCH Verlagsgesellschaft GmbH.

Cairns EJ, Tevebaugh AD (1964). CHO gas phase compositions in equilibrium with carbon, and carbon deposition boundaries at one atmosphere. J Chem Eng Data 9(3):453-462.

Caton JA (2000). On the destruction of availability (exergy) due to combustion processes – with specific application to internal-combustion engines. Energy 25:1097-1117.

Dunbar WR, Lior N (1994). Sources of combustion irreversibility. Combust Sci Techol 103:41-61.

Grassman P (1950). On the common definition of efficiency. Chemie-Ingenieur-Technik 22(4):77-80 (in German).

Groot A de (2004). Advanced exergy analysis of high temperature fuel cell systems. Petten: Energy research Centre of the Netherlands.

Kotas TJ (1980). Exergy criteria of performance for thermal plant. Int J Heat & Fluid Flow 2:147-163.

Lior N (2001). Irreversibility in combustion. In: Öztürk A, Gögüs YA, editors. Proceedings of ECOS 2001: efficiency, costs, optimization, simulation and environmental aspects of energy systems, Istanbul, Turkey, vol. 1., p. 39-48.

Moran MJ, Shapiro HN (1998). Fundamentals of engineering thermodynamics. 3rd ed. New York: Wiley.

Rath J, Wolfinger MG, Steiner G, Krammer G, Barontini F, Cozzani V (2003). Heat of wood pyrolysis. Fuel 82:81-91.

Simbeck DR, Dickenson RL, Oliver ED (1983). Coal gasification systems: a guide to status, application and economics, report AP-3109. Palo Alto, CA: EPRI.

Chapter 5

From coal to biomass gasification: comparison of thermodynamic efficiency[‡]

The effect of fuel composition on the thermodynamic efficiency of gasifiers and gasification systems is studied. A chemical equilibrium model is used to describe the gasifier. It is shown that the equilibrium model presents the highest gasification efficiency that can be possibly attained for a given fuel.
Gasification of fuels with varying composition of organic matter, in terms of O/C and H/C ratio as illustrated in a Van Krevelen diagram, is compared. It was found that exergy losses in gasifying wood (O/C ratio around 0.6) are larger than those for coal (O/C ratio around 0.2). At a gasification temperature of 927°C, a fuel with O/C ratio below 0.4 is recommended, which corresponds to a lower heating value above 23 MJ/kg. For gasification at 1227°C, a fuel with O/C ratio below 0.3 and lower heating value above 26 MJ/kg is preferred. It could thus be attractive to modify the properties of highly oxygenated biofuels prior to gasification, e.g. by separation of wood into its components and gasification of the lignin component, thermal pre-treatment, and/or mixing with coal in order to enhance the heating value of the gasifier fuel.

5.1 Introduction

Gasifiers can be designed to gasify almost any kind of organic feed. A wide variety of fuels, such as many types of wood, agricultural residues, peat, coal, anthracite, oil residues and municipal solid waste may be considered. During the oil crisis in the late 1970's and through to the middle of the 1980's, coal was regarded as a very important substitute for oil. Reserves of coal are abundant and more geographically spread over the world than crude oil. In this period, several coal gasifiers were developed and commercialized. However, due to a large drop in the oil price, coal gasification did not gain a much larger share of the energy market, although heavy oil gasification is commercially practiced at several refineries.

During the last decennium, there has been renewed interest in gasification. Focus is less on coal, but more on biomass gasification as a form of renewable energy. Introduction of biomass as a renewable energy source is vital for the transition to a more sustainable society. An example for the shift from coal to biomass is the

[‡] Presented at the ECOS 2003 conference, Copenhagen, Denmark.

power station in Buggenum, the Netherlands, which integrates coal gasification and combined cycle technology. Recently, a decision was made to co-gasify up to 50% of biomass in order to generate a high proportion of 'green energy' (van Veen, 2002). The Kyoto protocol emphasizing the need to combat carbon dioxide emission has also been an impetus for the interest in biomass gasification. Carbon dioxide emissions from using biomass as a fuel are perceived as neutral because this carbon dioxide is fixed by photosynthesis in a relatively short period. Nevertheless, it has been argued that society should try to use biomass with the same thermodynamic efficiency as fossil fuels, regardless of its perceived CO_2-neutrality (Hirs, 2001). It is important from an energy saving and environmental point of view to find out whether biomass can be gasified with the same efficiency as coal.

An interesting difference between coal and biomass lies in the composition of their organic matter: woody biomass contains typically around 50 wt% carbon and 45 wt% oxygen, whereas coal contains (depending on coal rank) 60-85 wt% carbon and 5-20 wt% oxygen. One might argue that the high oxygen content of biomass is beneficial because less oxygen needs to be added for gasification; on the other hand, biomass has a relatively low calorific value, which would not be beneficial for gasification. The fundamental question which fuel composition is more advantageous for gasifiers is addressed in this study.

The evaluation of gasification efficiency is based on exergy analysis (formerly known in the USA as availability analysis). The exergetic efficiency is based on the first as well as the second law of thermodynamics, which is useful because it considers not only the decrease in energy of combustion of the product gas compared to the solid fuel (due to partial oxidation) but also increases in entropy (as a solid fuel is decomposed into many smaller molecules). In the 1980's, exergy analysis was applied to evaluate coal gasification processes (Rodriguez et al., 1980; Tsatsaronis, 1982; Wen, 1983). Later, biomass gasifiers were analyzed (Chern et al., 1989; Anikeev et al., 1996; Chapter 3, this thesis). These analyses show that second-law efficiencies are considerably lower than first-law efficiencies, e.g. for a coal gasifier, the first law efficiency is nearly 100% for a well-insulated gasifier with negligible heat losses, whereas the second law efficiency equals 79% (Rodriguez et al., 1980). However, the results of these analyses are difficult to compare because the gasification processes are not always analyzed on the same basis, e.g. both autothermal and allothermal gasifiers have been considered, complete and incomplete carbon conversions, etc. Therefore, this chapter comprises a comprehensive analysis of the effect of the fuel type and related fuel composition on the efficiency that can be attained in a gasifier.

The chapter starts with a description of the applied methodology, notably: which fuels are considered, what their thermodynamic properties are, and how the gasification efficiency is defined. As a chemical equilibrium model is applied

throughout this study to describe the performance of gasifiers, its main assumptions and their validity for practical gasifiers is considered in a separate section. It is demonstrated that the equilibrium model indicates the maximum efficiency that can possibly be attained when gasifying a fuel. Finally, results are given that compare the attainable gasification efficiency for the various fuels considered.

5.2 Methodology

5.2.1 Gasifier fuel properties

As a gasifier fuel, biomass and coal vary in many properties, such as their heating values, proximate analyses (fixed carbon, volatile material, ash content and moisture content), ultimate analyses (amounts of carbon, hydrogen, oxygen, sulphur, nitrogen, chloride and other impurities) and sulphur analyses (type of sulphur present). For example, the organic matter in biomass contains a lot of volatile material, namely 70-80 wt%. Coals range from lignite with approximate volatile matter of 27% to anthracite with an average of 5%, with sub-bituminous and bituminous coals intermediate between these values.

The change in composition from biomass to coal is illustrated using a diagram developed by van Krevelen (1993). Figure 5.1 shows the change in atomic ratios H/C and O/C from biomass to peat, lignite, coal and anthracite. The figure specifically shows the composition of lignocellulose, i.e. wood, since this is the most abundant biofuel. Wood is related to coal because it is the precursor for its formation in nature by various coalification processes. Vitrinite, the most important constituent of coal, descends from woody tissue (van Krevelen, 1993).

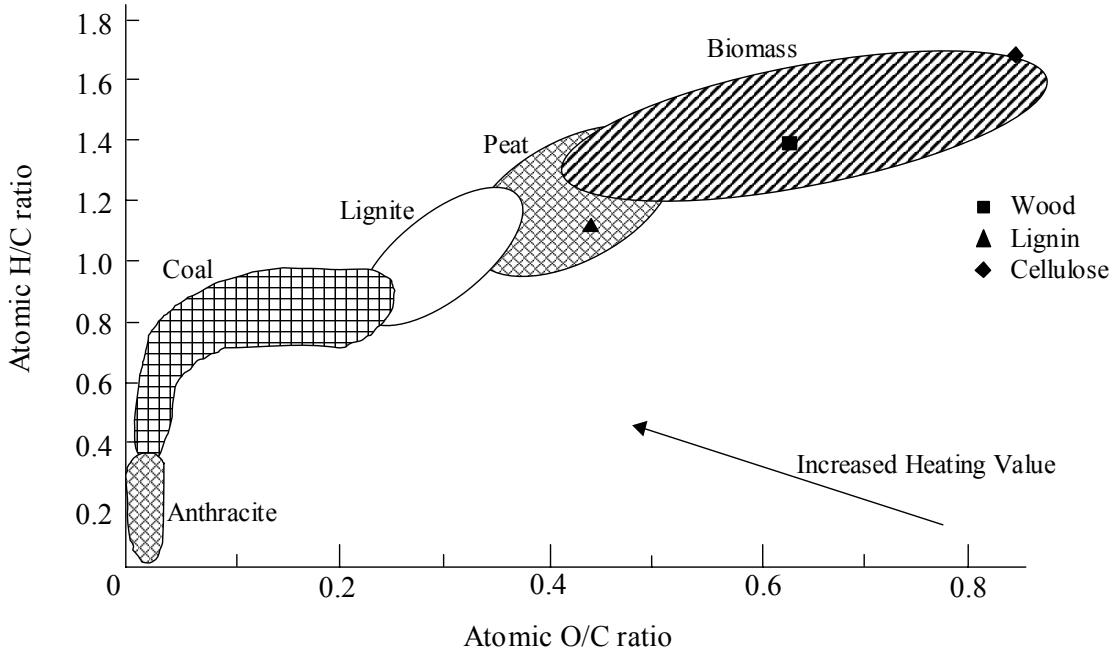

Figure 5.1: Van Krevelen diagram

This chapter aims to compare gasification efficiencies that can be attained for all fuels mentioned in the Van Krevelen diagram. Focus is on the composition of the organic material in the fuel, i.e. on dry- and ash-free fuels, taking into account only the most important constituents: carbon, hydrogen and oxygen.

In order to perform thermodynamic calculations for reacting fuels with oxygen, their thermodynamic properties must be available, such as the heating values and chemical exergies (or alternatively, enthalpy and entropy of formation). Thermodynamic properties of most fuels are not exactly known, except those for cellulose, because the structure of these fuels is not well defined. Statistical correlations are used to overcome this problem. The higher heating value can be accurately predicted by the correlation developed by Channiwala and Parikh (2002) (in MJ/kg):

$$HHV_{fuel} = 0.3491\, z_C + 1.1783 z_H - 0.1034 z_O - 0.0151 z_N + 0.1005 z_S - 0.0211 z_A \qquad (5.1)$$

In this equation, HHV_{fuel} is the higher heating value of the fuel in MJ/kg, and z_A, z_C, z_H, z_N, z_O and z_S the weight fractions of ashes, carbon, hydrogen, nitrogen, oxygen and sulphur (wt% dry), respectively.

The equation was developed for a wide spectrum of fuels, including the whole range from coal to biomass. It has a standard deviation from experimentally determined values of only 1.45% and the bias error is negligible. Since the gasifier is regarded as a CHO system, only the first three terms apply. The higher heating value is converted to lower heating value using the enthalpy of evaporation for water formed during combustion. Finally, the statistical correlation of Szargut and Styrylska (1964) was used to calculate the chemical exergy of the fuel:

$$\varepsilon_{ch,\,fuel} = \beta \cdot LHV_{fuel} \qquad (5.2)$$

with:

$$\beta = 1.0438 + 0.0158 \cdot \frac{H}{C} + 0.0813 \cdot \frac{O}{C} \qquad \text{for: } \frac{O}{C} \le 0.5 \qquad (5.3)$$

$$\beta = \frac{1.0414 + 0.0177 \cdot \frac{H}{C} - 0.3328 \cdot \frac{O}{C} \cdot \left[1 + 0.0537 \cdot \frac{H}{C}\right]}{1 - 0.4021 \cdot \frac{O}{C}} \qquad \text{for: } 0.5 < \frac{O}{C} \le 2 \qquad (5.4)$$

In these equations, LHV_{fuel} is the lower heating value of fuel in MJ/kg, $\varepsilon_{ch,fuel}$ the chemical exergy of fuel in MJ/kg, β the ratio of chemical exergy and lower heating value of fuel, and C, H, O the mole fractions of carbon, hydrogen and oxygen in the fuel, respectively.

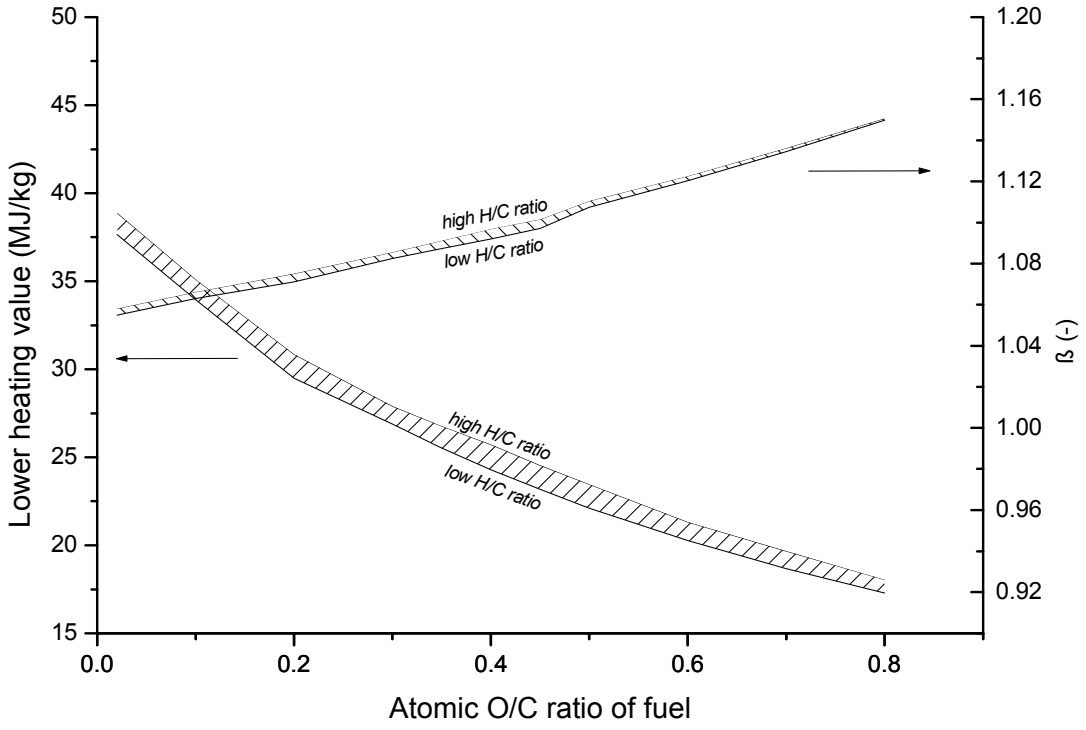

Figure 5.2: Lower heating value and ratio of chemical exergy to lower heating value of fuels shown in the Van Krevelen diagram

Figure 5.2 displays the lower heating values and the ratios of chemical exergies to lower heating values as a function of the fuel composition shown in the Van Krevelen diagram. The effect of H/C ratio on these parameters is much smaller than that of the O/C ratio. Therefore, they are plotted only as a function of O/C ratio with the area representing realistic H/C ratios, as these occur in the van Krevelen diagram. This approach is also followed in the rest of this chapter. Obviously, fuels with high O/C ratio have a smaller heating value than those with low O/C ratio.

However, the factor β increases with increasing O/C ratio, which indicates that by decomposing a fuel with high O/C ratio, relatively more work may be delivered. This effect is known from structurally well-defined compounds, e.g. when comparing the ratio between chemical exergy and lower heating value for methane (O/C of 0) and methanol (O/C of 1). For methane, this ratio is 1.037 (831.65 kJ/mol / 802.33 kJ/mol), whereas for methanol the ratio is 1.125 (718/638.4). The high value for β is related to the high reactivity of oxygenated compounds.

5.2.2 Gasification efficiency

The gasification efficiencies are determined for a gasifier as well as a gasification system. For the gasifier, shown in Fig. 5.3a, the thermodynamic efficiency is defined as the exergy increase of the gas divided by the exergy decrease of the solid

fuel. The gasifier efficiency $\Psi_{gasifier}$ of gasifying a fuel with pure oxygen and optionally steam is therefore given by:

$$\Psi_{gasifier} = \frac{\Phi_{m,gas}\,(\varepsilon_{ch,gas} + \varepsilon_{ph,gas}) - \Phi_{m,oxygen}\varepsilon_{ch,oxygen} - \Phi_{m,steam}(\varepsilon_{ch,steam} + \varepsilon_{ph,steam})}{\Phi_{m,fuel}\varepsilon_{ch,fuel} - \Phi_{m,fuel\_unconv}\,(\varepsilon_{ch,fuel\_unconv} + \varepsilon_{ph,fuel\_unconv})} \quad (5.5)$$

Where: $\varepsilon_{ch,fuel\_unconv}$, $\varepsilon_{ch,oxygen}$, $\varepsilon_{ch,steam}$, and $\varepsilon_{ch,gas}$ are the chemical exergy of unconverted fuel, oxygen, steam and gas, respectively; $\varepsilon_{ph,fuel\_unconv}$, $\varepsilon_{ph,steam}$ and $\varepsilon_{ph,gas}$ are the physical exergy of unconverted fuel, steam and gas, respectively, all in MJ/kg. The mass flow rates of fuel, unconverted fuel, oxygen, steam, and gas are indicated by $\Phi_{m,fuel}$, $\Phi_{m,fuel\_unconv}$, $\Phi_{m,oxygen}$, $\Phi_{m,steam}$ and $\Phi_{m,gas}$, respectively, all in kg/s.

The gasifier is part of a gasification system, shown in Fig. 5.3b, which includes steam, oxygen and electricity production units. Since these units consume exergy, irreversibilities also take place outside of the gasifier. To enable a fair comparison between all fuels, the above-mentioned efficiencies have to be corrected with the irreversibilities occurring in these production units. This correction is done on the basis that electricity required for oxygen production and process steam are generated from gasification product gas. This leads to the following definition:

$$\Psi_{system} = \frac{\Phi_{m,gas}\,(\varepsilon_{ch,gas} + \varepsilon_{ph,gas}) - I_{oxygen\_production} - I_{electricity\_production} - I_{steam\_production}}{\Phi_{m,fuel}\,\varepsilon_{ch,fuel} - \Phi_{m,fuel\_unconv}\,(\varepsilon_{ch,fuel\_unconv} + \varepsilon_{ph,fuel\_unconv})} \quad (5.6)$$

In which I is the irreversibility in MJ/s, with the subscript indicating the type of (sub-) process.

For large-scale oxygen production, cryogenic separation of air is the most widely applied process. The electricity consumption of large-scale cryogenic oxygen plants is approximately 380 kWh/ton oxygen (Simbeck et al., 1983). This is equivalent to an exergetic efficiency of 9.1%. Electricity required for oxygen production can be generated from gasification product gas in gas turbines or fuel cells; an exergetic efficiency of 50% is assumed for this process. Steam can be produced by heat exchange with the product gas. This study considers steam at 500 K and atmospheric pressure. This relatively low steam quality is preferably produced by heat exchange with product gas, rather than in a boiler. For a well-designed heat exchanger, a thermodynamic efficiency of 50% can be achieved. The chemical exergy of all gaseous components is obtained from Szargut et al. (1988). Finally, the exergy of air and water, required for oxygen and steam production, is negligible.

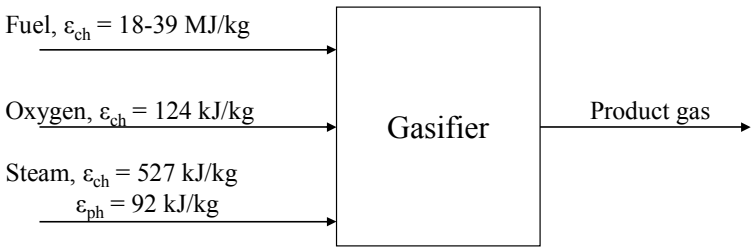

(a)

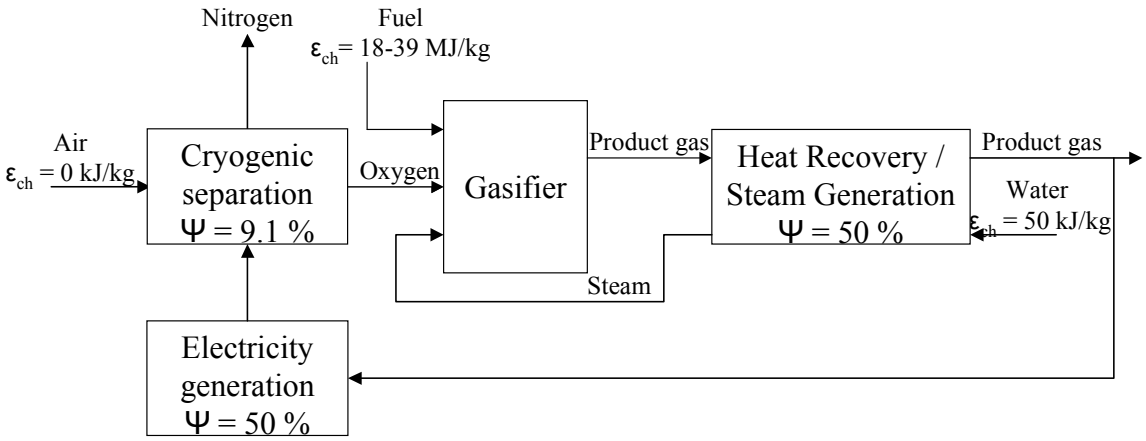

(b)

Figure 5.3: Block diagram of (a) gasifier and (b) gasification system

For the calculation of physical exergy, it is essential to use accurate data for the enthalpy and entropy in order to obtain accurate results. Thermodynamic data depend on the heat capacity as a function of temperature. Commonly used third-order polynomial equations give large deviations at temperatures above 1000 K. To overcome this problem, a more advanced equation developed by Barin (1989) is used for all components. The physical exergy of the product gas consists only of a temperature-dependent term, i.e. the work content of the sensible heat of the product gas. A pressure-dependent term is not included because gasification at atmospheric pressure is considered.

This chapter also uses the so-called chemical efficiency, which is calculated by neglecting the physical exergy of product gas in Eq. 5.5 and/or Eq. 5.6. The chemical efficiency indicates how well the chemical exergy of fuel is preserved in the chemical exergy of product gas.

5.2.3 Process losses

To gain more understanding of the observed thermodynamic efficiency, it is possible to analyze the various sub-processes occurring in a gasifier. This methodology has been described in more detail in Chapter 4. Gasification is

conceptually assumed to be a sequence of the following steps: heating of solid fuel and reactant gases to the gasification temperature, mixing of reactant gases, instantaneous chemical reaction, heat transfer to the reactant molecules, and product mixing. The rate of heat transfer determines at which temperature the chemical reaction takes place. If heat transfer is very fast, the gasifier is isothermal so that the product molecules have the same temperature as the reactant molecules. However, if heat transfer is slow, the temperature of product molecules may be much higher than the reactant molecules. For practical purposes, only the isothermal case is considered here.

For each sub-process, the irreversibilities can be calculated. The overall irreversibilities equal the sum of the irreversibilities of the subprocesses:

$$I_{\text{overall}} = I_{\text{heating\_fuel}} + I_{\text{heating\_O}_2} + I_{\text{heating\_steam}} + I_{\text{reactant\_mixing}} + I_{\text{chemical\_reaction}} + I_{\text{product\_mixing}} \quad (5.7)$$

The irreversibilities for heating of the solid fuels cannot be calculated separately because the heating capacities of complex fuels are not known as a function of temperature, and also pyrolysis takes place when these fuels are heated. Therefore, the irreversibilities for heating of fuel and chemical reaction are combined. The irreversibilities can be divided by the expended exergy, so that they are expressed as relative exergy losses. The sum of these relative exergy losses is the fraction of the expenditures lost through irreversibility. Irreversibilities occurring in oxygen, electricity and steam production units gasification systems can also be taken into account as relative exergy losses.

5.3 Gasifier models

5.3.1 Equilibrium model

A chemical equilibrium model is applied to predict the product gas composition, gas amount and carbon conversion in gasifiers. Equilibrium models are valuable because they predict the thermodynamic limits of the gasification reaction system. The equilibrium model has been extensively documented in literature (Gumz, 1950; Cairns and Tevebaugh, 1964; Baron et al., 1976; Kovacik et al., 1990) and applied for performance evaluations (Desrosiers, 1979; Chern, 1989). However, it remains important to realize that the main assumptions behind this model may not always be valid for practical gasifiers. These assumptions are discussed below:

- The gasifier is often regarded as a perfectly insulated apparatus, i.e. heat losses are neglected. In practice, gasifiers have heat losses to the environment, but this term can be incorporated in the enthalpy balance of the equilibrium model.

- Perfect mixing and a uniform temperature are assumed for the gasifier. Different hydrodynamics are observed in practice, depending on the design of the gasifier. Gasification technologies utilize fixed bed, moving bed, fluidized bed or entrained bed reactors, in which the contacting pattern of gas and solid, and their residence times differ. For example, if wood is gasified in a counter-current moving bed gasifier, devolatilization takes place before the particles reach the hot zone in the bottom of the gasifier, volatiles are contained in the product gas stream, and the composition of this gas stream will be very different from the equilibrium composition. In a cocurrent moving bed gasifier, these volatiles pass through a narrow cross section, the so-called throat, in which the temperature is high. The equilibrium model has much better predictive potential for this gasifier (Hos et al., 1980). The hydrodynamics of large-scale gasifiers, such as fluidized bed and entrained flow gasifiers, are more favourable than for moving bed gasifiers, but the residence time of the solids is much shorter.
- The model assumes that gasification reaction rates are fast enough and residence time is sufficiently long to reach the equilibrium state. The kinetics of gasification reactions are complicated: in the gasifying process, thermal pyrolysis, homogeneous gas phase and heterogeneous gas-solid reactions take place, so that thousands of chemical reactions may occur (Kovacik et al., 1990). Although it is difficult to determine the intrinsic kinetics of these reactions, many researchers agree that steam and carbon dioxide reforming reactions of char are kinetically limited at gasification temperatures lower than 1000°C (Kersten, 2002). Furthermore, the product gas of fluidized bed gasifiers generally contains tar, which is not considered in equilibrium models, and much more hydrocarbons (especially methane) than predicted. For entrained flow gasifiers, which operate at temperatures in the range of 1050-1400°C, the approach to equilibrium is much better. E.g. for a Shell coal gasifier, all predicted gas species are within 0.7% absolute of the measured values, and equilibrium temperatures are very close to the gasifier exit temperatures (Watkinson et al., 1991).

5.3.2 'Quasi'-equilibrium models

In order to describe the behaviour of fluidized bed gasifiers more accurately, modifications have been made to the equilibrium model. Empirical parameters have been added, such as the amount of methane in the product gas (Maniatis et al., 1994) and/or the carbon conversion (Li et al., 2001). Inclusion of empirical parameters leads to a better agreement with experimental data, but the model looses much of its predictive capabilities.

Another approach is the use of 'quasi'-equilibrium temperatures, whereby the equilibria of the reactions defined in the model (see Eqs. 5.8-5.10) are evaluated at a temperature, which is lower than the actual process temperature.

$$C + 2\,H_2 = CH_4 \qquad (5.8)$$

$$C + H_2O = CO + H_2 \qquad (5.9)$$

$$C + CO_2 = 2\,CO \qquad (5.10)$$

This approach was introduced by Gumz (1950). For fluidized bed gasifiers, the average bed temperature can be used as the process temperature, whereas for downdraft gasifiers, the outlet temperature at the throat exit should be used. Bacon (1982) defined 'quasi'-equilibrium temperatures for each independent chemical reaction. Li et al. (2001) found that the kinetic carbon conversion for pressurized gasification of subbituminous coal in the temperature range of 747-877°C is seen to be comparable to equilibrium predictions for a temperature of about 250°C lower. Based on 75 operational data points measured in circulating fluidised bed (CFB) gasifiers operated on biomass, Kersten (2002) has shown that for operating temperatures in the range of 740-910°C, the reaction equilibria of Eqs. 5.8-5.10 should be evaluated at much lower temperatures (respectively 457 ± 29°C, 531 ± 25°C, and 583 ± 25°C). These 'quasi'-equilibrium temperatures appear to be independent of process temperature in this range.

An important subject, which has not yet been studied thoroughly in the gasification literature, is whether kinetic limitations increase or decrease the efficiency of gasifiers. To this end, Appendix C compares gasification at equilibrium conditions with 'quasi' equilibrium conditions. The conclusion is reached that the gasification efficiency is severely affected when the gasification reactions of Eqs. 5.9 and 5.10 are kinetically limited and do not contribute sufficiently to the carbon conversion. The equilibrium model therefore indicates the maximum efficiency that can possibly be attained when gasifying a fuel. This model is applied in the next section to study the effect of changes in fuel composition on the maximum gasification efficiency. As a word of caution, it must be realized that it is difficult to reach this maximum at gasification temperatures below 1000°C, even for reactive fuels such as biomass. This may require operation at prolonged residence times (e.g. in a bubbling fluidized bed, the carbon conversion appears to be higher than in a CFB (Kersten, 2002)), higher pressures to increase the char reforming rates (although less favourable for the equilibrium of these reactions), which is demonstrated by the relatively high carbon conversion of the Värnamö gasifier (Ståhl et al., 2001), and/or catalytically active bed materials such as dolomite or olivine (Corella et al., 2004).

5.4 Results

5.4.1 Gasification temperatures and equivalence ratios

The gasification efficiency that can be achieved as a function of fuel composition is evaluated at three different temperatures: the carbon boundary temperature (the temperature obtained when exactly enough oxygen is added to achieve complete gasification), and reference temperatures of 927°C and 1227°C. It was shown in Chapter 4 that the reference temperature of 927°C is beneficial to preserve the chemical exergy of the fuel in the product gas. However, it is evident from the previous section that higher temperatures may very well be required in practice, in order to reduce kinetic limitations. Therefore, a temperature of 1227°C is also included as a reference temperature. Figure 5.4 shows the carbon boundary temperatures for gasification of fuels with different O/C and H/C ratios, as well as the reference temperatures. It can be observed that lower oxygen content in the fuel corresponds to a higher carbon boundary temperature. Optimum gasification temperatures were found to increase from 782°C for biomass (average composition $CH_{1.4}O_{0.6}$) to 1668°C for gasification of coal (average composition $CH_{0.95}O_{0.2}$) gasification.

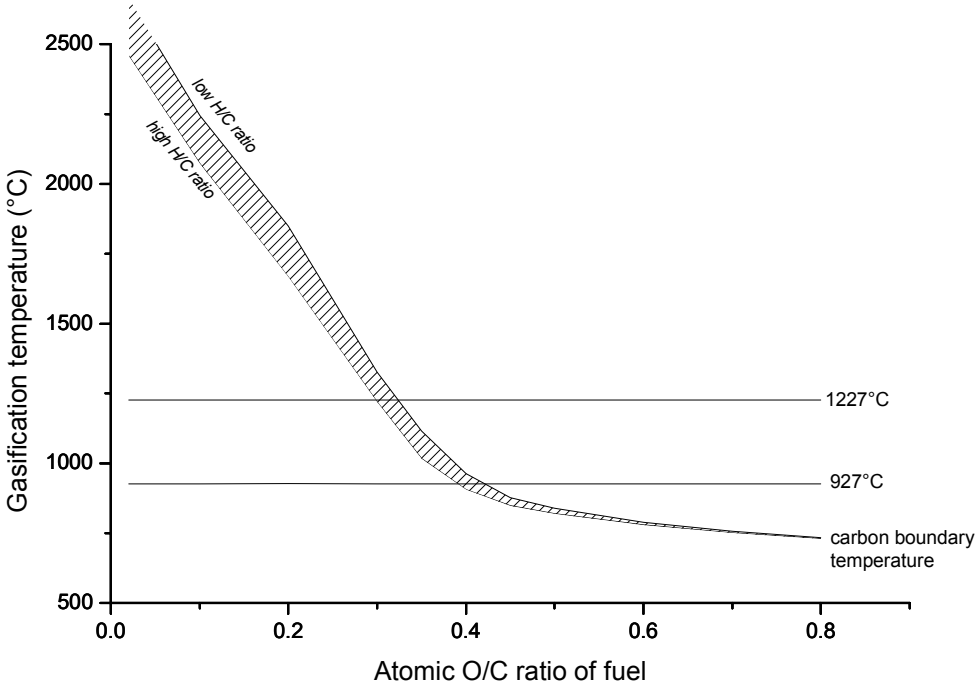

Figure 5.4: Gasification temperatures for fuels of varying O/C and H/C ratio

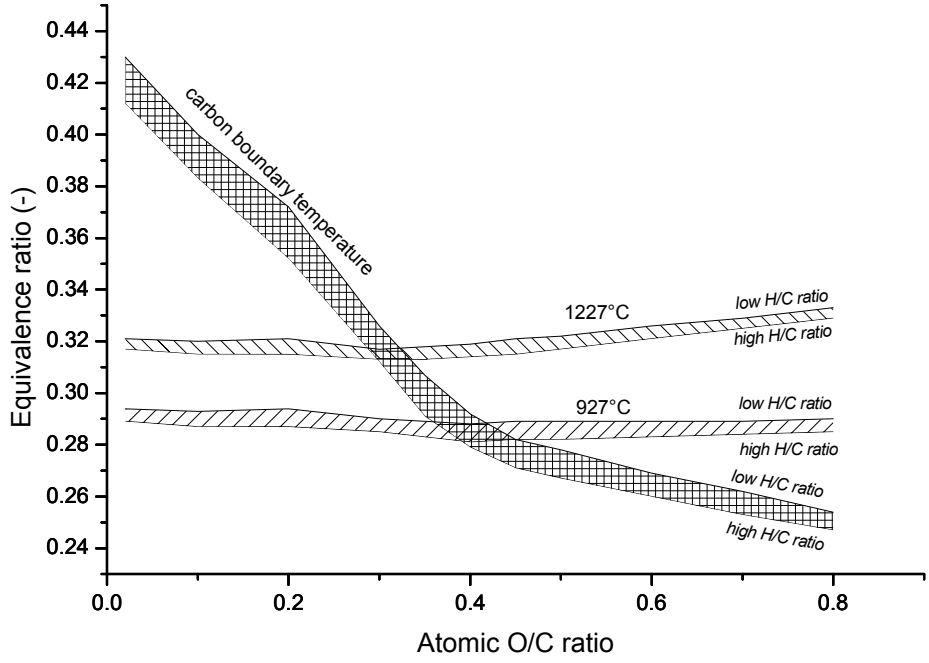

Figure 5.5: Minimum equivalence ratios for gasification of fuels of varying O/C and H/C ratio at different temperatures

Figure 5.5 shows the equivalence ratio required, depending on the desired gasification temperature, for different O/C and H/C ratios of the fuel. The equivalence ratio expresses the amount of oxygen required for gasification relative to the amount required for combustion. Equivalence ratios may range from 0.244 for cellulose to 0.500 for pure carbon (graphite), as exemplified in the equations below.

Cellulose gasification:

$$C_6(H_2O)_5 + 1.461\ O_2 = 4.567\ CO + 1.295\ CO_2 + 0.138\ CH_4 + 3.958\ H_2 + 0.766\ H_2O \quad (5.12)$$

Cellulose combustion:

$$C_6(H_2O)_5 + 6\ O_2 = 6\ CO_2 + 5\ H_2O \quad (5.13)$$

Carbon gasification:

$$C + \tfrac{1}{2}\ O_2 = CO \quad (5.14)$$

Carbon combustion:

$$C + O_2 = CO_2 \quad (5.15)$$

As expected, it becomes clear from Fig. 5.5 that coal gasifiers operated at the carbon boundary temperature require much higher equivalence ratios than biomass gasifiers. For fuels with O/C ratios above 0.4 (corresponding to carbon boundary

temperatures below 927°C), the required equivalence ratio increases only moderately with decreasing O/C ratios. This happens because the increased extent of oxidation is accompanied by an increased extent of reforming, as the reaction equilibria of Eqs. 5.9 and 5.10 become more favourable at higher temperature. If gasification is carried out at a fixed reference temperature, the difference in equivalence ratios levels out. The equivalence ratios become fairly constant for all fuels, around 0.29 for a gasification temperature of 927°C and 0.32-0.33 for a gasification temperature of 1227°C. At low O/C ratios, steam partly replaces oxygen, so that lower equivalence ratios are sufficient, whereas at high O/C ratios, more oxygen is required to reach the desired temperatures. In other words, biomass is gasified above its carbon boundary temperature by over-oxidizing the fuel, where coal may be gasified below its carbon boundary temperature by moderation with steam.

5.4.2 Gasification efficiencies

Figure 5.6a shows the thermodynamic efficiencies corresponding to oxygen-blown gasification of fuels with different O/C and H/C ratio. For gasification at the carbon boundary temperature, the overall efficiency as well as chemical efficiency rises when decreasing the O/C ratio from 0.8 to 0.4. Beyond this point, the overall efficiency increases only marginally, whereas the chemical efficiency decreases. This is caused by the sharp temperature increase at O/C ratios below 0.4 (see Fig. 5.4), which results in a high physical exergy of the product gas has, but low chemical exergy. For gasification at 927°C respectively 1227°C, the chemical efficiency in the O/C region below 0.4 is improved substantially due to moderation of the temperature with steam, with the chemical efficiency at 927°C approximately 2 %-points higher than at 1227°C. Moderation of the temperature hardly changes the overall efficiency. For fuels with high O/C ratios, such as biomass, the efficiencies at a gasification temperature of 927°C or 1227°C are considerably lower than at the carbon boundary temperature. These fuels need to be over-oxidized in order to reach the desired gasification temperature. Therefore, more oxygen is used than necessary for complete gasification, which causes thermodynamic losses.

Figure 5.6b shows thermodynamic efficiencies for gasifying fuels of varying composition, when exergetic losses for production of oxygen, electricity and steam are taken into account. The effect of these additional exergetic losses is substantial. The losses incurred for producing oxygen are most obvious for gasification of fuels with low O/C ratios at the carbon boundary temperature, which need high equivalence ratios to be gasified. The curves for overall and chemical efficiency flatten somewhat; this happens below an O/C ratio of 0.4 for gasification at 927°C and an O/C ratio of 0.3 for gasification at 1227°C.

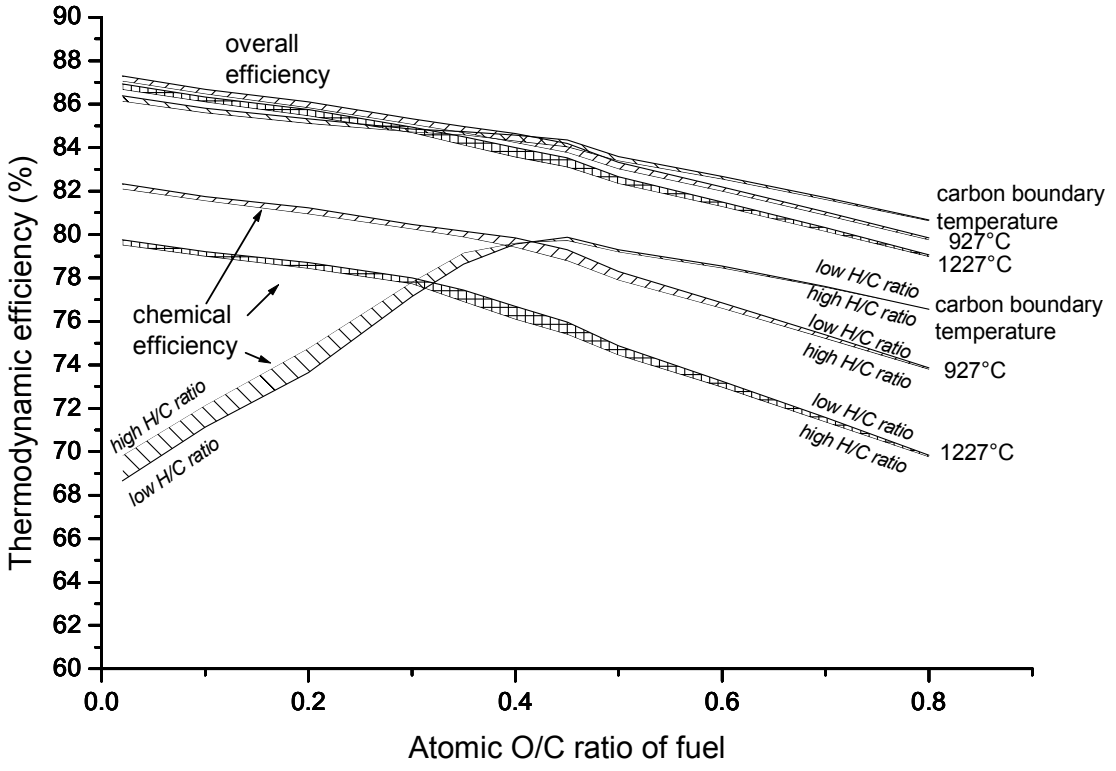

(a)

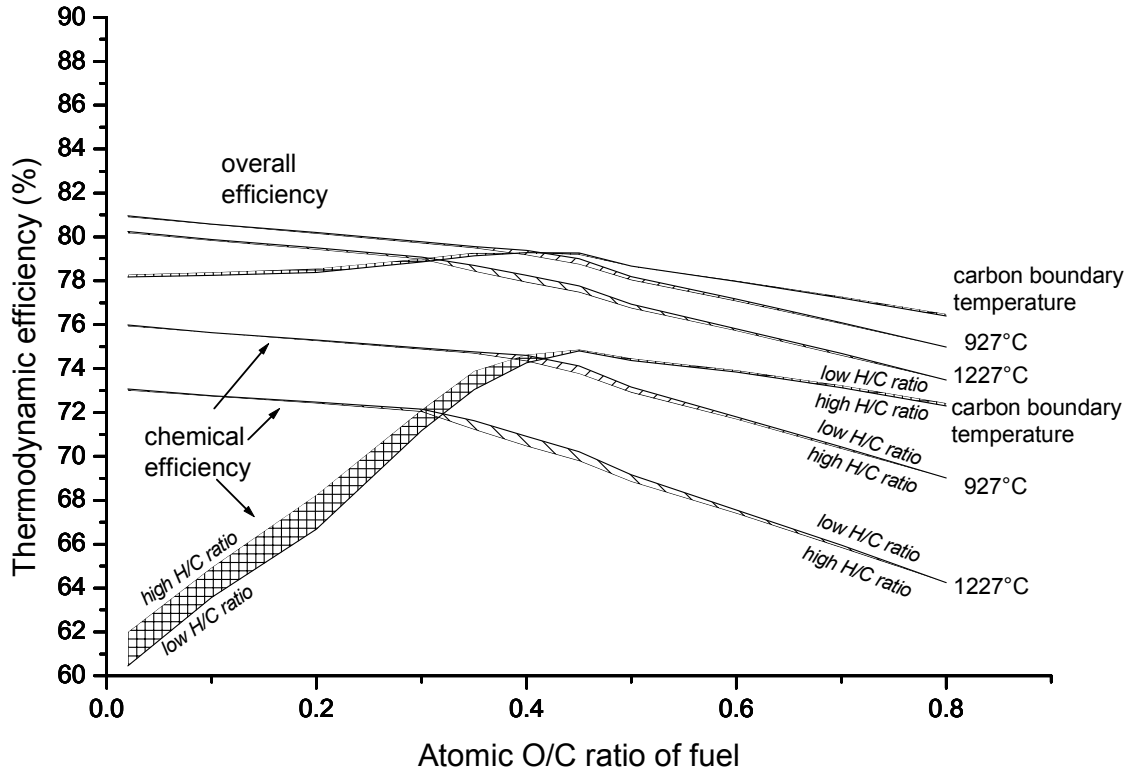

(b)

Figure 5.6: Thermodynamic efficiency of gasification of fuels of varying O/C and H/C ratio at different temperatures for (a) gasifier and (b) gasification system

5.4.3 Process losses

Figure 5.7 shows, as an illustration, the relative exergy losses for gasification at 927°C. Apart from exergy losses occurring in sub-processes in the gasifier, also exergy losses for production of oxygen, electricity and steam are shown. The exergy losses due to heating of fuel and chemical reaction are by far the largest contribution to the overall exergy losses. These losses correlate very well with β, the ratio of chemical exergy to lower heating value. Therefore, it can be concluded that fuels with a low β are preferred in order to achieve high exergetic efficiency.

Exergy losses due to oxygen and electricity production consume 5-6% of the fuel's exergy. These losses increase only slightly with decreasing O/C ratio because the required equivalence ratio is nearly constant. Figure 5.7 explains the slight flattening of efficiency curves below an O/C ratio of 0.4, observed in Figure 5.6b. Below this ratio, steam is introduced to moderate the gasification temperature. Although the exergetic losses due to heating of fuel and chemical reaction continue to decrease below 0.4, these are partially compensated by the losses incurred for steam production, and to a smaller extent for heating of steam and mixing of reactant gases.

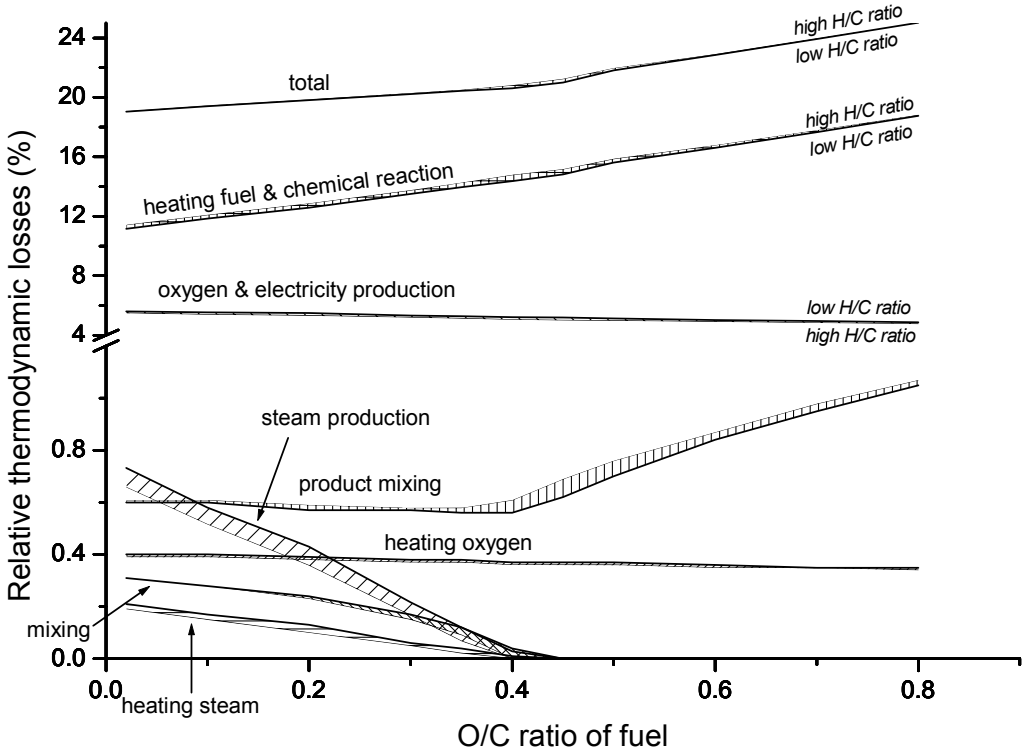

Figure 5.7: Relative exergy losses for sub-processes in gasification of fuels (including steam and oxygen production) of varying O/C and H/C ratio at 927°C

5.5 Conclusions and discussion

It was shown that the presence of kinetically limited char gasification reactions in gasifiers negatively influences the efficiency of a gasifier. Therefore, a relatively simple equilibrium model predicts the maximum efficiency that could be attained.

In order to gasify fuels with high thermodynamic efficiency, it is recommended to use a gasification temperature around 927°C, and fuels with O/C ratio smaller than 0.4 (corresponding to a preferred lower heating value above 23 MJ/kg). To minimize kinetic restrictions, higher temperatures may be preferred. At a gasification temperature of 1227°C, the recommended O/C ratio of the fuel is 0.3 or less (corresponding to a preferred lower heating value above 26 MJ/kg). Fuels with higher O/C ratios, such as wood, have larger exergy losses because of their high ratio of chemical exergy to lower heating value. Furthermore, such fuels are over-oxidized in the gasifier in order to reach the required gasification temperature. In practice, due to heat losses and the presence of ash in the fuel, the extent of over-oxidation will be more severe.

Based on the above, it becomes clear that highly oxygenated biofuels are not ideal fuels for gasifiers from an exergetic point of view. However, this does not mean that woody biomass is less attractive than coal as a gasification fuel. Apart from the composition of the organic matter in a fuel, there are many other factors that need to be taken into consideration, such as the lower ash, sulphur and nitrogen content of biomass and the high reactivity of biomass char compared to coal char. Rather than gasifying biofuels directly, it could be attractive to modify their properties. For example, wood could be separated into its components, e.g. by extraction of lignin with phenol, and only the lignin component could be gasified. Another approach uses thermal pre-treatment of wood at temperatures around 250°C (a process known as biomass torrefaction (Bourgois and Doat, 1985)), which lowers the O/C ratio prior to gasification. Lignin or torrefied wood could also be mixed with coal to enhance the gasification fuel properties.

Appendix C: Gasification efficiency at equilibrium and non-equilibrium conditions

Figure 5.8a illustrates gasification of biomass at equilibrium conditions at typical gasification temperature of 877°C. Preheating of fuel or gasifying medium is not considered, which means that the fuel and oxygen enter the gasifier at a temperature T_0 = 25°C. The biomass fuel is represented by a general formula of $CH_{1.4}O_{0.6}$ (with net heat of combustion of 19.6 MJ/kg) and indicated by point A in the triangular diagram. Assuming that 10% moisture is present in the fuel, the composition of the wet biomass is given by point B. When oxygen is added, the composition moves into the direction of point C; at this point, all carbon is present in the gaseous phase

as carbon monoxide, carbon dioxide or methane. The required equivalence ratio, defined as the amount of oxygen added for gasification relative to the amount of oxygen required for complete combustion, is 0.295. Notice that point C does not lie on the carbon boundary line (line I), because this line has to be crossed over in order to reach the desired temperature. The thermodynamic efficiency of air or oxygen-blown gasification, based on the first and second law of thermodynamics, reaches a maximum at the carbon boundary temperature (see Chapter 3). Theoretically, the biomass could be gasified more efficiently at a slightly lower equivalence ratio.

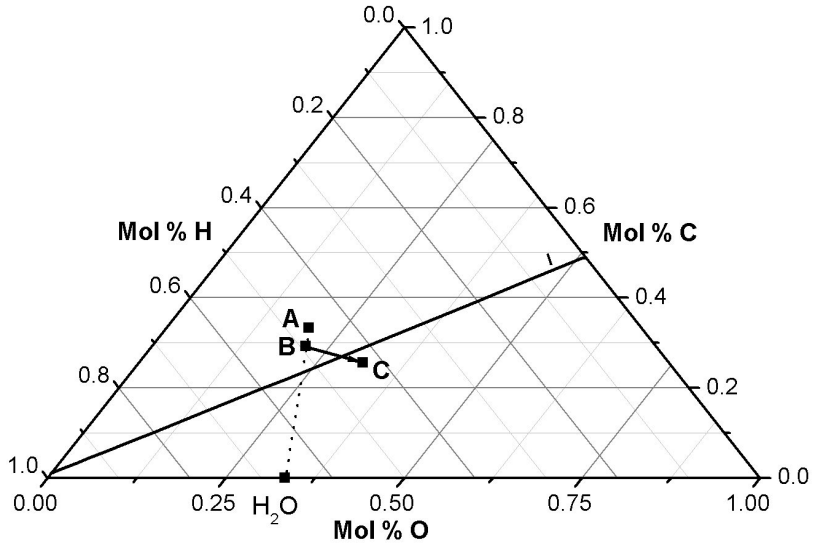

(a)

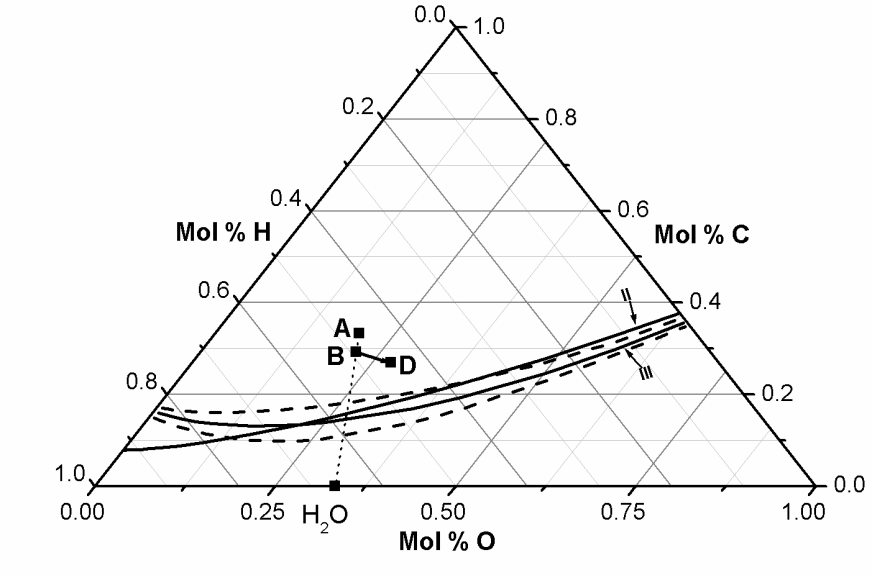

(b)

Figure 5.8: Biomass ($CH_{1.4}O_{0.6}$, point A), wet biomass (containing 10 wt% moisture, point B) and gasification of wet biomass, (a) at equilibrium conditions (to point C) and (b) at non-equilibrium conditions (to point D).

The triangular diagram in Fig. 5.8b illustrates gasification of biomass at a gasification temperature of 877°C at 'quasi'-equilibrium conditions, with the reaction equilibria evaluated at lower temperatures. Figure 5.8b shows several carbon boundary lines that we have determined: line II is the carbon boundary line (at 627°C) based on the research of Li et al. (2001) and line III (including lines to indicate uncertainty) is based on the research of Kersten (2002). These lines have shifted downwards compared to line I in Fig. 5.8a, which indicates that as a result of kinetic limitations, more oxygen is required for complete gasification. This is the combined net result of two effects. If the exothermic reaction of Eq. 5.8 is kinetically limited and more methane (and higher hydrocarbons) is formed than predicted, it is favourable because hydrocarbon formation contributes to the carbon conversion. However, if the endothermic reactions of Eqs. 5.9 and 5.10 are also kinetically limited, it is not favourable because this means that these reactions are effectively 'frozen in', and more oxygen must be added to obtain complete carbon conversion.

Again, the biomass fuel considered in this work is represented by a general formula of $CH_{1.4}O_{0.6}$, indicated by point A in the triangular diagram, and the composition of the wet biomass including 10% moisture is given by point B. When oxygen is added, the composition moves into the direction of point D. At this point, 60% of the carbon is present in the gaseous phase and 40% remains unconverted. Interestingly, the required equivalence ratio to reach the desired process temperature is only 0.151, which is lower than for the unmodified equilibrium model. This is because the endothermic char reforming reactions, which normally act as a temperature ceiling in a gasifier, hardly occur. In practice, higher equivalence ratios need to be used to compensate for heat losses from the gasifier and warm up inert components (such as ash in the fuel, and nitrogen if air is used as gasifying medium). More carbon is thus converted, but the total carbon conversion in fluidized bed gasifiers operating at atmospheric pressure and bed temperatures below 910°C remains rather low, in the range of 70-85% at equivalence ratios of 0.2-0.3 and complete carbon conversion only above 0.4 (Kersten et al., 2002).

The process parameters for atmospheric gasification at a temperature of 877°C at equilibrium and 'quasi'-equilibrium conditions are compared in Table 5.1. The gas composition is very different for these scenarios. At 'quasi' equilibrium conditions, much less carbon monoxide is present in the gas, and more methane, steam and carbon dioxide. Methane formed in gasifiers, probably by thermal cracking of tar, reforms too slowly and hence its concentration is higher than at equilibrium conditions. The concentrations of steam and carbon dioxide are higher due to kinetic limitations of the char reforming reactions.

Table 5.1 compares the thermodynamic efficiency of the gasification processes. It shows that the thermodynamic efficiency is highest at equilibrium conditions. For

the gasifier, the process losses amount to 19.3% for the equilibrium case and 23.0% for the 'quasi'-equilibrium case. Due to losses incurred for oxygen production, these numbers are higher for the total gasification systems, but the conclusion that the equilibrium case is more efficient still holds. Analysis of the process losses, also shown in Table 5.1, indicates that the losses for heating the fuel and chemical reaction have the largest contribution. These losses are higher for the 'quasi'-equilibrium case. The reason that gasification at equilibrium conditions is more efficient is that the exothermic oxidation reactions are effectively coupled with endothermic reforming reactions, so that the driving force for the overall chemical reaction (difference in chemical potential) is lower.

In the definitions of Eqs. 5.5 and 5.6, unconverted carbon is not regarded as a loss because, in principle, it can be recycled into the gasifier. However, this is problematic in practice as unconverted carbon is contained in the ashes. If unconverted carbon is regarded as a loss, the thermodynamic efficiency for gasification at 'quasi'-equilibrium conditions drops below 50%. This number may be somewhat improved by processing the unconverted carbon rather than to dispose of it, e.g. it can be burned out in a separate reactor.

Table 5.1: Gasification at 877°C, equilibrium and 'quasi'-equilibrium conditions

	Equilibrium conditions	**'Quasi' equilibrium conditions**
Equivalence ratio	0.295	0.151
Carbon conversion	100%	60%
Gas composition (mol%)		
H_2O	9.6%	17.9%
H_2	36.0%	37.0%
CO	44.3%	19.5%
CO_2	10.0%	21.3%
CH_4	< 0.1%	4.3%
Gasifier efficiency (%)		
chemical	75.2%	70.3%
physical	5.5%	6.7%
total	80.7%	77.0%
Process losses		
heating oxygen	0.4%	0.3%
heating fuel & chemical reaction	17.9%	21.4%
product mixing	1.0%	1.3%
total	19.3%	23.0%
Gasification system efficiency (%)		
total	75.6%	73.0%
total if unconverted carbon is lost		48.7%

References

Anikeev VI, Gudkov AV, Ermakova A (1996). Exergetic analysis of biomass gasification for co-production of methanol and energy. Theoretical Foundations of Chemical Engineering 30(5):461-468.

Bacon DW, Downie J, Hsu JC, Peters J (1982). Modeling of fluidized bed wood gasifiers. In: Overend RP, Milne TA, Mudge LK, editors. Fundamentals of thermochemical biomass conversion. London: Elsevier Applied Science. p. 717-32.

Barin I (1989). Thermochemical Data of Pure Substances: Part I and II. Weinheim (Germany): VCH Verlagsgesellschaft GmbH.

Baron RE, Porter SH, Hammond OH (1976). Chemical equilibria in carbon-hydrogen-oxygen systems. Cambridge: MIT Press.

Bourgois JP, Doat J (1985). Torrefied wood from temperate and tropical species. Advantages and prospects. In: Egnéus H, Ellegård A, editors. Bioenergy 84. London: Elsevier. vol III, p.153-159.

Cairns EJ, Tevebaugh AD (1964). CHO gas phase compositions in equilibrium with carbon, and carbon deposition boundaries at one atmosphere. Journal of Chemical and Engineering Data 9(3):453-462.

Channiwala SA, Parikh PP (2002). A unified correlation for estimating HHV of solid, liquid and gaseous fuels. Fuel 81:1051-1063.

Chern SM, Walawender WP, Fan LT (1989). Mass and energy balances of a downdraft gasifier. Biomass 18(2):127-151.

Chern SM (1989). Equilibrium and kinetic modeling of co-current (downdraft) moving-bed biomass gasifiers. Ph.D. thesis. Manhattan, Kansas: Kansas State University.

Corella J, Toledo JM, Padilla R (2004). Olivine or dolomite as in-bed additive in biomass gasification with air in a fluidized bed: which is better? Energy & Fuels 18:713-720.

Desrosiers R (1979). Thermodynamics of gas-char reactions. In: T.B. Reed (Ed.), A survey of biomass gasification. Colorado: Solar Energy Research Institute.

Gumz W (1950). Gas producers and blast furnaces. New York: John Wiley and Sons Inc.

Hirs GG (2001). Efficiency of biomass simply too low. Duurzame Energie 10:35 (in Dutch).

Hos JJ, Groeneveld MJ, Swaaij WPM van (1980). Gasification of organic solid wastes in cocurrent moving bed reactors. In: Energy from biomass and wastes IV, Lake Buena Vista, Florida. Chicago: Institute of Gas Technology.

Kersten SRA (2002). Biomass gasification in circulating fluidized beds. Ph.D. thesis. Enschede: Twente University Press.

Kovacik G, Oğuztöreli M, Chambers A, Özüm B (1990). Equilibrium calculations in coal gasification. Int. J. Hydrogen Energy 15(2):125-131.

Krevelen DW van (1993). Coal – Typology – Physics – Chemistry - Constitution. 3rd edition. Amsterdam: Elsevier Science Publishers B.V.

Li X, Grace JR, Watkinson AP, Jim CJ, Ergüdenler A (2001). Equilibrium modeling of gasification: a free energy minimization approach and its application to a circulating fluidized bed gasifier. Fuel 80:195-207.

Maniatis K, Vassilatos V, Kyritsis S (1994). Design of a pilot plant fluidized bed gasifier. In: Bridgwater AV, editor. Advances in thermochemical biomass conversion, vol. 1. London: Blackie. p. 403-10.

Rodriguez L, Gaggioli RA (1980). Second-law efficiency of a coal gasification process. Canadian Journal of Chemical Engineering 58(3):376-381.

Tsatsaronis G (1982). Thermodynamic analysis of a coal gasification process. In: Energy: money, materials and engineering, symposium series no. 78, London: Institution of Chemical Engineers. p. T5/1-11.

Simbeck DR, Dickenson RL, Oliver ED (1983). Coal gasification systems: a guide to status, application and economics. Palo Alto, CA: EPRI (report AP-3109).

Ståhl K, Nieminen J, Neergaard M (2001). Värnamö demonstration programme, final report. In: Bridgwater AV, editor. Progress in thermochemical biomass conversion, vol. 1. Oxford: Blackwell Science. p. 549.

Szargut J, Styrylska T (1964). Approximate evaluation of the exergy of fuels. Brennstoff Wärme Kraft 16(12):589-596 (in German).

Szargut J, Morris DR, Steward FR (1988). Exergy analysis of thermal, chemical and metallurgical processes. New York: Hemisphere Publishing Corporation.

Veen A van (2002). Switchover of coal gasifier in Buggenum goes successfully. Duurzame Energie 10:44-47 (in Dutch).

Watkinson AP, Lucas JP, Jim CJ (1991). A prediction of performance of commercial coal gasifiers. Fuel 70:519-527.

Wen CY (1983). Coal gasification availability analysis. Gov. Rep. Announce. Index (U.S.) 83(15):3580.

Chapter 6

Exergetic optimisation of a production process of Fischer-Tropsch fuels from biomass[‡]

An exergy analysis of Biomass Integrated Gasification – Fischer Tropsch process is presented. The process combines an air-blown, atmospheric gasifier, using sawdust as feedstock, with a Fischer-Tropsch reactor and a steam-Rankine cycle for electricity generation from the Fischer-Tropsch tail gas. Results show that the rational (exergetic) efficiency is 36.4%, consisting of 34.5 % efficiency to Fischer-Tropsch diesel and wax and 1.9% efficiency to electricity. The largest exergy losses take place in biomass gasification and in generation of electricity from the Fischer-Tropsch tail gas. Recommendations are given for process improvements, which increase the rational efficiency to 46.2%.

6.1 Introduction

6.1.1 General background

The production of liquid hydrocarbon fuels from biomass is receiving increased attention. This is motivated by the Kyoto protocol emphasizing the need for renewable, CO_2-neutral fuels. There is also an economic interest for wood-producing countries or countries with large agricultural residues. Finally, transport of liquid is easier and cheaper than transport of the original biomass, especially since the mass to be transported is reduced more than threefold due to removal of moisture, ash and deoxygenation of the organic fraction.

A variety of biomass liquefaction processes are under development, including direct processes, such as fermentation, fast pyrolysis and hydrothermal upgrading. In indirect liquefaction processes, biomass is first gasified, followed by conversion of the formed synthesis gas to methanol (Ptasinski et al., 2002) or Fischer-Tropsch (FT) liquids (Larson and Jin, 1999; Daey Ouwens et al., 2001; Boerrigter and den Uil, 2002; Tijmensen et al., 2002). This chapter focuses on the thermodynamic efficiency of producing hydrocarbon fuels by biomass gasification integrated with Fischer-Tropsch synthesis (BIG-FT).

[‡] Published in Fuel Processing Technology 86 (4):375-389, 2005.

Comparing FT synthesis with methanol synthesis, an important difference is that much higher conversions per pass can be obtained. This is beneficial for integration with biomass gasification, as it allows for a so-called once-through process: synthesis gas is converted in a single pass to mainly liquid hydrocarbons and the unconverted gas (as well as gaseous products) is not recycled. Air can be used as gasification medium in order to avoid an oxygen separation process, which is expensive on the relatively small scale of most biomass gasifiers. The tail gas from the FT reactor can be converted into electricity, and if desired, into heat. This concept has been termed tri-generation (Daey Ouwens et al., 2001).

6.1.2 Objectives

The main objective of this chapter is to determine the exergetic efficiency of the production process of FT fuels from biomass. There are several reasons for using exergy (previously called: available energy) in this study. First, biomass can be regarded as a certain amount of work potential, which should be conserved in the produced FT fuels as much as possible. Furthermore, the process produces not only FT fuels, but also electricity as a co-product. Using the concept of exergy analysis, these different products can both be expressed in the same unit, i.e. units of rate of work (Joule per second). Finally, exergy analysis allows identification of those process units where the largest process losses occur.

A second objective of this chapter is to optimise the exergetic efficiency of this process. Although guidelines have been presented to reduce exergy losses (Sama, 1995), the results of exergy analysis do not necessarily indicate how improvements can be made. In our case, the process could be optimised by studying the effect of design changes as well as process operating parameters on the magnitude of exergy losses.

The outline of this chapter is as follows: background is given about FT synthesis and its integration with biomass gasification. The process design is modelled in Aspen Plus (version 11.1) to establish mass and energy balances; these are the input for the exergy calculations. Results of exergy analysis are presented, including possibilities for process optimisation, followed by conclusions.

6.2 Background

6.2.1 Fischer-Tropsch synthesis

The FT synthesis has a lively history of about seventy years. An overview is given by Schulz (1999). In the FT synthesis, synthesis gas containing carbon monoxide and hydrogen is converted in the following catalytic reaction:

$$n\,CO + 2n\,H_2 \rightarrow \left[-CH_2-\right]_n + n\,H_2O \qquad \Delta H = -159.2\ kJ/mol \qquad (6.1)$$

The Fischer-Tropsch reaction follows a chain-growth mechanism, whereby the product spectrum adheres to an Anderson-Schulz-Flory distribution characterized by the chain growth probability factor alpha. Typical operating pressures for FT synthesis are 15-40 bar, while two temperature modes can be distinguished: high temperature Fischer-Tropsch (300-350°C) and low temperature Fischer-Tropsch (200-260°C). At lower temperature, the chain growth probability is higher. Less gaseous products, such as gasoline and light olefins, are formed and more liquid products, such as diesel and wax. The wax may be hydrocracked with good selectivity to FT diesel, which has very favourable properties in terms of cetane number and biodegradability. Therefore, most interest today is in low temperature Fischer-Tropsch technology.

6.2.2 Fischer-Tropsch feedstock

The most popular feedstock to provide synthesis gas for the FT synthesis has varied throughout the years. During World War II, German vehicles were fuelled with coal-derived FT liquids, while from 1955 FT fuels and chemicals have been produced from low rank coal in South Africa. Today, natural gas is the most important feedstock for synthesis gas production. Sources of gas are either large, remote reserves of natural gas or so-called associated gas that cannot be flared any more due to more severe CO_2 emission regulations. Biomass has not yet been commercially applied as a feedstock for the FT synthesis; the integration of biomass gasification with FT synthesis has been demonstrated in laboratory work only recently (Boerrigter and den Uil, 2002).

6.2.3 Integration of Fischer-Tropsch synthesis with biomass gasification

The design of a biomass gasifier integrated with a Fischer-Tropsch synthesis reactor must be aimed at achieving a high yield of liquid hydrocarbons. For the gasifier, it is important to avoid methane formation as much as possible, and convert all carbon in the biomass to mainly carbon monoxide and carbon dioxide. Methane formed in the gasifier does not participate in the FT reaction and therefore decreases the overall selectivity to liquids. For this reason, atmospheric gasification may be preferred over pressurized gasification, although the latter saves synthesis gas compression costs.

A second very important aspect is gas cleaning. Advanced utilisation of biomass synthesis gas, such as electricity generation by means of gas engines or gas turbines, is still hampered by the formation of condensable organic compounds, referred to as biomass tars. Gas cleaning is even more important for the integration of a biomass gasifier and a catalytic reactor. To avoid poisoning of FT catalyst, tar, hydrogen sulphide, carbonyl sulphide, ammonia, hydrogen cyanide, alkali and dust particles must be removed thoroughly. For this reason, a dry gas clean-up section is

not sufficient and conventional wet gas cleaning has to be used (Tijmensen et al., 2002).

Another important design parameter for integrating a biomass gasifier and a Fischer-Tropsch reactor is the hydrogen to carbon monoxide (H_2/CO) ratio. The ratio of hydrogen to carbon monoxide in the raw gas from the biomass gasifier typically is between 0.8 and 1.6, while the F-T reactor consumes at least two times more hydrogen than carbon monoxide. In the absence of make-up hydrogen, e.g. from steam reforming of methane or from solar-driven water electrolysis, a catalytic water gas shift (WGS) reactor can be used to obtain the right ratio between hydrogen and carbon monoxide.

Including a WGS reactor in the process scheme inevitably leads to formation of carbon dioxide. There is general consensus in the literature that carbon dioxide does not have an inhibiting effect on the rate of FT synthesis for catalysts that are not active for the water gas shift (WGS) reaction, such as cobalt catalyst (Espinoza et al, 1999). Removing carbon dioxide increases the partial pressure of carbon monoxide in the feed gas to the FT reactor, which improves the FT selectivity to liquids. For our system, which is based on air-blown gasification, the synthesis gas is already diluted with nitrogen, so that the increase in FT selectivity by removal of carbon dioxide is relatively small. However, carbon dioxide removal requires a lot of energy: for process configurations based on absorption/stripping using methyldiethanolamine (MDEA), together with an activator, energy requirements are around 0.68 GJ/ton CO_2 (Desideri and Palucci, 1999). We have found that the increased energy use outweighs the increase in FT selectivity caused by removal of carbon dioxide. Therefore, a carbon dioxide removal section is not included.

Finally, heat integration must be considered. Due to the high exothermic nature of the FT reaction, a lot of reaction heat is available that may be used to dry the biomass. Additional heat is available from cooling the hot synthesis gas. Even if the biomass is very moist, there is an excess of heat in the process that must be utilized.

6.2.4 Process description

Figure 6.1 shows a block diagram of a biomass gasification process integrated with FT synthesis (BIG-FT). Heat integration is indicated with dotted lines. Sawdust is considered as a feedstock, with the composition shown in Table 6.1 (from: Tillmann, 2000). The biomass is dried to 10 wt% moisture by indirect drying using reaction heat from the Fischer-Tropsch section. It is autothermally gasified with air at a temperature of 900°C and atmospheric pressure. The product gas is cooled to 90°C, generating 50 bar-g as well as 20 bar-g steam, which are used in steam cycles for electricity production. The gas is subsequently cleaned: ash particles are separated by filtration and acid gases, ammonia and salts are washed by water from the synthesis gas.

Table 6.1 Composition of sawdust feedstock (Tillmann, 2000)

Proximate analysis (wt%)	
Fixed carbon	14.36
Volatile matter	84.58
Ash	1.06
Moisture	34.93
Ultimate analysis (wt%)	
Carbon	49.29
Hydrogen	5.93
Oxygen	43.31
Nitrogen	0.40
Sulphur	0.02
Ash	1.06
Higher heating value, dry (MJ/kg)	19.4

The gas is compressed to 25 bar using an inter-cooled, adiabatic three-stage compressor with isentropic efficiency of 0.72, and catalytically shifted in a water-gas-shift (WGS) reactor. The gas is converted to gaseous and liquid hydrocarbons at a temperature of 260°C by cobalt-catalysed Fischer-Tropsch synthesis. The total single-pass H_2+CO conversion is 80%. The products from the FT reactor are cooled to 40°C, so that hydrocarbon liquids are condensed from the tail gas, which contains most of the naphtha (C5-C8). Diesel (C9-C22) and wax (C23+) are recovered as liquid products. These final products would be transported to a refinery for further work-up (e.g. fractionation, hydrocracking and/or hydroisomerisation).

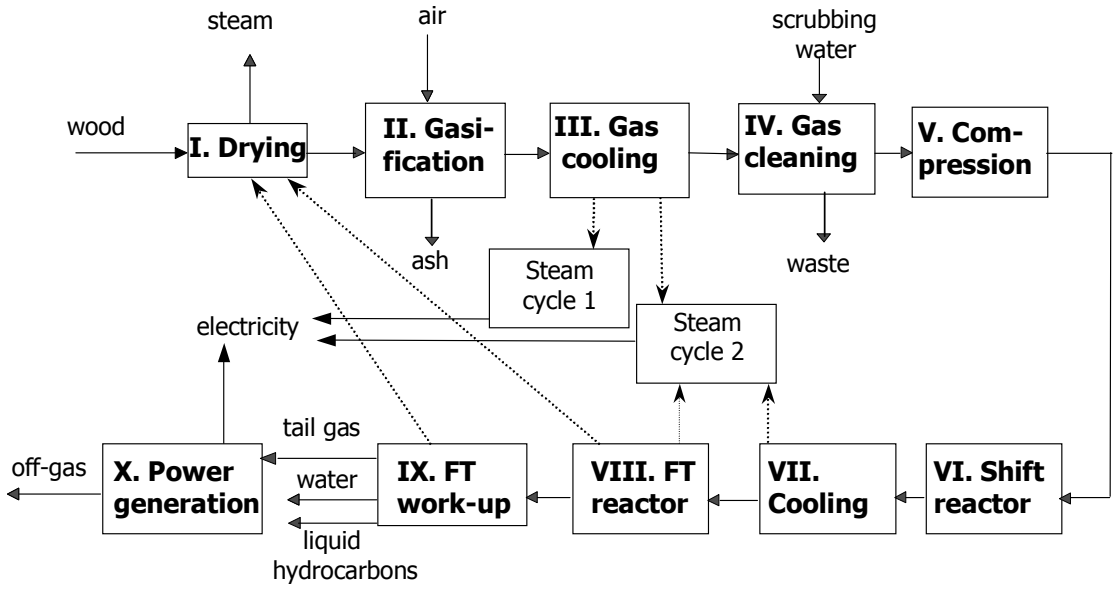

Figure 6.1: Block diagram of a BIG-FT process

The tail gas from the FT work-up section has a lower heating value less than 3 MJ/m^3_n (the synthesis gas typically has 5.5 MJ/m^3_n, which reduces in the FT reactor due to conversion of carbon monoxide and hydrogen) and it is not suitable for burning in a gas turbine or gas engine. Therefore, similar to many biomass-fuelled power plants in operation today, a traditional steam-Rankine cycle is applied for electricity generation. The tail gas is incinerated in a boiler and electricity is generated by means of a condensing steam turbine.

6.3 Energy and exergy calculations

6.3.1 Process modelling

Mass and energy balances were obtained from Aspen Plus simulations based on the process parameters included in the process description. Thermodynamic equilibrium was assumed for the gasifier, with H_2, H_2O, CO, CO_2 and CH_4 considered as the only stable gaseous components at elevated temperatures. Thermodynamic equilibrium was also assumed for the WGS reactor. For the FT reactor, the hydrocarbon product distribution was calculated from the following equation for the chain growth probability factor alpha (Lox and Froment, 1993):

$$\alpha = \frac{k_{HC1} P_{CO}}{k_{HC1} P_{CO} + k_{HC5} P_{H_2} + k_{HC6}} \qquad (6.2)$$

with:

k_{HC1} *rate constant for adsorption of carbon monoxide on active site, mol/(g s bar)*

k_{HC5} *rate constant for desorption of paraffins by hydrogenation of active site, mol/(g s bar)*

k_{HC6} *rate constant for desorption of olefins from active site, mol/(g s)*

P_{CO} *partial pressure of carbon monoxide, bar*

P_{H2} *partial pressure of hydrogen, bar*

This equation reflects that selectivity increases with carbon monoxide partial pressure, and decreases with hydrogen partial pressure. The equation was based on experiments using a precipitated iron catalyst; however, it is assumed that industrial cobalt catalysts show similar selectivities. Predicted alpha values at FT conditions of 260°C, 20 bar and 80% conversion are in the range of 0.946-0.956 for undiluted synthesis gas (H_2/CO ratio of 2) and these reduce to 0.930-0.949 for synthesis gas diluted with 50% nitrogen. The higher values correspond to a reactor with the liquid in plug flow (e.g. a fixed bed, multi-tubular reactor) while the lower values, which were used in the process simulations, correspond to a reactor in which the liquid is well mixed (e.g. a slurry reactor).

The power generation section was not modelled in Aspen Plus. This section comprises a steam-Rankine cycle, for which the efficiency was estimated at 25% based on lower heating value. The boiler in this section is fed by a relatively small volume of Fischer-Tropsch tail gas, and therefore has a relatively small capacity. In practice, vendors would use lower grade steels in the boiler tubes to minimize costs. This requires modest steam pressures and temperatures (60 bar, 480°C) compared to large-scale coal plants (100-240 bar, 510-540°C), thereby leading to reduced efficiency (Williams and Larson, 1993).

6.3.2 Exergy balances

The mass and energy balances obtained in Aspen Plus formed the basis for exergy calculations in a separate spreadsheet. For each section in the process, an exergy balance was made, which can be written as follows:

$$\sum_{in} E_i - \sum_{out} E_i + E^Q - W = I \qquad (6.3)$$

where:

$\sum_{in} E_i$: *exergy accompanying incoming mass flows*

$\sum_{out} E_i$: *exergy accompanying outgoing mass flows*

E^Q : *exergy accompanying heat transfer*

W : *exergy accompanying work transfer*

I : *process irreversibility or internal exergy loss*

The aim of applying this balance is to identify units or areas in a system with the largest process irreversibilities. These units or system areas have the largest degradation of energy and materials, leading to a reduction in work potential. Apart from internal losses, external exergy losses can also take place if process streams are emitted to the environment.

The overall exergetic efficiency is defined as:

$$\eta_{overall} = \frac{E_{liquid\ fuels} + W_{net}}{E_{biomass}} \qquad (6.4)$$

where:

$\eta_{overall}$: *overall exergetic efficiency*

$E_{liquid\,fuels}$: *exergy of liquid fuel product*

W_{net} : *electricity produced in the process (net work)*

$E_{biomass}$: *exergy of biomass feed*

The overall efficiency can be seen as the sum of the efficiency to fuels and the efficiency to electricity. The exergy of incoming mass streams other than the biomass feed stock may be neglected (e.g. air for biomass gasification). Chemical exergy of the biomass was calculated from the lower heating value using the method of Szargut and Styrylska (1964).

6.4 Results and discussion

6.4.1 Results of exergy analysis

The overall mass and energy balance for production of Fischer-Tropsch hydrocarbons and electricity is given in Table 6.2. On a process scale of 36.7 ton/hr of organic material (57 ton/hour of biomass), the plant produces approximately 5.6 ton/hr of liquid Fischer-Tropsch products. The net output of hydrocarbon fuels is therefore 15.2% on weight basis. Based on higher heating values, the efficiency to fuels is 36.5%, which is slightly lower than a preliminary value of 40% reported by Larson and Jin (1999).

Figure 6.2 shows a Grassman-diagram, depicting the exergy flows within the process. It shows that the biomass feed contains chemical exergy of 210.8 MW and the final liquid products contain 72.9 MW with co-production of 4.0 MW of electricity. The overall process efficiency is calculated at 36.4%, of which the exergy content of the liquid F-T fuels is 34.5% of the exergy content in the biomass feedstock, while the electricity generated in the process amounts to 1.9% of the feed.

Table 6.2: Overall mass and energy balance of BIG-FT process

	Mass (ton/hr)	Energy (MW)
Process input		
Biomass input, organic fraction	36.7	200[1]
Process outputs		
Fischer-Tropsch hydrocarbons	5.56	72.9[1]
Net Electricity		4.0
Production		
Steam cycle (50 bar-g)		5.8
Steam cycle (20 bar-g)		6.6
Power generation section		12.7
Consumption		
Synthesis gas compression		20.3
Other equipment		0.8

[1] Higher heating value (gross heat of combustion)

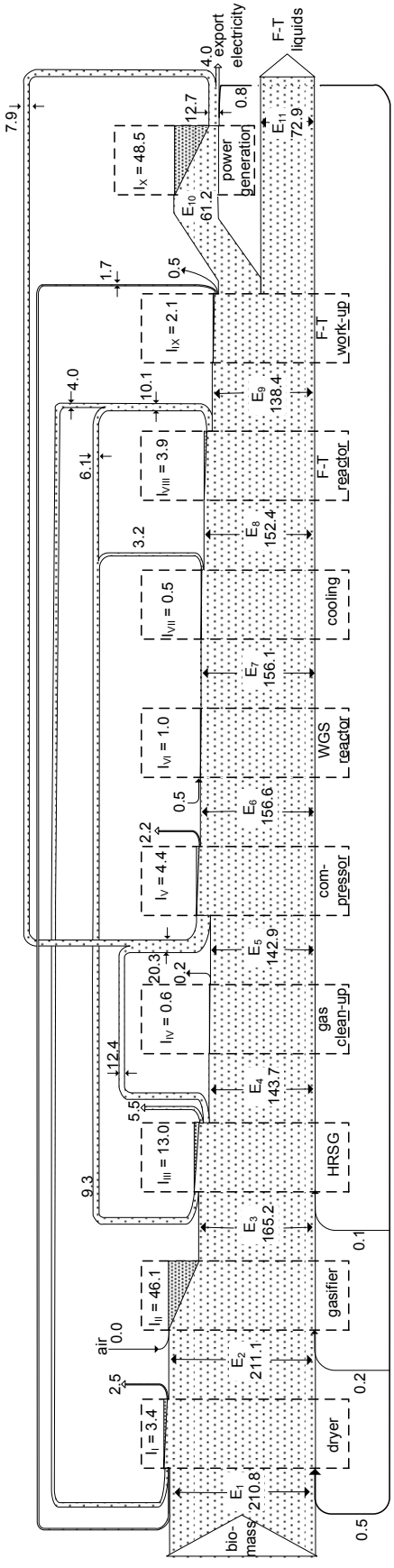

Figure 6.2: Grassman diagram of a BIG-FT process

Figure 6.3 identifies sections of the process with the largest exergy losses. External losses occur in the dryer (exergy of produced steam), steam cycle (steam turbine exhaust is condensed by air cooling), gas clean up (scrubber water) and compression (interstage cooling). However, over 90% of the losses are irreversibilities due to internal degradation of energy. The largest internal losses occur in biomass gasification and generation of power from Fischer-Tropsch tail gas; these will be discussed in the next two sub-sections. Moderate exergy losses take place in the drier, compressor and the Fischer-Tropsch reactor. The Fischer-Tropsch unit is relatively efficient. Based on only the first law of thermodynamics, it would be tempting to state that the process efficiency of this unit is 80% because 20% of the combustion value of the synthesis gas is 'lost' as reaction heat in the FT synthesis. However, the exergetic efficiency is higher (88%) due to an entropy decrease, as small molecules of hydrogen and carbon monoxide are ordered into large organic molecules. If the thermal exergy of the produced reaction heat is also taken into account, the total exergetic efficiency is almost 95%.

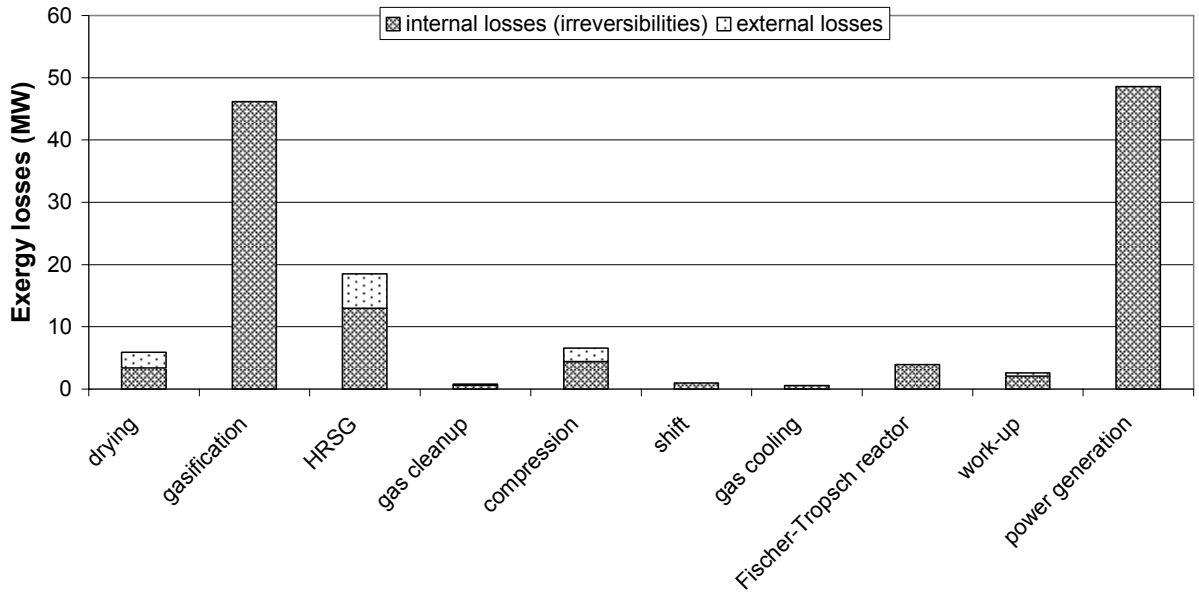

Figure 6.3: Exergy losses per process section

6.4.2 Exergy losses in biomass gasifier

Exergy losses occurring in the gasifier are intrinsic because gasification is a partial oxidation process leading to a decrease in heating value. However, the losses may be minimized by the use of a dry feedstock and optimisation of the gasification temperature.

6.4.2.1 Influence of biomass drying

In the base case design, the biomass was dried from 34.9 wt% moisture to 10 wt% moisture. Other simulations included drying to 15 wt% as well as 20 wt% moisture. The results are shown in Figure 6.4. It can be seen that drying has a small effect on the overall efficiency to electricity. Although less extensive drying increases the duty of the synthesis gas compressor, this is partly compensated because more electricity can be generated in steam cycles and from the F-T tail gas (because more methane is formed in a wet gasifier). However, the effect on the hydrocarbon yield was much larger: it decreased from 15.2 to 14.2 wt% when the extent of drying was decreased from drying to 10 wt% moisture to drying to 20 wt% moisture. As a result, the thermodynamic efficiency of the overall process decreases from 36.4% to 34.2%. This can be explained in the following way: at the same gasification temperature, a wetter feedstock requires addition of more gasifying medium in order to generate heat for water evaporation. The biomass feedstock is thus oxidized at a higher equivalence ratio (defined as the amount of oxygen added for gasification relative to the amount of oxygen required for complete combustion), so that less usable synthesis gas is available for production of hydrocarbons. As a conclusion, it is advantageous to dry the biomass as thoroughly as possible, although moisture contents lower than 10 wt% are difficult to achieve in technical drying processes.

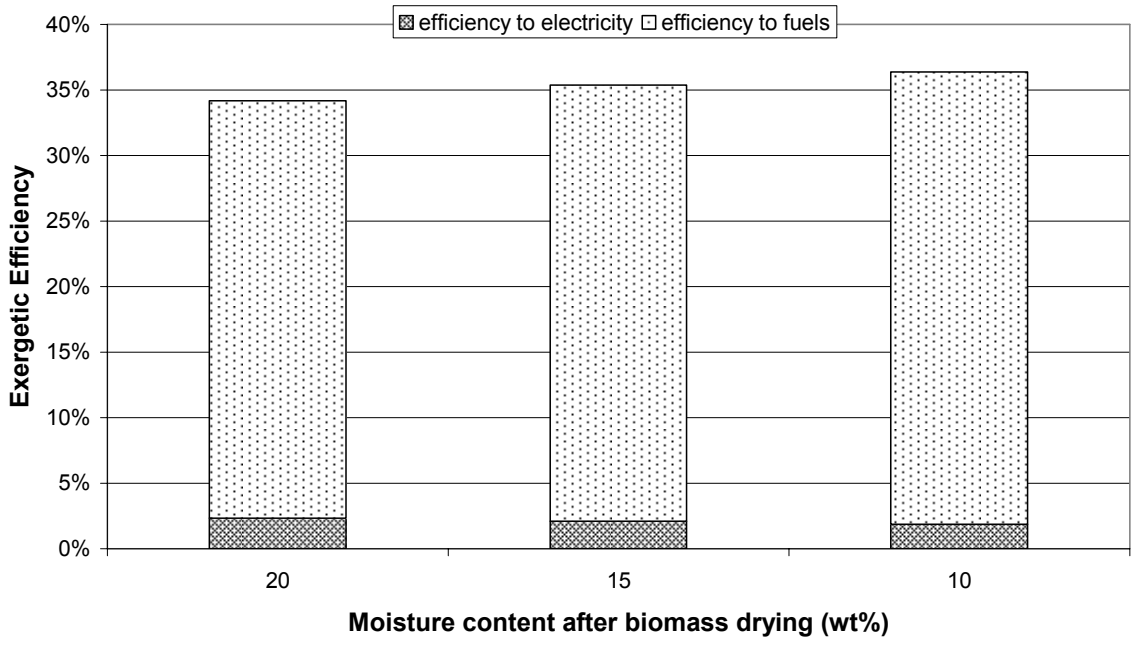

Figure 6.4: Effect of biomass drying on overall exergetic efficiency

6.4.2.2 Optimisation of gasification temperature

One of the most important parameters for biomass gasification is the gasifier temperature. For various extents of drying, the effect of gasification temperature on gasifier efficiency and overall efficiency are shown in Figure 6.5a and 6.5b, respectively.

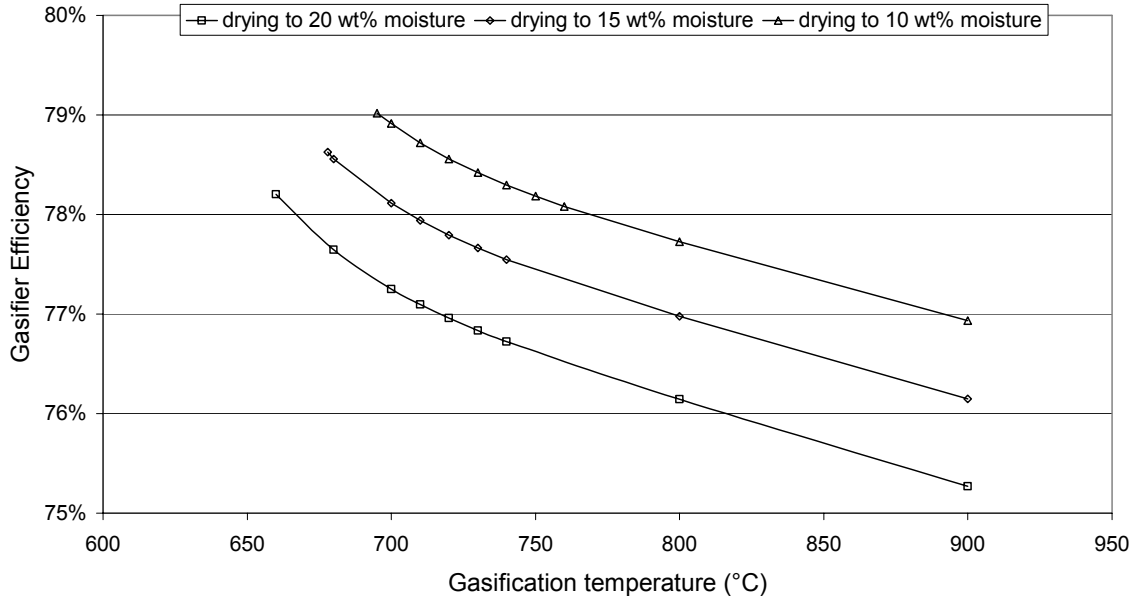

(a)

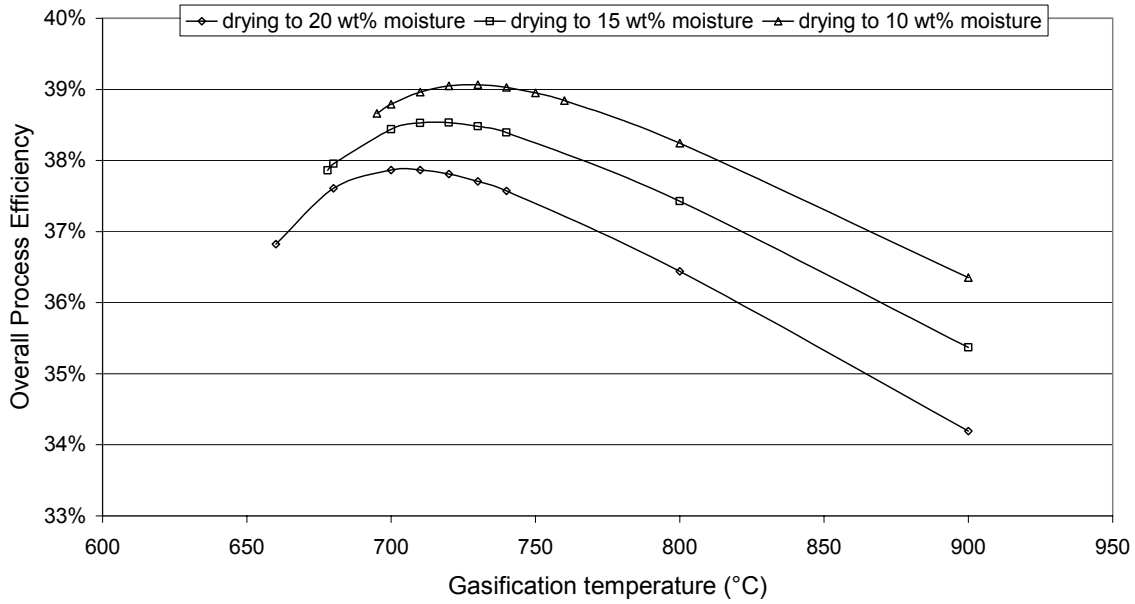

(b)

Figure 6.5: Effect of gasification temperature on gasifier exergetic efficiency (a) and overall exergetic efficiency (b)

Focusing on the efficiency of the gasifier, from literature it is known that optimal operation is achieved when just enough oxygen is added for complete gasification (Gumz, 1950; Chapter 3, this thesis). This point is called the carbon boundary point and it increases in temperature from 660°C for biomass with 20% moisture to 695°C for biomass with 10% moisture. Above these temperatures, more oxygen is added than required and the gasifier efficiency decreases. However, one can observe that the overall efficiency as a function of the operating temperature in the gasifier goes through a maximum. A low temperature in the gasifier (< 700°C) results in a too much methane formation, whereas a high temperature (>800°C) requires a higher equivalence ratio leading to increased irreversibilities in the gasifier. In other words, the gasifier cannot be operated at its optimum conditions and the biomass feed must be over-oxidized. This shows an advantage of exergy analyses, namely that integrated processes can be optimised with regard to thermodynamic efficiencies. This is relevant because a thermodynamic improvement in one unit may have negative effects in other units. Note that temperatures higher than the optimum gasification temperature of 740°C may be required in practice because equilibrium is not always reached in biomass gasifiers, which leads to increased methane formation and lower process efficiency.

6.4.3 Exergy losses in power generation section

The exergy losses in the power generation section can be reduced by a number of process improvements: by optimising the yield of liquid hydrocarbons in the FT reactor, by improving the recovery of the liquids in the FT work-up section and by using more efficient electricity generation technology from the FT tail gas.

6.4.3.1 Production of liquids in Fischer-Tropsch reactor

The ratio between liquid fuels production and power generation is determined by the yield of hydrocarbon liquids in the Fischer-Tropsch reactor. Figure 6.6 shows the relationship between CO conversion in the FT reactor and the exergetic efficiency to fuels and electricity as well as the overall exergetic efficiency. At low conversion levels, increasing the conversion leads to an almost linear increase in exergy of the liquid products and almost linear decrease in net electricity production. At conversions above 85%, the selectivity to liquid fuels in the FT reactor decreases strongly due to the low partial pressure of carbon monoxide in the reactor. This leads to a decrease in the yield of liquids and an increase in electricity generation from the tail gas. Further more, F-T reaction rates become very low at high conversions, which would lead to a substantial increase in reactor volume and investment costs. As a conclusion, it is recommended to operate the FT reactor at conversion levels around 80% in order to optimise the yield of liquid hydrocarbons.

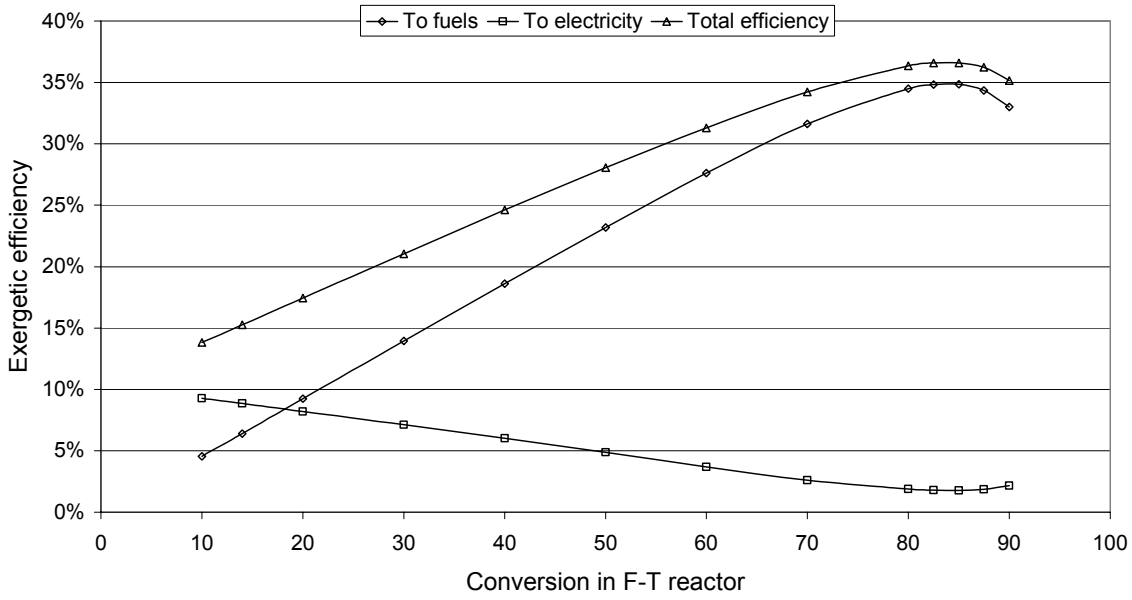

Figure 6.6: Effect of Fischer-Tropsch conversion on overall exergetic efficiency

6.4.3.2 Recovery of liquids in Fischer-Tropsch work-up

Another process improvement that reduces process losses in the power generation section would be to minimize the exergy contained in the FT tail gas. After the Fischer-Tropsch work-up section, 46% of the exergy content goes to the steam-Rankine cycle and only 54% is contained in the liquid products, even though the synthesis gas conversion in the FT reactor is 80%. This is caused by the presence of C1-C8 hydrocarbons in the tail gas. It seems attractive to include C5-C8 naphtha in the liquid products. This increases the exergetic efficiency from 36.4 to 41.8%, where all exergy is in the FT fuels and there is no net output of electricity.

6.4.3.3 Power generation technology

A large benefit is expected by using a more efficient technology to generate electricity from the FT tail gas than a steam-Rankine cycle. If a combined cycle were used for electricity generation, the efficiency of the power generation section would improve from 25 to approximately 50% (Elliott and Booth, 1990) and the overall exergetic efficiency of the plant from 36.4 to 42.4%. For the case where C5-C8 naphtha is included in the liquid FT products, the efficiency would improve further to 46.2%, where 41.8% is efficiency to fuels and 4.4% is electricity.

In practice, this would require improvement of the heating value of FT tail gas, either by addition of external methane or by using oxygen or enriched air for biomass gasification (in order to avoid or reduce dilution of synthesis gas with nitrogen). Using oxygen as a gasifying medium also has other benefits: this reduces process losses in the biomass gasifier and synthesis gas compressor, whereas improving the selectivity to hydrocarbon liquids in the FT reactor due to higher

partial pressure of carbon monoxide. Although these benefits have not been quantified, they may outweigh the electricity input needed to separate oxygen from air.

6.5 Conclusions and recommendations

The process for producing FT fuels from biomass, which integrates biomass gasification with Fischer-Tropsch synthesis, converts a renewable feedstock into a clean fuel. For air-blown, atmospheric gasification, the maximum thermodynamic efficiency that may be achieved is 46.2%, consisting of 41.8% fuels and 4.4% electricity. The largest process losses occur in power generation from FT tail gas and in the biomass gasifier.

The power generation section may be avoided if oxygen-blown gasification is considered. This creates the possibility of (partial) recycling of FT tail gas to the FT reactor, so that exclusively FT fuels are produced without co-production of electricity. However, such a plant is expected to be capital intensive and economic analysis is recommended to determine its economic feasibility.

The thermodynamic analysis showed that process losses occurring in the biomass gasifier are intrinsic. Biomass is not an ideal feedstock for this process because its optimum gasification temperature is rather low (695°C; for biomass containing 10% moisture), which leads to undesired formation of methane. A mild thermal pre-treatment of the biomass may be considered in order to improve its gasification properties, such as heating value and moisture content.

References

Boerrigter H, Uil H den (2002). Green diesel from biomass with the Fischer-Tropsch synthesis. In: Palz W, Spitzer J, Maniatis K, Kwant K, Helm P, Grassi A, editors. Proceedings of the 12th European Biomass Conference, Amsterdam, Netherlands, 17-21 June 2002. Florence: ETA-Florence and WIP-Munich. p. 1152-1153.

Daey Ouwens C, Faaij A, Ruyter HP (2001). Flexible, competitive production of electricity, heat, bio-fuels and ethanol by tri-generation. In: Kyritsis S, Beenackers AACM, Helm P, Grassi A, Chiaramonti D, editors. Proceedings of the 1st World Conference on Biomass for Energy and Industry, Sevilla, Spain 5-9 June 2000. London: James & James (Science Publishers) Ltd. p. 1483-.1485

Desideri U, Palucci A (1999). Performance modelling of a carbon dioxide removal system for power plants. Energy Conversion and Management 40(18):1899-1915.

Elliott P, Booth R (1990). Sustainable Biomass Energy, Selected paper PAC/233. London: Shell International Petroleum Co.

Espinoza RL, Steynberg AP, Jager B, Vosloo AC (1999). Low temperature Fischer-Tropsch synthesis from a Sasol perspective. Applied Catalysis A: General, 186(1-2):13-26.

Gumz W (1950). Gas producers and blast furnaces: theory and methods of calculation. New York: Wiley.

Larson ED, Jin H (1999). Biomass conversion to Fischer-Tropsch liquids: preliminary energy balances. In: Overend RP, Chornet E, editors. Proceedings of the 4th Biomass Conference of the Americas, Oakland, CA, 29 August-2 September 1999. Oxford: Pergamon. p. 843-853.

Lox ES, Froment GF (1993). Kinetics of the Fischer-Tropsch reaction on a precipitated promoted iron catalyst. 2. Kinetic modeling. Ind. Eng. Chem. Res. 32:71-82.

Ptasinski KJ, Hamelinck C, Kerkhof PJAM (2002). Exergy analysis of methanol from the sewage sludge process. Energy Conversion and Management, 43 (9-12):1445-1457.

Sama DA (1995). The use of the second law of thermodynamics in process design. Journal of Energy Resources Technology, Transactions of the ASME, 117(3):179-185.

Schulz H (1999). Short history and present trends of Fischer–Tropsch synthesis. Applied Catalysis A: General, 186(1-2):3-.12

Szargut J, Styrylska T (1964). Approximate evaluation of the exergy of fuels. Brennstoff Wärme Kraft 16(12):589-596 (in German).

Tillmann DA (2000). Biomass cofiring: the technology, the experience, the combustion consequences. Biomass and Bioenergy 19(6):365-384.

Tijmensen MJA, Faaij APC, Hamelinck CN, Hardeveld MRM van (2002). Exploration of the possibilities for production of Fischer Tropsch-liquids and power via biomass gasification. Biomass and Bioenergy 23(2):129-152.

Williams RH, Larson ED (1993). Advanced gas-based biomass power generation. In: Johansson TB, Kelly H, Reddy AKN, Williams RH, editors. Renewable Energy: Sources for Fuels and Electricity. Washington: Island Press. p. 731.

Chapter 7

Weight loss kinetics of wood torrefaction

Torrefaction is a thermal treatment step in the relatively low temperature range of 225-300°C, which aims to produce a fuel with increased energy density by decomposing the reactive hemicellulose fraction. The weight loss kinetics for torrefaction of willow, a deciduous wood type, was studied by isothermal thermogravimetry. A two-step reaction in series model was found to give an accurate description. For the two steps, activation energies of 76.0 kJ/mol and 151.7 kJ/mol respectively and pre-exponential factors of 2.48 10^4 kg kg^{-1} s^{-1} and 1.10 10^{10} kg kg^{-1} s^{-1} respectively were found. The first reaction step has a high solid yield (70-88 wt%, decreasing with temperature), whereas less mass is conserved in the second step (41 wt%). The fast initial step may be representative for hemicellulose decomposition, whereas the slower subsequent reaction represents cellulose decomposition and secondary charring of hemicellulose fragments. The kinetic model is applied to give recommendations for industrial torrefaction process conditions, notably operating temperature, residence time and particle size.

7.1 Introduction

Thermal degradation of wood is a complex research topic because wood contains different fractions. On microscopic scale, wood cells are composed of so-called microfibrils, bundles of cellulose molecules 'coated' with hemicellulose. In between the microfibrils (and sometimes within the amorphous regions of the microfibril) lignin is deposited. These wood fractions show different thermal behaviour. Three zones may therefore be distinguished in weight loss curves of wood: hemicelluloses, the most reactive compounds, decompose at temperatures in the range of 225-325°C, cellulose at 305-375°C and lignin gradually over the temperature range of 250-500°C (Shafizadeh, 1985). This research addresses specifically the first zone, i.e. decomposition of hemicellulose in the relatively low temperature range of 225-300°C, a process also known as torrefaction (Bourgois and Doat, 1984; Pentananunt et al., 1990; Girard and Shah, 1991; Lipinsky et al., 2002). The solid product of such a process, roasted or so-called torrefied wood, has found applications as a barbecue fuel and firelighter (Girard and Shah, 1991). It may be attractive in future as a renewable fuel with increased energy density (compared to raw wood) for gasification and/or co-combustion.

Although a wealth of research data is available about pyrolysis of wood, relatively few address the temperature range of torrefaction. Therefore, more research is required to obtain better understanding of the chemical and physical processes occurring in torrefaction, especially reaction mechanism, reaction kinetics, optimization of process conditions and selection of particle size. This chapter focuses on the determination of the weight loss kinetics of wood torrefaction by experiments in a thermogravimetric analyser (TGA). In Chapter 8, the products formed in the torrefaction process are quantified and analyzed, with emphasis on the properties of torrefied wood.

The weight loss kinetics of lignocellulosic fuels have been determined in many different experimental devices. Such devices include thermogravimetric analysers, tube furnaces, and fluidized bed reactors. Experiments can be carried out under dynamic conditions, in which the sample is submitted to an assigned heating rate, but experimental heating rates are often much slower than those achieved in process equipment such as gasifiers or combustors. The research described below uses static conditions, in which the sample is kept at a constant temperature. In this case, the heating rate is important too, because the sample has to be heated from environmental temperature to the reaction temperature at which the weight loss kinetics is studied. If the heating rate is too high, the results may be affected by heat transfer limitations within the sample. If a too slow heating rate is applied, the weight loss that takes places during the warm-up phase is not negligible, which complicates the interpretation and deduction of kinetic data. However, for the low temperatures applied in torrefaction (225-300°C), the warm-up phase is relatively short, even for low heating rates of 10-100 K/min common in TGA equipment and the error introduced by the weight loss during this phase is acceptable.

An important research parameter is the type of biomass, the composition of which determines its behaviour in the torrefaction process. Deciduous wood types as well as coniferous wood types are considered. These types are often referred to as hard wood and soft wood, respectively. There is not much difference in the distribution of the three wood fractions between these types. Coniferous wood may contain slightly more lignin than deciduous wood (25-35 wt% versus 18-25 wt%), slightly less cellulose (35-50 wt% versus 40-50 wt%) and, on average, comparable amounts of the hemicelluloses (20-32 wt% versus 15-35 wt%) (Wagenführ and Scheiber, 1974). However, the composition of the polysugars that form the hemicelluloses fraction is very different. In the case of deciduous wood, the hemicelluloses contain 80-90 wt% of 4-O methyl glucoronoxylan (referred to as xylan) whereas they contain 60-70 wt% of glucomannan and 15-30 wt% of arabinogalactan for coniferous wood (Wagenführ and Scheiber, 1974). The thermal behaviour of these components may be different. Therefore, it is an important question whether the thermal behaviour of deciduous and coniferous wood types is the same, i.e. do they

react with comparable rates in the torrefaction temperature range. Furthermore, weight loss kinetics of wood is compared to wood components such as xylan.

Finally, the kinetic model obtained in this work is applied to make recommendations for industrial torrefaction process conditions, such as temperature, residence time and particle size.

7.2 Experimental

7.2.1 Materials

Several biomass types have been tested in the experiments: deciduous wood (beech and willow), coniferous wood (larch) and straw. The deciduous wood types were obtained from Rettenmaier, Germany, the coniferous wood from Praxis, Netherlands, and wheat straw was taken from a field in North-Holland. Particle sizes were in the range of 0.7-2.0 mm in all cases, except for straw where it was < 5 mm.

Model compounds of wood, such as cellulose and 4-O methyl glucuronoxylan, extracted from oak spelt, were also used. These were purchased from Sigma Aldrich in powdered form.

7.2.2 Equipment and procedures

TGA measurements were carried out with a Perkin Elmer Pyris 6 TG apparatus with autosampler. The analysed sample weights varied from 2 to 10 mg. Analysis was carried out with a nitrogen flow rate of 20 ml/min. Ceramic crucibles loaded with biomass particles were placed inside the TG apparatus where the weight was constantly measured. The temperature was varied from 230 to 300°C and the heating rate from 10 to 100 °C/min. A temperature program consisting of a dynamic heating period followed by an isothermal heating period was applied. During the dynamic heating period the biomass was thoroughly dried. The weight loss graphs of the dry biomass were used for determination of reaction kinetics.

Due to variations in ash content of the various samples, the measured weights were corrected in the following way:

$$\left(\frac{M_t}{M_o}\right)_{\exp} = \frac{W_{TGA} - W_{ash}}{W_{initial} - W_{ash}} \qquad (7.1)$$

Where $W_{initial}$ is the solid weight of the dry sample, W_{ash} the weight of the ash in the dry sample, and W_{TGA} the solid weight that is measured as a function of time.

7.3 Results and discussion

7.3.1 Thermal degradation of different biomass types

Figure 7.1 shows the weight loss curves of the various biomass types at 248°C and 267°C obtained from isothermal TGA experiments. The weight loss observed during heating of the sample from 200°C, the temperature at which thermal decomposition begins to occur, to the required temperature is relatively small, except for xylan. From Fig. 7.1 it can be concluded that xylan, the main hemicellulose component of deciduous wood, is the most reactive component. It starts decomposing around 200°C and has a high weight loss. The cellulose decomposition rate is very low in the temperature range used. This is in agreement with results of other studies, e.g. Gaur and Reed (1988) mention that cellulose may depolymerise at low temperatures, but volatilization of the cellulose is very slow below 250°C. At 267°C, limited weight loss of cellulose is found.

The hardwoods beech and willow have comparable reactivity. The weight loss observed lies between that of xylan and cellulose, which was expected as wood contains these fractions (and other fractions, such as lignin). High xylan content also explains the relatively high weight loss of wheat straw, although catalytic effects due to the presence of mineral matter could also play a role. Finally, the coniferous larch reacts a lot slower than the hardwoods. Although some researchers have attributed the lower weight loss for coniferous wood to higher lignin content, Ramiah (1970) has experimentally shown that differences in composition of the hemicellulose fractions in deciduous and coniferous wood (xylan- and mannan-based, respectively) may be the main explanation.

As a preliminary conclusion, hardwood looses considerably more weight than softwood and therefore a higher increase in energy density (J/g) may be expected, a topic that is studied in Chapter 8. This makes hardwood an attractive feedstock for torrefaction processes. In the rest of this section, a kinetic model is therefore developed for torrefaction of willow, a classical hardwood.

7.3.2 Kinetic model for willow torrefaction

Because the pyrolysis of wood is a very complex set of reactions, simplified kinetic models are generally applied. For pyrolysis of cellulose and biomass at temperatures higher than 300°C, the Broido-Shafizadeh model (Broido, 1976; Bradbury et al., 1979) is the mostly used, consisting of an activation step followed by two subsequent reactions. Other models consisting of three first-order consecutive reactions or of a simple first-order reaction (global one step) have been proposed as well (Várhegyi et al., 1989; Várhegyi et al., 1997).

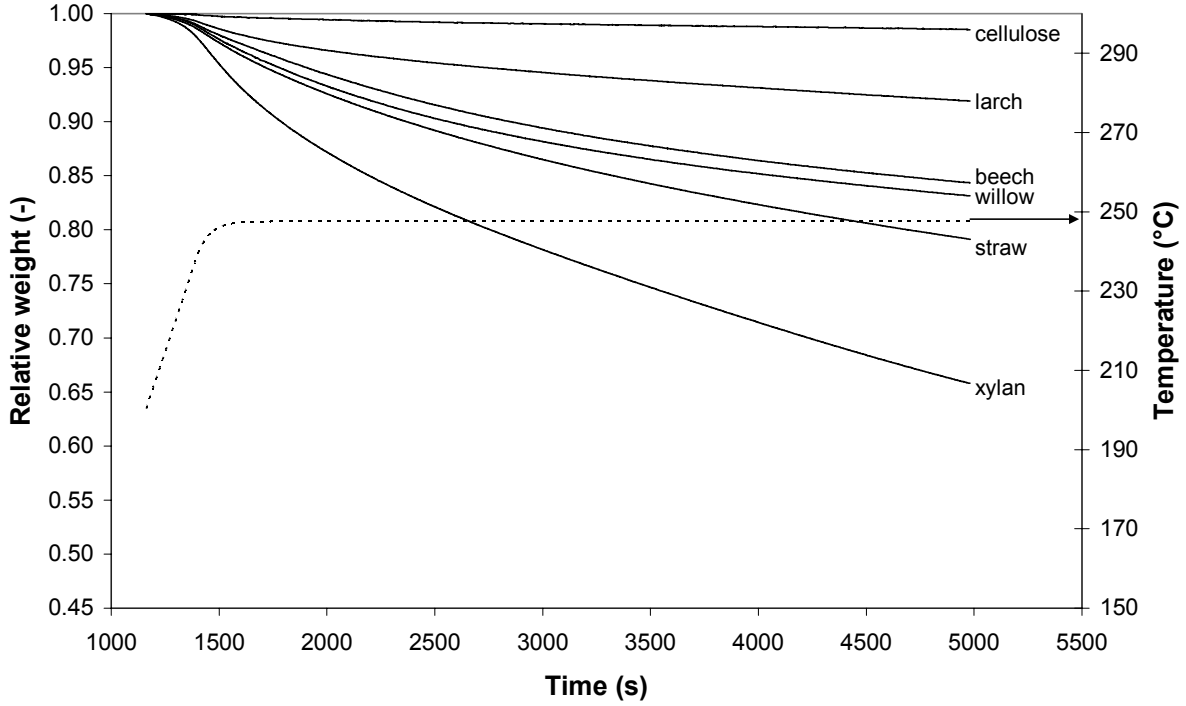

(a)

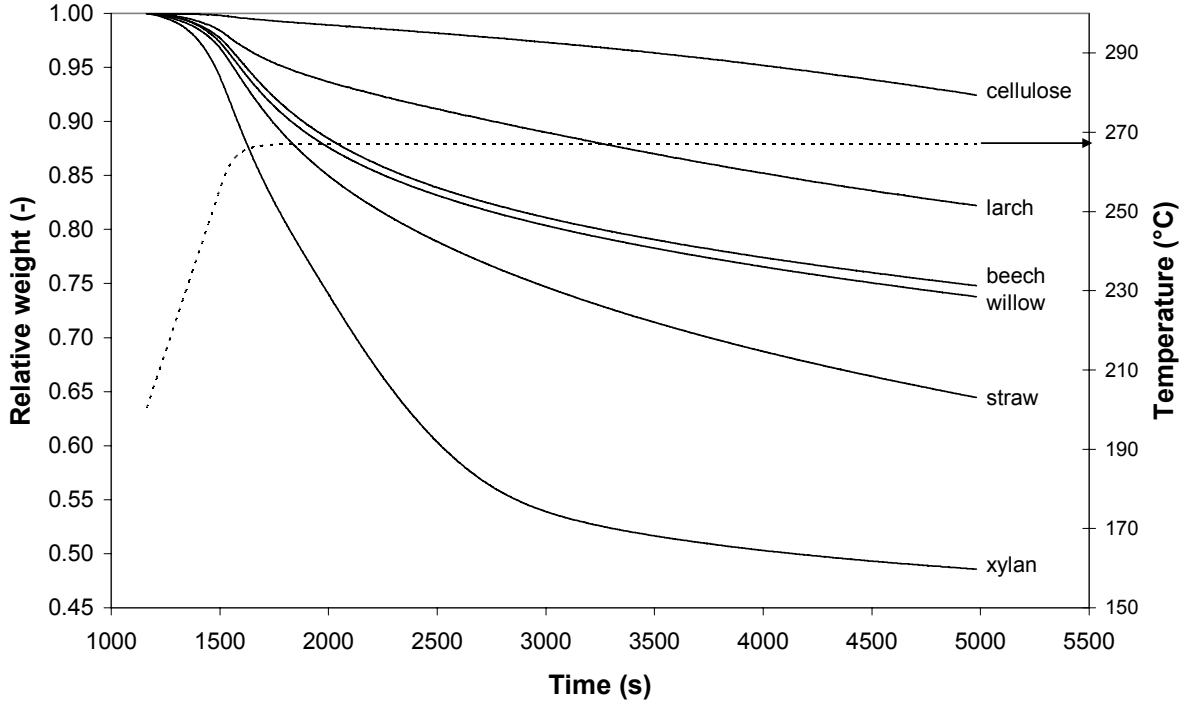

(b)

Figure 7.1: TGA of various biomass compounds, (a) at 248°C and (b) at 267°C. Heating rate 10°C/min, particle size 0.5-2 mm; dotted line is the heating curve

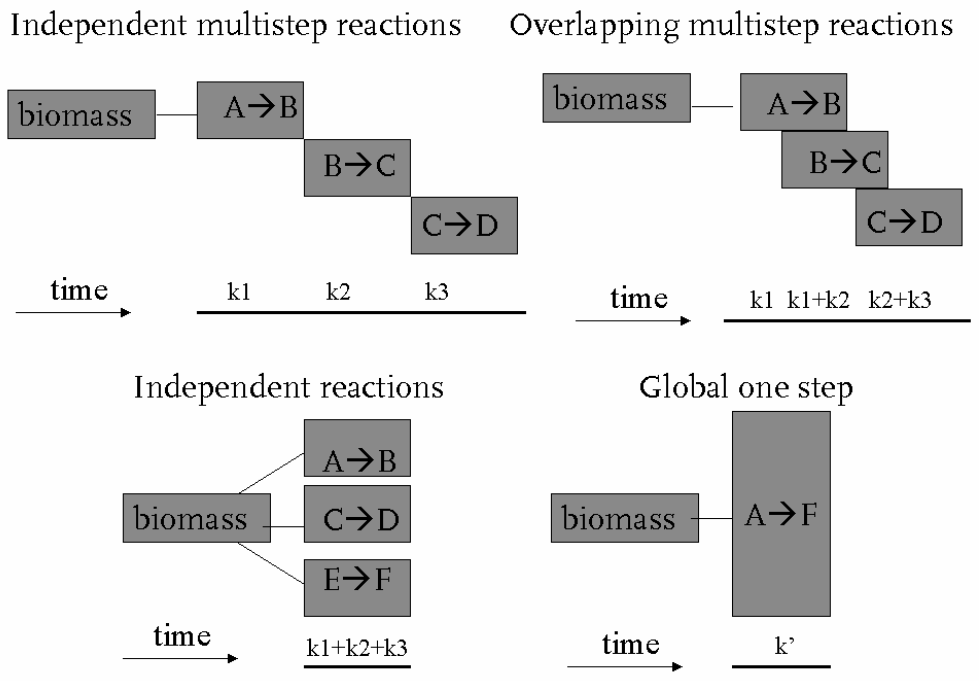

Figure 7.2: Different mechanisms used in the evaluation of biomass kinetics

The main kinetic schemes described in literature for hemicellulose decomposition are shown in Fig. 7.2. A global one-step reaction gives a very rough impression of kinetics of the overall reaction but it is difficult to compare parameters consistently with other researchers (Di Blasi and Lanzetta, 1997). Órfão et al. (1999) concluded that hemicellulose decomposition could not be modelled by simple kinetics. Research done on multi-step reaction mechanisms gives better results (Várhegyi et al., 1989; Várhegyi et al., 1997; Ward and Braslaw, 1985; Koufopanos et al., 1989). However, the models used in these papers fail to take into account the change of char yield with temperature. Di Blasi and Lanzetta (1997) used isothermal TGA measurements for evaluation of the kinetic parameters of torrefaction of xylan. They modeled the kinetics by a combination of a two-step mechanism with parallel reactions for the formation of solids and volatiles. In the mechanism of Di Blasi and Lanzetta, xylan is assumed to form an intermediate reaction product, which is a solid with a reduced degree of polymerization. This intermediate then reacts to the final product. The first reaction was found to be substantially faster than the second one.

For this research, it was decided to verify whether a two-step mechanism is also suitable to describe the weight loss kinetics of wood in the torrefaction temperature range, and how the char yields and reaction rates of the first and second step for wood compare with xylan. The mechanism used to model the torrefaction kinetics of willow is given in Eq. 7.2. As in the model of Di Blasi and Lanzetta, the formation of an intermediate product B is assumed and volatiles are formed in both reactions.

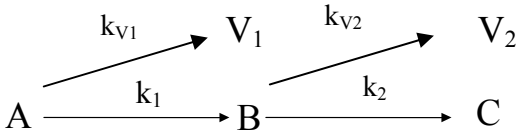

(7.2)

The differential rate equations, on the basis of weight, are given for the solids by Eqs. 7.3a-c. Similar equations may be derived for the volatile products.

$$r_A = \frac{\partial A}{\partial t} = -(k_1 + k_{V1})\, A^{n_A} \qquad (7.3a)$$

$$r_B = \frac{\partial B}{\partial t} = k_1\, A^{n_A} - (k_2 + k_{V2})\, B^{n_B} \qquad (7.3b)$$

$$r_C = \frac{\partial C}{\partial t} = k_2 B^{n_B} \qquad (7.3c)$$

If all reactions are assumed to be of first order, the system of equations can be solved analytically. Integration of the differential equations, with the initial condition that only A is present at the beginning of the reactions, and addition gives an expression for the relative solid weight:

$$M = A + B + C \qquad (7.4)$$

$$\frac{M_t}{M_0} = \left(1 + \left[\frac{k_1 K_1 - k_1 k_2}{K_1 (K_2 - K_1)}\right]\right) * e^{-K_1 t} + \left[\frac{-k_1 K_2 + k_1 k_2}{K_2 (K_2 - K_1)}\right] * e^{-K_2 t} + \frac{k_1 k_2}{K_1 K_2} \qquad (7.5)$$

Where:

$$K_1 = k_1 + k_{V1} \qquad (7.6a)$$

$$K_2 = k_2 + k_{V2} \qquad (7.6b)$$

For higher reaction orders, e.g. a second order reaction followed by a first order sequential reaction, the system of equations is non-linear and of stiff nature. This system can be solved numerically using a suitable algorithm; e.g. in Matlab Release 12, a one-step solver based on a modified Rosenbrock formula of order 2 may be applied.

The final char yield, which can be determined experimentally, is equivalent to the last term in Eq. 7.5:

$$\frac{C_{t\to\infty}}{M_0} = \frac{k_1 k_2}{K_1 K_2} = y_1 y_2 \qquad (7.7)$$

The yields of solid product are denoted as the parameters y_1 and y_2 for the first and second reaction respectively. Várhegyi et al (1989; 1997) have regarded these parameters as temperature-independent, e.g. for xylan decomposition, constant

values for the solid yields of the first and second reactions were obtained. Antal (1985) states that the separate formation of different product classes may be questioned from the viewpoint of analytical chemistry. Nevertheless, the solid product yields may decrease with temperature, as the hemicellulose fraction of the wood is dehydrated to a larger extent. Therefore, this study does consider solid formation and volatile formation as parallel reactions and aims to determine k_1, k_2, k_{V1} and k_{V2}.

7.3.3 Fitting of weight loss curves

Figure 7.3 shows the experimental weight loss curve for decomposing willow at various temperatures for a time interval of 3 hours. This interval includes a heating period of 3-10 minutes, required to heat the sample from 200°C to the final temperature (at a heating rate of 10°C min^{-1}). The weight loss curves for wood and wood components are modelled by a reaction in series model as this gives more accurate results than a global one-step reaction. If the first reaction is must faster than the second reaction, as is the case for xylan decomposition, a demarcation time exists after which the first reaction is completed and the second one starts. For decomposition of willow wood, it was possible to establish a demarcation time at temperatures in excess of 250°C. From this temperature, it seems that secondary charring reactions begin to occur.

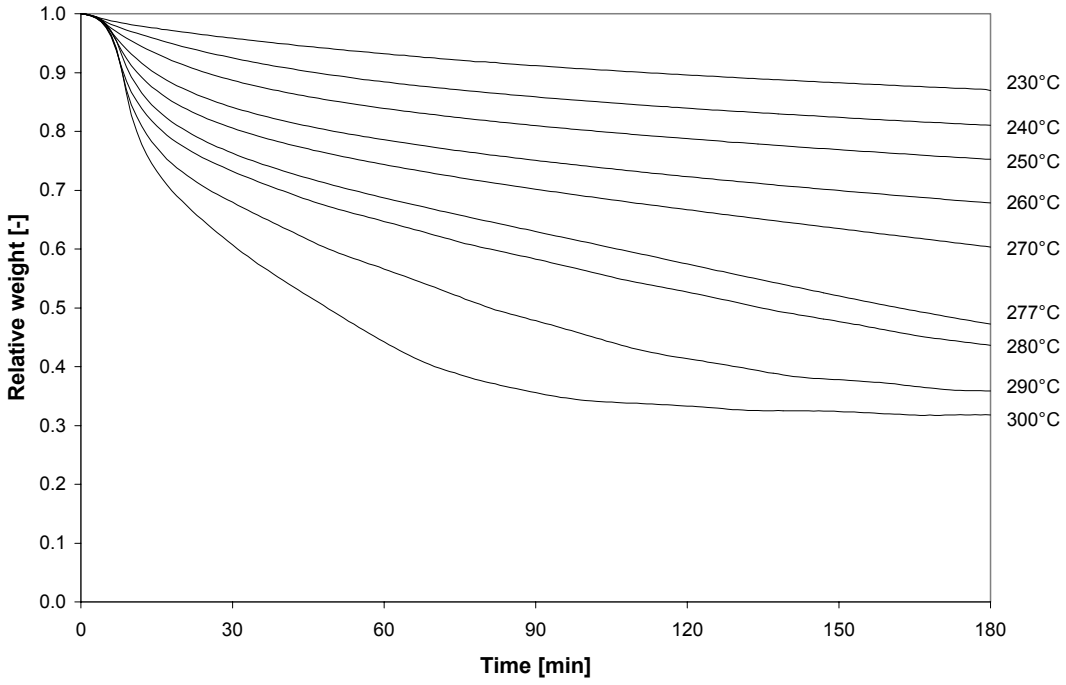

Figure 7.3: Experimental weight loss curve for willow decomposition at various final temperatures. Starting weight defined at 200°C; time includes a heating period of 3-10 minutes (heating rate = 10°C/min)

To determine the reaction orders, a plot of the logarithm of the non-dimensional solid weight versus time is shown in Fig. 7.4 (for clarity, experimental data points are shown with 5-10 minute intervals). Straight lines are observed before and after the demarcation time, so that a model with two first order reactions is valid. This is advantageous as it gives an analytical expression for the weight loss, whereas heat transfer limitation calculations become a lot more complicated for higher order models.

Since the volatile formation reactions are responsible for the solid weight loss, the reaction rate constants k_{V1} and k_{V2} can be graphically derived from the slopes of the lines before respectively after the demarcation time. The best fit for k_1 and k_2 was achieved by minimizing the sum of squares function:

$$F = \sum_i \left(\left(\frac{M_t}{M_o}\right)_{\exp,i} - \left(\frac{M_t}{M_o}\right)_{theor,i}\right)^2 \qquad (7.8)$$

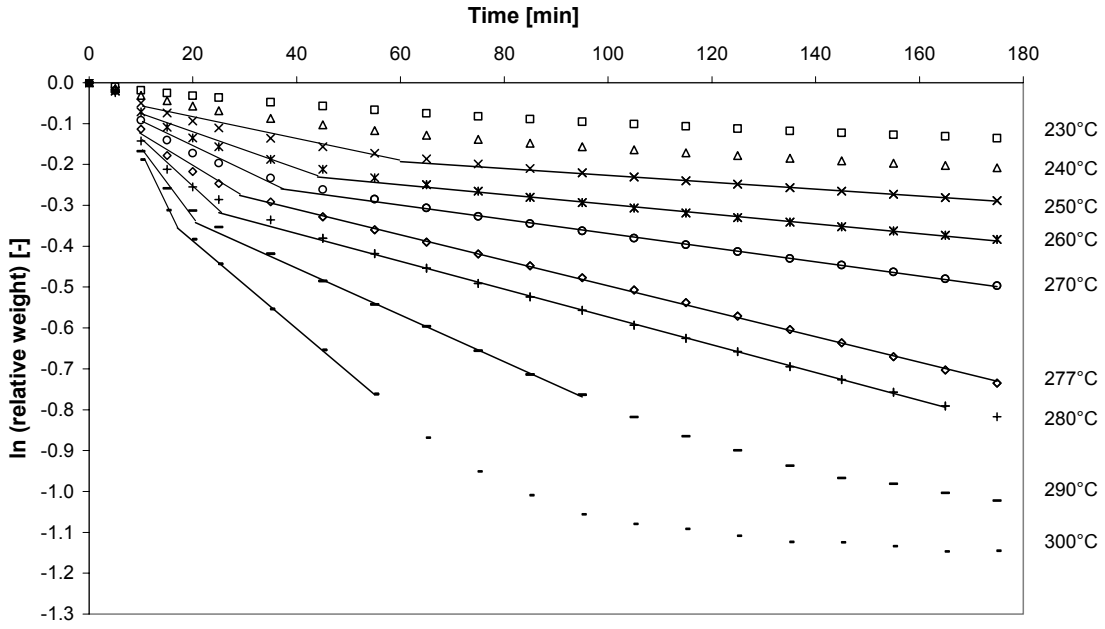

Figure 7.4: Logarithmic relative weight of willow versus time, at various final temperatures. Starting weight defined at 200°C; time includes a heating period of 3-10 minutes (heating rate = 10°C/min)

7.3.4 Kinetic parameters

The kinetic parameters obtained using the method described are as follows:

$$k_1 = 2.48 \times 10^4 \exp(-75976/RT) \qquad (7.9a)$$

$$k_{V1} = 3.23 \times 10^7 \exp(-114214/RT) \qquad (7.9b)$$

$$k_2 = 1.10 \times 10^{10} \exp(-151711/RT) \qquad (7.9c)$$

$$k_{V2} = 1.59 \times 10^{10} \exp(-151711/RT) \qquad (7.9d)$$

All rate constants are expressed in kg kg^{-1} s^{-1}, the temperature T in K and the gas constant R in J mol^{-1} K^{-1}. The kinetic parameters have been obtained using experiments with a low heating rate of 10 K/min, taking into account the weight loss during the heating phase.

In agreement with literature, it was found that the first reaction stage is remarkably faster than the second stage. Activation energies for the first and second stages are very close to those reported by Branca and Di Blasi (1997) of 76 kJ/mol and 143 kJ/mol respectively. The latter values have been determined by isothermal thermogravimetry for beech wood, for which the thermal behaviour has been demonstrated to be very similar to willow wood. Compared to the parameters published by Di Blasi and Lanzetta for xylan torrefaction, willow wood decomposes approximately one order of magnitude slower than xylan. This can be partly explained because willow contains only 25-30 wt% of xylan, but also because extraction of pure xylan from a wood matrix may make the xylan more reactive.

7.3.5 Model verification

To verify the final char yield predicted by the model, TGA experiments with a longer reaction time of 435 minutes were carried out (including a heating period of 7-10 minutes at a heating rate of 10°C min^{-1}). The results are shown in Fig. 7.5. At temperatures of 280-300°C, predicted char yields of 29-31% showed good agreement with experimental data, whereas determination of the final char yield at 270°C was not possible because the weight had not stabilized yet within 435 minutes.

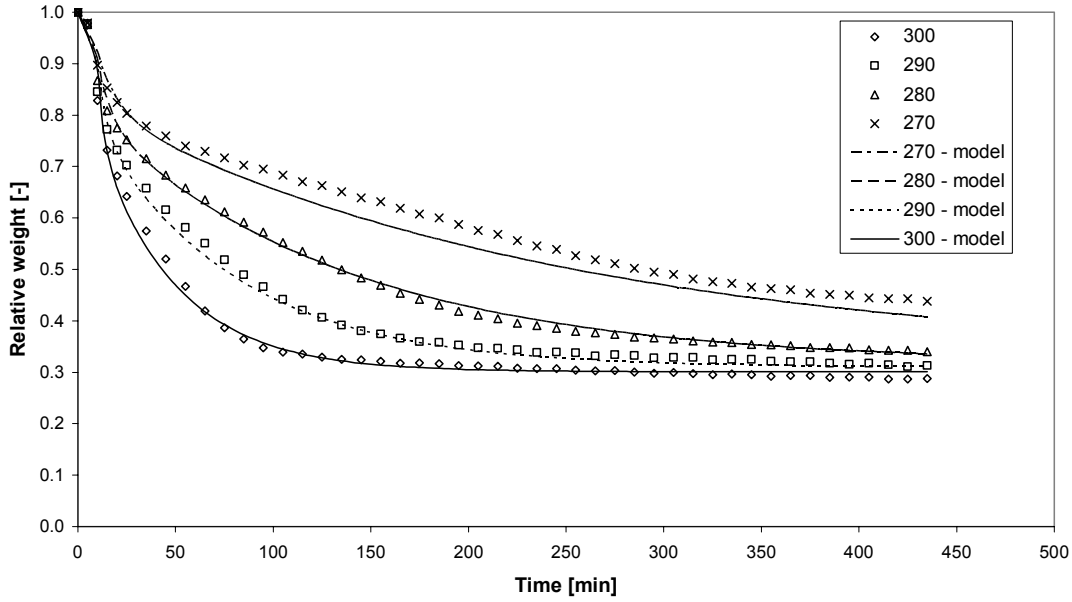

Figure 7.5: Experimental and modelled relative weight of willow versus time, for various temperatures. Starting weight defined at 200°C; time includes a heating period of 7-10 minutes (heating rate = 10°C/min)

The final char yield is the product of the solid yield for the first decomposition reaction (y_1) and the second decomposition reaction (y_2). For the temperature range studied, y_1 decreases from 88% at 230°C to 70% at 300°C, whereas y_2 is fairly constant at 41%. The first reaction with a relatively low weight loss could very well be representative of decomposition of the reactive xylan in willow wood, since hardwood contains up to 30% of xylan. The high weight loss in the second reaction can be explained by decomposition of the other fractions contained in the wood, notably the cellulose fraction, perhaps in combination with charring of the remaining hemicellulose fraction. This is also plausible because the activation energy found for the second weight loss step is close to literature values, such as those of Wagenaar et al. (1993). It may be that the primary decomposition products of xylan decomposition, e.g. acids, initiate decomposition of cellulose fraction. This hypothesis has been formulated previously (Lipinsky et al., 2002) and contradicts the approach of others who have considered the rate of biomass decomposition as the sum of the rates of main biomass components that react individually (Alves and Figueiredo, 1989; Órfão et al., 1999).

The model has also been tested at higher heating rates up to 100°C min^{-1}. Figure 7.6 shows the sample temperature and relative weight as a function of reaction time for heating rates of 10, 50 and 100°C min^{-1} and a final temperature of 260°C. It can be observed that the trend in weight loss is predicted accurately also at higher heating rates. At a heating rate of 100°C min^{-1}, the required heating time is less than a minute and the associated weight loss less than 1%.

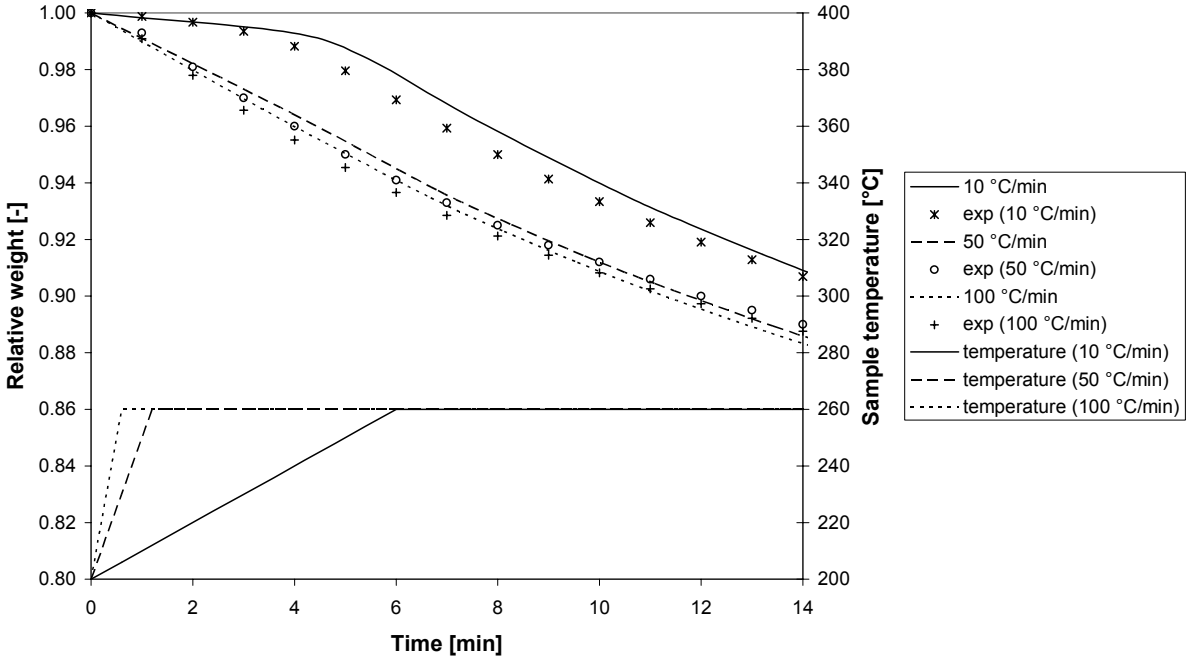

Figure 7.6: Experimental and modeled relative weight of willow versus time, with varying heating rates and final temperature of 260°C. Bottom lines indicate sample temperatures

7.3.6 Recommendations for industrial torrefaction process conditions

The kinetic data may be used to make recommendations for industrial torrefaction process conditions and for process scale-up. In torrefaction, the fast initial reaction, in which the highly reactive hemicellulose is decomposed, is important. This reaction stage should go more or less to completion. The second reaction stage, which could represent cellulose decomposition and secondary charring reactions of hemicellulose reaction products, takes much more time to complete, which may lead to uneconomically large equipment. Figure 7.7 shows the time required to obtain the maximum yield of intermediate product B. This time reduces from over 3 hours at 230°C to 10 minutes at 300°C. The latter reaction time appears short enough for commercially viable processes, since the estimated reactor volume may be fitted into a single reactor even at large capacity up to 10 kg s^{-1}.

The maximum yield of B, which is also shown in Fig. 7.7, decreases with temperature since more volatiles are formed at higher temperature. This may be favourable if these volatiles consist of species that carry little energy, such as water vapour or carbon dioxide. However, at temperatures above 300-320°C, fast thermal cracking of cellulose may cause tar formation, so that operation below 300°C is recommended. This also ensures a good selectivity to the intermediate product; the selectivity to B decreases with temperature because the activation energy of the secondary reactions is higher than that of the primary reactions.

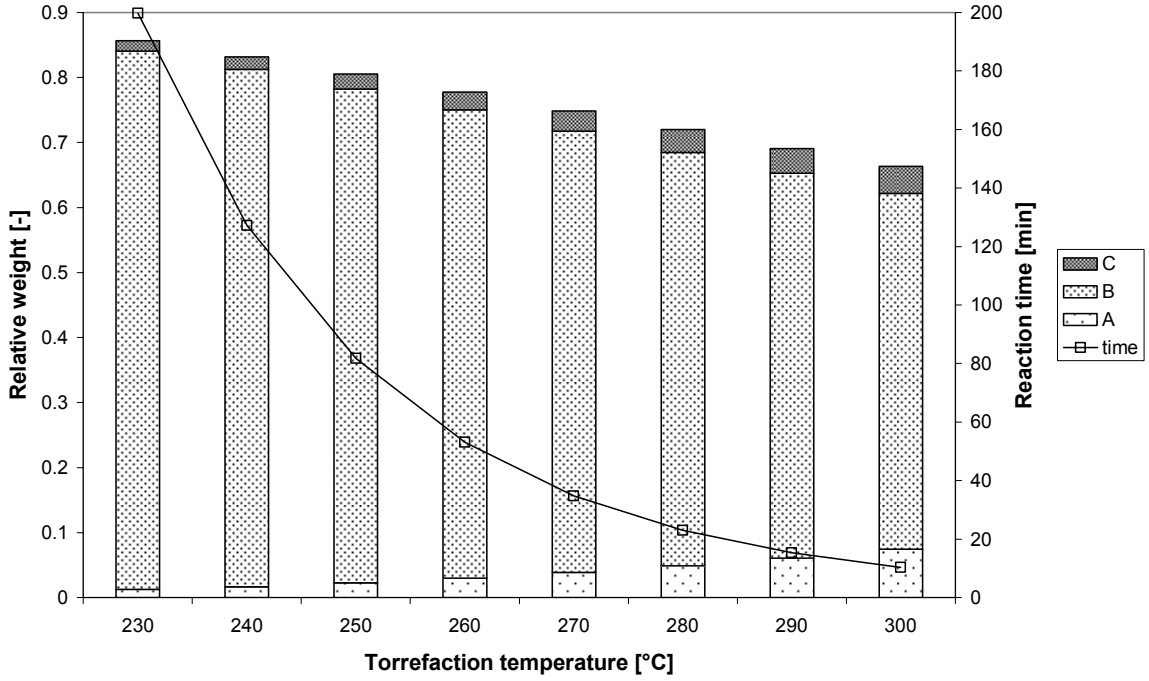

Figure 7.7: Time required for maximum yield of intermediate product B and corresponding yields of A, B and C at different temperatures

Another important process parameter for torrefaction is the particle size. To ensure the minimum residence time, it is important that the rate of heat transfer to and within the particle is fast, as compared with the reaction rate. This means that the solid temperature will be essentially the same as the surrounding temperature, and the overall controlling factor is the intrinsic kinetics. The ratio between heat convection and conduction rates is expressed by the Biot number:

$$Bi = \frac{\alpha r_p}{\lambda} << 1 \qquad (7.10)$$

While the ratio of heat convection rate and reaction rate is expressed by the (external) Pyrolysis number (Pyle and Zaror, 1984):

$$Py' = \frac{\alpha}{K_1 \rho c_p r_p} >> 1 \qquad (7.10)$$

In these equations, α is the external heat transfer coefficient in W m^{-2} K^{-1}, r_p is the radius of the particle in m (assuming spherical particles), λ is the thermal conductivity in W m^{-1} K^{-1}, ρ is the density in kg m^{-3} and c_p is the heat capacity in J kg^{-1} K^{-1} of the biomass particle. Figure 7.8 shows these parameters at a reaction temperature of 250°C and 300°C for an external heat transfer coefficient of 100 W m^{-2} K^{-1}. At a Biot number of unity, equivalent to a particle size of 2 mm, the Pyrolysis number is sufficiently high. For pyrolysis of wood below 300°C, it follows that the reactions are the rate limiting step, provided that the particle size is sufficiently small and internal heat transfer does not play a role.

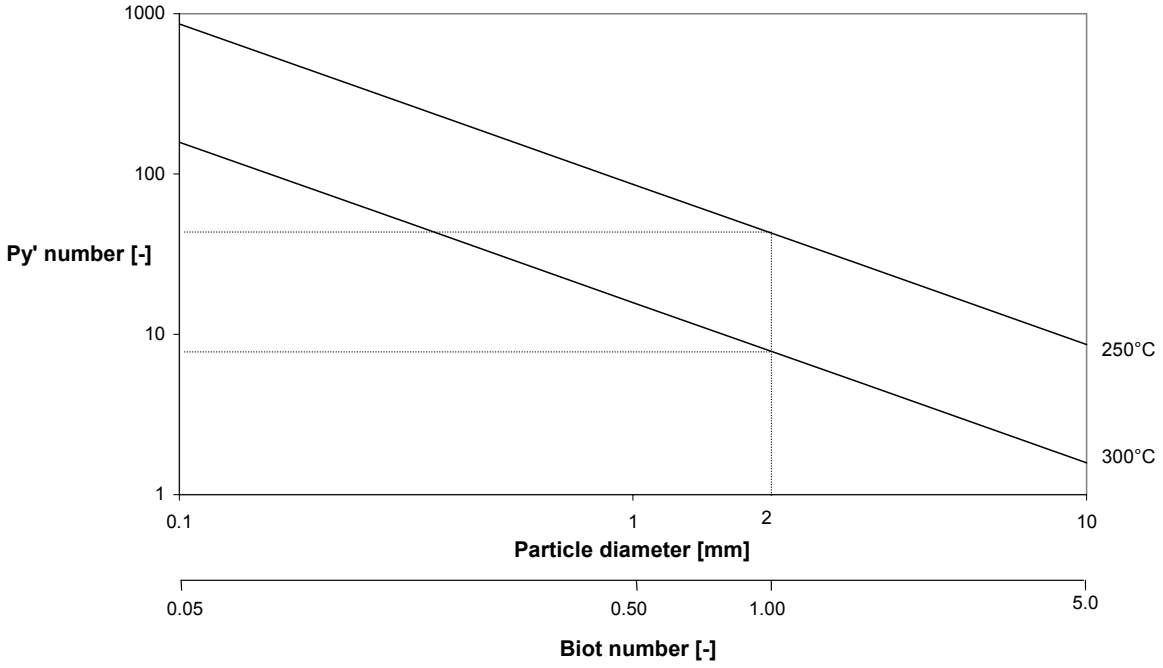

Figure 7.8: Biot number and Pyrolysis number (for reaction at 250°C and 300°C) as a function of biomass particle diameter. Biomass properties: λ = 0.1 W/mK, ρ = 1500 kg/m3 and cp = 2000 J/kgK

7.4 Conclusions

The kinetics of torrefaction reactions in the temperature range of 230-300°C can be described accurately by a two-step mechanism. The first step is much faster than the second step, so that these steps can be demarcated in time. The first step is representative of hemicellulose decomposition, while the second step represents cellulose decomposition. The solid yield for the first step is higher than for the second step: 70-88% (decreasing with temperature) versus 41%. This may be explained because deciduous wood, such as willow, contains less xylan (the reactive component in its hemicellulose fraction) than cellulose.

Comparison of the kinetic parameters of willow with those of xylan shows that xylan reacts approximately one order of magnitude faster than willow, a classical hardwood containing up to 30% xylan. It is recommended to determine reaction kinetics also for softwood, such as larch. However, initial experiments have shown that softwood is much less reactive and therefore lower rate constants can be expected. Research into thermal degradation of model components such as glucomannan, which constitutes 60-70 wt% of the hemicellulose fraction in softwoods, is recommended to confirm this finding.

References

Alves SS, Figueiredo JL (1989). A model for pyrolysis of wet wood. Chemical Engineering Science 44:2861-2869.

Antal MJ (1985). Biomass Pyrolysis: a Review of the Literature. Part II – Lignocellulose pyrolysis. In: Boer KW, Duffie JA, editors. Advances in Solar Energy. Boulder, CO: American Solar Energy Society. p. 175-255.

Bradbury AGW, Sakai Y, Shafizadeh F. J (1979). A kinetic model for pyrolysis of cellulose. Journal of Applied Polymer Science 23: 3271-3280.

Branca C, Di Blasi C (2003). Kinetics of the isothermal degradation of wood in the temperature range 528-708 K. Journal of Analytical and Applied Pyrolysis 67:207-219.

Broido A (1976). Kinetics of solid phase cellulose pyrolysis. In: Shafizadeh F, Sarkanen KV, Tillman DA, editors. Thermal uses and properties of carbohydrates and lignins. New York: Academic Press.

Bourgois JP, Doat J (1984). Torrefied wood from temperate and tropical species, advantages and prospects. In: Egnéus H, Ellegård A. Bioenergy 84. London: Elsevier Applied Science Publishers. p. 153-159.

Di Blasi C, Lanzetta M (1997). Intrinsic kinetics of isothermal xylan degradation in inert atmosphere. Journal of Analytical and Applied Pyrolysis 40-41:287-303.

Gaur S, Reed TB (1988). Thermal data for natural and synthetic materials. New York: Marcel Dekker.

Girard P, Shah N (1991). Recent developments on torrefied wood, an alternative to charcoal for reducing deforestation. REUR Technical series 20: 101-114.

Koufopanos CA, Maschio G, Lucchesi A (1989). Kinetic modelling of the pyrolysis of biomass and biomass components. Canadian Journal of Chemical Engineering 67:75-84.

Lipinsky ES, Arcate JR, Reed TB (2002). Enhanced wood fuels via torrefaction. Fuel Chemistry Division Preprints 47 (1):408-410.

Órfão JJM, Antunes FJA, Figueiredo JL (1999). Pyrolysis kinetics of lignocellulosic materials – three independent reactions model. Fuel 78:349-358.

Pentananunt R, Mizanur Rahman ANM, Bhattacharya S (1990). Upgrading of biomass by means of torrefaction. Energy 15 (12): 1175-1179.

Pyle DL, Zaror CA (1984). Heat transfer and kinetics in the low temperature pyrolysis of solids. Chemical Engineering Science 39:147-158.

Ramiah MV (1970). Thermogramietric and differential thermal analysis of cellulose, hemicellulose, and lignin. Journal of Applied Polymer Science 14: 1323-1337.

Shafizadeh F (1985). Pyrolytic Reactions and Products of Biomass. In: Overend RP, Milne TA, Mudge LK, editors. Fundamentals of Biomass Thermochemical Conversion. London: Elsevier. p. 183-217.

Várhegyi G, Antal MJ, Szekely T, Szabo P (1989). Kinetics of the thermal decomposition of cellulose, hemicellulose, and sugar cane bagasse. Energy & Fuels 3:329-335.

Várhegyi G, Antal MJ, Jakab E, Szabó P (1997). Kinetic modeling of biomass pyrolysis. Journal of Analytical and Applied. Pyrolysis 42:73-87.

Wagenführ R, Scheiber C (1974). Wood atlas. Leipzig: VEB Fachbuchverlag. (in German)

Ward SM, Braslaw J (1985). Experimental weight loss kinetics of wood pyrolysis under vacuum. Combustion and Flame 61:261-269.

Wagenaar BM, Prins W, Swaaij WPM van (1993). Flash pyrolysis kinetics of pine wood. Fuel Processing Technology 36:291-298.

Chapter 8

Analysis of products from wood torrefaction

Torrefaction is a mild pyrolysis process carried out at temperatures ranging from 225 to 300°C, in which hemicellulose, the most reactive fraction of wood, is decomposed. Dehydration and decarboxylation reactions cause a mass loss of the wood, whereas the lower heating value of the wood is largely conserved. Deciduous wood types (beech and willow) and straw were found to produce more volatiles than coniferous wood (larch), especially more methanol and acetic acid. These originate from acetoxy- and methoxy-groups present as side chains in xylose units present in the xylan-containing hemicellulose fraction. The torrefied wood product has a brown/black colour, reduced volatile content and increased energy density: 20.7 MJ/kg (after 15 min reaction time at 270°C) versus 17.7 MJ/kg for untreated willow. It has favourable properties for application as a fuel for gasification and/or (co-)combustion.

8.1 Introduction

In the transition to a more sustainable energy supply, there is a clear need for better biofuels. Untreated woody biomass has a relatively low energy density, high moisture content and is difficult to comminute into small particles. These properties make transport of wood relatively expensive. After drying, it can regain moisture and may rot during storage. Furthermore, enhancement of the energy density is advisable because a large amount of wood is required to replace an equivalent amount of coal in applications such as combustion and gasification. A technology that could help to overcome these problems is a thermal processing step known as torrefaction. In this process, wood is roasted in the temperature range of 225-300°C under an inert atmosphere. The weight loss kinetics of the process have been treated in Chapter 7. This chapter focuses on the products obtained, which consist of three phases: a solid product of a dark colour, an acidic aqueous phase of yellowish colour and permanent gases such as carbon monoxide and carbon dioxide. The solid product, torrefied wood, has attractive fuel properties, such as an improved heating value, low moisture content, and ease of size reduction (Bergman et al., 2004).

Research focused on the torrefaction process was already performed in France in the 1930's but no significant publications remain. In the 1980's, the process was pioneered by Bourgois and Doat (1984), who published the results of torrefaction experiments with two temperate and two tropical wood samples. For the deciduous

wood types, eucalyptus and a mixture of chestnut and oak, torrefaction at 270-275°C increased the lower heating value of the wood from 18.6 to 22.7 MJ/kg and 17.9 to 21.5 MJ/kg respectively, while retaining over 90% of the energy. The coniferous wood types, maritime and Caribbean pine, required a higher temperature of 280-285°C, while the increase in energy density was slightly less. This research resulted in the building of a continuous wood torrefaction plant in 1987. Torrefied wood from this plant was used as a reducer in the production of silicon metal. Two batch plants were also built for the production of barbeque fuel and firelighters. Torrefaction of wood has recently attracted more interest. Pentananunt et al (1990) carried out torrefaction experiments at the Asian Institute of Technology in Bangkok. They compared combustion characteristics of torrefied wood produced after 2-3 hours of torrefaction and concluded that torrefied wood produces less smoke compared with untreated wood. Felfli et al. (1998) used a bench unit to determine the effect of raw material, temperature, and residence time on the properties of torrefied wood. Similar research has been carried out at by Pach et al. (2002) and Nimlos et al. (2003).

In torrefaction, the most reactive fraction of biomass, i.e. the hemicellulose fraction, is decomposed so that torrefied wood and volatiles are formed. Gaur and Reed (1998) summarize the hemicellulose degradation as a two-step reaction where light volatiles (mono- and polysaccharide fractions and dehydrosugars) are formed in the first step followed by their catalytic degradation (by mineral matter) resulting in the formation of CO and CO_2. Thermal cleavage of carbon bonds of the carboxylic groups might result in the formation of acids. Acid catalyzed dehydration and thermal cleavage reactions form CO_2 and carbonyls like hydroxy acetone, methanol, propanal etc, most of them consisting of 1-3 carbon atoms and 1-2 oxygen atoms. They differ a lot due to stereochemistry and internal rearrangements like retro aldol reactions. When the biomass particles are relatively small the main part of the acids diffuses out of the particle.

The research described in this chapter aims to give a good insight into the overall mass balance of the process. This requires analysis of all reaction products, i.e. both the torrefied wood and the volatile product (the latter is seldom analyzed in the torrefaction literature). An important research parameter is the type of wood: both deciduous and coniferous wood types are considered since the composition of their hemicellulose fraction differs. The torrefaction behavior of straw is also tested because it is an abundant and cheap biomass feedstock. The effect of process conditions such as temperature and residence time on the yield and composition of solid product and volatile products is studied. Special emphasis is given to the fuel properties and the energy conserved in torrefied wood.

8.2 Experimental

8.2.1 Equipment

Figure 8.1 presents a schematic view of the experimental setup. The bench-scale torrefaction unit consists of a quartz fixed-bed reactor placed inside an oven. A continuous flow of argon is controlled with a Brooks mass flow controller. The argon flow is used to keep the system inert and remove volatile products from the reactor. The volatile products are split into a liquid and gas phase in a cold trap at –5°C. Gases are collected in a gasbag. The sample temperature is measured by a thermocouple in a glass well inside the reactor bed and controlled with a Eurotherm master slave controller. Tracing the inlet and outlet of the reactor prevents condensation of products in the reactor and tubing. The argon inlet lines are also traced in order to preheat the gas for a more stable temperature control. A batch of 10 gram of biomass is loaded in the reactor resulting in a bed height of approximately 5 cm. The biomass is heated with a heating rate of 10-20 °C/min to the torrefaction temperature. After the isothermal heating period the reactor is cooled in approximately 5 minutes with pressurized air until the temperature is below 200°C. In order to prevent condensation of reaction products the tracing is continued for another 15 minutes.

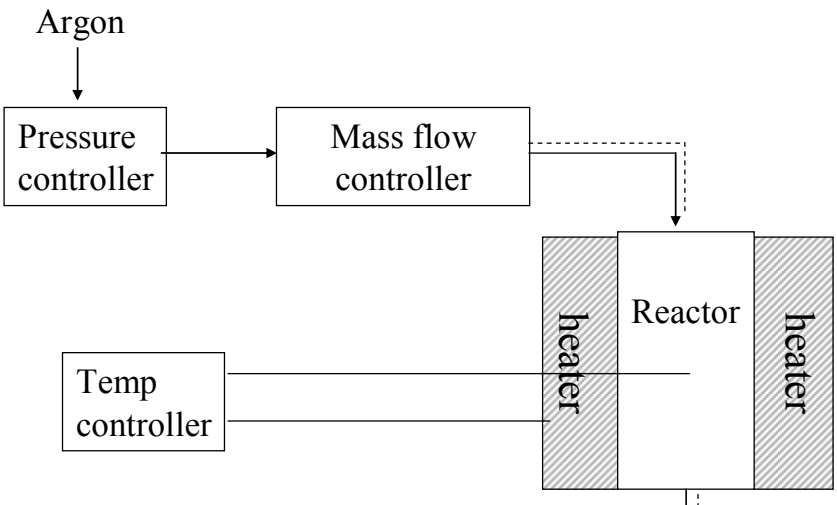

Flow	10-50 ml/min
Pressure	Atmospheric
Temp	230-300 ºC
Tracing inlet	120 ºC
Tracing outlet	180 ºC

Figure 8.1: Schematic setup of the bench scale torrefaction unit

8.2.2 Experimental plan

The biomass used was beech, willow, larch and straw, the properties of which are shown in Table 8.1. Particle sizes were in the range of 0.7 to 2.0 mm in all cases, except for straw where it was < 5 mm. Experiments were carried out with beech and willow at temperatures in the range of 220-300°C and residence times in the range of 10-60 minutes. For comparison, the coniferous larch wood was torrefied at 230°C (50 min.), 250°C (30 min.), 270°C (15 min.), 290°C (10 min.) and straw at 250°C (30 min.). Note that the residence time excludes the heating time, e.g. to heat the reactor bed from 200°C (at which the torrefaction reactions begin to occur) to a torrefaction temperature of 250°C takes approximately 8 minutes.

Table 8.1: Properties of biomass types

	Ash	Volatiles	C	H	N	O	O/C Ratio	HHV (dry)	LHV (dry)
	wt% of dry material						-	MJ/kg	MJ/kg
Beech	1.2	82.7	47.2	6.0	0.40	45.2	0.72	18.3	17.0
Willow	1.6	81.4	47.2	6.1	0.34	44.8	0.71	19.0	17.7
Larch	0.1	82.8	48.8	6.1	0.10	44.9	0.69	19.5	18.2
Straw	7.1	79.0	44.3	5.8	0.40	42.4	0.72	17.4	16.1

8.2.3 Analyses

All the reaction products were collected and weighed in order to make an overall mass balance. The solid product, the produced liquid and the produced gases were analyzed with different techniques. The composition of the solid product was determined by proximate and ultimate analysis and its heating value was measured in a bomb calorimeter. Liquid products collected in the cold trap were diluted with 2-butanol because not all the products dissolve in water. The diluted liquid was analyzed with HPLC using a Chrompack Organic Acids column with detection based on refraction index. The composition of produced gas was analyzed with a Varian Micro GC with a Poraplot Q and a Molsieve column.

8.3 Results and discussion

8.3.1 Overall mass balance

Figure 8.2 displays the overall mass balance of several torrefaction experiments using willow, larch and straw. The overall mass balance of the torrefaction experiments closed quite well and was generally in the range of 95-100%. This high accuracy is possible because the solid product, which can be recovered and weighed accurately, constitutes the largest proportion of the product yield. The amount of lost material increases with temperature, which means that experimental error in recovery and weighing of volatiles is larger than for the solid.

8.3.2 Yield of solid product

Figure 8.3 shows the amount of solid product recovered, for beech, willow, straw and larch at various conditions. The yield of solid product decreases with temperature and, to a lesser extent, residence time, whereas the yield of volatiles increases accordingly. Clearly, the extent of devolatilisation increases with temperature and reaction time. The two lines shown in Fig. 8.3 have been calculated using the kinetic model for torrefaction of willow obtained in Chapter 7. The upper line is for a residence time of 15 minutes and the lower line for 30 minutes. For willow and beech wood, the measured data points are in the range described by the kinetic model. Therefore, there is good agreement between thermogravimetric weight loss data and the data from the fixed bed reactor set-up.

Figure 8.3 also shows a number of data points for larch (coniferous wood) and straw. The observed weight loss for straw is comparable to willow and beech wood (both deciduous woods). However, the total weight loss for larch is much smaller, which agrees with the results in Chapter 7. This is probably caused because the hemicellulose fraction in coniferous wood has a different chemical composition, i.e. the amount of the most reactive hemicellulose (xylan) is less than for the deciduous wood types (Wagenführ and Scheiber, 1974). The hemicellulose fraction of coniferous wood contains a high proportion of glucomannan, which is less reactive and has lower weight loss in this temperature range than xylan (Ramiah, 1970).

8.3.3 Yield of volatile products

The volatiles consist of a condensable and a non-condensable fraction. For both fractions, the amount formed increases with torrefaction temperature. Figure 8.4 shows the yields of condensable products (weight formed divided by the dry- and ash-free weight of wood) for willow, larch and straw at varying experimental conditions.

Acetic acid and water are the main liquid torrefaction products of willow, while smaller quantities of methanol, formic acid, lactic acid, furfural, hydroxyl acetone and traces of phenol are found. Šimkovic et al. (1988), who used TG/MS to study thermal decomposition of xylan have also observed these compounds. Thus, the products found stem mainly from the decomposition of the hemicellulose fraction.

The amount of acetic acid formed from willow increases with temperature: the amount of acetic acid formed is as much as 13% at 290°C.Straw yields similar condensable products in comparable quantities as for willow, but these differ from larch: the weight loss of larch is mainly due to dehydration and the main acid formed is formic acid. For larch wood, the yield of condensable products is much smaller, in agreement with the observed lower weight loss, and also increases with temperature. The difference in product distribution between willow and larch may be explained from differences in hemicellulose composition. The hemicellulose of

deciduous woods has acetoxy- and methoxy-groups attached to the polysugars (in particular to xylose units), which form acetic acid and methanol when the wood is heated to temperatures around 200°C (White and Dietenberger, 2001).

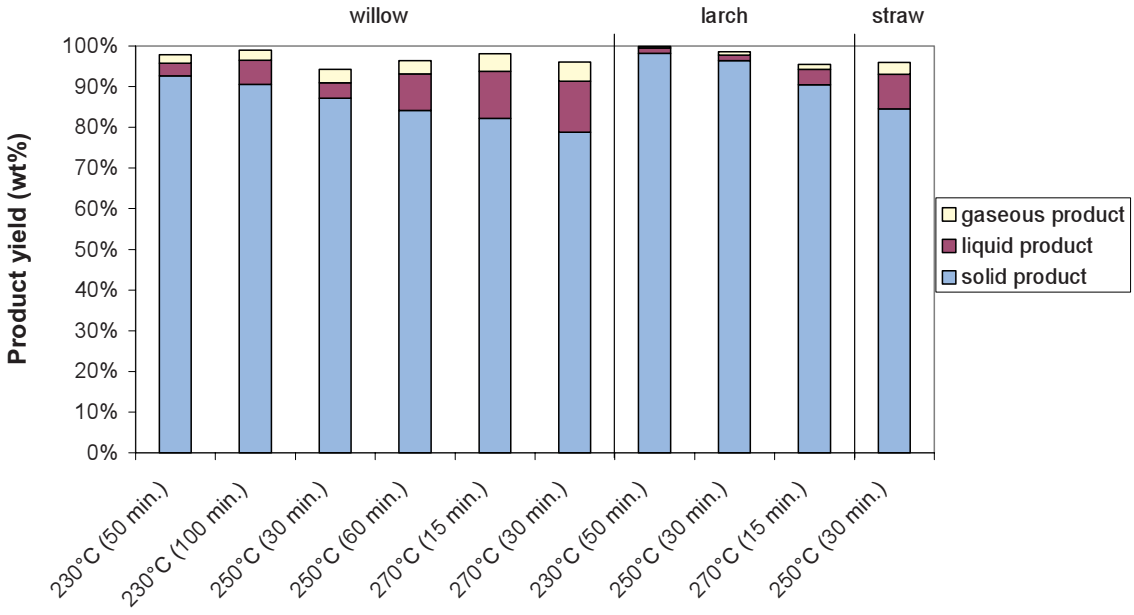

Figure 8.2: Overall mass balance of several torrefaction experiments

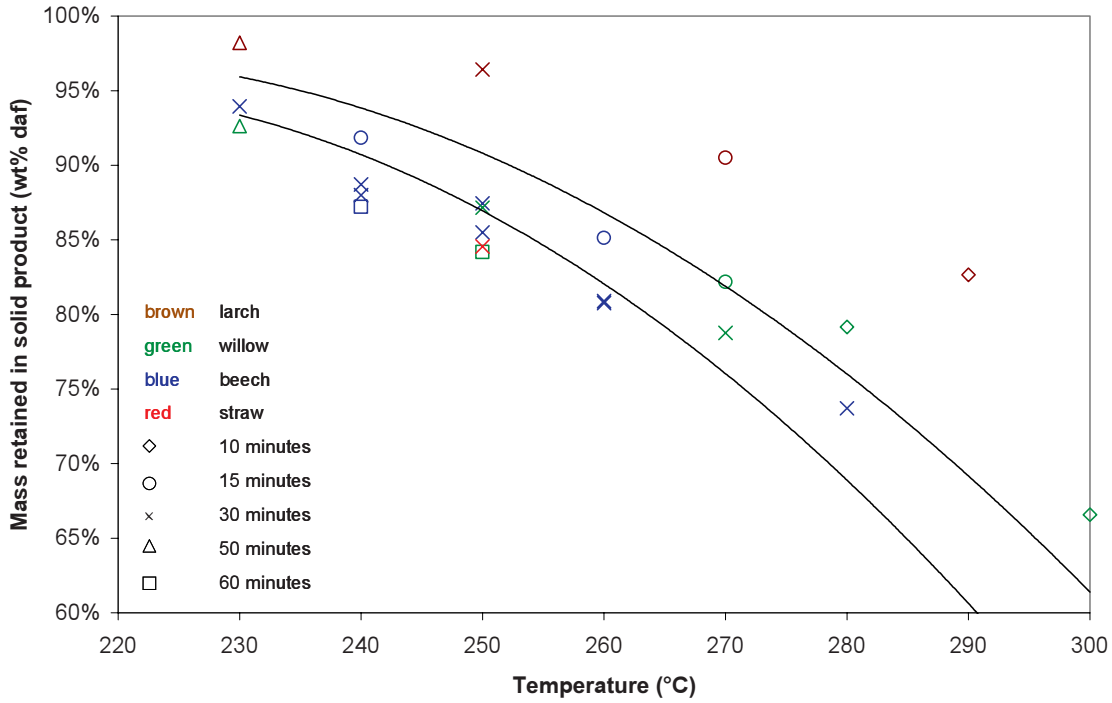

Figure 8.3: Yield of torrefied wood as a function of temperature and residence time, for different biomass types; solid lines from kinetic model for torrefaction of willow at 15 minutes (upper line) and 30 minutes (lower line) residence time

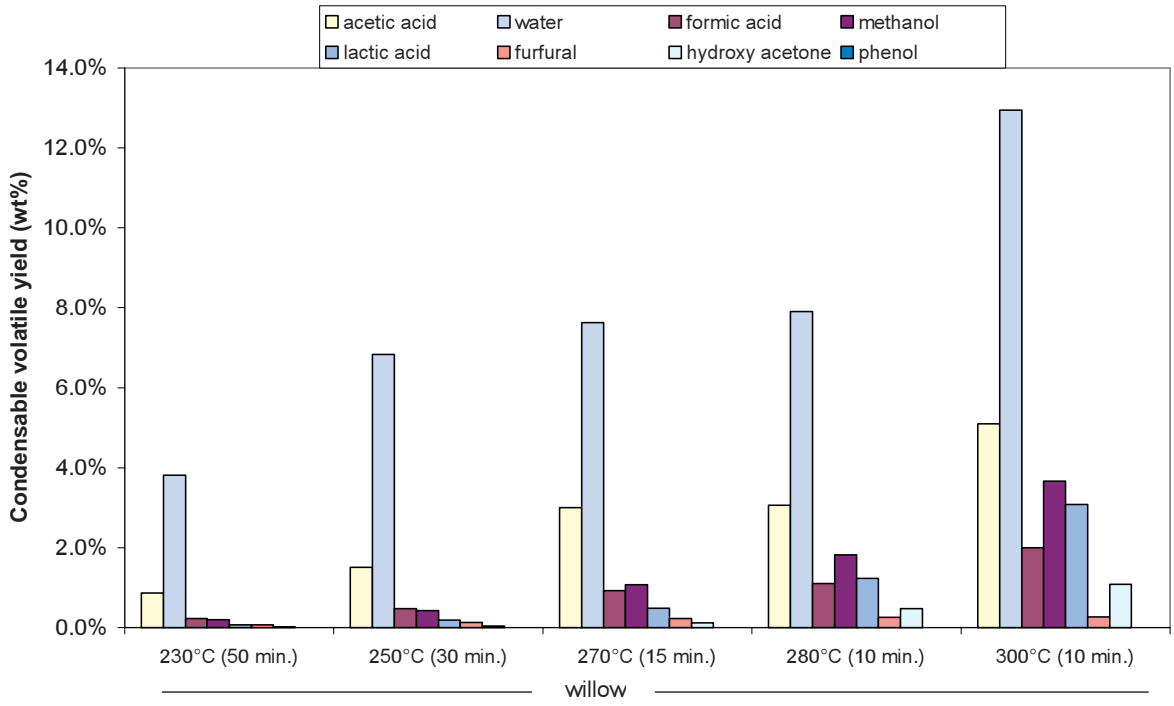

(a)

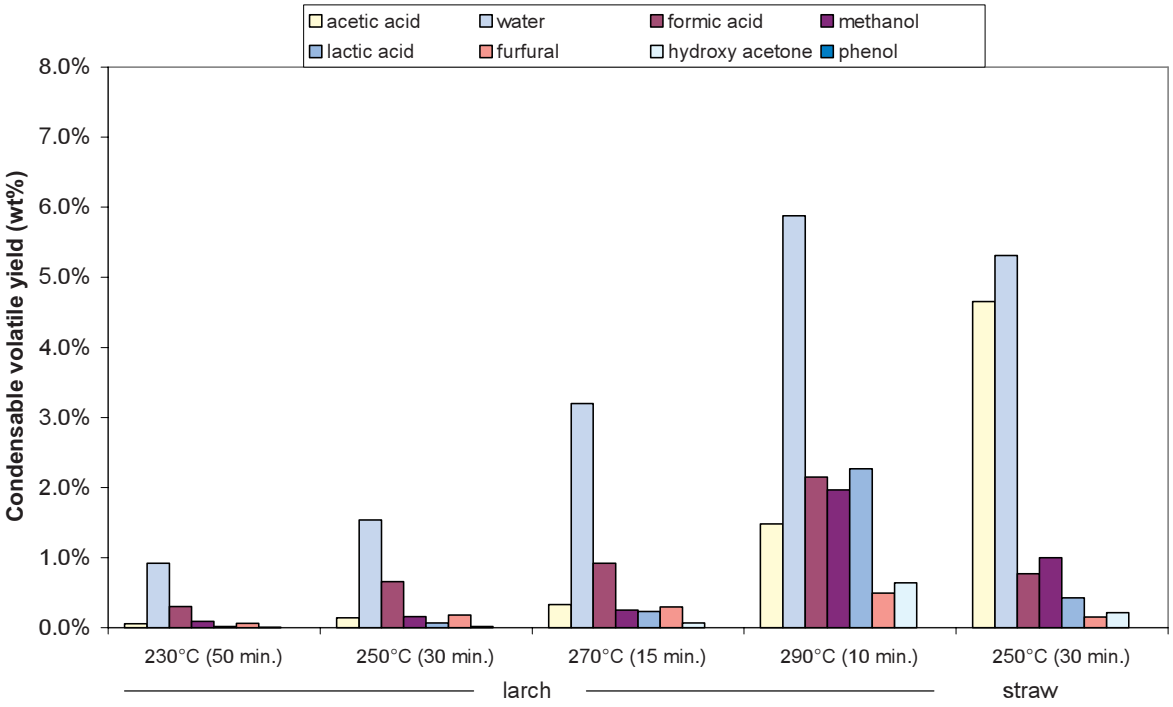

(b)

Figure 8.4: Product yields of condensable volatiles formed in torrefaction at different conditions, for (a) willow and (b) larch and straw

The composition of the non-condensable volatile product obtained from torrefaction is depicted in Fig. 8.5a for willow and Fig. 8.5b for larch and straw at various conditions. The amount of non-condensable volatiles is again higher for willow and straw than that for larch, which further exemplifies the higher degree of devolatilisation for deciduous, xylan-containing wood. The permanent gases formed are mainly carbon dioxide and carbon monoxide. Traces of hydrogen and methane are detected as well.

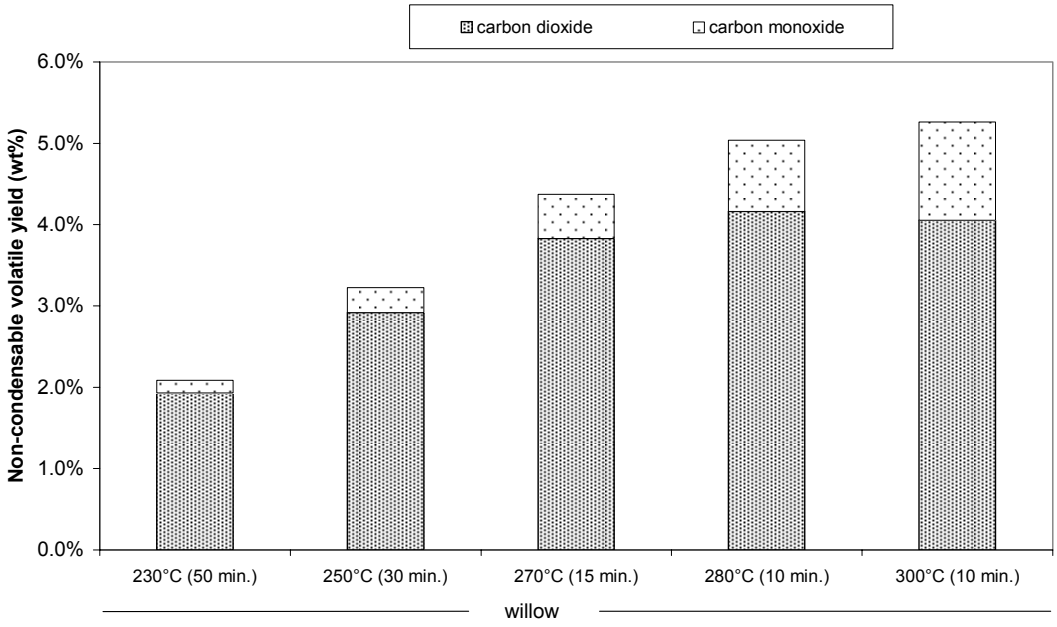

(a)

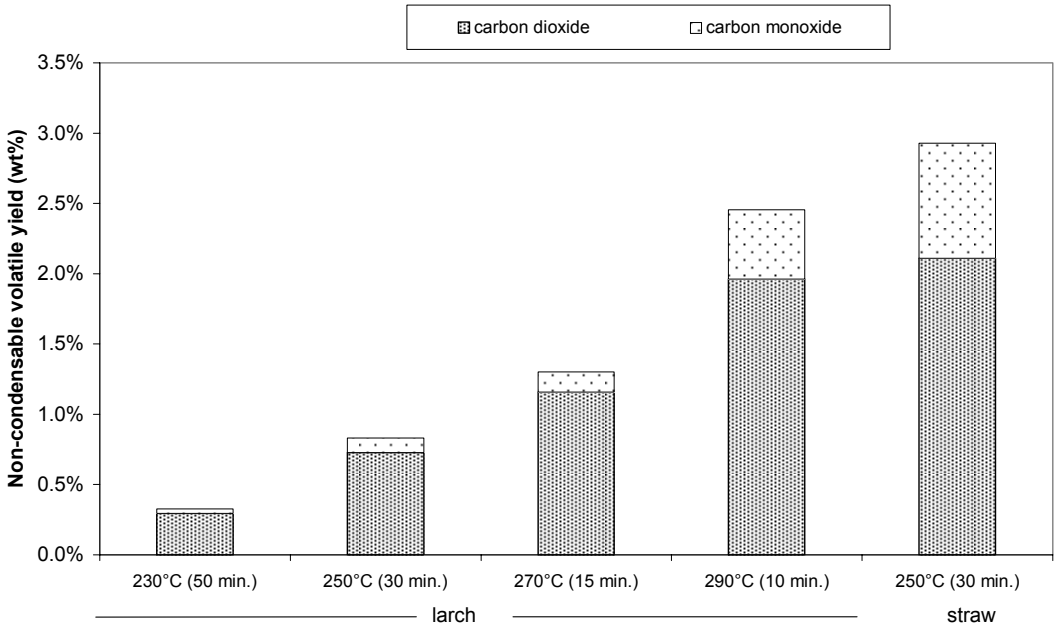

(b)

Figure 8.5: Product yields of non-condensable volatiles formed in torrefaction at different conditions, for (a) willow and (b) larch and straw

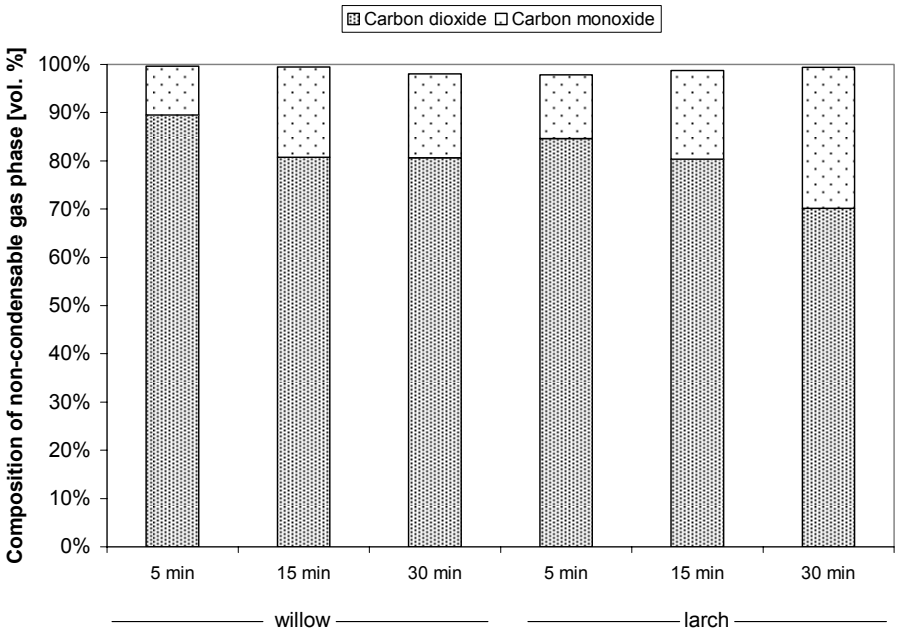

Figure 8.6: Change in gas composition with time for torrefaction at 250°C

The formation of carbon dioxide may be explained by decarboxylation of acid groups in the wood. However, the formation of carbon monoxide cannot be explained by dehydration or decarboxylation reactions. The increased carbon monoxide formation is reported in literature (White and Dietenberger, 2001) as the reaction of carbon dioxide and steam with porous char to carbon monoxide with increasing temperature. Mineral matter may catalyze such reactions, especially since the gases formed in the torrefaction experiment using straw contained a relatively higher amount of carbon monoxide than the experiments using wood (which contains much less mineral matter).

Figure 8.6 shows the gas composition of the non-condensable product with time (the totals do not add exactly to 100% because the main components, carbon dioxide and carbon monoxide, are shown). These results were obtained by torrefaction of larch and willow at 250°C and analysis of non-condensable gases after 5, 15 and 30 minutes. It was found that the ratio of carbon dioxide to carbon monoxide decreases with time, in line with the theory that carbon monoxide is formed in a secondary reaction.

8.3.4 Properties of the solid product

The torrefied wood samples obtained at temperatures above 250°C contained less than 0.1% moisture. The volatile content of deciduous wood decreases during torrefaction from 81-83% to 70-75%. Torrefaction decreases the atomic O/C ratio of the solid product from approximately 0.70 to 0.52-0.60; this decrease becomes larger at higher reaction temperature and prolonged reaction times. There was a marked difference between willow, beech and straw compared to larch. For the latter, a smaller decrease was observed, with O/C ratios in the range of 0.60-0.65.

This is explained because in torrefaction of larch, mainly water is formed, and relatively little carbon dioxide, carbon monoxide, and other carbon containing species, as in torrefaction of beech and willow. The chemical composition of torrefied wood is comparable to that of peat. Torrefied wood is an intermediate between wood and charcoal, which requires much higher temperatures to produce.

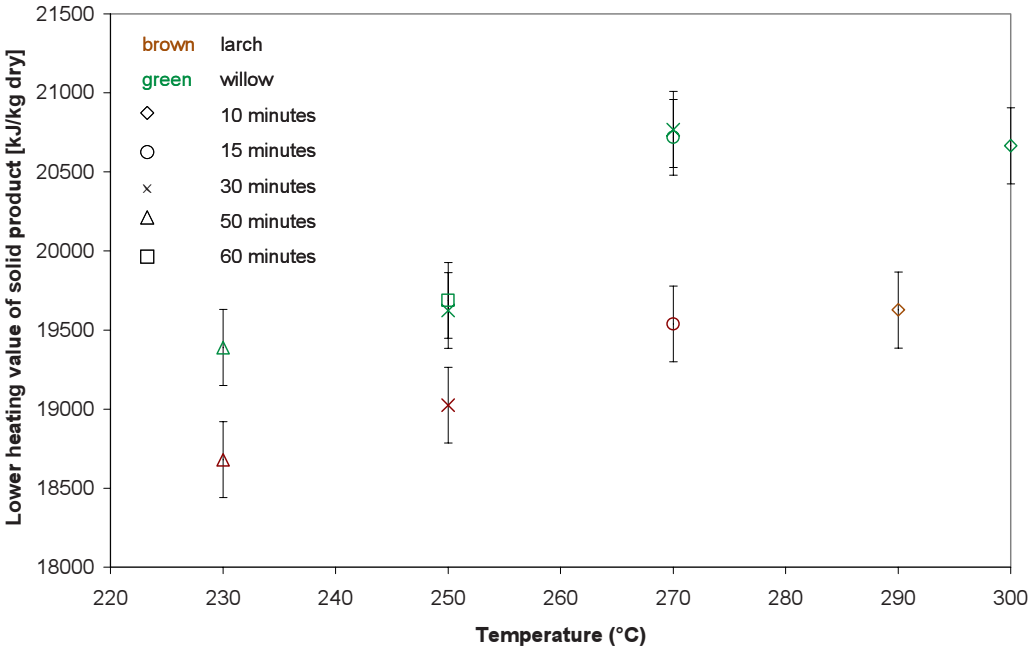

(a)

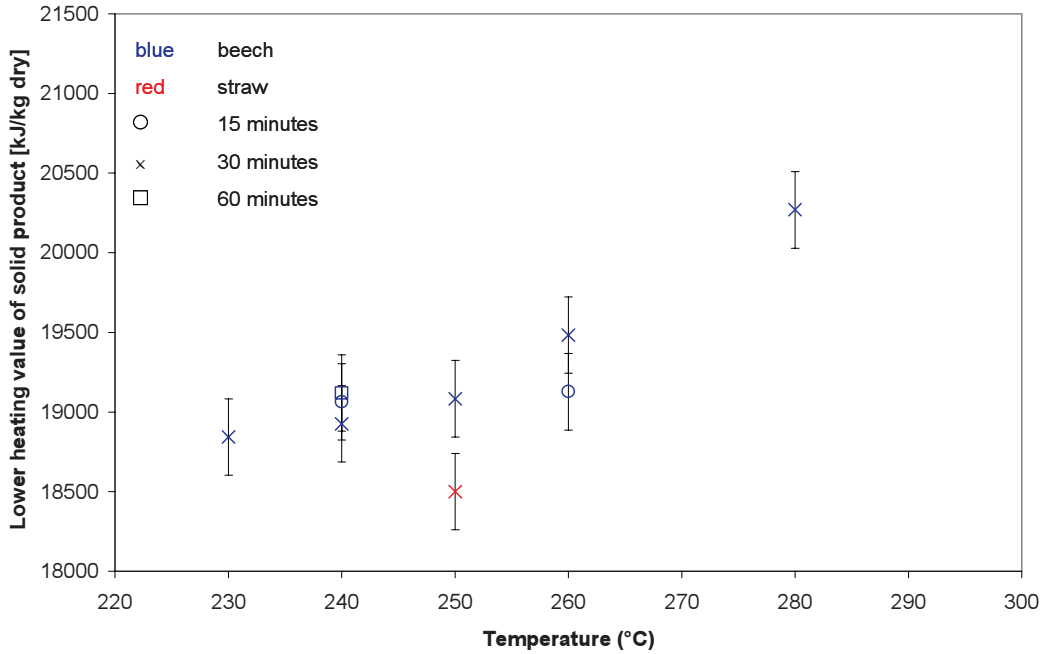

(b)

Figure 8.7: Lower heating value of torrefied wood on dry basis as a function of temperature and residence time, for (a) willow and larch and (b) beech and straw. Bars indicate error margin of 240 J/g in the ASTM method for bomb calorimetry

A very important property is the increase in energy density of the torrefied wood compared to untreated wood. Due to the loss of water vapour and carbon dioxide, for which the lower heating value is zero, relatively more mass is lost than energy. Figure 8.7 shows the lower heating value of the solid product on dry basis for willow, larch, beech and straw for various process conditions. The errors bars represent a standard error of 240 J/g for determination of heating values in a bomb calorimeter. Clearly, the energy density increases with temperature: for willow a 17% increase was observed at 270°C (from 17.7 to 20.7 MJ/kg) and for beech an increase of almost 20% at 280°C (from 17.0 to 20.3 MJ/kg). It is also expected to increase with reaction time, but in many cases such an increase could not be observed due to the error margin in determination of lower heating values. For softwood such as larch, a smaller but statistically relevant increase in energy density of up to 7% is observed. As has been argued earlier, the smaller weight loss due to the lower reactivity of softwood explains this. It must be remarked that the torrefied wood samples produced at temperatures above 250°C contained less than 0.1% moisture, whereas the untreated wood did contain moisture, e.g. for beech approximately 8.6%. If the lower heating value of untreated wood is corrected for the enthalpy of evaporation of present moisture, the actual increase in energy density brought about by torrefaction is up to 30% for deciduous wood types.

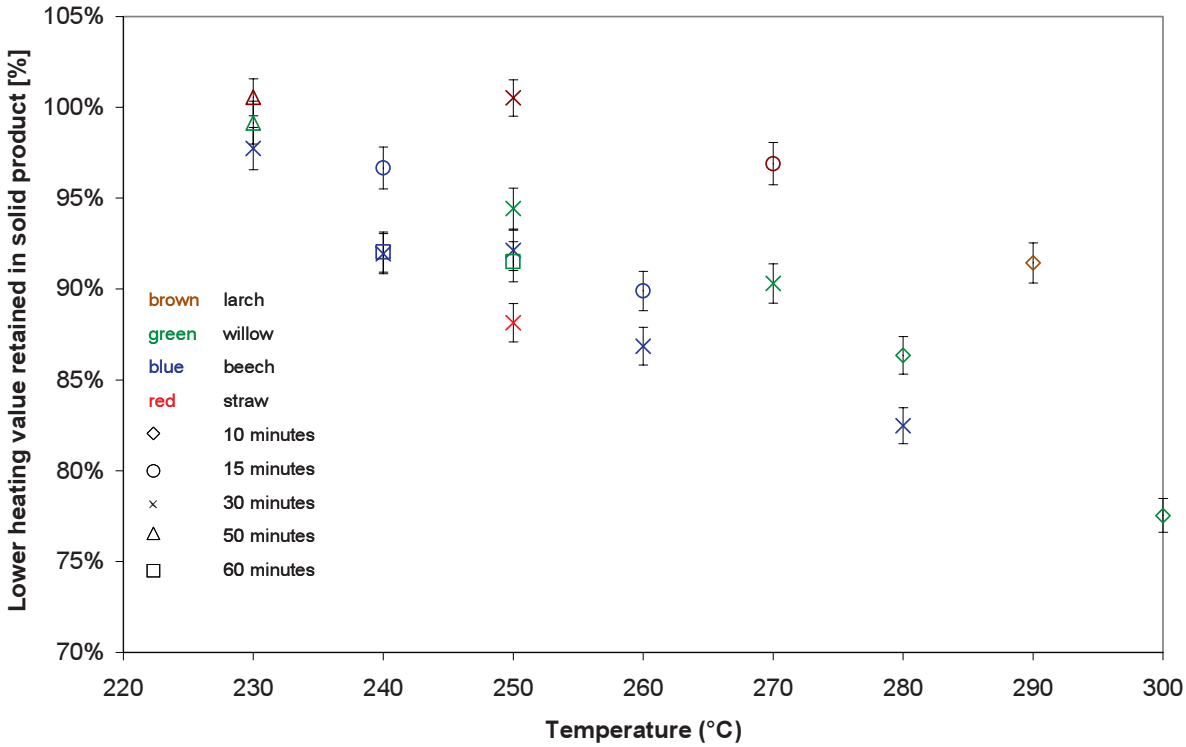

Figure 8.8: Lower heating value retained in torrefied wood on dry basis as a function of temperature and residence time, for different biomass types. Bars indicate error margin of 240 J/g in the ASTM method for bomb calorimetry

The energy retained in the solid product is shown in Fig. 8.8. Clearly, in torrefaction of the deciduous wood types and straw, more energy is transferred with the volatiles in the form of combustibles such as methanol, acetic acid and carbon monoxide. The energy contained in volatiles increases with temperature and reaction time. For torrefaction of larch, energy conservation is almost complete below 250°C as volatile formation is very low.

8.4 Conclusions and recommendations

It can be concluded that deciduous xylan-containing wood (beech and willow) and straw are more reactive in the torrefaction process than coniferous wood (larch). In the first case, the mass conserved in the torrefied wood is lower: 73-83% (depending on residence time) versus 90% at a temperature of 270°C. Much more volatiles are formed, such as acetic acid and methanol, which mainly originate from acetoxy- and methoxy-groups present as side chains in xylose units present in the hemicellulose fraction. These are not present in the hemicellulose fraction of coniferous wood. For deciduous wood and straw, also more non-condensable gases such as carbon dioxide and carbon monoxide are produced and the extent of dehydration is higher. At a torrefaction temperature of 270°C and a reaction time of 15 minutes, the increase in energy density of the solid product is much higher for deciduous wood than for coniferous wood: 17% versus 7%. Torrefaction of deciduous wood at these conditions still retains 90% of the energy in the solid material. Therefore, this process is an attractive method to produce a renewable fuel with favorable properties for gasification and/or (co-)combustion.

It is recommended to obtain more insight into the torrefaction reactions by analyzing the chemical composition of torrefied wood in more detail, to determine its main components and degree of polymerisation. Knowledge of the hemicellulose content could enable more accurate determination of the required residence time at different temperatures.

The chemical properties of torrefied wood could also be related to its mechanical properties, e.g. depending on the extent of decomposition of the hemicellulose fraction in the torrefaction process (and possibly depolymerisation of the cellulose fraction), the friability can be expected to increase. Initial experiments for size reduction and fluidization of torrefied wood have shown promising results (Bergman et al., 2004).

References

Bergman PCA, Boersma AR, Kiel JHA, Prins MJ, Ptasinski KJ, Janssen FJJG (2004). Torrefaction for entrained flow gasification of biomass. In: Swaaij WPM van, Fjällström T, Helm P, Grassi A, editors. Proceedings of 2nd World Biomass Conference, Rome, Italy, May 10-14, 2004. p. 679-682.

Bourgois JP, Doat J (1984). Torrefied wood from temperate and tropical species, advantages and prospects. In: Egnéus H, Ellegård A. Bioenergy 84. London: Elsevier Applied Science Publishers. p. 153-159.

Felfli FF, Luengo CA, Bezzon G, Beaton Soler P (1998). Bench unit for biomass residues torrefaction. In: Kopetz H, Weber T, Palz W, Chartier P, Ferrero GL, editors. Proceedings of the 10th Eur. Conf. Biomass for Energy & Industry, Würzburg, Germany, June 8-11, 1998.

Gaur S, Reed TB (1998). Thermal data for natural and synthetic materials. New York: Marcel Dekker.

Nimlos MN, Brooking E, Looker MJ, Evans RJ (2003). Biomass torrefaction studies with a molecular beam mass spectrometer. Prepr. Pap.-Am. Chem. Soc., Div. Fuel Chem. 48:590-591.

Pach M, Zanzi R, Bjørnbom E (2002). Torrefied biomass a substitute for wood and charcoal. In: Proceedings of the 6th Asia-Pacific International Symposium on Combustion and Energy Utilization, Kuala Lumpur, Malaysia, May 20-22, 2002.

Pentananunt R, Mizanur Rahman ANM, Bhattacharya S (1990). Upgrading of biomass by means of torrefaction. Energy 15 (12): 1175-1179.

Ramiah MV (1970). Thermogramietric and differential thermal analysis of cellulose, hemicellulose, and lignin. Journal of Applied Polymer Science 14: 1323-1337.

Šimkovic I, Varhegyi G, Antal MJ (1988). Thermogravimetric/Mass Spectrometric characterization of the thermal decomposition of (4-O-Methyl-D-Glucorono)-D-Xylan. Journal of Applied Polymer Science 36:721-728.

Wagenführ R, Scheiber C (1974). Wood atlas. Leipzig: VEB Fachbuchverlag. (in German)

White RH, Dietenberger MA (2001). Wood products: thermal degradation and fire. In: Buschow KHJ, Cahn RW, Flemings MC, Ilschner B, Kramer EJ, Mahajan S, editors. The encyclopedia of materials: science and technology. Amsterdam: Elsevier. p. 9712-9716.

Chapter 9

More efficient biomass gasification via torrefaction[‡]

Wood torrefaction is a mild pyrolysis process that improves the fuel properties of wood. At temperatures between 230°C and 300°C, the hemicellulose fraction of the wood decomposes, so that torrefied wood and volatiles are formed. Mass and energy balances for torrefaction experiments at 250°C and 300°C are presented. Advantages of torrefaction as a pre-treatment prior to gasification are demonstrated. Three concepts are compared: air-blown gasification of wood, air-blown gasification of torrefied wood (both at a temperature of 950°C in a circulating fluidized bed) and oxygen-blown gasification of torrefied wood (at a temperature of 1200°C in an entrained flow gasifier), all at atmospheric pressure. The overall exergetic efficiency of air-blown gasification of torrefied wood was found be lower than that of wood, because the volatiles produced in the torrefaction step are not utilized. For the entrained flow gasifier, the volatiles can be introduced into the hot product gas stream as a 'chemical quench'. The overall efficiency of such a process scheme is comparable to direct gasification of wood, but more exergy is conserved in as chemical exergy in the product gas (72.6% versus 68.6%). This novel method to improve the efficiency of biomass gasification is promising; therefore, practical demonstration is recommended.

9.1 Introduction

Motivated by transition to a more sustainable society, renewable biofuels are expected to replace fossil fuels gradually. Carbon dioxide emissions from using biomass as a fuel are perceived as neutral because carbon dioxide is fixed by photosynthesis in a relatively short period. Nevertheless, it is important to use efficient biomass conversion technologies. For example, the future energy industry could use gasification rather than combustion of biomass. Relatively inefficient combustion of solid fuels in boilers and production of electricity in steam-Rankine cycles was common practice in the 20th century and remains so today. The use of producer gas from wood gasifiers, which could be used in modern devices such as gas turbines, fuel cells or catalytic reactors, is still limited.

[‡] Presented at the ECOS 2004 conference, Guanajuato, Mexico, and selected for publication in Energy.

Many of the problems in wood gasification are related to the properties of the fuel. Although wood is a clean fuel with low nitrogen, sulphur and ash content, it is thermally unstable which may lead to formation of condensable tars in gasifiers, thus giving problems in down-stream equipment such as choking and blockage of piping (for a recent review, see Devi et al., 2003). Other disadvantages are the low energy density of wood, typically 18 MJ/kg, in combination with its high moisture content as a result of its hygroscopic character, typically around 10 wt% even after drying. Moreover, we have shown in Chapter 5 that higher gasification efficiencies can be achieved for fuels with low O/C ratios, such as coal, than for fuels with high O/C ratios, such as wood. Firstly, this can be explained due to the high chemical exergy of wood, which is not fully utilized when wood is gasified. Secondly, the optimum temperature for wood gasification is rather low, below 700°C, but higher gasification temperatures are required in practice, so that wood becomes over-oxidized in the gasifier. Therefore, highly oxygenated biofuels are not ideal fuels for gasifiers from an exergetic point of view. Rather than gasifying these fuels directly, it could be attractive to modify their properties prior to gasification.

A process that lowers the O/C ratio of biomass is known as torrefaction (Bourgois and Doat, 1984; Bourgois and Guyonnet, 1988; Pentananunt et al., 1990, Pach et al, 2002), which comprises thermal pre-treatment of wood at temperatures from 230°C to 300°C. The main application of torrefied wood is as a renewable fuel for combustion or gasification. In the 1980's, a commercial plant with a capacity of 14,000 ton/year was operated in France, mainly for the production of barbecue fuel (Girard and Shah, 1991). Although torrefied wood was recognized as a clean-burning fuel with little acids in the smoke, commercial success was hampered because it burns much faster than charcoal, which is conventionally used for barbecues. Other uses such as fuel for district heating and for gasifiers were explored. The use of torrefied wood was successfully tested in an air-blown downdraft gasifier: a higher gasification temperature was observed and the product heating value increased from 5.3 to 6.0 MJ/m^3_n (Girard and Shah, 1991). Novel combinations of torrefaction and gasification have been proposed recently (Daey Ouwens and Küpers, 2003). It is also worth noting that the electricity requirements for size reduction of torrefied wood are 50-85% smaller (depending on torrefaction conditions) in comparison with fresh wood (Bergman et al., 2004). This facilitates its use in entrained flow, oxygen-blown pressurized gasifiers.

This chapter aims to compare gasification of torrefied wood with conventional gasification of wood. The main question is whether wood may be gasified in a more efficient way than direct gasification by using torrefaction as pre-treatment. Attention is focused first on the mass and energy balances of torrefaction. Using these energy balances, several proposed process schemes combining wood torrefaction and gasification are evaluated by process modelling and their efficiencies are compared with conventional direct gasification.

9.2 Wood torrefaction

9.2.1 Introduction

In our laboratory, torrefaction experiments have been carried out in a small-scale (5-10 g sample) fixed bed reactor placed inside an oven as shown in Fig. 9.1. The experiments, described in Chapter 8, were aimed at recovering and identifying all reaction products, which are present in three phases: a solid product (which retains at least 80% of the energy content of the wood feedstock), condensable gases (such as moisture, acetic acid and other oxygenates) and non-condensable gases (mainly carbon dioxide, carbon monoxide and small amounts of hydrogen and methane). By determining the amount and composition of each phase, it was possible to obtain good quantitative closure of the elemental carbon, hydrogen and oxygen balances.

Various types of biomass have been tested: deciduous wood such as beech and willow, straw and coniferous wood such as larch. Deciduous wood has been found to be much more reactive than coniferous wood under torrefaction conditions. This may be explained because the hemicellulose fraction in deciduous wood contains mainly xylan, which is much more reactive than the mannan found in coniferous wood. Important thermal decomposition reactions in torrefaction processes are dehydration, decarboxylation and deacetylation of the xylan-containing hemicellulose polymers. Results are therefore given mainly for beech and willow, of which the thermal behaviour is very similar.

Figure 9.1: Bench-scale experimental set-up for wood torrefaction

9.2.2 Properties of torrefied wood

Figure 9.2 compares the elemental composition of fresh beech wood and the torrefied product. The latter was obtained after heating beech wood from 200°C (around this temperature, wood starts to decompose) to temperatures between 220-280°C in 3-12 minutes respectively, where after the temperature is kept constant for 30 minutes. The triangle points closest to the original beech wood were measured at the lower temperatures (220-230°C) and those furthest away at the higher temperatures (270-280°C). Due to removal of water and carbon dioxide, the composition of the torrefied product has a lower O/C and H/C ratio. The product composition is still very different from charcoal, which requires much higher temperatures to produce. Torrefied wood has a brown color and retains 70-90% of the weight of the biomass feed. The properties of torrefied wood were found to be in between wood and coal. Compared to the original wood, torrefaction decreases the content of volatiles from ca. 80% to 60-75% and the moisture content from typically 10% to 0-3%, whereas the heating value increases by 5-25%. The properties of torrefied wood depend on the type of wood used, and the reaction temperature and residence time that is applied; the required reaction time decreases with temperature and may be calculated from a kinetic model, such as the one described in Chapter 7.

Table 9.1 presents the composition of wood and torrefied wood, obtained by two experiments using willow: at a reaction temperature of 250°C and reaction time of 30 minutes, and 300°C and 10 minutes respectively. Reaction times exclude a heating time from 200°C to the reaction temperature of 8.5 and 17 minutes respectively. As a result of the torrefaction process, the lower heating value of the wood increases from 17.6 MJ/kg to 19.4 MJ/kg and 21.0 MJ/kg respectively.

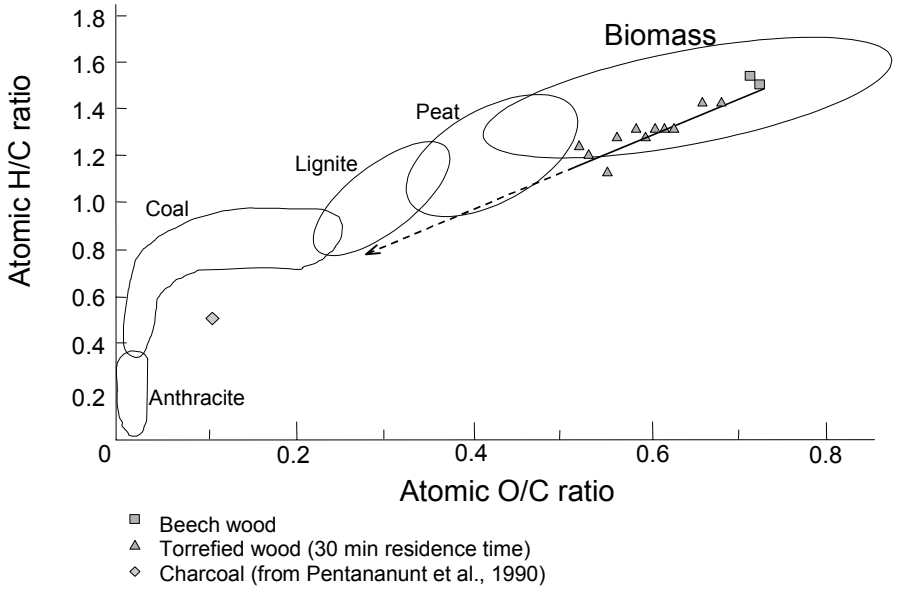

Figure 9.2: Composition of beech wood and torrefied beech wood (obtained at temperatures from 220-280°C) in van Krevelen diagram

Table 9.1: Composition of wood and torrefied wood (for willow).

	Wood	Torrefied wood (250°C, 30 min.)	Torrefied wood (300°C, 10 min.)
Carbon	47.2%	51.3%	55.8%
Hydrogen	6.1%	5.9%	5.6%
Oxygen	45.1%	40.9%	36.2%
Nitrogen	0.3%	0.4%	0.5%
Ash	1.3%	1.5%	1.9%
LHV(MJ/kg)	17.6	19.4	21.0

Torrefaction has a large effect on the strength of the cell wall in wood material. This is most probably caused by decomposition of hemicellulose, the main fraction reacting in the temperature range of torrefaction. The polysaccharides in woody plant cell walls are physically aggregated into very long strands known as microfibrils. These microfibrils are essentially a core of crystalline cellulose encased in a shell of hemicellulose (Panshin and de Zeeuw, 1980). The microfibrils are enclosed in a continuous system of amorphous lignin. By decomposing hemicellulose in the torrefaction process, the orientation of the microfibrils in the lignin matrix may change, which influences the viscoelastic properties of the wood. Furthermore, depolymerization of cellulose and thermal softening of lignin may play a role.

9.2.3 Mass and energy balances

Table 9.2 presents mass and energy balances for the experiments of Table 9.1. At higher temperature, more volatiles are formed so that the mass yield for the two cases is 87% and 67% respectively. The main volatile product is steam, which is formed by dehydration reactions of the wood. Many organic products are formed, mainly acetic acid, but also furfural, formic acid, methanol, lactic acid, phenol and others. The gaseous product typically consists of 80% carbon dioxide and 20% carbon monoxide, with small amounts of hydrogen and methane.

Figure 9.3 shows the overall mass and energy balances for the two experiments. The energy balance shows that 95% and 79% of the respective energy input (the lower heating value of the wood plus heat supplied to the process) is retained in the solid product. These values have been determined by an ASTM method using an adiabatic bomb calorimeter, which has an inaccuracy of approximately 240 kJ/kg. This complicates the determination of the net reaction enthalpy, which is calculated from the difference of the in- and outgoing process streams. To determine the reaction enthalpy more accurately, other experiments are required, e.g. by differential scanning calorimetry in combination with thermogravimetry. In practice, wood always contains a certain amount of moisture, typically 7-10% after drying, so that heat is required to evaporate moisture and the overall process is certainly endothermic.

Table 9.2: Mass and energy balances for torrefaction of (dry) willow at a temperature of 250°C (reaction time of 30 minutes) and 300°C (reaction time of 30 minutes). Data per kg of wood input.

	Torrefaction (250°C, 30 min.)			Torrefaction (300°C, 10 min.)		
	Mass (kg/kg)	LHV (kJ/kg)	Sensible heat (kJ/kg)	Mass (kg/kg)	LHV (kJ/kg)	Sensible heat (kJ/kg)
Torrefied wood						
Org. material	0.859			0.655		
Ash	0.013			0.013		
Total	0.872	16883	202	0.668	14024	189
Volatiles						
Steam	0.057	0	24	0.066	0	35
Acetic acid	0.021	300	6	0.072	1001	28
Other organics	0.018	258	6	0.142	2280	59
Carbon dioxide	0.029	0	6	0.040	0	11
Carbon monoxide	0.003	30	1	0.012	121	3
Hydrogen	trace	1	0	trace	1	0
Methane	negl.	0	0	trace	2	0
Total	0.128	589	43	0.332	3405	136

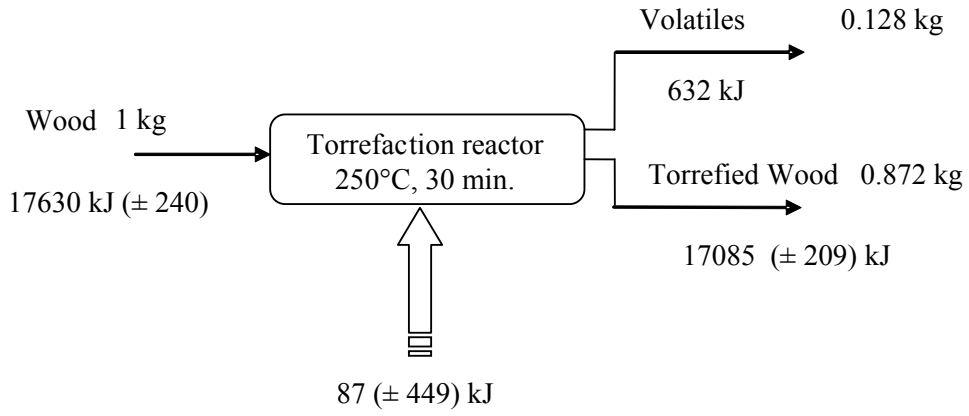

(a)

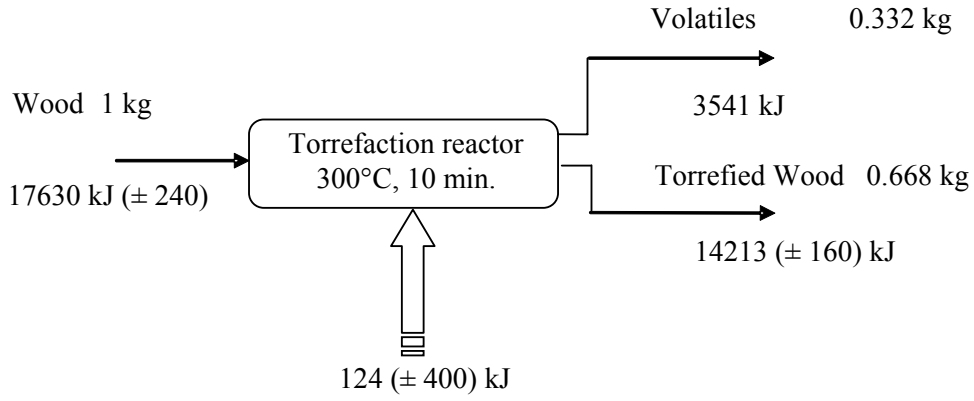

(b)

Figure 9.3: Overall mass and energy balances for torrefaction of (dry) willow at temperature and reaction time of (a) 250°C and 30 minutes (b) 300°C and 10 minutes

9.3 Wood torrefaction combined with gasification

9.3.1 Process options

The main idea behind combining biomass torrefaction and gasification is as follows: in gasifiers, biofuels such as wood are converted into combustible product gas and heat. This heat is normally recovered in the form of medium or high pressure steam, which may be exported and/or used for electricity generation. Alternatively, steam can be partially used to supply the heat for the torrefaction process. Bone-dry torrefied wood with increased heating value is formed, which is subsequently gasified. In this way, advantage is taken of the high reactivity of wood (which is related to its relatively high chemical exergy), and part of the sensible heat of gasification product gas is put 'back into' the gasifier. The design of a torrefaction reactor, which is placed in front of the gasifier, is similar to a drier. In this case, indirect heat transfer based on heat conduction is selected which allows precise temperature control. A steam tube drier, possibly with rotation to promote contact between the solid particles and hot steam tubes, may be used.

The concept of torrefaction aided gasification is similar to two-stage pyrolysis-gasification, but differs in two aspects. Firstly, the temperature of the torrefaction stage is carefully controlled at or below 300°C in order to minimize pyrolysis of cellulose and avoid tar formation. Secondly, the heat requirements for torrefaction are smaller than those for pyrolysis at higher temperatures. Therefore, instead of taking heat from the gasifier itself (e.g. by recirculation of hot sand), sufficient heat can be taken from the gasifier product gas.

Figure 9.4 shows process options for gasification of wood or torrefied wood.

- Conventional biomass gasification in a circulating (CFB) fluidized bed is shown in Fig. 9.4a. Alternatively, bubbling fluidized beds and (on a small scale) moving bed gasifiers may be applied. The operating temperature in CFB gasifiers is below 1000°C, in order to avoid problems with ash softening and melting, and operating pressure is mostly atmospheric. Air is generally used as a gasifying medium.
- In Fig. 9.4b, the solid product of the torrefaction reactor is fed to an air-blown CFB gasifier. The volatile product is not used in the process and regarded as a waste stream. To dispose of this waste stream, acidic water can be condensed and sent to a biological wastewater treatment plant, while the non-condensable gases could be (catalytically) combusted.

- Figure 9.4c shows gasification of torrefied wood in an oxygen-blown entrained flow (EF) gasifier. Prior to its introduction into the gasifier, torrefied wood is pulverized to a particle size of 100 μm, which behaves as a Geldart A powder suitable for fast fluidization (Bergman et al., 2004). The torrefied wood is gasified at a very high temperature, with flame temperatures up to 1700°C and gas outlet temperatures ranging from 1000-1400°C. The hot gas leaving the gasifier is normally physically quenched, e.g. with cold recycle gas, but it is also possible to use the torrefaction volatiles in order to induce a 'chemical quench' (Kerkhof and Das, 1996). Due to the high temperature, the thermally unstable volatiles from the torrefaction step will decompose into carbon monoxide and hydrogen and provide a cooling effect so that the temperature drops by 100-400°C (depending on the amount of volatiles that are introduced, which in turns depends on the torrefaction conditions). This method avoids the loss of organic material from the torrefaction reactor, because all product streams are effectively used in the gasification system and contribute to the production of synthesis gas.

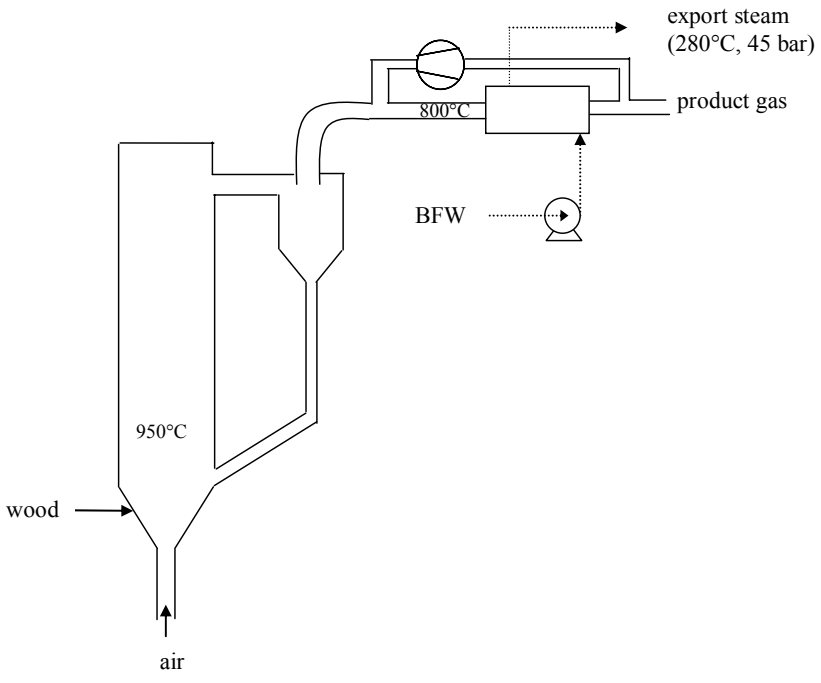

(a)

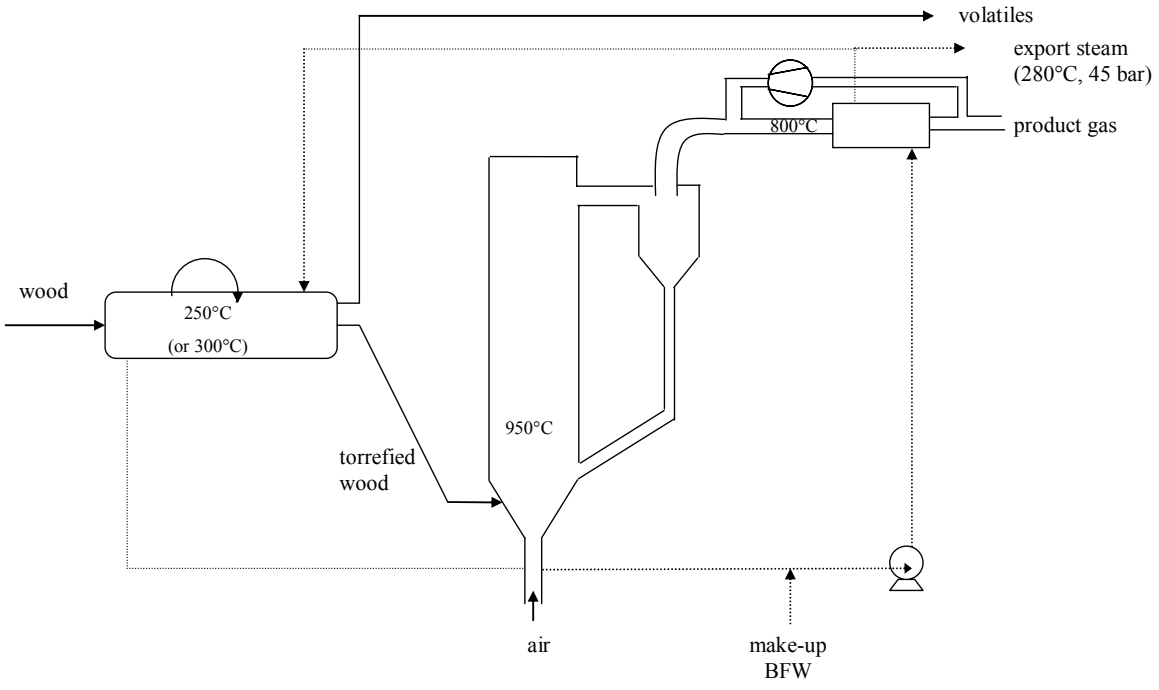

(b)

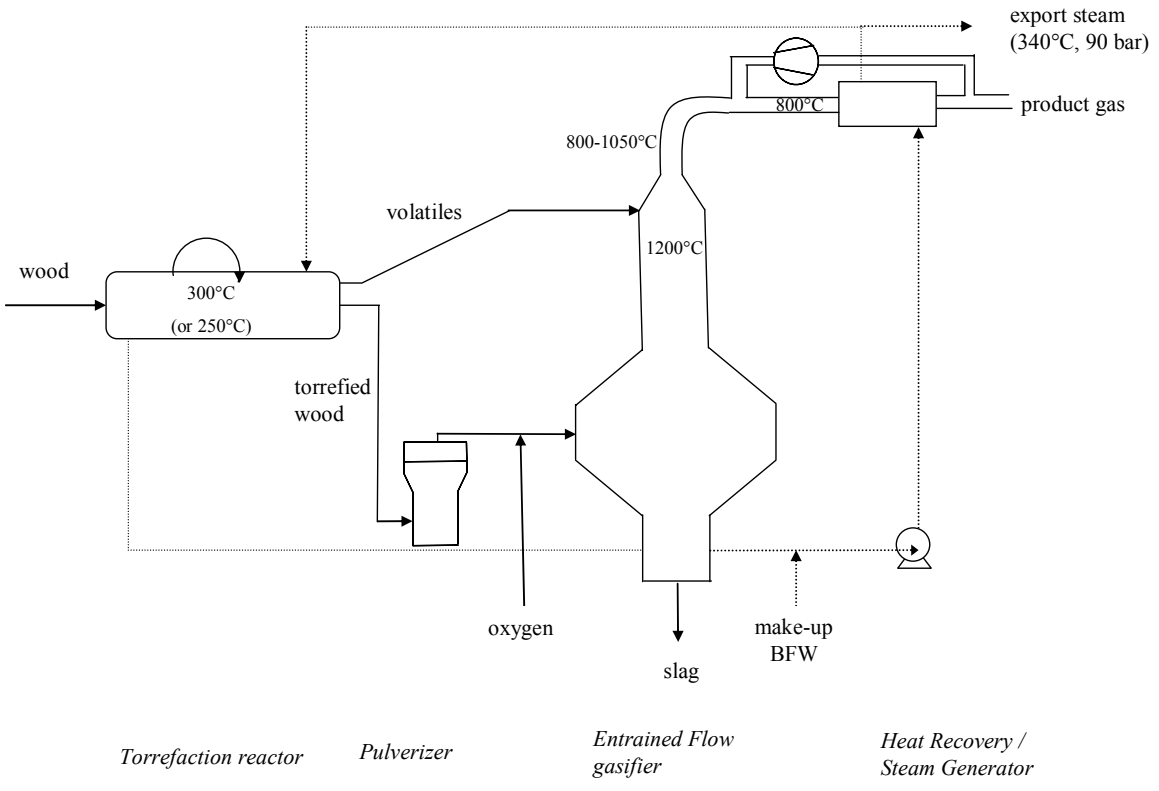

(c)

Figure 9.4: Gasification process schemes, (a) CFB gasification of wood (air-blown), (b) wood torrefaction and CFB gasification of torrefied wood (air-blown), (c) wood torrefaction integrated with EF gasification of torrefied wood (oxygen-blown)

9.3.2 Process modeling

The three process flow sheets have been simulated in Aspen Plus, version 11. The model is based on dry wood as a fuel, because the main interest was to check the effect of modifying the chemical composition prior to gasification, thereby excluding the effect of drying. The model is based on the following input parameters:

- The wood feedstock is initially reduced in size to particle diameters of a few centimeters, both for use in a CFB gasifier and in a torrefaction reactor. Since the requirements of the different options are similar and the electricity required is expected to be relatively small, this term is not taken into account.
- The mass and energy balances of the torrefaction cases at 250°C and 300°C were used as an input for the simulation.
- The required power for pulverizing torrefied wood (at room temperature) to a particle size of 100 μm is approximately 10-20 kWe/MWth (Bergman et al., 2004). Assuming that the production of electricity from wood has an overall efficiency of 40%, this amounts to 2.5-5% of the fuel. Values of 3% and 2.5% were applied for torrefaction at 250°C and 300°C respectively. These are conservative estimates because the energy required for size reduction may be even less if torrefied wood is pulverized while it is hot.
- For cryogenic air separation, electricity requirement of 380 kWh/ton oxygen is used (Simbeck et al., 1983) with generation efficiency from produced gas of 50%.
- The gasifier has been modelled using an equilibrium model. This indicates the maximum thermodynamic efficiency that may be achieved in the three processes. Operating temperatures of 950°C and 1200°C were assumed for CFB respectively EF gasification, whereas operating pressure was atmospheric in all cases.
- At a gasification temperature of 1200°C, melting of ash and formation of a slag is unlikely (although indicated in Fig. 9.4c). Therefore, the heat of fusion of the ash is not considered.
- The hot product gases from the gasifier are physically quenched with cold product gas (after a possible chemical quench) to a temperature of 800°C, as is common in many gasifiers such as the high-temperature coal gasifier developed by Shell. This allows for relatively cheap construction materials in the Heat Recovery/Steam Generator (HRSG). Steam produced in this unit is partially used to provide heat for the torrefaction process and partially exported. The pressure of the steam generated in the HRSG is

tailored for controlling the torrefaction temperature: 45 bar for torrefaction at 250°C and 90 bar for torrefaction at 300°C.

9.3.3 Efficiency of process options

To compare the gasification efficiencies of the various process options, the exergetic efficiency is used. The efficiency, based on the exergy of product gas and steam relative to the exergy of the wood fuel is defined as:

$$\Psi_{overall} = \frac{(\varepsilon_{product\ gas} - \varepsilon_{air}) + \varepsilon_{steam} - \dfrac{E_{air\ separation} + E_{size\ reduction} + E_{recycle\ compressor}}{\Psi_{electricity\ generation}}}{\varepsilon_{wood}} \qquad (9.1)$$

In this equation, ε_{wood}, ε_{air}, $\varepsilon_{product\ gas}$ and ε_{steam} represent the exergy of wood, air, product gas and produced steam, $E_{air\ separation}$ is the electricity required for cryogenic air separation, $E_{size\ reduction}$ the electricity required for size reduction of torrefied wood, $E_{recycle\ compressor}$ the electricity for recycling cold synthesis gas for gas quenching, and Ψ is the efficiency for generating electricity from product gas (estimated at 50%). The electricity for the boiler feed water (BFW) pump may be neglected. Thermodynamic data of all components were obtained from Szargut et al. (1988). The chemical exergy of wood was calculated from its lower heating value, while the chemical exergy of air is zero because it is a component of the environmental reference system.

Figures 9.5a and 9.5b show the overall gasification efficiencies as a function of gasification temperature for the various process options: air-blown CFB gasification of wood (see Fig. 9.4a) and torrefied wood (see Fig. 9.4b), for torrefaction at 250°C and 300°C respectively, and oxygen-blown integrated EF gasification of torrefied wood (see Fig. 9.4c), for torrefaction at 250°C and 300°C respectively. The overall efficiency of air-blown CFB gasification is lower for torrefied wood than for wood, especially at a high torrefaction temperature when a lot of energy is contained in the volatiles, which are not used in the process. Compared to air-blown CFB gasification of wood, the overall efficiency for oxygen-blown integrated EF gasification of torrefied wood is slightly lower if torrefied wood is produced at 250°C, but quite comparable if torrefied wood is produced at 300°C. Several typical operating temperatures (I, IIa, IIb, IIIa and IIIb) have been indicated in Fig. 9.5, for which more detail is given below.

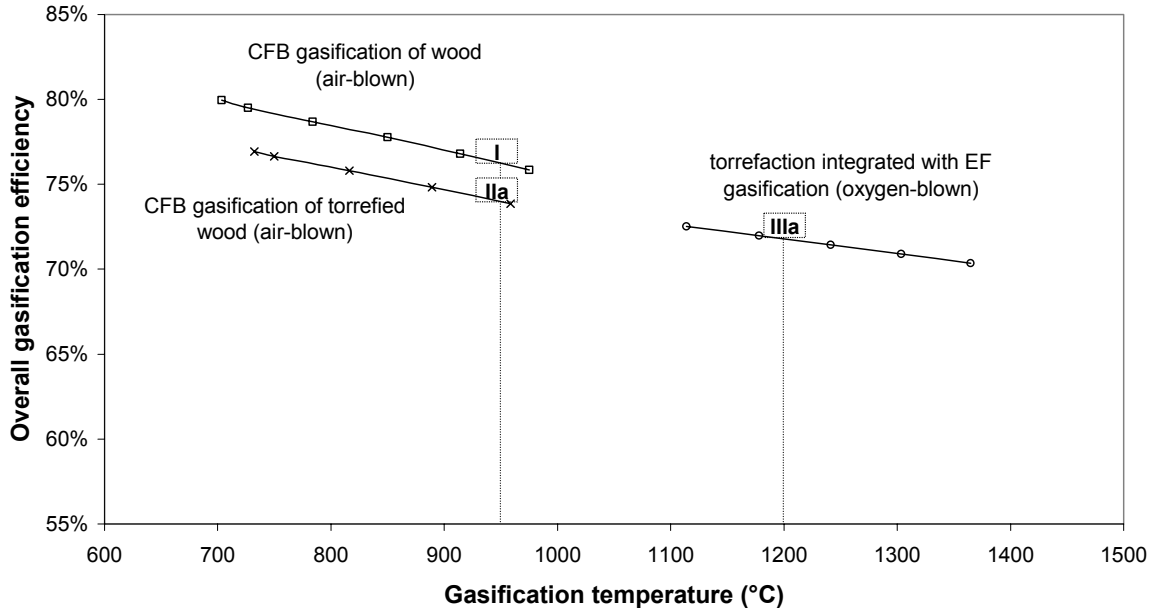

(a)

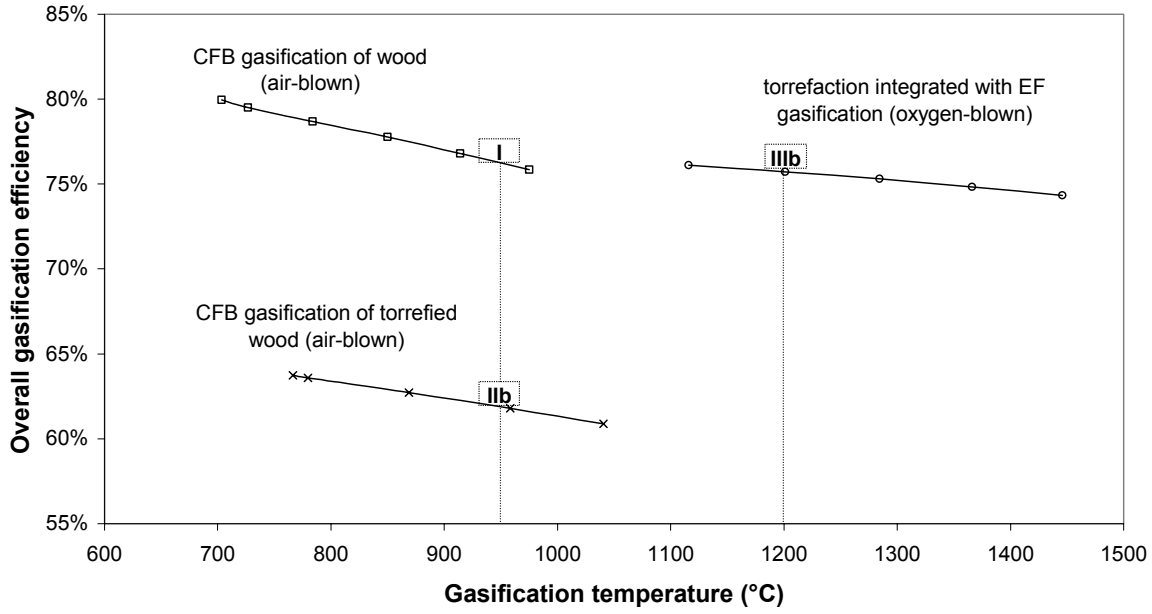

(b)

Figure 9.5: Overall gasification efficiency at varying gasification temperature for different process schemes

Figure 9.6 splits out the overall efficiency at the indicated operating temperatures. The overall efficiency is the sum of several contributions: chemical exergy of product gas, physical exergy of product gas (at the outlet temperature of the HRSG) and exergy of steam. The highest amount of chemical exergy conserved is observed for case IIIb (torrefaction at 300°C integrated with gasification at 1200°C). For this option, little steam is generated due to the smaller gas volume when oxygen is used as gasifying medium and most of this steam is required for torrefaction.

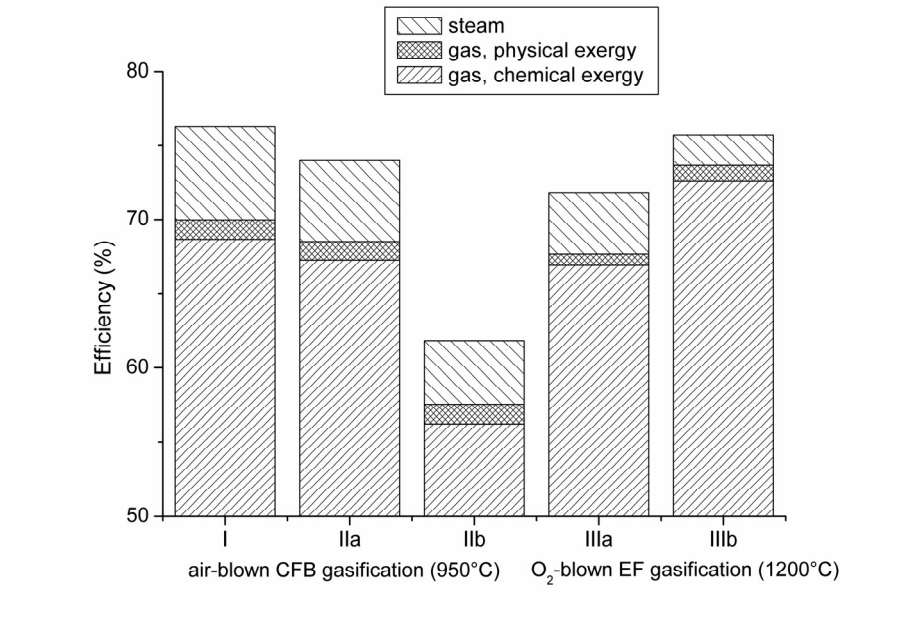

Figure 9.6: Exergetic efficiency of different process schemes

In order to understand the observed trends, the process losses are analyzed and shown in Fig. 9.7. These process losses consist of internal losses (irreversibilities) and external losses. The external losses consist of volatiles lost as a waste stream (for CFB gasification of torrefied wood) and of hot ash emitted from the gasifier. The latter term was found to be very small and is therefore not shown. From Fig. 9.7, it becomes clear that the exergy contained in the torrefaction volatiles can be substantial, especially at 300°C, which explains why the concept of CFB gasification of torrefied wood has a lower efficiency than for gasification of wood. In cases IIIa and IIIb, in which the volatiles from wood torrefaction are used to quench the gasifier product gas, this external loss is avoided. Internal losses occur in all unit operations: torrefaction, gasification, and air separation (4.7% and 3.8% for gasification of torrefied wood prepared at 250°C and 300°C respectively) and size reduction (3.0% and 2.5% respectively). The internal losses occur mostly in the gasifier; these are reduced when torrefied wood is fed to the gasifier instead of wood. This might have been expected because the amount of solid material that needs to be gasified is smaller. However, even the combined irreversibilities for torrefaction and gasification are smaller than those for direct gasification. This can be understood by realizing that torrefaction (hemicellulose decomposition) conventionally takes place in the gasifier itself. To this end, heat from the oxidation zone in the gasifier is released at high temperature and downgraded to a lower temperature. If the torrefaction step is performed outside of the gasifier, a lower quality heat can be used, i.e. steam produced from cooling the gasification product gas, which is beneficial.

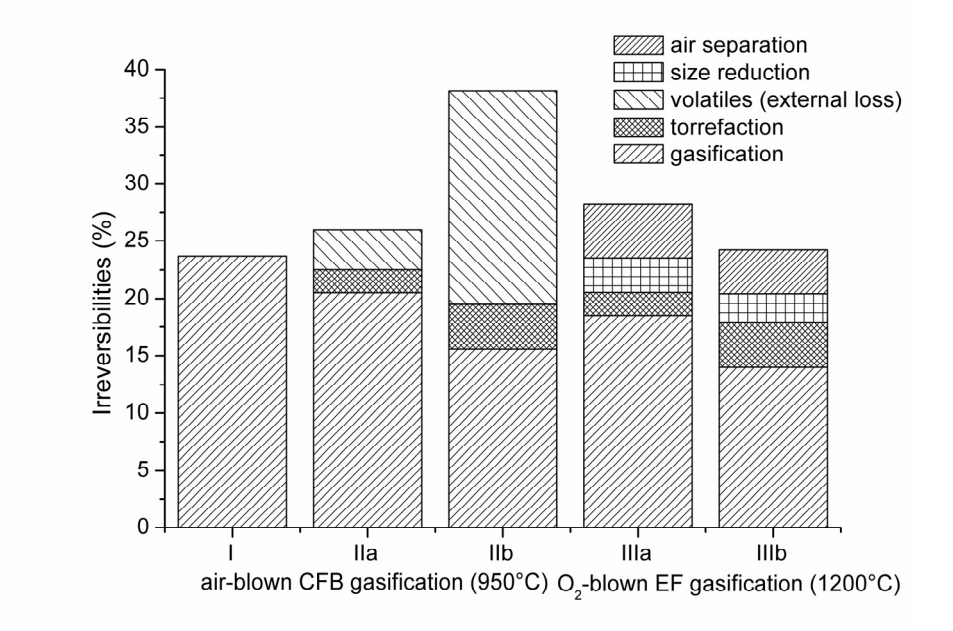

Figure 9.7: Thermodynamic losses of different process options

The triangular CHO-diagram in Figure 9.8 presents another reason for the increased gasification efficiency of torrefied wood. In this diagram, the so-called carbon boundary line (see e.g. Cairns and Tevebaugh, 1964) is shown at a temperature of 950°C. This line has to be crossed in order to avoid formation of solid carbon. The thermodynamic optimum is on the carbon boundary line, where exactly enough oxygen is added to achieve complete gasification. Considering gasification of wood at 950°C, there is a considerable amount of over-oxidation which negatively influences the gasification efficiency. If wood is modified by torrefaction, its composition becomes more favourable so that it is over-oxidized less in the gasifier.

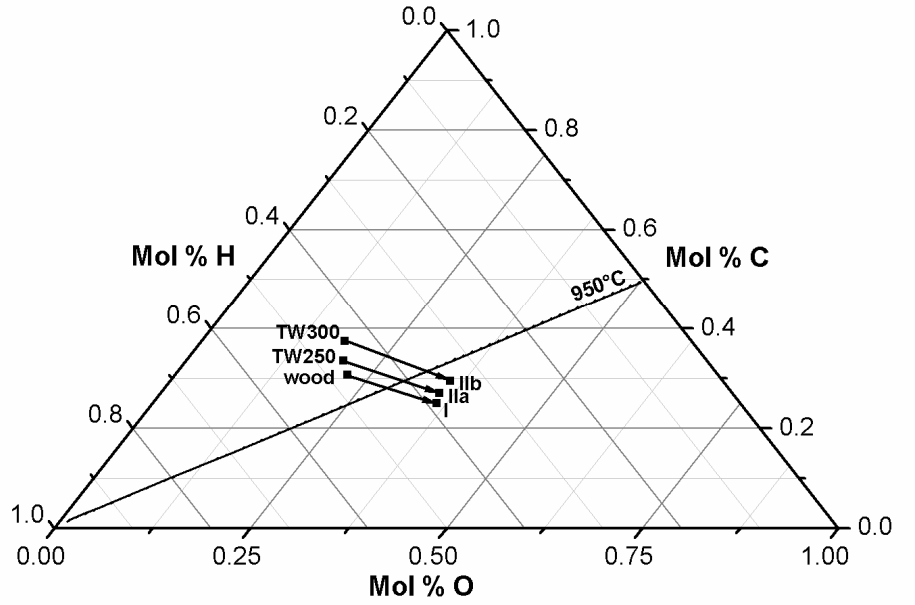

Figure 9.8: Gasification of wood and torrefied wood (TW; produced at 250°C and 300°C) at a temperature of 950°C illustrated in a CHO-diagram

9.3.4 Discussion

In several input parameters for the process models, such as the torrefaction energy balances, inaccuracies exist so that the results presented in Figs. 9.5 and 9.6 do not provide firm evidence that one process option is more efficient than the other. Nevertheless, oxygen-blown EF gasification of torrefied wood seems an attractive option to conserve the chemical exergy of wood in the product gas maximally, at a high gasification temperature. Direct gasification of wood at this temperature would have a much lower efficiency.

There are several advantages for oxygen-blown EF gasification of torrefied wood which should be mentioned. Firstly, the process simulations were based on dry wood, but wood always contains some moisture which is physically adsorbed. By decomposing the hemicellulose fraction in a torrefaction reactor, moisture present will evaporate so that always a bone-dry solid product is gasified. In CFB gasification of wood, the efficiency drops quickly with moisture content of the fuel. For example, if wood is used with a moisture content of 8.6%, the efficiency drops by 1.5 percentage points compared to only 0.7 percentage points for torrefaction (at 250°C) integrated with EF gasification. Secondly, the gasification reactions in the gasifier were assumed to reach chemical equilibrium. However, at the operating temperature of CFB gasifiers, these reactions are too slow and do not contribute sufficiently to the carbon conversion (Kersten 2002). Typical carbon conversions are around 90%, whereas at higher gasification temperatures of EF gasifiers, almost complete conversion can be expected. However, this has yet to be verified experimentally. Thirdly, the possibility exists for operating the EF gasifier at elevated pressure, which is beneficial for many downstream operations such as gas turbines and catalytic reactors for production of hydrogen, methanol, dimethylether or Fischer-Tropsch hydrocarbons. It would then also be attractive to operate the torrefaction reactor at elevated pressure, but this has not yet been tested experimentally either. Finally, the catalytic reactors mentioned also benefit from the fact that the product gas from high temperature gasifiers contains very little methane, which is inert and passes these reactors unconverted.

Several studies, e.g. by Ciferno and Marano (2002), have identified high temperature gasification of biomass as a promising option. We regard torrefaction as an enabling pre-treatment technology which solves two problems simultaneously: the high energy requirements for size reduction as well as the low heating value and the high moisture content of untreated wood.

9.4 Conclusions and recommendations

Although wood is clean and renewable fuel which, compared to coal, contains little ash, sulphur and nitrogen, it is not an ideal fuel for gasifiers. Its optimum gasification temperature is rather low (below 700°C) due to the high O/C ratio of

the fuel and high moisture content. As a result, wood is generally over-oxidized in gasifiers leading to thermodynamic losses. This chapter has shown that it is possible to reduce these thermodynamic losses by prior thermal pre-treatment in the range of 250-300°C, i.e. wood torrefaction. If the heat produced in the gasifier is used to drive the wood torrefaction reactions, the chemical exergy preserved in the product gas has been shown to increase provided that both torrefied wood and volatiles are introduced into the gasification process. This is a novel, promising method to achieve more efficient gasification of wood. It is thus recommended to test this integrated process in practice and also to consider the effect of a torrefaction pre-treatment step on process economics.

References

Bergman PCA, Boersma AR, Kiel JHA, Prins MJ, Ptasinski KJ, Janssen FJJG (2004). Torrefaction for entrained flow gasification of biomass. In: Swaaij WPM van, Fjällström T, Helm P, Grassi A, editors. Proceedings of 2nd World Biomass Conference, Rome, Italy, May 10-14, 2004. p. 679-682.

Bourgois JP, Doat J (1984). Torrefied wood from temperate and tropical species, advantages and prospects. In: Egnéus H, Ellegård A. Bioenergy 84. London: Elsevier Applied Science Publishers. p. 153-159.

Bourgois J, Guyonnet R (1988). Characterization and analysis of torrefied wood. Wood Science and Technology 22: 143-155.

Cairns EJ, Tevebaugh AD (1964). CHO gas phase compositions in equilibrium with carbon, and carbon deposition boundaries at one atmosphere. Journal of Chemical and Engineering Data 9(3):453-462

Ciferno JP, Marano JJ (2002). Benchmarking biomass gasification technologies for fuels, chemicals and hydrogen production. Prepared for National Energy Technology Laboratory, US Department of Energy. See also: http://www.netl.doe.gov/.

Daey Ouwens C, Küpers G (2003). Lowering the cost of large-scale, biomass based, production of Fischer-Tropsch liquids. In: Proceedings of Bioenergy 2003, International Nordic Bioenergy Conference; Editor: D. Asplund, Jyväskylä, Finland, 384-388.

Devi L, Ptasinski KJ, Janssen FJJG (2003). A review of the primary measures for tar elimination in biomass gasification processes. Biomass and Bioenergy 24: 125-140.

Girard P, Shah N (1991). Recent developments on torrefied wood, an alternative to charcoal for reducing deforestation. REUR Technical series 20: 101-114.

Kerkhof FPJM, Das A (1996). Process for cooling a hot gas stream. Patent nr. WO 96/06901.

Kersten SRA (2002). Biomass gasification in circulating fluidized beds. Ph.D. thesis. Enschede: Twente University Press.

Pach M, Zanzi R, Björnbom E (2002). Torrified Biomass a substitute for Wood and Charcoal. 6th Asia-Pacific International Symposium on Combustion and Energy Utilization, Kuala Lumpur, 20-22 May 2002.

Panshin AJ, de Zeeuw C (1980). Textbook of wood technology, fourth edition. New York: McGraw-Hill Book Company.

Pentananunt R, Mizanur Rahman ANM, Bhattacharya S (1990). Upgrading of biomass by means of torrefaction. Energy 15 (12): 1175-1179.

Simbeck DR, Dickenson RL, Oliver ED (1983). Coal gasification systems: a guide to status, application and economics, report AP-3109. Palo Alto, CA: EPRI.

Szargut J, Morris DR, Steward FR (1988). Exergy analysis of thermal, chemical and metallurgical processes. New York: Hemisphere Publishing Corporation.

Chapter 10

Concluding remarks

The final chapter summarizes the main conclusions of the thesis, gives recommendations for R&D topics in the area of biomass torrefaction and torrefied wood gasification and presents an outlook for biomass-based energy.

10.1 Main conclusions

The objective of this study was to find out how the exergy (i.e. the work content) of a biofuel can be preserved as much as possible in the product gas of a gasifier. Furthermore, the thesis aimed to answer the question: what is the effect of the composition of the fuel on the efficiency that can be attained in a gasifier?

These questions have been addressed by a thermodynamic approach described in Chapter 3-6, which formed the first part of the thesis. The main conclusions in this part are:

- The thermodynamic efficiency of gasification processes should be defined based on exergy content of biomass feed and gaseous and solid products. The gasification efficiency reaches a maximum at the carbon boundary point, where exactly enough air/oxygen is added for complete gasification.
- By gasification of solid carbon rather than complete combustion, thermodynamic losses due to internal thermal energy exchange are reduced from 14-16 to 5-7% of expended exergy, while the chemical reactions are relatively efficient for both processes. For oxygen-blown gasification of fuels with high calorific value, moderation of the gasification temperature by addition of steam is advisable, with optimum temperatures in the ranges of 1100-1200 K (for atmospheric pressure) and 1200-1300 K (for 10 bar pressure).
- The maximum efficiency that may be reached for gasifying a given fuel, with varying fuel composition as given in a Van Krevelen diagram, is indicated by an equilibrium model. For gasification at 927°C, fuels with O/C ratio below 0.4 are recommended. However, higher temperatures may be required in practice. At 1227°C, fuels with O/C ratio below 0.3 would be preferred. Therefore, it would be attractive to modify biomass (with O/C ratio around 0.6) prior to gasification.

- When integrating (air-blown) biomass gasification with Fischer-Tropsch synthesis, the gasifier is one of the largest sources of internal exergy losses (irreversibilities). Losses in the gasifier may be reduced by proper drying of the biomass. To avoid formation of methane, which remains unconverted in the Fischer-Tropsch process, operation at temperatures higher than the optimum temperature for biomass gasification is needed. This effectively over-oxidizes the biomass. To reduce such over-oxidation, pre-treatment of biomass aiming to enhance its calorific value is desirable.

Summarizing, the most important conclusion is that pre-treatment of biomass is advisable in order to obtain an improved gasification feedstock. There are various methods for enhancement of the calorific value of biomass. One possibility is separation of lignin from the holocellulose fraction of woody biomass, e.g. by extraction with hot phenol, and gasification of only the lignin component. However, such a separation is not easy, and furthermore this would greatly reduce the available amount of biomass for energy purposes. Another approach is to carry out a thermal pre-treatment in the range of 230-300°C, using a process known as torrefaction. Such as process aims to remove water and carbon dioxide from the biomass, so that energy is concentrated in the solid product. The properties of torrefied wood lie between those of coal and biomass; it can be easily reduced in size and (if desired) mixed with coal for co-gasification.

Therefore, the torrefaction process has been the subject of research in Chapters 7-9, which formed the second part of the thesis, focusing on kinetics, product analysis, and possibilities for integrating the processes of torrefaction and gasification. The main conclusions in this part are:

- The weight loss kinetics for torrefaction of willow can be accurately described by a two-step reaction in series model. The aim of torrefaction is to carry out the relatively fast, initial step, representative of hemicellulose decomposition, and avoid the slower, subsequent reaction which represents further charring. The time required to reach the maximum amount of intermediate product decreases from over 3 hours at 230°C to 10 minutes at 300°C.
- Deciduous wood types, such as beech and willow, were found to be more reactive than coniferous wood in the range of 225-300°C. Deciduous wood types produce more volatiles, especially more acetic acid and methanol than coniferous wood. The solid product, torrefied wood, has a brown colour, reduced volatile content and improved lower heating value, e.g. thermal treatment at 270°C for 15 minutes increases the lower heating value from 17.7 to 20.7 MJ/kg (for willow).

- Overall mass and energy balances for torrefaction at 250°C and 300°C show that the process is mildly endothermic. Three concepts have been compared: air-blown gasification of wood, air-blown gasification of torrefied wood (both a temperature of 950°C in a fluidized bed) and oxygen-blown gasification of torrefied wood (at a temperature of 1200°C in an entrained flow gasifier). For the third option, an attractive option is to introduce the volatiles formed during torrefaction into the product gas of the gasifier. The overall efficiency of such a concept is comparable to direct gasification wood at a much lower temperature, but more exergy is conserved in the form of chemical exergy.

Therefore, a general conclusion from this thesis is that the concept of wood torrefaction, followed by high temperature entrained flow gasification of the torrefied wood, is very promising. This avoids the kinetic restrictions of fluidized bed gasifiers operating at relatively lower temperatures.

10.2 Recommendations for future work

10.2.1 Research and development of biomass torrefaction

Although thermal decomposition of biomass has been extensively studied, more research is needed for the temperature range of torrefaction, i.e. 230-300°C. Specific topics are the determination of the maximum allowable operating temperature (although a high temperature reduces the required reaction time, more reaction heat may be required and at some point cellulose decomposition begins to occur with possible formation of undesired tars) and the link between chemical composition, reactivity and mechanical strength. The reaction enthalpy could be accurately determined as a function of feed type and operating conditions by using thermogravimetry simultaneously with differential scanning calorimetry (TGA/DSC). It would also be interesting to check whether torrefaction is influenced by elevated pressures, as the development of pressurized torrefaction processes is beneficial for integration with pressurized entrained flow gasifiers.

Based on more detailed research data, a suitable torrefaction reactor could be developed. If heat is available in the form of medium pressure steam, it becomes possible to condense the steam in order to supply the heat for the torrefaction reactor. A steam tube drier, i.e. a vessel containing wood heated indirectly by steam tubes, may be suitable due to its simple construction, low cost and maintenance, and narrow temperature control. Also, these can be built very large as the required residence time for torrefaction is in the order of minutes. Steam tube driers need to be demonstrated at higher temperatures because they have not yet been used at temperatures above 150°C. Material selection, final sizing and costing are needed to determine the economic feasibility of the torrefaction process.

10.2.2 Research and development of torrefied wood gasification

As mentioned in Chapter 1, biomass gasification at elevated temperatures largely avoids the tar formation and gas clean-up problems of fluidized bed gasifiers operating below 950°C. By torrefaction of woody biomass, the calorific value is increased, moisture is removed and the biomass becomes more suitable for gasification at higher temperatures. An option that could therefore be investigated is the use of torrefied wood in bubbling fluidized bed (BFB) gasifiers at elevated temperatures, possibly up to 1100°C. At this temperature, in combination with the longer residence time, much less tar formation can be expected.

Another major advantage of thermal pre-treatment is that the fibrous structure is destroyed, so that the product can be used in an entrained flow gasifier. This is an exciting new route to the production of clean synthesis gas from biomass. Research into entrained flow gasification of torrefied wood has not yet been carried out. A very important practical problem is posed by the removal of ash from the gasifier. The required operating temperature for entrained flow gasification of torrefied wood will be lower than for coal. The question is whether the ashes in biomass will melt under the required conditions. By different lab-scale tests and thermodynamic modelling, Van der Drift et al. (2004) have found that ash from clean wood does not or hardly melts at operating temperatures in the range of 1300-1500°C. This is caused by the fact that the ashes are rich in CaO, while alkali metals (which reduce melting temperatures) are removed by the gas phase. Two approaches can therefore be conceived, which both warrant further research:

- Development of a non-slagging gasifier specifically for torrefied wood. Care must be taken to operate the gasifier below the ash melting temperature. A little bit of melting can probably not be avoided, but may be not be serious given the low ash content of the torrefied wood.
- Development of a slagging gasifier. This would require the addition of fluxing agents and possibly slag recycling to ensure coverage of the gasifier wall. Such a gasifier would be more flexible, as it allows for co-gasification of coal and torrefied wood.

Besides torrefied wood, another research option is the use of wood-derived pyrolysis oil in entrained flow gasifiers, which circumvents the problem of ash removal (Stassen et al., 2002). It would be very interesting to develop these different pyrolysis-gasification concepts further and compare them with regard to technical feasibility and economic viability.

Tests are also required for the use of torrefaction volatiles as a chemical quench for the gasifier, as proposed in Chapter 9. Problems are not expected because these volatiles are highly unstable and should decompose very quickly into synthesis gas components.

10.3 Outlook

10.3.1 Electricity from biomass

Figure 10.1 shows various applications for the gaseous feedstock produced by biomass gasifiers. This has traditionally been used in gas engines, boilers, with applications in gas turbines in an early phase of development. The world's first biomass-fired IGCC (integrated gasification combined cycle) is the Värnamo plant, which uses a circulating fluidized bed gasifier. It was built between 1991 and 1993 and can produce 6 MW of electricity and 9 MW of heat from wood chips. The greatest hurdle towards wider commercialization of this technology remains the requirement, set by the gas turbine, to produce tar- and particulate-free gas. The development of entrained flow gasifiers may be important to overcome this hurdle.

Assuming that entrained flow gasifiers can indeed be technically fully proven and ultra-clean synthesis gas produced, an even better option is application of this gas in fuel cells. Biomass derived synthesis gas could be directly converted into electricity using a stationary fuel cell, such as a Molten Carbonate Fuel Cell (MCFC) or Solid Oxide Fuel Cell (SOFC). Such cells can handle methane-containing synthesis gas, which is reformed inside the cell. The successful operation of a SOFC using gasified biomass has been shown for the first time in a one-day demonstration on August 7th, 2002 in Littleton, Colorado (Community Power Corporation, 2002). Three different biomass fuels were individually gasified in a downdraft gasifier and converted to electric power in a small laboratory fuel cell.

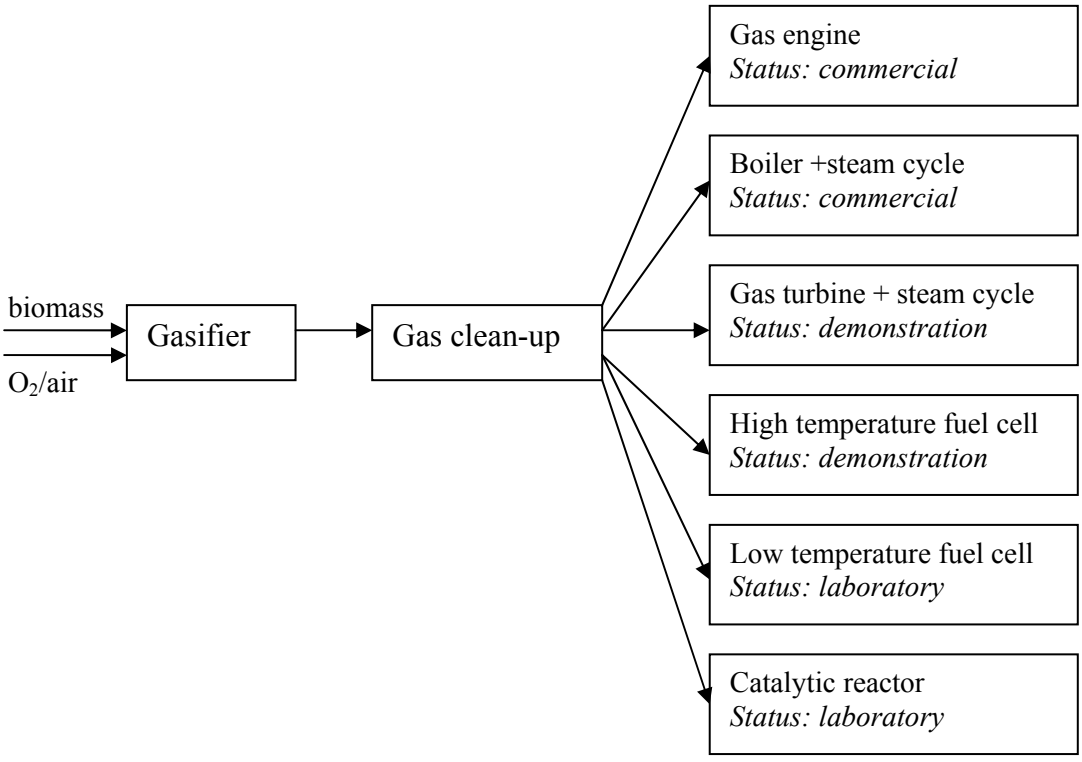

Figure 10.1: Applications for product gas from biomass gasifiers

Pure hydrogen was also run on the same fuel cell to calibrate power output. As expected, pure hydrogen produced the highest power level (2.76 Watts), followed by coconut shells (1.97 Watts), pecan shells (1.96 Watts) and wood chips (1.88 Watts). The robustness of the technology must still be proven on longer time scale.

Entrained flow gasifiers operating at very high temperature produce synthesis gas with very low methane content. Another option that thus becomes possible is the production of hydrogen from biomass ('green hydrogen') for Proton Exchange Membrane (PEM) fuel cells. The PEM fuel cell is the type of fuel cell considered most often for mobile applications, due to its fast start-up, dynamic response and favourable power-to-weight ratio. The cost price of these cells has been reduced to less than 200 Euro per kW of peak power, and looks set to decrease further to price levels that can compete with internal combustion engines (Middelman, 2004).

10.3.2 Hydrogen from biomass

Figure 10.2 shows three possibilities for the production of hydrogen by gasification of torrefied wood. These possibilities differ in the way that wood is transported: as wood itself, as torrefied wood (which has an increased energy density; furthermore the bulk density can also be increased by densification) or as a liquid hydrogen carrier. Transport is needed when the demand for hydrogen is in a different location than where biomass is produced. A techno-economic evaluation of these options, whereby investment costs are balanced against transport costs, is recommended. Such an evaluation will answer the question whether torrefaction should preferably be carried out small-scale (locally) or large-scale. For all options in Fig. 10.2, it may be advisable to obtain oxygen required for gasification by water electrolysis (instead of cryogenic air separation), whereby the obtained hydrogen is additional product or can be used to increase the H_2/CO ratio of gas for dimethylether (DME) synthesis.

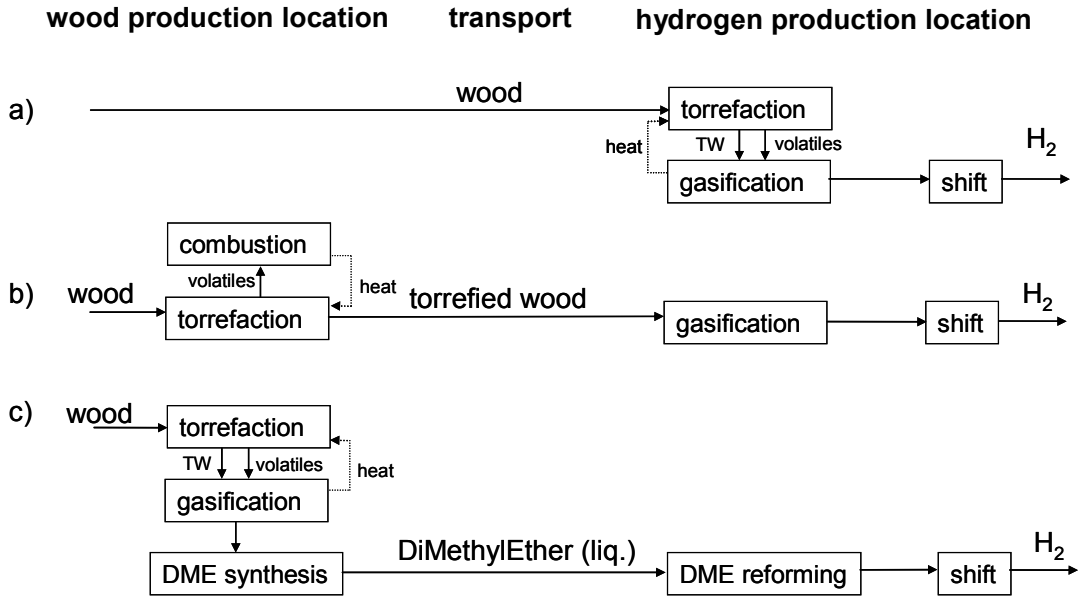

Figure 10.2: Options for production of hydrogen from imported biomass

Methanol has been most frequently considered as a liquid hydrogen carrier. An extensive research programme was carried out in the 1980's in the European Community entitled "Advanced gasification: methanol production from wood" (Beenackers and Van Swaaij, 1986). Due to recent progress in the direct synthesis of DME, its production may be cheaper in the future. DME synthesis is characterized by high per pass conversions (up to 60%) and flexibility for the H_2/CO ratio in the feed gas because the water gas shift reaction occurs inside the reactor. Another advantage compared to methanol is that DME is not toxic; in fact, it is already used in everyday life as a propellant. Similar to LPG, DME requires a pressure over 5 bar to keep it in liquid state. In the presence of steam, both methanol and DME can be catalytically reformed selectively to hydrogen, avoiding thermal decomposition. DME reforming requires higher temperatures than methanol reforming (350°C versus 200°C) and needs technology development, especially improved reforming catalysts (Semelsberger et al., 2004).

The production of hydrogen from biomass by oxygen-blown gasification competes with many other methods, such as gasification in super-critical water (Antal et al., 2000), catalytic reforming of biomass derived components such as sorbitol, glycerol and ethylene glycol in sub-critical water (Huber et al, 2003) and biological production from sorghum by thermophilic bacteria (Claassen et al., 2004). Hydrogen can also be produced from water electrolysis powered by electricity from renewable resources such as wind energy and solar energy. More advanced methods that produce hydrogen directly from sun light (without electricity as intermediate), such as photoelectrochemical production in photovoltaic cells and photobiological production using algae or bacteria, are being developed and appear highly promising. The capture efficiency of a multicrystalline silicon photovoltaic cell amounts to 13-14% (van Zolingen, 2000) and may exceed 20% in future. In contrast, the efficiency of solar energy conversion into biomass is calculated by Hall et al. (1993) to be at most 6.7% for C_4 plants (plants whose first product is a 4-carbon sugar) and 3.3% for C_3 plants (for which the first product of photosynthesis is a 3-carbon sugar). Practical biomass yields for C_3 plants will be just about 1% of the solar exergy influx, and even in warm climates where C_4 plants can thrive the conversion efficiencies are between 2% and 3% at best. This means that to produce the same amount of hydrogen, much more land area is needed for biomass than for solar cells (Mulder et al., 2000). At the moment, the energy output to input ratio of solar cells is rather low because a lot of energy is used to refine silicon, and they are still expensive, but cheaper plastic solar cells are being developed with less energy intensive production. This justifies the question: 'should we produce hydrogen from biomass (and send carbon contained in the biomass straight back into the atmosphere as carbon dioxide), if we can make it directly from solar energy?'

A key issue that must be considered in this regard is storage, because the availability of solar energy (which peaks in summer in the industrialized Northern

Hemisphere) may not always coincide with the demand for hydrogen. Unfortunately, hydrogen is the smallest molecule on earth, which makes storage difficult. Storage as a liquid requires a temperature below 20 K, whereas storage in compressed form requires very high pressures, at least 34 MPa (5000 psi) for hydrogen-fuelled cars, in order to reach an acceptable driving range. Both methods are costly and require a lot of compression energy. Attempts to store hydrogen in metal hydrides or in carbon nanotubes have so far not led to a practical solution. If hydrogen is present together with carbon monoxide, obtained from biomass, it can be effectively stored in the form of methanol or DME. These can subsequently be steam reformed back to hydrogen at a convenient time. However, it would be preferable if these compounds could be used in direct methanol fuel cells and direct DME fuel cells. The development of such cells currently lags behind hydrogen fuel cells and breakthroughs are required, e.g., new electrolyte materials that can withstand increased operating temperatures up to 200°C and avoid fuel cross-over from anode to cathode.

10.3.3 Biomass in the year 2525

"In the year 2525

If man is still alive

If woman can survive

They may find....."

(Evans, 1969)

Imagine a society in the year 2525 where fossil fuels have become so scarce that nobody can afford them. A society based completely on renewable energy that will look back on our time as the "fossil fuel age". An interesting question is: will biomass be used in such a society, and how?

Of course, biomass will still be grown for food production. Furthermore, people will still need materials, e.g. for packaging, construction, etc. Since biomass is the only renewable carbon source, it will be indispensable for many carbon-containing materials, such as chemicals and plastics that are currently produced from crude oil. E.g., bio-ethylene (obtained from bio-methanol, bio-DME or bio-ethanol) can serve as a raw material to produce bio-plastics, or smarter ways might be used to produce bio-plastics directly.

The world in 2525 can rely on solar energy to produce electricity; photo-voltaic cells would be commonplace. People's houses could be heated by solar energy, geothermal energy or heat pumps (i.e. boilers, stoves and furnaces would be extinct); although they may have more need for air-conditioning as a result of global warming.

The future world inhabitants would enjoy their mobility. Therefore, a modern transport system powered by fuel cells could be in place. Solar hydrogen, assuming that it can be effectively stored, might have made the hydrogen economy a reality. Another scenario, advocated by Nobel laureate George Olah, is a methanol economy. In order to produce methanol, Olah (2003) suggests using nuclear energy to produce hydrogen, and subsequently hydrogenate carbon dioxide present in the atmosphere, thus chemically recycling carbon dioxide. As man will probably live in better harmony with nature in 2525, it is hard to imagine that nuclear energy would be used in a sustainable society (although nuclear fusion might be). Moreover, the process proposed by Olah would be hampered by the low concentration of CO_2 in the atmosphere (even if it were a magnitude higher than the 360 ppm it is today). Scientists of the 26th century would realize that a sophisticated process which takes up CO_2 from the atmosphere and, even better, uses water as a source of hydrogen, already exists in nature: photosynthesis. They would understand and have the ability to control photosynthesis in order to produce carbohydrates and modify them into a compound that is suitable for storage and application in future fuel cells. This compound could be methanol, DME, or even glucose, which might be used in fuel cells, containing enzymes that mimic the human body, in a far-fetched future. Such a scenario may be truly characterized as: ‘biomass as a sustainable energy source’.

References

Antal MJ, Allen SG, Schulman D, Xu, X, Divilio RJ (2000). Biomass Gasification in Supercritical Water. Industrial & Engineering Chemistry Research 39(11):4040 – 4053.

Beenackers AACM, Swaaij WPM van, editors (1986). Advanced gasification: methanol production from wood – results of the EEC pilot programme. Solar Energy R&D in the European Community, Series E, Vol. 8, Energy from Biomass. Dordrecht, Netherlands: D. Reidel Publishing Company.

Claassen PAM, de Vrije T, Budde MAW (2004). Biological Hydrogen Production from sweet sorghum by Thermophilic Bacteria. In: Proceedings of 2nd World Biomass Conference, Rome, Italy, May 10-14, 2004.

Community Power Corporation (2002). Fuel cell operates on coconut shells, pecan shells and wood chips. Press release, August 15, 2002.

Drift A van der, Boerrigter H, Coda B, Cieplik MK, Hemmes K (2004). Entrained flow gasification of biomass: ash behaviour, feeding issues, and system analyses. Report nr. ECN-C-04-039. Petten: Energy research Centre of the Netherlands.

Evans R (1969). In the year 2525. Sung by Zager and Evans, reached #1 on Billboard Charts on December 7, 1969.

Hall DO, Rosillo-Calle F, Williams RH, Woods J (1993). Biomass for energy: supply prospects. In: Johansson TB, Kelly H, Reddy AKN, Williams RH, editors. Renewable Energy: Sources for Fuels and Electricity. Washington: Island Press.

Huber GW, Shabaker JW, Dumesic Ja (2003). Raney Ni-Sn catalyst for H_2 production from biomass-derived hydrocarbons. Science 300:2075-2077, 27 June 2003.

Middelman E (2004). Nedstack halves price of fuel cell each year; oil companies are slowing down introduction of hydrogen (interview in Dutch). Utilities, May 2004.

Mulder JM, van der Kooi HJ, De Swaan Arons J (2000). Alternative routes for ethanol production from renewable resources. In: Hirs GG, editor. Proceedings of 13th Int. Conf. on Efficiency, Costs, Optimization, Simulation and Environmental Impact of Energy Systems (ECOS 2000), University of Twente, Netherlands.

Olah GA (2003). It's elemental: the periodic table – carbon. Chemical and Engineering News 81 (36): September 8, 2003.

Semelsberger TA, Brown LF, Borup RL, Inbody MA (2004). Equilibrium products from autothermal processes for generating hydrogen-rich fuel-cell feeds. International Journal of Hydrogen Energy 29 (10), 1047-1064, 2004.

Stassen HEM, Prins W, Swaaij WPM van (2002). Thermal conversion of biomass into secondary products: the case of gasification and pyrolysis. In: Palz W, Spitzer J, Maniatis K, Kwant K, Helm P, Grassi A, editors. Twelfth European Biomass Conference, Amsterdam, Netherlands. p.38-44.

Zolingen RJC van (2000). Photovoltaic conversion. In: Berkel J van, Daey Ouwens C, Helden WGJ van, Kuik GAM van, Prasad KK, Wit MJ de, Zolingen RJC van, editors. Sustainable energy resources, Lectures notes, Eindhoven University of Technology.

List of publications

Articles

Prins MJ, Ptasinski KJ, Janssen FJJG (2003). Thermodynamics of gas-char reactions: first and second law analysis. Chemical Engineering Science 58 (13-16):1003-1011.

Prins MJ, Ptasinski KJ (2005). Energy and exergy analyses of oxidation and gasification of carbon. Energy 30 (7):982-1002.

Prins MJ, Ptasinski KJ, Janssen FJJG (2005). Exergetic optimisation of a production process of Fischer–Tropsch fuels from biomass. Fuel Processing Technology, 86 (4):375-389.

Prins MJ, Ptasinski KJ, Janssen FJJG. From coal to biomass gasification: comparison of thermodynamic efficiency. Submitted to Energy.

Prins MJ, Ptasinski KJ, Janssen FJJG. Torrefaction of wood. Part I: Weight loss kinetics. Submitted to Journal of Analytical and Applied Pyrolysis.

Prins MJ, Ptasinski KJ, Janssen FJJG. Torrefaction of wood. Part II: Analysis of products. Submitted to Journal of Analytical and Applied Pyrolysis.

Prins MJ, Ptasinski KJ, Janssen FJJG. More efficient biomass gasification via torrefaction. Accepted for publication in Energy.

Refereed proceedings

Prins MJ, Ptasinski KJ, Janssen FJJG (2002). Thermodynamics of gas-char reactions: first and second law analysis. In: Proceedings of 17th Int. Symp. on Chemical Reaction Engineering, Hong Kong, China, August 25-28, 2002.

Prins MJ, Ptasinski KJ, Janssen FJJG (2003). From coal to biomass gasification: comparison of thermodynamic efficiency. In: Houbak N, Elmegaard B, Qvale B, Moran MJ, editors. Proceedings of 16th Int. Conf. on Efficiency, Costs, Optimization, Simulation and Environmental Impact of Energy Systems (ECOS 2003), Copenhagen, Denmark, June 30-July 2, 2003. p. 1097-1103.

Prins MJ, Ptasinski KJ, Janssen FJJG (2004). More efficient biomass gasification via torrefaction. In: Rivero R, Monroy L, Pulido R, Tsatsaronis G, editors. Proceedings of 17th Int. Conf. on Efficiency, Costs, Optimization, Simulation and Environmental Impact of Energy Systems (ECOS 2004), Guanajuato, Mexico, July 7-9, 2004. p. 1485-1494.

Prins MJ, Pierik A, Janssen FJJG, Ptasinski KJ (2005). Exergy efficiency of biomass gasification for various biofuels. Submitted for 18th Int. Conf. on Efficiency, Costs, Optimization, Simulation and Environmental Impact of Energy Systems (ECOS 2005), Trondheim, Norway, June 20-23, 2005.

Non-refereed proceedings

Prins MJ, Ptasinski KJ, Janssen FJJG (2002). Exergy analysis of a production process of Fischer-Tropsch fuels from biomass. In: Palz W, Spitzer J, Maniatis K, Kwant K, Helm P, Grassi A, editors. Proceedings of 12th European Biomass Conference, Amsterdam, Netherlands, June 17-21, 2002. p. 1154-1157.

Bergman PCA, Boersma AR, Kiel JHA, Prins MJ, Ptasinski KJ, Janssen FJJG (2004). Torrefaction for entrained flow gasification of biomass. In: Swaaij WPM van, Fjällström T, Helm P, Grassi A, editors. Proceedings of 2nd World Biomass Conference, Rome, Italy, May 10-14, 2004. p. 679-682.

Summary

This thesis addresses the question how biomass may be used more efficiently and economically than it is being used today. Biomass already plays a large role in the energy supply, especially in developing countries, but it is often used inefficiently. Rather than combustion of biomass, it could be gasified, and the gas subsequently used in modern energy devices such as gas turbines, fuel cells, and catalytic reactors. Gasification of biomass has been practiced since World War II but technical bottlenecks (e.g. tar formation) and non-technical bottlenecks (e.g. cost and availability of biomass) are still hampering large-scale implementation.

The thesis is presented in two parts. In the first part, the thermodynamic efficiency of gasification processes is analysed. The second part is aimed at improving the properties of biomass prior to gasification.

The first part defines gasification efficiency, on the basis of the first and second law of thermodynamics, as the exergy increase of the gas divided by the exergy decrease of the solid fuel. It is shown that the efficiency of gasifying a fuel reaches a theoretic maximum at the so-called carbon boundary point. This is the point where the fuel is reacted with exactly enough oxygen so that gasification is complete and solid carbon formation does not occur. A detailed explanation is given why gasification is more efficient than combustion.

The gasification efficiency that can be achieved for different fuels, ranging from biomass to coal, is compared. These fuels are distinguished by their atomic O/C and H/C ratios as shown in a Van Krevelen diagram. The amount of oxygen to be added for complete gasification relative to the amount required for combustion is lower for biomass than for coal. Consequently, a lower gasification temperature is theoretically required. However, at practical gasification temperatures in the range of 1200 K to 1500 K, biomass becomes over-oxidized. Furthermore, the chemical exergy of biomass is high relative to its heating value, but this work potential is not fully utilized in the process.

For the combination of an air-blown biomass gasifier with a catalytic Fischer-Tropsch reactor, it is shown that the gasifier has a large contribution to the exergy losses. The optimum temperature for gasification of wood is rather low (around 700°C), but the overall efficiency is higher at elevated temperatures where methane formation is avoided.

The main conclusion of the first part of this thesis is that it may be advantageous to improve the heating value of biomass prior to gasification, which enables higher gasification temperatures and higher thermodynamic gasification efficiency.

The second part of this thesis focuses on biomass torrefaction, a thermal pretreatment in the range of 230-300°C in the absence of oxygen. In this process, mainly the hemicellulose fraction (which amounts to 20-35 wt% of the wood) decomposes, whereby deciduous wood types, such as beech and willow, were found to be more reactive than coniferous wood types, such as larch, due to different compositions of their hemicellulose fractions.

The weight loss kinetics of torrefaction of willow are determined by thermogravimetric analysis. It can be described by a two-stage mechanism: a fast first stage, in which hemicellulose decomposes, followed by a slower second stage in which secondary charring occurs. Volatile formation occurs in both reactions. The torrefaction kinetics are described by first-order consecutive reactions, with an activation energy of 76.0 kJ/mol for the first reaction and 151.7 kJ/mol for the second reaction. The required residence time in an industrial torrefaction process decreases from over 3 hours at 230°C to 10 minutes at 300°C.

The products formed by torrefaction of wood have been determined in a small fixed bed reactor set-up. The torrefied wood, an aqueous phase and non-condensable gases have been analysed. Torrefaction lowers the O/C ratio of wood from 0.70 to 0.52-0.60 (depending on process conditions). At a temperature of 270°C and a reaction time of 15 minutes, the lower heating value is increased from 17.7 MJ/kg up to 20.7 MJ/kg. The liquid product contains mainly water and acetic acid and the gaseous product of mainly carbon dioxide and carbon monoxide.

Possibilities for integration of biomass torrefaction with gasification are studied. Three concepts are compared: circulating fluidized bed gasification of wood and torrefied wood, both at 950°C, and entrained flow gasification of torrefied wood at 1200°C. Steam generated from the hot gasifier product gas is used to heat the torrefaction reactor. For the entrained flow gasifier, the volatiles from the torrefaction process can be introduced into the gasifier product gas as a ‘chemical quench’. Such as system offer a thermodynamic improvement compared to direct gasification of wood, since more chemical exergy is conserved in the product gas.

The thesis recommends that the integrated processes of torrefaction and gasification be demonstrated in practice, as this presents a novel method to convert biomass more efficiently to synthesis gas than conventional gasification processes.

Samenvatting

Dit proefschrift behandelt de vraag, hoe biomassa efficiënter en economischer benut kan worden dan nu gebeurt. Biomassa speelt reeds een grote rol in de energievoorziening, vooral in ontwikkelingslanden, maar wordt vaak inefficiënt gebruikt. In plaats van verbrand, kan deze beter vergast worden, waarbij het product gas gebruikt kan worden in moderne apparatuur, zoals in gas turbines, brandstofcellen of katalytische reactoren. Vergassing van biomassa werd al toegepast tijdens de Tweede Wereldoorlog, maar technische belemmeringen (zoals teervorming) en niet-technische belemmeringen (zoals kosten en beschikbaarheid van biomassa) staan grootschalige implementatie in de weg.

Het proefschrift wordt in twee delen gepresenteerd. In het eerste deel wordt de thermodynamische efficiëntie van vergassingsprocessen geanalyseerd. Het tweede deel richt zich op het verbeteren van de eigenschappen van biomassa, voorafgaande aan vergassing.

In het eerste deel wordt de efficiëntie van een vergasser gedefinieerd, op basis van de eerste en tweede hoofdwet van de thermodynamica, als de toename van de exergie van het gas gedeeld door de afname van de exergie van de vaste brandstof. Aangetoond wordt dat de efficiëntie een theoretisch maximum bereikt bij het punt waarop precies genoeg zuurstof toegediend wordt voor volledige vergassing, waarbij zich geen vaste koolstof vormt. Een gedetailleerde onderbouwing wordt gegeven waarom adiabatische vergassing efficiënter is dan verbranding.

De efficiëntie die gehaald kan worden bij vergassing van verschillende brandstoffen, variërend van biomassa tot steenkool, is vergeleken. Deze brandstoffen onderscheiden zich door hun O/C en H/C verhoudingen, zoals in een Van Krevelen diagram. De hoeveelheid zuurstof die nodig is voor vergassing, in verhouding tot verbranding, is lager voor biomassa dan voor steenkool. Echter, bij praktische vergassingstemperaturen tussen 1200 en 1500 K wordt biomassa over-geoxideerd. Bovendien is de chemische exergie hoog in verhouding tot de verbrandingswarmte en wordt deze potentiële arbeid in het proces niet volledig benut.

Voor de combinatie van een biomassa vergasser met lucht als oxidans en een katalytische Fischer-Tropsch reactor is aangetoond dat de vergasser een grote bron van exergieverliezen vormt. De optimale temperatuur voor vergassing van hout is nogal laag (circa 700°C), maar het totale proces is het meest efficiënt bij hogere vergassingstemperaturen waarbij de vorming van methaan vermeden wordt.

De hoofdconclusie van het eerste deel van het proefschrift is dat het gunstig zou kunnen zijn om de verbrandingswarmte van de biomassa voorafgaande aan het vergassingsproces te verbeteren, hetgeen hogere vergassingstemperaturen en een hogere thermodynamische efficiëntie van biomassa vergassers mogelijk maakt.

Het tweede deel van het onderzoek concentreert zich op torrefactie van biomassa, een thermische voorbehandeling in het temperatuurbereik van 230 tot 300°C in afwezigheid van zuurstof. In dit proces ontleedt met name de hemicellulose fractie (circa 20-35 gewichtsprocent van het hout), waarbij loofhout, zoals beuk en wilg, reactiever is dan naaldhout, zoals larix, als gevolg van verschillende samenstellingen van de hemicellulose fracties.

De snelheid van gewichtsafname bij torrefactie van beuk is gemeten met behulp van thermogravimetrische analyse. Deze kan beschreven worden met een twee-traps mechanisme: een snelle eerste stap, waarin hemicellulose ontleedt, gevolgd door een tragere volgstap, waarbij zgn. ‘charring’ reacties optreden. In beide stappen vormen zich vluchtige stoffen. De kinetiek wordt beschreven door eerste orde reacties in serie, met een activeringsenergie van 76.0 kJ/mol voor de eerste reactie en 151.7 kJ/mol voor de tweede reactie. De benodigde reactietijd in een industrieel torrefactie proces daalt van meer dan 3 uur bij 230°C tot 10 minuten bij 300°C.

De producten die gevormd worden bij torrefactie van hout zijn bepaald in een kleine vast bed reactoropstelling. Het getorreficeerde hout, een vloeistoffase en niet-condenseerbare gassen zijn geanalyseerd. Torrefactie verlaagt de O/C verhouding van hout van 0.70 tot 0.52-0.60 (afhankelijk van de procescondities). Bij een temperatuur van 270°C en reactietijd van 15 minuten wordt de onderste verbrandingswaarde verhoogd van 17.7 MJ/kg tot 20.7 MJ/kg. Het vloeibare product bevat voornamelijk water en azijnzuur en het gas bestaat vooral uit kooldioxide en koolmonoxide.

Mogelijkheden om biomassa torrefactie te integreren met vergassing zijn bestudeerd. Drie concepten zijn vergeleken: circulerend wervelbed vergassing van hout en getorreficeerd hout, beide bij 950°C, en ‘entrained flow’ vergassing van getorreficeerd hout bij 1200°C. Stoom verkregen uit het hete produkt gas van de vergasser wordt gebruikt om de torrefactie reactor te verwarmen. De vluchtige stoffen, die bij torrefactie vrijkomen, kunnen gebruikt worden om het product gas van de ‘entrained flow’ vergasser af te koelen. Een dergelijk concept betekent een thermodynamische verbetering ten opzichte van directe vergassing van hout, aangezien meer chemische exergie geconserveerd blijft in het product gas.

Het proefschrift doet de aanbeveling om de geïntegreerde processen van torrefactie en vergassing in de praktijk te demonstreren, aangezien dit een nieuwe methode is om biomassa efficiënter om te zetten in synthese gas dan conventionele vergassingsprocessen.

Dankwoord

Graag wil ik iedereen bedanken die een bijdrage geleverd heeft aan de totstandkoming van dit proefschrift en zeker ook iedereen die mij de afgelopen jaren gesteund en gemotiveerd heeft.

Mijn begeleiders Frans Janssen en Krzysztof Ptasinski wil ik bedanken voor de mogelijkheid die ze mij gaven om onderzoek te doen op een aansprekend vakgebied, de vrijheid die ik kreeg om hier invulling aan te geven en voor hun opbouwende feedback. Ik ben 'biomassa-goeroe' Cees Daey Ouwens erkentelijk voor zijn enthousiasme en interesse in mijn werk, en voor het initïeren van onderzoek op het gebied van torrefactie van biomassa. De hieruit voortvloeiende samenwerking met Patrick Bergman en Jaap Kiel van ECN-Biomassa en Hans Haan van Shell Global Solutions heb ik als zeer prettig en vruchtbaar ervaren.

Anneloes Meijnders, Gundula Hübner en Wouter van den Hoogen uit de onderzoeksgroep Mens-Techniek Interactie van prof. Cees Midden bij de faculteit Technologie Management wil ik bedanken voor de positieve, open discussies, die ertoe geleid hebben dat wetenschappers van verschillende achtergronden bijgedragen hebben aan de kwaliteit van elkaars onderzoek. Wouter, nog speciaal bedankt voor het maken en beschikbaar stellen van de foto op de kaft.

Binnen het promotieproject zijn vier studenten afgestudeerd: Tamara Loonen (2001), Ronald Verrips (2002), Barry van Dongen (2003) en Marijn Kappers (2004). Het was prettig met jullie samen te werken en jullie hebben allen een belangrijke bijdrage aan het onderzoek geleverd. In het bijzonder wil ik vermelden dat Marijn zo enthousiast was dat hij zelfs na zijn afstuderen nog enige tijd onderzoek heeft gedaan aan torrefactie van biomassa, hulde! Mijn dank ook voor de inbreng van research stagiaires Anke Pierik en Daan van Eck en afstudeerder Johann Venter van de Universiteit van Pretoria (baie dankie!).

De praktische ondersteuning van Anton Bombeeck bij de constructie van de torrefactie set-up, Marlies Coolen, Peter Lipman en Wim Groenland bij het uitvoeren van GC en HPLC analyses, en de secretariële ondersteuning van Denise Tjallema-Dekker heb ik zeer gewaardeerd.

Ik ben dank verschuldigd aan Lex Lemmens en Ria Overwater van TDO (Technologie voor Duurzame Ontwikkeling) voor het beschikbaar stellen van TU/e gelden om de nodige apparatuur aan te kunnen schaffen. De leden van de biomassa werkgroep binnen de Technische Universiteit Eindhoven dank ik voor de faculteits-overschrijdende interesse in elkaars onderzoek.

I would like to thank my roommates Lopamudra Devi and Zacharia Masende for the nice atmosphere and our discussions about everything that can be done to make this world a better place. Let me say to you: Dhanyabaad! Asante sana! Furthermore I would like to acknowledge Jieheng Guo for the pleasant manner in which we wrote a project proposal together. I am grateful for the help in Matlab modeling by fellow Ph.D. students Sreejit Nair, Chaitanya Khare, Charl Stemmet and Vinit Chilekar. Thanks also to many Indian Ph.D. students for the nice cricket games that we played on the TU/e grounds!

Graag wil ik enkele personen noemen, die (misschien zonder het te weten) mij beïnvloed hebben in de keuze van het onderwerp van het promotieonderzoek. Allereerst dr. Johannes Penninger, die mij tijdens mijn afstudeertijd bij Akzo Nobel leerde dat koppeling van exotherme en endotherme reacties efficienter is dan deze reacties afzonderlijk uitvoeren. Emeritus prof. Gerard Hirs liet mij als TwAIO tijdens een PAOK-cursus kennis maken met exergie; in dit kader heb ik in 1995 al een exergieanalyse van een biomassavergasser uitgevoerd. Met dr. Ben Jager van Sasol Technology heb ik verschillende keren gediscussieerd over de voor- en nadelen van ‘natte’ vergassers (bv. Lurgi) en ‘droge’ vergassers (bv. Shell, Texaco). Ek het dit baie geniet!

Tanja Gielen wil ik bedanken voor het prachtige ontwerp van de kaft en, samen met Geert van Gameren, voor alle hulp en advies bij het editen van het proefschrift.

Tenslotte dank ik mijn familie. Jullie betekenen zeer veel voor mij en ik heb jullie de laatste tijd heel erg nodig gehad. Mijn ouders en mijn broer Daniël, bedankt voor alle liefde, hulpvaardigheid en ondersteuning. Esther, als jij me niet gestimuleerd had, dan was ik misschien wel nooit aan het promotieonderzoek begonnen. Het was ontzettend fijn om de steun te hebben van iemand die zelf gepromoveerd is en de problemen, die zich voordoen bij promotieonderzoek, kan relativeren. Bedankt voor alle hulp, begrip en troost. Een glimlach van jou en van Marianne maken mijn dag altijd goed.

14 december 2004,

Mark Prins

Curriculum vitae

Mark Jan Prins was born on the 3rd of June 1970 in Haaksbergen, situated in the region of Twente, the Netherlands, as the eldest of three sons (see picture below). Mark is married to Esther Gielen and they have a daughter: Marianne Carina.

After attending primary and secondary school in his hometown, he studied chemical engineering at the University of Twente. His M.Sc. research was carried out at Akzo Nobel in Hengelo under supervision of prof.dr.ir. K.R. Westerterp and completed on 29th of April 1994. The topic was thermal decomposition of chelating agents such as EDTA in liquid water at elevated temperatures. He then specialized at the University of Twente in chemical process design and development by completing the two-year postgraduate process technology course.

Mark's industrial career started on 1st of July 1996 in Sasolburg, South Africa, where he worked as a process engineer for Sasol Technology. Sasol is the only company in the world that produces liquid fuels from coal. He was involved in the production of Fischer-Tropsch diesel from wax on pilot-plant scale, and co-authored two patents on this topic. After his return to the Netherlands in 1999, he worked in basic and detailed plant engineering with Fluor Daniel in Bergen op Zoom.

In January 2001, his continuing interests in renewable energy and thermodynamic analysis of processes merged and the research described in this thesis was started.

Michiel, Daniel and Mark,
brothers and basketball teammates